Energy Management and Environmental Sustainability of the Canadian Oil Sands Industry

by

Mohamed Elsholkami

A thesis

presented to the University of Waterloo
in fulfillment of the

thesis requirement for the degree of

Doctor of Philosophy

in

Chemical Engineering

Waterloo, Ontario, Canada, 2018

Examining Committee Membership

The following served on the Examining Committee for this thesis. The decision of the Examining Committee is by majority vote.

External Examiner	Dr. Qipeng (Phil) Zheng Professor
Supervisor	Dr. Ali Elkamel Professor
Internal Member	Dr. William A. Anderson Professor
Internal Member	Dr. Boxin Zhao Professor
Internal-external Member	Dr. Sagar Naik Professor

Author's Declaration

I hereby declare that I am the sole author of this thesis. This is a true copy of the thesis, including any required final revisions, as accepted by my examiners.

I understand that my thesis may be made electronically available to the public.

Abstract

By 2030 the worldwide energy demand is expected to increase by twofold, in which fossil fuels inevitably will still play a major role in this transition. Canadian oil sands, the second largest proven oil reserves, represent a major pillar in providing energy and economic security in North America. Their development on a large scale is hindered due to associated environmental impacts, which include greenhouse gas emissions, water usage, and management of by-products of downstream operations (e.g. Sulfur, petroleum coke, etc.). In this work optimization techniques are employed to address the management of various environmental issues while minimizing the cost of operations of the oil sands industry. In this context, this thesis makes four principal contributions.

First, an extensive review is conducted on potential production pathways of renewable energy that can be integrated in the energy infrastructure of oil sands. Renewable technologies such as wind, geothermal, hydro, bioenergy, and solar are considered the most environmentally benign options for energy production that would contribute in achieving significant carbon emissions reductions. A mixed integer non-linear optimization model is developed to simultaneously optimize the capacity expansion and new investment decisions of both conventional and renewable energy technologies, and determine the optimal configurations of oil producers. The rolling horizon approach is used for the consecutive planning of multiple operational periods. To illustrate the applicability of the model, it was applied to a case study based on operational data for oil sands operators in Alberta for the period of 2010 – 2025.

Second, a generalized optimization model was developed for the energy planning of energy intensive industries. An extensive superstructure was developed that incorporates

conventional, renewable, nuclear, and gasification of alternative fuels (e.g. petroleum coke, asphaltenes, etc.) technologies for the production of energy in the form of power, heat and hydrogen. Various carbon mitigation measures were incorporated, including carbon capture and sequestration, and purchase of carbon credits to satisfy emission targets. Finally, the superstructure incorporated the possibility of selling excess energy commodities in competitive markets. The superstructure is represented by a multi-period mixed integer optimization model with the objective of identifying the optimal set of energy supply technologies to satisfy a set of demands and emission targets at the minimum cost. Time-dependent parameters are incorporated in the model formulation, including energy demands, fuel prices, emission targets, carbon tax, construction lead time, etc. The model is applied to a case study based on the oil sands operations over the planning period 2015–2050. A scenario based approach is used to investigate the effect of variability in energy demand levels, various carbon mitigation policies, and variability in fuel and energy commodity prices.

Third, a multi-objective and multi-period mixed integer linear programming model is developed for the integrated planning and scheduling of the energy infrastructure of the oil sands industry incorporating intermittent renewable energy. The contributions of various energy sources including conventional, renewable, and nuclear are investigated using a scenario based approach. Power-to-gas for energy storage is incorporated to manage surplus power generated from intermittent renewable energy sources, particularly wind. The wind-electrolysis system incorporates two hydrogen recovery pathways, which are power-to-gas and power-to-gas-to-power using natural gas generators. The model takes into account interactions with the local Alberta grid by incorporating unit

commitment constraints for the grid's existing power generation units. Three objective functions are considered, which are the total system cost, grid operating cost and total emissions. The epsilon constraint method is used to solve the multi-objective aspect of the proposed model.

Fourth, extensive research has been done on the components that constitute the sulfur supply chain, including sulfur recovery, storage, forming, and distribution. These components are integrated within a single framework to assist in the design optimization of sulfur supply chains. This represents a starting point in understanding the trade-offs involved in the sulfur supply chain from an optimization point of view. Optimization and mathematical modeling techniques were implemented to generate a decision support system that will provide an indication of the optimal design and configuration of sulfur supply chains. The resulting single-period mixed-integer linear programming model was aimed at minimizing total capital and operating costs. The model was illustrated through a case study based on Alberta's Industrial Heartland. A deterministic approach in an uncertain environment was implemented to investigate the effect of supply and demand variability on the design of the supply chain. This was applied to two scenarios, which are steady state operation and sulfur surplus accumulation. The model identified the locations of forming facilities, the forming, storage and transportation technologies, and their capacities.

The contributions of this thesis are intended to support effective carbon mitigation policy making and to address the environmental sustainability of the oil sands industry.

Acknowledgments

I express my utmost gratitude and attribute every achievement in my life to my parents, Zamzam ElMarsafy and Ahmed Elsholkami. My deepest love and appreciation also goes to my siblings Yasmin Elsholkami and Amro Elsholkami. Their unconditional love and support have been the root of every success in my life.

I express my sincere gratitude to my supervisor, Dr. Ali Elkamel. It has been a privilege to be his student and to have him as a role model. I am appreciative for all his support and advice for all of my endeavors at the University of Waterloo, which helped me define the bases of my research and teaching skills. His generous advice extends into improving who I am as a person. Dr. Elkamel has been truly an inspiration and I will always look up to him.

During my graduate studies, I had the pleasure of working with an exceptional group of graduate and undergraduate students at the department of chemical engineering. I also would like to take this opportunity to thank the chemical engineering department faculty and the administrative staff for their support and assistance during my graduate studies.

I acknowledge the financial support received for my doctoral research through grants and scholarships, Ontario Graduate Scholarship and Natural Sciences and Engineering Research Council.

I acknowledge many friends who have encouraged and supported me during my studies and stay in Waterloo. I wish to specifically thank my friends, Riz Hossain, Shadya Kabir, Yaseen Hossain, Yousuf Hossain, Mohab ElDeeb, Mohammed ElDeeb, Ahmed Tareq, Emir Burazerovic, Chato Hajizadeh, Omar Alkubaisi, Henry Balodaki, and Greg Bernard.

Dedication

To my parents.

Table of Contents

List of Tables

List of Figures

Nomenclature

Sets and indices

B, b	Set of boiler technologies (*B'*: Set of preheat options ∈ *B*). (Chapter 3, 4, 5)
	Set of sulfur blocks. (Chapter 6)
C, c	Set of industrial gas fired combined heat and power technologies. (Chapter 3)
	Set of available capacity levels of electrolyzers. (Chapter 5)
	Set of customers. (Chapter 6)
D, d	Set of available capacity levels of hydrogen transportation pipeline. (Chapter 5)
	Set of all distribution centers $U \subset D$. (Chapter 6)
E, e	Set of existing energy production units (i.e. power, hydrogen, steam and hot water producers). (Chapter 3)
	Set of all energy commodities required (i.e. power, hydrogen, low and high pressure steam, etc.). (Chapter 4, 5)
	Set of all nodes in the supply chain ($I \cup J \cup G \cup D \cup U \cup C$). (Chapter 6)
F, f	Set of fuels (i.e. natural gas, coal, biomass, petcoke, asphaltene, etc.) (Chapter 4)
	Set of natural gas combined cycle units. (Chapter 5)
	Set of formed sulfur products. (Chapter 6)
G, g	Set of natural gas combined heat and power units. (Chapter 5)
	Set of newly established forming facilities. (Chapter 6)
H, h	Set of hydrogen production plants
I, i	Set of all types of energy production technologies ($P \cup H \cup B \cup U \cup C \cup K \cup R$) ∈ I (Chapter 3, 4).
	Set of existing generating units belonging to the Alberta grid. (Chapter 5)
	Set of sulfur recovery units. (Chapter 6)
J, j	Set of an industry's production routes (e.g. bitumen extraction and upgrading routes). (Chapter 3)
	Set of all forming facilities $G \subset J$. (Chapter 6)
K, k	Set of gasification technologies. (Chapter 4)
	Set of regional buses comprising the Alberta grid. (Chapter 5)
M, m	Set of integrated mining / upgrading SCO production routes
N, n	Set of energy production units considered for each technology. (Chapter 4)
	Set of number of units available for each production technology p. (Chapter 5)
	Set of all forming technologies. (Chapter 6)
	Nf: Set of forming technologies associated with product form f
O, o	Set of all SCO production routes
P, p	Set of standalone power production technologies (Chapter 3, 4)
	Set of all energy production technologies. (Chapter 5)
Q, q	Set of products produced through industrial production routes f (e.g. bitumen, synthetic crude oil, etc.).
R, r	Set of processing options of syngas produced from gasification. (Chapter 4)
	Set of raw material i.e. liquid sulfur. (Chapter 6)
S, s	Set of integrated SAGD / upgrading SCO production routes. (Chapter 3)
	Set of storage facilities. (Chapter 6)
	S_f: Set of storage facilities associated with formed sulfur
	S_r: Set of storage facilities associated with liquid sulfur
	S_b: Set of storage facilities associated with blocked sulfur
T, t	Set of time period included in the planning period. (Chapters 4, 5)
	Set of transportation modes. (Chapter 6)
	T_r: Set of transportation modes associated with liquid sulfur
	T_f: Set of transportation modes associated with formed sulfur
U, u	Set of nuclear production technologies. (Chapter 4, 5)
	Set of newly established distribution centers. (Chapter 6)

Parameters

AWP	Annual energy yield of VESTAS wind turbine (kWh)
CCB_b	Amortized capital cost of boiler type b ($/yr)
$CCGEO$	Amortized capital cost of geothermal plants ($/yr)
CCH_h	Amortized capital cost of hydrogen plant type h ($/yr)
$CCHE$	Amortized capital cost of electrolyzer ($/yr)
CCP_p	Amortized capital cost of power plant type p ($/yr)
CO_2E	Maximum allowable level of CO_2 emissions (tonne CO_2/h)
d_m	Distance between mining location and extraction plant (m)
DR	Fraction of diluent
dT_m	Distance between extraction plant and tailing ponds (m)
ECB	Electricity requirement for the production of commercial crude bitumen (kWh/tonne)
ECC_i	Electricity requirement for compressing CO_2 for transport (kWh/tonne/km)
ECR	Power requirement for centrifugation (kWh/m^3)
ED_o	Electricity requirement for delayed cokers (kWh/tonne)
EER	Electrolyzer energy requirement (kWh/Nm^3)
EL_o	Electricity requirement for LC-finers (kWh/tonne)
$EPVF$	Annuity factor for existing technologies
$ESMR$	Electricity requirement of steam methane reforming plants (kW/tonne H_2)
ΔHSS	Change in enthalpy of SAGD steam (MJ/ton)
ΔHPS	Change in enthalpy of process steam (MJ/ton)
ΔHHW	Change in enthalpy of hot water (MJ/ton)
HHG	Hydrogen requirement for hydrotreatment of HGO (tonne H_2/tonne LGO)
HH_h^{max}	Maximum production capacity of hydrogen plant h (tonne/h)
HHV_b	High heating value of fuel used in boiler technology b i.e. natural gas, biomass etc. (MJ/tonne)
HHV_h	High heating value of fuel used in hydrogen technology h i.e. coal, natural gas, etc. (MJ/tonne)
HHV_p	High heating value of fuel used in power technology p i.e. coal, natural gas, etc. (MJ/tonne)
HLG	Hydrogen requirement for hydrotreatment of LGO (tonne H_2/tonne LGO)
HN	Hydrogen requirement for the hydrotreatment of naphtha (tonne H_2/tonne naphtha)
HNG	Heating value of natural gas (GJ/Nm^3)
HP_h^{cogen}	Power co-produced or consumed by hydrogen plants (kW/tonne H_2)
HRP_p	Heat rate of power plant p (MJ/kWh)
HRH_h	Heating rate of hydrogen production technology h (MJ/tonne H_2)
HRU_o	Hydrogen requirement for hydrocracking in low and high conversion LC-finers (tonne H_2/tonne feed)
$HRGEO^{max}$	Maximum heat rate provided by a geothermal plant (MJ/h)
FR_o	Natural gas requirement for LC-finers and delayed cokers (GJ/tonne VTB)
L	Length of CO_2 pipeline (km)
MDC	Diesel consumption for mining extraction (L diesel/bbl bitumen)
η_b	Efficiency of boiler type b
OMB_b	Operating and maintenance cost of boiler type b ($/yr)
$OMGEO$	Operating and maintenance cost of geothermal plants ($/yr)
OMH_h	Operating and maintenance cost of hydrogen plant h ($/yr)
$OMHE$	Operating and maintenance cost of electrolyzer ($/yr)
OMP_p	Operating and maintenance cost of power plant p ($/yr)
PFB_b	Unit cost of fuel utilized by SAGD boiler b ($/GJ or $/tonne)
PF_m	Pumping factor for hydrotransport (kWh/tonne/m)
PFH_h	Unit cost of fuel utilized by hydrogen plant h ($/GJ or $/tonne)
PFP_p	Unit cost of fuel utilized by power plant p ($/GJ or $/tonne)
PFT_m	Pumping factor for transport of tailings (kWh/tonne/m)
PD	Unit cost of diesel ($/L)
PNG	Unit cost of natural gas utilized by natural gas boilers ($/GJ)

PP_p^{max}	Maximum power production capacity of plant *p* (kWh)
PVF	Annuity factor for newly established technologies
EPVFe	Annuity factor for existing technologies
S_b^{max}	Maximum production capacity of boiler type *b* (tonne/h)
SSC	Unit sequestration cost ($/tonne CO_2)
SC_m	Steam requirement for conditioning stage (tonne steam/tonne feed)
SF	Steam requirement for bitumen extraction (tonne steam/tonne froth)
SOR	Steam to oil ratio (tonne of steam/tonne of bitumen)
SRD	Steam requirement for the diluent recovery unit (tonne steam/tonne feed)
SRF	Steam requirement for the fluid coker (tonne steam/tonne feed)
SRV	Steam requirement of vacuum distillation units (tonne steam/tonne feed)
t	Annual hours of operation (8760 hr/yr)
TC	Unit transportation cost of CO_2 ($/tonne CO_2/km)
WC_m	Water requirement for conditioning (tonne water/tonne oil sands)
WH	Water requirement for hydrotransport (tonne water/tonne oil sands)
WR	Water requirement for bitumen recovery (tonne water/tonne oil sands)
WTCF	Wind turbine capacity factor
%RED	Percentage reduction of CO_2 emission levels
%S	Fraction of boiler capacity dedicated for steam production

$BMAX_b$	Maximum production capacity of boiler technology *b* (t h^{-1})
CCB_b	Capital cost factor for boiler production technology *b* during time period *t* (CAD/t h^{-1})
CCH_{ht}	Capital cost factor for hydrogen production technology *h* during time period *t* (CAD/tH_2 h^{-1})
CCK_{kt}	Capital cost factor for gasification production technology *k* during time period *t* (CAD/t syngas h^{-1})
$CCNU_{ut}$	Capital cost factor for nuclear production technology *u* during time period *t* (CAD/MWth)
$CCO_{ct}^{GT/ST}$	Capital cost factors for gas and steam turbines in combined heat and power production technology *c* during time period *t* (CAD/MW)
CCP_{pt}	Capital cost factor for power production technology *p* during time period *t* (CAD/MW)
CCR_r	Capital cost factor for syngas processing option *r* during time period *t* (CAD/t syngas h^{-1})
CF_{pt}^R	Is the estimated annual capacity factor of renewable power production technology *p* during time period *t* (%)
CFB_{bt}	Unit cost of fuel utilized by boiler production technology *b* (e.g. CAD/GJ)
$CFCO_{ct}$	Unit cost of fuel utilized by CHP production technology *c* (e.g. CAD/GJ)
CFH_{ht}	Unit cost of fuel utilized by hydrogen production technology *h* (e.g. CAD/GJ)
CFK_k	Unit cost of fuel utilized by gasification technology *k* (e.g. CAD/kg)
CFP_{pt}^F	Unit cost of fuel utilized by power production technology *p* (e.g. CAD/GJ)
$CMAX_{iet't}^{LT}$	Maximum production capacity matrix of energy production technology *i*, incorporating construction lead time
$CMIN_{iet't}^{LT}$	Minimum production capacity matrix of energy production technology *i*, incorporating construction lead time
CNA	Cost of nuclear accident (CAD)
$CO2_t^{limit}$	Carbon dioxide emission cap for time period t (tCO_2 h^{-1})
$COMAX_c^{GT/ST}$	Maximum capacity of CHP technology *c* (MW)
$CostCredit_t$	Cost of purchasing carbon credits (CAD tCO_2^{-1})
$CostCS$	CO_2 sequestration cost (CAD tCO_2^{-1})
$CostCT$	CO_2 transport cost (CAD tCO_2^{-1} km^{-1})
$ECO2_{int}$	Total CO_2 emissions generated from energy production unit *n* of technology *i* (tCO_2 h^{-1})
EI_{eqj}	Energy intensity factor represent the amount consumed of energy commodity *e* for the production of a unit of *q* using production route *j* (units of *e*/units of *q*)
ε_i	CO_2 capture factor for energy production technology *i* (%)
FC_f	Cost of fuel *f* (CAD kg^{-1} or GJ^{-1})

$FCO_{ct}^{GT/ST}$	Fixed operating cost of cogeneration production technology *c* (CAD/MW)
FOB_b	Fixed operating cost of boiler production technology *b* (CAD/t h^{-1})
FOH_h	Fixed operating cost of hydrogen production technology *h* (CAD/tH_2 h^{-1})
FOK_k	Fixed operating cost of gasification technology *k* (CAD/t syngas h^{-1})
$FONU_u$	Fixed operating cost of nuclear technology *u* (CAD/MWth)
FOP_{pt}	Fixed operating cost of power production technology *p* (CAD/kW)
FOR_r	Fixed operating cost of syngas processing option *r* (CAD/t syngas h^{-1})
FRH_h^F	Fuel requirement for hydrogen technology *h* (kg or GJ of fuel/tH_2)
$H2Price_t$	Selling price of hydrogen during time period *t* (CAD/tH_2)
$Heat_h^H$	Heat requirement for hydrogen technology *h* (GJ/tH_2)
$HMAX_h$	Maximum production capacity of hydrogen technology *h* (tH_2 h^{-1})
$HRMAX_{b'}^{Preheat}$	Maximum preheating rate available from preheating technology *b'* (GJ h^{-1})
$KMAX_k$	Maximum production capacity of gasification technology *k* (t syngas h^{-1})
NPY_{pt}	Nominal power production capacity of renewable power production technology *p* during time period *t* (kW)
$NUMAX_u$	Maximum production capacity of nuclear technology *u* (MWth)
PKM	Pipeline length for CO_2 transport (km)
$PMAX_p$	Maximum production capacity of power production technology *p* (MW)
PNA	Probability of occurrence of a nuclear accident (reactor.yr)$^{-1}$
$PowPrice_t$	Power buying and selling price from and to the grid during time period *t* (CAD/kWh)
$PReq_h^H$	Power requirement for hydrogen technology *h* (kWh/tH_2)
$QPCE_{qjt}^{MAX}$	Maximum capacity expansion available for the production of product *q* through route *j* during time period *t* (units of *q*/units of time)
$QPCE_{qjt}^{MIN}$	Minimum capacity that can be added for the production of product *q* through route *j* during time period *t* (units of *q*/units of time)
QPR_{qt}	Rate of production of q during time period t (units of q/units of time) (e.g. bbl of SCO h^{-1})
RAF	Individual risk perception parameter for a nuclear accident
$RMAX_r$	Maximum capacity of syngas processing option *r* (t syngas h^{-1})
δYK_k^{syn}	Yield of syngas from gasification technology *k* (t syngas/t fuel)
δYR_{re}^{EC}	Yield of energy commodity *e* from syngas processing option *r* (units of *e*/t syngas)
δYU_{ue}^{E}	Yield of energy commodity *e* from nuclear production technology *u* (units of *e*/MWth)
$VCO_{ct}^{GT/ST}$	Variable operating cost of cogeneration technology *c* (CAD/kWh)
VOB_b	Variable operating cost of boiler production technology *b* (CAD/t)
VOH_h	Variable operating cost of hydrogen production technology *h* (CAD/tH_2)
VOK_k	Variable operating cost of gasification production technology *k* (CAD/t syngas)
$VONU_u$	Variable operating cost of nuclear production technology *u* (CAD/kWh)
VOP_{pt}	Variable operating cost of power production technology *p* (CAD/kWh)
VOR_r	Variable operating cost of syngas processing option *r* (CAD/t syngas)

$AELZ$	Electrolyzer constant (kg H_2/kWh)
A_{rotor}	Rotot area of the wind turbine (m^2)
$\phi_{emissions}^{SYSTEM}$	Weight set on emissions of the energy system [0,1]
$\phi_{emissions}^{GRID}$	Weight set on emissions of the grid [0,1]
$\beta_{kk'}$	Transmission line susceptance
CH_MIN_c	Minimum generation capacity of electrolyzer of capacity level *c* (kg H_2)
CH_MAX_c	Maximum generation capacity of electrolyzer of capacity level *c* (kg H_2)
DEC_{et}	Demand for energy commodity *e* during time period *t* of oil sands operators
ε_2	Epsilon constraint on objective function 2
ε_3	Epsilon constraint on objective function 3
$Grid\_demand_{kt}$	Total demand of regional bus *k* of the grid during period *t* (MW)
$Grid\_Demand_t^{Tota}$	Total power demand of the grid during period *t* (MW)
$GU\_Min\_uptime_i$	Minimum uptime of grid generating unit *i* (hour)
$GU\_Min\_downtim$	Minimum downtime of grid generating unit *i* (hour)

$HR\_MAX_u^{NU}$	Maximum heat production from nuclear unit *u* (MWth)
$H\_storage\_MAX$	Maximum storage capacity of storage tanks (kg H_2)
$H\_Transport_d^{MAX}$	Maximum capacity of transportation mode *p* (kg H_2)
HV_{H_2}	Heating value of hydrogen (GJ/kg)
HV_{NG}	Heating value of natural gas (GJ/kg)
$Min\_downtime_{ngc}$	Minimum up time of NGCC generators (hours)
Min_uptime_{ngcc}	Minimum down time of NGCC generators (hours)
Max_CR^{ngcc}	Maximum capacity rate of NGCC unit (MW)
Min_CR^{ngcc}	Minimum capacity rate of NGCC unit (MW)
$Min\_downtime_{cog}$	Minimum down time of cogeneration units (hours)
Min_uptime_{cogen}	Minimum up time of cogeneration units (hours)
Max_HRSG^{cogen}	Maximum heat produced from heat recovery steam generators (GJ h^{-1})
Min_CR^{cogen}	Minimum capacity rate of cogeneration units (MW)
Max_CR^{cogen}	Maximum capacity rate of cogeneration units (MW)
η^{WT}	Efficiency of wind turbine
$\eta_{turbine}$	Efficiency of gas turbine of cogeneration units
$\eta_{generation}$	Efficiency of generation from heat recovery steam generators of cogeneration units
$\eta_{recovery}$	Efficiency of recovery of heat of heat recovery steam generators of cogeneration units
η_{NGCC}	Efficiency of NGCC units
$P\_Ramp_i^{gu}$	Maximum ramping rate of generation unit *i* of the grid (MW hr^{-1})
ρ_{air}	Density of air (kg m^{-3})
ρ_{H_2}	Density of hdyrogen (kg m^{-3})
ρ_{NG}	Density of natural gas (kg m^{-3})
$RA_{it}^{hydro\&wind}$	Resource availability of hdyro and wind resources
$Ramp^{ngcc}$	Ramping rate of NGCC units (MW hr^{-1})
$Ramp^{cogen}$	Ramping rate of cogeneration units (MW hr^{-1})
SR_t	Spinning reserve requirement of the grid during period *t* (MW)
$SR\_lim_i^{MAX}$	Spinning reserve limit for each unit *i* (MW)
δP_{ue}^{NU}	Yield of energy commodity *e* from nuclear unit *u* (units of e /MWth)
TEC_{MIN}^{SYSTEM}	Minimum emissions of the energy system (tCO_2)
TEC_{MAX}^{SYSTEM}	Maximum emissions of the energy system (tCO_2)
TEC_{MIN}^{Grid}	Minimum emissions of the grid (tCO_2)
TEC_{MAX}^{Grid}	Maximum emissions of the grid (tCO_2)
$Trans_{kk'}^{Max}$	Capacity of power transmissions between buses *k* and *k'* of the grid (MW)
V_t	Wind speed during period *t* (m/s)
$Wind\_Potential_t$	Wind potential during period *t* (MWh)
ω	Weight used to calculate epsilon constraint 3 [0, 1]
z_3^{max}	Maximum value of objective function 3 used to calculate epsilon constraint 3
z_3^{min}	Minimum value of objective function 3 used to calculate epsilon constraint 3
$\varphi_{H_2}^{HENG}$	Maximum allowable share of hydrogen in hydrogen enriched natural gas sent to NGCC units (%)
$\emptyset^{TE}$	Allowable amount of excess power generated from the grid units and installed energy production units presented as a share of the total demand (%). Set to zero in this study.

g_{rfn}	Yield of product form *f* to raw material *r* using technology *n*
ρ_{cp}	A binary indicator of whether or not customer *c* accepts product form *p*
QF_{nq}^{min}	Minimum capacity of forming technology *n* of a capacity level *q*, T yr^{-1}
QF_{nq}^{max}	Maximum capacity of forming technology *n* of a capacity level *q*, T yr^{-1}
F_{jfn}^{min}	Lower limit on the amount of product *f* produced by technology *n* at site *j*, T yr^{-1}
F_{jfn}^{max}	Upper limit on the amount of product *f* produced by technology *n* at site *j*, T yr^{-1}
λ_{es}	Storage holding period of storage facility s at forming facilities and distribution centers ($e \in J \cup D$), d yr (365 d^{-1})

QST_{sq}^{min}	Minimum storage capacity for storage type *s* of capacity level *q*, T
QST_{sq}^{min}	Maximum storage capacity for storage type *s* of capacity level *q*, T
ST_{es}^{min}	Lower limit on the amount of product stored in technology *s* at site *e*, T
ST_{es}^{max}	Upper limit on the amount of product stored in technology *s* at site *e*, T
αn_{nq}	Area required for forming technology *n* of capacity level *q*, m^2
αs_{sq}	Area required for storage facility of type *s* of capacity level *q*, m^2
A_e^T	Total area available at site *e*, m^2
QT_t^{min}	Minimum flow rate by transportation mode *t*, T yr^{-1}
QT_t^{max}	Maximum flow rate by transportation mode *t*, T yr^{-1}
LC_e	Investment cost (e.g. cost of land) for establishing forming or storage facilities at a given location ($e \in G \cup U$) , $
FFC_{gnq}	Investment cost of technology *n* of capacity level *q* at forming facility *g*, $ yr^{-1}
FSC_{esq}	Investment cost for technology *s* of capacity level *q* at any of the forming facilities and distribution centers ($e \in G \cup U$), $ yr^{-1}
FCF_{jn}	Fixed production cost for forming technology *n* at forming facility *j*, $ yr^{-1}
FCS_{es}	Fixed storage cost for storage technology *s* at any of the forming facilities and distribution centers ($e \in J \cup D$), $ yr^{-1}
OFC_{jn}	Variable production cost for forming technology *n* at forming facility *j*, $ T^{-1}
OSC_{es}	Variable storage cost for storage technology *s* at any of the forming facilities and distribution centers ($e \in J \cup D$), $ T^{-1}
$FIT_{ee't}$	Fixed cost of establishing transportation link *t* between nodes *e* and *e'*, $ yr^{-1}
$FTC_{ee'pt}$	Fixed cost of transporting product form *p* between nodes *e* and *e'* using mode *t*, $ T^{-1}
$VTC_{ee'pt}$	Variable cost of transporting product form *p* between nodes *e* and *e'* using mode *t*, $ T^{-1} km^{-1}
$D_{ee'}$	Distance between nodes *e* and *e'*, km
D_c^T	Total demand of customer *c* for sulfur, T

Continuous variables

A	Annual cash flow ($/yr)
ATB_o	Atmospheric topped bitumen fraction sent to vacuum distillation unit and/or LC-finers (tonne/h)
$ATBF_o$	Atmospheric topped bitumen transferred from the DRU to the fluid cokers (tonne/h)
BIT_m	Amount of bitumen produced from mining production route *m* (tonne/h)
BIT_s	Amount of bitumen produced from SAGD production route *s* (tonne/h)
BMF_m	Bitumen froth in primary extraction (tonne froth/h)
BF_o	Amount of bottoms from LC-fining sent to fluid cokers in combined thermocracking and hydrocracking upgrading route (tonne/h)
C_i	Amount of CO2 captured from power and hydrogen plants (tonne CO_2/h)
CB	Flow rate of commercial bitumen (tonne/h)
$CCPD$	Total power requirement for carbon capture and transportation (kWh)
$CCSC$	Total net present value of carbon capture and sequestration cost ($)
CO_2e_i	CO_2 emission of energy producer *i* (tonne CO_2/h)
CO_2T	Total CO_2 emission of energy producers (tonne CO_2/h)
$CSCP_p$	Total CO_2 captured from power technology *p* (tonne CO_2/h)
$CSCH_h$	Total CO_2 captured from power technology *h* (tonne CO_2/h)
DBC_m	Amount of diluted bitumen transferred to the centrifugation stages (m^3/h)
EFC	Total net present value of extraction fuel (NG + Diesel) cost ($)
FH_h	Amount of fuel consumed by hydrogen plant *h* (fuel/h, e.g. Nm^3 of NG/h)
FP_p	Amount of fuel consumed by power plant *p* (unit fuel/h, e.g. Nm^3 of NG/h)
GW	Hot water produced by a geothermal plant (tonne/h)
HC	Total net present value of hydrogen production cost ($)

HGO_o	Heavy gas oil flow rate (tonne/h)
HH_h	Hydrogen produced by plant *h* (tonne H_2/h)
HHE	Hydrogen produced by electrolyzers (tonne H_2/h)
HRGEO	Heat rate provided by a geothermal plant (MJ/h)
HW_b	Total amount of hot water produced by boiler type b (tonne/h)
HWGC	Total net present value of geothermal hot water production cost ($)
LGO_o	Light gas oil flow rate (tonne/h)
MEDD	Total diesel demand for mining extraction (L/h)
MEPD	Total power demand for mining extraction (kWh)
MEPSD	Total process steam demand for mining extraction (tonne/h)
MEWD	Total hot water demand for mining extraction (tonne/h)
MO_m	Oil sands mining rate (tonne oil sands/h)
N_o	Naphtha flow rate (tonne/h)
NPV	Total net present value of energy production cost for oil sands operations ($)
PC	Total net present value of power cost ($)
PH_h	Power co-produced or consumed by hydrogen (kWh)
PP_p	Electricity produced by power plant *p* (kWh)
PS_b	Total process steam produced by boiler *b* (tonne/h)
PWT	Total power production by wind turbines (kWh)
SC_m	Process steam consumption for conditioning stage (tonne steam/tonne oil sand)
SEPD	Total power demand for SAGD extraction operations (kWh)
SESD	Total SAGD steam demand (tonne/h)
SF	Process steam required for mining bitumen extraction (tonne steam/tonne froth)
SL_m	Oil sands slurry rate (tonne/h)
SMRPD	Total power requirement of SMR plants (kWh)
SS_b	Total SAGD steam produced by boiler *b* (tonne/h)
SC	Total net present value of steam production cost ($)
TPE_m	Tailings production from primary extraction stage (tonne/h)
TSE_m	Tailings production from secondary extraction stage (tonne/h)
UHD	Total hydrogen demand for hydrocracking and hydrotreatment stages in upgrading operations (tonne H_2/h)
UFD	Total fuel demand (natural gas) for upgrading operations (GJ/h)
UPD	Total power requirement for upgrading operations (kWh)
UPSD	Total process steam requirement for upgrading operations (tonne/h)
VTB_o	Vacuum topped bitumen feed to LC-finers or delayed cokers (tonne/h)
XB_b	Amount of fuel consumed by steam boiler *b* (unit fuel/h, e.g. Nm^3 of NG/h)

BC_t^{total}	Total production cost from boilers during time period *t* (CAD)
BP_{bnt}	Production rate from boiler unit *n* of technology *b* during period *t* (t h^{-1})
$BP_{bnb'n't}^{GtoP}$	Flow rate of water between unit *n* of boiler *b* and unit *n'* of preheat option *b'* (t h^{-1})
COC_t^{total}	Total cost of production from combined heat and power technology *c* during time period t (CAD)
$Creditbuy_t$	Carbon credits purchased from global carbon markets or carbon exchanges to offset the emissions of industries that are not capable of meeting their emission reduction requirements (tCO_2 h^{-1})
$Creditsell_t$	Carbon credits sold by industries that are capable of achieving emission below the imposed cap and have a surplus of carbon credits (tCO_2 h^{-1})
DEC_{et}	Total requirement of energy commodity *e* during time period *t* (Units of *e*/units of time)
$ECO2_{int}^{new}$	Total CO_2 emissions from all newly installed energy producing units during time period t (tCO_2 h^{-1})
$ECO2_{int}^{exist}$	Total CO_2 emissions from all existing energy producing units during time period t (tCO_2 h^{-1})

EC_{rent}^{PCK}	Amount of energy commodity *e* produced from syngas processing option *r* (units of *e* h^{-1})
EC_{inet}^{new}	Amount of energy commodity *e* produced from energy production technology *i* (units of *e* h^{-1})
EPU_{uent}^{NU}	Amount of energy commodity *e* produced from nuclear production technology *u* (units of *e* h^{-1})
FCB_{bnt}	Fuel consumption rate of unit *n* of technology *b* during time period *t* (GJ h^{-1})
FCC_{cnt}^{Tot}	Total fuel consumption by cogeneration technology *c* during time period *t* (GJ h^{-1})
FCC_{cnt}^{GT}	Fuel consumption by gas turbines in combined heat and power technology *c* (GJ h^{-1})
$FCC_{cnt}^{GR-post}$	Fuel consumption for post firing of exhaust gas in HRSG's in combined heat and power technology *c* (GJ h^{-1})
FCG_{knt}	Fuel consumption (coal, petcoke, biomass, etc.) in unit *n* of gasification technology *k* during time period *t* (t h^{-1})
FCH_{hnt}	Fuel consumption rate of unit *n* of technology *h* during time period *t* (GJ h^{-1})
FCH_{hnt}^{heat}	Fuel consumption rate for heat production used by unit *n* of technology *h* during time period *t* (GJ h^{-1})
FCP_{pnt}^{F}	Fuel consumption rate of unit *n* of technology *p* during time period *t* (GJ h^{-1})
$Fuel_{ft}$	Fuel consumption for industrial operations such as transportation, heating, etc. (GJ h^{-1})
$GASC_t^{total}$	Total cost of production of energy from gasification during time period *t* (CAD)
$H2Sell_t$	Hydrogen sold to the market during time period t (tH_2 h^{-1})
HC_t^{total}	Total cost of hydrogen production during time period *t* (CAD)
$HeatU_{unt}^{UPG}$	Direct heat from nuclear energy used for industrial operations (e.g. heat used in thermocracking for upgrading bitumen) (kWh)
$HeatU_{unt}^{H}$	Heat from nuclear energy used for hydrogen production technologies (e.g. steam methane reforming) (kWh)
HHC_{hnt}^{H}	Heat consumption rate of unit *n* of technology *h* during time period *t* (GJ h^{-1})
HP_{hnt}	Hydrogen production rate from unit *n* of technology *h* during period *t* (tH_2 h^{-1})
HPC_{hnt}	Power consumption rate of unit *n* of technology *h* during time period *t* (kWh)
HRU_{unt}^{NU}	Heat production rate of nuclear technology *u* (MWth)
$HRX_{bnt}^{Preheat}$	Preheating rate provided by unit *n* of preheat technology *b'* during period *t* (GJ h^{-1})
NUC_t^{total}	Total cost of production from nuclear energy during time period *t* (CAD)
PC_t^{total}	Total production cost of power during time period *t* (CAD)
PP_{pnt}	Power production rate of unit *n* of technology *p* during time period *t* (kWh)
PP_{pnt}^{GRID}	Power sold to the grid from technology *p* during *t* (kWh)
PP_{pnt}^{DEM}	Power used to satisfy the demand of industrial operations from technology *p* during *t* (kWh)
PP_{pnt}^{H}	Power exported to hydrogen production facilities to satisfy the electricity requirement (e.g. electrolyzers) from technology *p* during *t* (kWh)
PPC_{cnt}^{GT}	Power production from gas turbines in cogeneration technology *c* (kWh)
PPC_{cnt}^{ST}	Power production from steam turbines in cogeneration technology *c* (kWh)
PPU_{unt}^{DEM}	Power produced from nuclear energy used to satisfy the electricity demand of industrial operations (kWh)
PPU_{unt}^{GRID}	Power produced from nuclear energy that is sold to the grid (kWh)
PPU_{unt}^{H}	Power produced from nuclear energy used to satisfy the electricity requirements of hydrogen production technologies (e.g. electrolyzers) (kWh)
PPU_{unt}^{NU}	Total power production from unit *n* of nuclear technology *u* in time period *t* (kWh)
$PurGrid_t$	Total power purchased from the local grid during time period *t* (kWh)
QP_{qft}^{T}	Production level of product q through production route f during time period t (Units of q/units of time)
$QPCE_{qft}$	Capacity of production of product q through route f added during time period t (units of q/units of time)
$SellGrid_t$	Total power sold to the local grid during time period *t* (kWh)
SP_{cnt}^{GR}	Steam produced from the heat recovery of exhaust gases from gas turbines of cogeneration facility *c* (t h^{-1})
SPC_{cnt}^{G-S}	Steam produced from the heat recovery of exhaust gases from gas turbines of cogeneration facility *c* that is sent to steam turbines (t h^{-1})

SPC_{cnt}^{HPB}	High pressure steam generated to be used in steam turbines of cogeneration facility *c* (t h^{-1})
SPC_{cnt}^{EXT2}	Steam extracted from steam turbines at a medium pressure level (t h^{-1})
SPC_{cnt}^{EXT3}	Steam extracted from steam turbines at a low pressure level (t h^{-1})
SPD_{cnt}^{HP}	High pressure steam produced from cogeneration technology *c* that is sent to satisfy the high pressure steam requirements of industrial operations (t h^{-1})
SYN_{knt}^{KT}	Syngas produced from gasification technology *k* (t syngas h^{-1})
SYN_{rnt}^{RT}	Syngas used by processing option *r* (t syngas h^{-1})
$SYN_{knrn't}$	Flow rate of syngas between unit *n* of gasification technology *k* and unit *n'* of syngas processing option *r* (t syngas h^{-1})
SYN_{knt}^{exp}	Syngas exported to other energy production facilities (e.g. boilers) (t h^{-1})
$SynS_{bnt}^{G}$	Syngas from gasification facilities consumed by utility boiler b (t h^{-1})

$C_{capex}{}_{pn}^{FF_{exist}}$	Capital cost of existing fossil fuel energy production unit n of technology p (CAD)
$C_{capex}{}_{pn}^{FF_{new}}$	Capital cost of new fossil fuel energy production unit n of technology p (CAD)
$C_{capex}{}_{pn}^{Nuclear}$	Capital cost of nuclear energy production unit n of technology p (CAD)
$C_{capex}{}_{pn}^{Solar\&Wind}$	Capital cost of renewable (i.e. solar and wind) energy production unit n of technology p (CAD)
$C_{capex}{}_{denn'}^{Transport}$	Capital cost of energy transportation technology *d* transporting energy commodity *e* between energy production units *n* and *n'* (CAD)
$C_{fuel}{}_{pnt}^{FF_{exist}}$	Cost of fuel utilized in existing fossil fuel production unit *n* of technology *p* during time period *t* (CAD)
$C_{fuel}{}_{pnt}^{FF_{new}}$	Cost of fuel utilized in new fossil fuel production unit *n* of technology *p* during time period *t* (CAD)
$C_{fuel}{}_{it}^{FF}$	Cost of fuel utilized in fossil fuel production unit *i* of the grid during time period *t* (CAD)
$C_{opex}{}_{pnt}^{FF_{exist}}$	Operating cost of existing fossil fuel energy production unit *n* of technology *p* during time period *t* (CAD)
$C_{opex}{}_{pnt}^{FF_{new}}$	Operating cost of new fossil fuel energy production unit *n* of technology *p* during time period *t* (CAD)
$C_{opex}{}_{pnt}^{Nuclear}$	Operating cost of nuclear energy production unit *n* of technology *p* during time period *t* (CAD)
$C_{opex}{}_{pnt}^{Solar\&Wind}$	Operating cost of renewable energy production unit *n* of technology *p* during time period *t* (CAD)
$C_{opex}{}_{denn't}^{Transport}$	Operating cost of energy transport of mode *d* of energy commodity *e* between units *n* and *n'* during time period *t* (CAD)
$C_{opex}{}_{it}$	Operating cost of power generating unit *i* belong to the Alberta grid during time period *t* (CAD)
$C\_system_{et}^{Import}$	Cost of importing energy commodity *e* during time period *t* into the energy system of the oil sands industry (CAD)
$C\_system_{et}^{Export}$	Revenue earned from selling energy commodity *e* during time period *t* (CAD)
$C_{startup}{}_{it}$	Cost of starting power generating unit *i* during time period *t* (CAD)
$C_{unserved\_demand}{}_{kt}$	Cost of unserved demand of regional bus *k* during time period *t* (CAD)
$C\_grid_{e=power,t}^{Import}$	Cost of power sent to the grid during time period *t* (CAD)
$C\_grid_{e=power,t}^{Export}$	Cost of power sold by the grid during time period *t* (CAD)
$CH1_{ct}$	Hydrogen produced by electrolyzer *c* during time period *t* in electrolyzer farm 1 (kg H_2)
$CH2_{ct}$	Hydrogen produced by electrolyzer *c* during time period *t* in electrolyzer farm 2 (kg H_2)
$ECO2_{pnt}^{FF_{exist}}$	Total emissions generated by existing fossil fuel generation unit *n* of technology *p* during time period *t* (tCO_2)
$ECO2_{pnt}^{FF_{new}}$	Total emissions generated by new fossil fuel generation unit *n* of technology *p*

	during time period *t* (tCO_2)
$ECO2_{denn't}^{Transport}$	Total emissions generated from energy transport of mode *d* of energy commodity *e* between units *n* and *n'* during time period *t* (tCO_2)
$ECO2_{it}^{operation}$	Total emissions generated from power generating unit *i* belong to the Alberta grid during time period *t* (tCO_2)
$ECO2_{it}^{startup}$	Total emissions generated from the startup of power generating unit *i* belong to the Alberta grid during time period *t* (tCO_2)
EC_{gt}	Power generated from combined heat and power unit *g* during time period *t* (MWh)
$EH\_to\_upgrader_t^{wind}$	Electrolytic hydrogen generated from wind power sent to bitumen upgraders in Alberta Industrial Heartland during time period *t* (kg H_2)
EPU_{uet}^{NU}	Production level of energy commodity *e* from nuclear unit *u* during time period *t* (units of e)
$Grid\_to\_OS_t$	Power sent to oil sands operators from the grid during time period *t* (MWh)
$Fuel\_T_{gt}$	Total amount of natural gas consumed by the turbines of CHP unit *g* during period *t* (GJ)
$Fuel\_G_{gt}$	Total amount of natural gas consumed by the heat recovery steam generators of CHP unit *g* during period *t* (GJ)
$Fuel\_cogen_{gt}^{total}$	Total amount of natural gas consumed by CHP unit *g* during period *t* (GJ)
$Fuel\_NGCC_{ft}$	Total amount of natural gas consumed by NGCC unit *f* during period *t* (GJ)
$Heat\_cogen_{gt}$	Total amount of heat produced by CHP unit *g* during time period *t* (GJ)
$H\_to\_NGCC_t$	Total amount of electrolytic hydrogen used in hydrogen enriched natural gas burned in NGCC units during time period *t* (GJ)
$H\_electrolyzer_t^{wind}$	Total amount of electrolytic hydrogen produced from wind power during time period *t* (kg H_2)
$H\_electrolyzer_t^{NU}$	Total amount of electrolytic hydrogen produced from nuclear power during time period *t* (kg H_2)
H_input_t	Total amount of excess electrolytic hydrogen sent to hydrogen storage tanks during time period *t* (kg H_2)
$H\_storage_t$	Hydrogen in inventory in storage tanks during time period *t* (kg H_2)
H_output_t	Hydrogen retrieved from storage during time period *t* (kg H_2)
HRP_{ut}^{NU}	Heat generated from nuclear energy from technology *u* during time period *t* (MW_{th})
NG_NGCC_t	Total amount of natural gas consumed in NGCC units during time period *t* (GJ)
$P\_EC_{gt}^{grid}$	Power sent to the grid from natural gas cogeneration unit g during time period *t* (MWh)
$P\_EC_{gt}^{demand}$	Power from natural gas cogeneration unit g used to satisfy the power requirements of the oil sands industry during time period *t* (MWh)
$Power\_NGCC_{ft}$	Total power production from natural gas generators (NGCC) unit *f* during time period *t* (MWh)
$P\_NU_{ut}^{electrolyzers}$	Total amount of nuclear power from technology *u* sent to electrolyzers during time period *t* (MWh)
pp_{it}	Total power generated from existing unit *i* in the Alberta grid during time period *t* (MWh)
$P_{unserved\,kt}$	Total amount of unserved power demand for regional bus *k* of the grid during period *t* (MWh)
$P_{excess\,kt}$	Total amount of excess power generated from regional bus *k* of the grid during period *t* (MWh)
$P\_NU_{ut}^{grid}$	Power sent to the grid from nuclear generation technology *u* during period *t* (MWh)
$P\_NU_{ut}^{demand}$	Power sent to oil sands operators from nuclear generation technology *u* during period *t* (MWh)
$SH\_to\_upgrader_t$	Hydrogen retrieved from storage and sent to bitumen upgraders (kg H_2)
δ_{kt}	
sr_{it}	Spinning reserve from generation unit *i* during period *t* (MWh)
TEC^{SYSTEM}	Total emissions of the energy system (tCO_2)
TEC^{Grid}	Total emissions of the grid (tCO_2)
TC^{SYSTEM}	Total cost of the energy system (CAD)

TC^{Grid}	Total operating cost of the grid (CAD)
$Wind\_P_t^{electrolyzers}$	Wind power sent to electrolyzers during period *t* (MWh)
$Wind\_P_t^{grid}$	Wind power sent to the grid during period *t* (MWh)
$z_1(x)$	Total cost of the energy system (CAD)
$z_2(x)$	Total operating cost of the grid (CAD)
$z_3(x)$	Total emissions generated from the energy infrastructure of oil sands operators and the Alberta grid (tCO_2)

RS_{ri}	Production rate of raw material *r* by producer *i*, T yr^{-1}
F_{jfn}	Production rate of product form *f* by forming technology *n* at forming facility *j*, T yr^{-1}
B_{jb}	Amount of sulfur sent to blocking facility *b* at facility *j*, T yr^{-1}
$Q_{ee'pt}$	Flow rate of product form *p* between nodes *e* and *e'* by transportation mode *t*, T yr^{-1}
ST_{es}	Inventory level for storage facility *s* at any of the forming facilities and distribution centers ($e \in J \cup D$), T

Binary variables

$EGEO_e$	=1 if existing geothermal plant number *e* is operating in the investigated year; 0 otherwise
ENB_{be}	=1 if existing boiler number *e* of type *b* is operating in the investigated year; 0 otherwise
ENH_{he}	=1 if existing hydrogen plant number *e* of type *h* is operating in the investigated year; 0 otherwise
$ENHE_e$	=1 if existing electrolyzer is operating in the investigated year; 0 otherwise
ENP_{pe}	=1 if existing power plant number *e* of type *p* is operating in the investigated year; 0 otherwise
EWT_e	=1 if existing wind turbine number *e* is operating in the investigated year; 0 otherwise
$IMBIT_m$	=1 if integrated mining upgrading route is selected; 0 otherwise
$ISBIT_s$	=1 if integrated SAGD upgrading route is selected; 0 otherwise

$bp_{bnb'n't}$	Indicates if that path between unit *n'* of preheating option *b'* and unit *n* of boiler type *b* exists (1), otherwise (0)
$kr_{knrn't}$	Indicates if that path between unit *n* of gasification option *k* and unit *n* of syngas processing option *r* exists (1), otherwise (0)
nb_{bnt}	Indicates if boiler production unit *n* of technology type *b* is constructed during time period *t* (1), otherwise (0)
$nc_{cnt}^{GT/ST}$	Indicates if gas or steam turbines in industurial cogeneration *c* facility *n* are constructed in time period *t* (1), otherwise (0)
nh_{hnt}	Indicates if hydrogen production unit *n* of technology type *h* is constructed during time period *t* (1), otherwise (0)
nk_{knt}	Indicates if gasification production unit *n* of technology type *k* is constructed during time period *t* (1), otherwise (0)
np_{pnt}	Indicates if power production unit *n* of technology type *p* is constructed during time period *t* (1), otherwise (0)
nr_{rnt}	Indicates if syngas processing option unit *n* of type *k* is constructed during time period *t* (1), otherwise (0)
nu_{unt}	Indicates if nuclear production unit *n* of technology *u* is constructed during time period *t* (1), otherwise (0)
yb_{bnt}	Indicates if boiler production unit *n* of technology *b* is operational during time period *t* (1),

	otherwise (0)
$yc_{cnt}^{GT/ST}$	Indicates if gas or steam turbines production unit *n* of cogeneration technology *c* are operational during time period *t* (1), otherwise (0)
yh_{hnt}	Indicates if hydrogen production unit *n* of technology *h* is operational during time period *t* (1), otherwise (0)
yk_{knt}	Indicates if gasification production unit *n* of technology *k* is operational during time period *t* (1), otherwise (0)
yp_{pnt}	Indicates if power production unit *n* of technology *p* is operational during time period *t* (1), otherwise (0)
yr_{rnt}	Indicates if syngas processing unit *n* of technology *r* is operational during time period *t* (1), otherwise (0)
yu_{unt}	Indicates if nuclear production unit *n* of technology *u* is operational during time period *t* (1), otherwise (0)
ze_{qjt}	Indicates if production capacity $QPCE_{qft}$ is added during time period t (1), otherwise (0)

uco_{gt}	Commitment of cogeneration unit *g* during period *t*
u_gu_{it}	Commitment of grid unit *i* during period *t*
u_ngcc_{ft}	Commitment of NGCC unit *f* during period *t*
Y_Hpipe_{d}	Investment in pipeline capacity *d*
$YNCO_{g}$	Investment in cogeneration unit *g*
$YNGCC_{f}$	Investment in NGCC unit *f*
yco_{gt}	Shutdown of cogeneration unit *g* during period *t*
y_gu_{it}	Shutdown of grid unit *i* during period *t*
y_ngcc_{ft}	Shutdown of NGCC unit *f* during period *t*
zco_{gt}	Startup of cogeneration unit *g* during period *t*
z_gu_{it}	Startup of grid unit *i* during period *t*
z_ngcc_{ft}	Startup of NGCC unit *f* during period *t*

X_{jn}	1 if forming technology *n* is selected at forming facility *j*, 0 otherwise
Z_{es}	1 if storage technology *s* is selected at any of the forming facilities or distribution centers ($e \in J \cup D$), 0 otherwise
V_e	1 if new forming or storage facilities are established at the given locations ($e \in G \cup U$), 0 otherwise
$Y_{ee't}$	1 if transportation link *t* exists between nodes *e* and *e'*, 0 otherwise

Integer variables

NB_b	Number of newly installed boilers of type *b*
NGEO	Number of newly installed geothermal plant
NH_h	Number of new installed hydrogen plant *h*
NHE	Number of new electrolyzers
NP_p	Number of newly installed power plant *p*
NWT	Number of newly installed wind turbines

$N\_electrolyzer_{c}^{farm1}$	Number of electrolyzer of capacity level *c* installed in electrolyzer farm 1
$N\_electrolyzer_{c}^{farm2}$	Number of electrolyzer of capacity level *c* installed in electrolyzer farm 2
NHT	Number of hydrogen storage tanks
NNU_u	Number of units of nuclear technology *u*
NWT	Number of wind turbines

NF_{gnq}	Number of units of technology n and capacity level q installed at forming facility g
NS_{esq}	Number of storage units of technology s and capacity level q installed at forming facilities and distribution centers ($e \in G \cup U$)

List of Abbreviations

ATB	Atmospheric Topped Bitumen
BCL	Battelle Columbus Laboratory biomass gasifiers
CCS	Carbon Capture and Sequestration
DC	Delayed Coker
DRU	Diluent Recovery Unit
EGS	Enhance Geothermal System
FC	Fluid Coker
GHG	Greenhouse gas emissions
GTI	Gas Technology Institute biomass gasifiers
HGO	Heavy Gas Oil
HT	Hydrotreatment
IGCC	Integrated Gasification Combined Cycle
LCF	LC-Fining
LGO	Light Gas Oil
MP1	Mined bitumen + Conditioning upgraded by LCF + FC + HT
MP2	Mined bitumen upgraded by LCF + FC + HT
MP3	Mined bitumen upgraded by DC + HT
MP4	Mined bitumen upgraded by LCF + HT
NGCC	Natural Gas Combined Cycle
NPV	Net Present Value
SAGD	Steam Assisted Gravity Drainage
SCO	Synthetic Crude Oil
SCPC	Supercritical Pulverized Coal
SOR	Steam-to-oil ratio
SP1	SAGD bitumen upgraded by LCF + FC + HT
SP2	SAGD bitumen upgraded by DC + HT
SP3	SAGD bitumen upgraded by LCF + HT
VDU	Vacuum Distillation Unit

Chapter 1

Introduction

1.1 Motivation

The majority of oil reserves in Canada are located in the Western Canada Sedimentary Basin, of which the oil sands in Alberta comprise the majority of reserves. The majority of Canadian oil sands are located in Alberta in three major deposits, which are Peace River, Cold Lake and Athabasca. The largest and most heavily developed among them is the Athabasca oil sands deposit, which includes deposits that can be surface mined and extensive in situ reserves. The Canadian Oil Sands is the third largest crude oil proven reserves in the world, which amount to proven reserves of about 168 billion barrels constituting approximately 97% of Canada's total oil reserves [1]. The oil sands are a mixture of bitumen, sand, clay and water. Bitumen is heavy viscous crude that requires significant amounts of energy for production, upgrading and transportation.

Oil still remains the major energy source and it is involved in a wide variety of applications. Even though, it is expected in the future that its use will mainly shift towards the transportation and petrochemicals sector, it will still dominate the energy market and be the premier energy resource for many years to come as its production is economically attractive compared to other energy alternatives, e.g. wind and solar energy, biofuels, etc. The reliance on unconventional oil resources is expected to significantly increase in the future as conventional resources are becoming scarce accompanied with demands and prices elevation [2]. According to the International Energy Agency (IEA) the growth of production of Canadian oil sands will continue over

the next decades, which will significantly contribute to the world's energy supply and security [3].

Currently available production capacity is 2.8 million barrels per day (MBPD) and additional projects will add a capacity of 0.9 MBPD by 2020. If proposed and announced projects are completed, it is expected that oil sands production will increase by more than two-folds from the current level reaching approximately 4.5 MBPD by 2035 [3]. The availability of energy commodities (i.e. power, hydrogen, steam, etc.), and management of the environmental impacts of production while maintaining economic feasibility are crucial factors to the further development of the oil sands industry. Alberta provincial government and Canadian Federal government are required to address various environmental issues that hinder the large-scale development of this resource, which include:

- *Greenhouse Gas (GHG) Emissions*: Operations of oil sands require significant amounts of energy derived from burning natural gas, making the industry the largest contributor to growth of GHG emissions in Canada, and an increase in production offsets achieved reductions in GHG emissions.
- *Sulfur By-product*: Imposes a physical problem due to its stockpiling in limited inventory.

According to a report from the Organization for Economic Co-operation and Development (OECD), for Canada to meet its climate change goals it will have to make significant reductions to emissions generated from oil sands operations. Moreover, the projected increase in oil production will add serious risks to the achievement of Canada's climate mitigation goals. Even though emissions have decreased in most Canadian

provinces, they increased by 18 per cent in Alberta since 2005, which is mostly attributed to the development in oil sands projects and results in the province accounting to over 40 per cent of Canada's emissions. In addition, Canada's environmental tax regime is considerably low in comparison to other OECD countries, which discourages industries including oil sands operators to further reduce their emissions. Consequently, the implementation of the Pan-Canadian Framework for Clean Growth and Climate Change is considered to be imperative for achieving Canada's emission reduction targets. This requires adequate approaches for pricing carbon pollution, and the incorporation of technologies and emission reduction measures that ensure competitiveness of Canadian industries in the global low-carbon economy. Moreover, an ensemble of proven energy production technologies is available to be utilized to contribute in the reduction of GHG emissions generated from the energy infrastructure of oil sands operations. These include nuclear, renewable (i.e. wind, geothermal, biomass, etc.), fossil based (i.e. coal, natural gas, petroleum coke, etc.) integrated with carbon capture and sequestration. Exploiting untapped non-emitting renewable and nuclear energy sources provide significant potential in achieving the required emission reduction targets while satisfying the rising energy requirements of Canada's industrial, transportation and household sectors.

Efficient and robust mathematical models that describe the operations of the Canadian oil sands industry are useful tools that can be used to assess current and future production scenarios, and their associated environmental impacts. These models are useful in order to determine the energy infrastructure required to meet the oil production demands projected over the upcoming years, which will be of great assistance as a decision making tool in planning future operations of the industry. Variability and uncertainties in key

process operational parameters, such as natural gas prices, GHG emission targets, etc., can be evaluated easily using these modeling tools.

Several mathematical models that address various operational aspects of the oil sands industry have been reported in the literature [4-7]. The main focus of these models was the estimation of the energy requirements of the oil sands operations and the quantification of the GHG emissions associated with these energy requirements. Furthermore, the models focused on the optimization of the energy infrastructure required to power the oil sands industry. These models provided promising results that give insight of the future operational scenarios of the oil sands industry. However, there are various limitations associated with these mathematical models that if addressed can provide a more realistic representation of future oil sands operations. The previous models considered only conventional technologies (i.e. fossil fuel based) in the proposed energy infrastructure disabling the model from reaching high emission reduction targets. Nuclear technologies can provide promising potential in terms of reducing GHG emissions. However, investing in them is judged critically since there are significant external costs associated with them for the national economy due to security reasons and very long construction times. Finally, all the previously formulated models were aimed at optimizing instances of oil sands operations eliminating the effects of time variable parameters.

1.2 Research Objectives and Contributions

Achieving emission reductions from the energy infrastructure of the oil sands industry requires investment in low carbon intensive energy production technologies. The existing energy infrastructure is considered to be economically long-lived, which complicates

incorporating investment decisions of new technologies in its planning. Increasing the favorability of these investments requires the design and implementation of effective carbon mitigation measures that result in the achievement of the highest possible emission reductions at the lowest possible costs. Similarly, encouraging the effective management of excess by-products generated from oil sands operations (e.g. petroleum coke, sulfur, etc.) instead of stockpiling them in limited inventory requires the application of supply chain management techniques. This research focuses on developing optimization mathematical models to assist policy makers in:

1- Determining the optimal energy commodities infrastructure required for oil sands operations considering conventional and non-conventional (i.e. renewables, low carbon footprint) energy sources
2- Designing, planning and operating the sulfur supply chain

To achieve the objectives, mathematical models geared towards minimizing costs and increasing operational efficiency, resource utilization and environmental sustainability will be formulated. This will require obtaining adequate estimates of marginal carbon mitigation costs of all the low-carbon intensive mitigation technologies considered (i.e. nuclear, renewable, fossil based, etc.). Renewable energy production technologies (i.e. wind, geothermal, hydro, bioenergy, etc.) are critical environmentally benign technologies that can play a significant role in achieving significant emission reductions from oil sands operations and any industrial sectors that exchange energy with oil sands operators (e.g. Alberta grid). This will require a thorough evaluation and review of renewable energy potential in Alberta, and outlining all the possible and feasible configurations that can be employed to provide the energy requirements of oil sands

operators. The incorporation of wind power in the energy infrastructure of oil sands requires the utilization of hydrogen as an energy carrier due to the geographical hindrance of transmitting wind power to oil sands operators. Moreover, due to the variable nature of wind power generation, incorporating a large wind generation capacity will require modeling interactions with the local Alberta grid, in which the effect on the unit commitment of power generation units is investigated. The feasibility of incorporating energy storage (i.e. hydrogen storage) to mitigate

One of the objectives of this thesis is to provide a generalized multiperiod optimization model that can be applied for the energy planning of energy-intensive industries. Moreover, a key feature of this work is the application of this generalized model. There has been no multi-period energy planning optimization models applied to the case study based on the energy intensive oil sands operations in Alberta over a long time horizon (i.e., 2015–2050). This facilitates the investigation of the economical and structural impact of time-dependent parameters on the energy production fleet. These parameters include the variability in oil sands production levels, energy demand intensities, carbon mitigation policies, and fuel prices. This will assist governmental or industrial policy makers in making decisions of the energy planning for oil sands operations. The development of the globally valuable oil sands resource is essential for Canada's economic growth, and it is dependent on the ability to comply with environmental regulations while maintaining economic competitiveness of Canadian oil industries. The research provides tools for oil sands industries to increase their development and production through cost-effective strategies that allow reaching higher environmental sustainability.

The final objective of this thesis is to investigate the components that comprise the sulfur supply chain (i.e. recovery, storage, forming and distribution) and implement optimization techniques in mathematical modeling to describe the design and operation of sulfur supply chains and integrate these components within a single framework. It could serve as a useful decision support system in the early stages of developing sulfur supply chains and understanding the trade-offs involved in the sulfur supply chains. The model will be used to estimate the total investments required to establish and operate sulfur forming and storage facilities and distribution networks. It will provide an indication about the optimal configuration of the sulfur supply chain, which will assist governmental or industrial policy makers in making strategic decisions. These decisions include the number, location, type, and capacity of sulfur forming plants and storage facilities, required transportation links among nodes in the network, and production rates of forming technologies and flow rates of sulfur.

1.3 Thesis Structure

The rest of the thesis is organized as follows.

Chapter 2: This chapter outlines the general methodology utilized to achieve the four contributions of this thesis.

Chapter 3: An energy optimization model for the integration of renewable technologies into the energy infrastructure of the oil sands industry is presented. The proposed model determines the optimal configuration of oil producers and the energy infrastructure required to meet their energy demands. The model is geared towards the minimization of cost subject to carbon dioxide emission constraints. A mixed integer non-linear optimization model is developed that simultaneously optimizes capacity expansion and

new investment decisions of conventional and renewable energy technologies. To illustrate its applicability, the proposed model was applied to a case study using data reported in the literature for various years of oil sands operations. A rolling horizon approach was implemented to determine the effect of investment decisions of previous operational years on the selection of new investment options. Results were compared with and without the incorporation of renewable energy technologies. The results obtained indicate that the proposed model is a practical tool that can be employed to evaluate and plan oil sands and energy producers for future scenarios. Moreover, the results show that renewable energy technologies have significant potential in reducing reliance on fossil-fuel based technologies and their associated CO2 emissions. The emission constraints set for the operational year 2025 can only be achieved by the incorporation of renewables in the energy production mix.

Chapter 4: A multi-period optimization model is developed for the energy procurement planning of industries including renewable energy. The model is developed with the objective of identifying the optimal set of energy supply technologies to satisfy a set of demands (e.g. power, heat, hydrogen, etc.) and emission targets at minimum cost. Time dependent parameters are incorporated in the model formulation, including demands, fuel prices, emission targets, carbon tax, lead time, etc. The model is applied to a case study based on the oil sands operations over the planning period 2015 – 2050. Various production alternatives were incorporated, including renewable, nuclear, conventional and gasification of alternative fuels. The results obtained indicated that the energy optimization model is a practical tool that can be utilized for identifying the key parameters that affect the operations of energy-intensive industrial operations, and can further assist in the planning and scheduling of the energy for these industries.

Chapter 5: The energy infrastructure for oil sands operations can be classified as a decentralized energy system, in which energy requirements (i.e. power, heat and hydrogen) are generated near the end-users, and can operate with interactions with the local Alberta grid, in which it feeds surplus power generated to it. In this study a mathematical optimization model is developed for the integrated planning and scheduling of the energy infrastructure of the oil sands industry. The contributions of various energy sources including conventional, renewables, and nuclear are investigated. Power-to-gas for energy storage is incorporated to manage surplus power generated from intermittent renewable energy sources, particularly wind. The wind-electrolysis system included incorporates two hydrogen recovery pathways, which are power-to-gas and power-to-gas-to-power using natural gas generators. The problem is modeled as a multiobjective and multiperiod mixed integer linear programming model that minimizes the system cost (energy production and storage), grid cost, and total greenhouse gas emissions. In addition to including the grid cost and emissions in the objective function, grid-interaction is incorporated in the optimization model through the unit commitment operations of the existing power generation units of the grid. The proposed model is designed to evaluate the optimal operation and sizing of the energy producers and the energy storage system, as well as the interactions between them. The epsilon constraint method is used to solve the multi-objective aspect of the proposed model. To illustrate its applicability, the model is applied to a case study based on the oil sands industry in Alberta for the integrated planning and scheduling of its energy infrastructure for the year 2017.

Chapter 6: Extensive research has been done on the components that constitute the sulfur supply chain, including sulfur recovery, storage, forming and distribution. The research focus was on improving the efficiency and environmental sustainability of each of these areas rather than focusing on the supply chain as a whole. The aim of this work is to design a sulfur supply chain that integrates these components within a single

framework. It represents a starting point in understanding the trade-offs involved in the sulfur supply chain from an optimization point of view. Optimization and mathematical modeling techniques were implemented to generate a decision support system that will provide an indication of the optimal design and configuration of sulfur supply chains. The resulting single-period mixed-integer linear programming (MILP) model was aimed at minimizing total infrastructural and operational costs. The model was illustrated through a case study based on Alberta's Industrial Heartland (AIH). A deterministic approach in an uncertain environment was implemented to investigate the effect of supply and demand variability on the design of the supply chain. This was applied to two scenarios, which are steady state operation and sulfur surplus accumulation. The results for the investigated case study reveal that the optimum sulfur supply chain might consist of medium-to-large sulfur forming facilities serving multiple producers. The model also identified the locations of forming facilities, the forming, storage and transportation technologies, and their capacities.

Chapter 7: This chapter summarizes the conclusions and the contributions of the thesis.

Chapter 2

Methodology

This section outlines the methodology undertaken to develop the optimization models used for determining the energy planning and sulfur supply chain for the Canadian Oil Sands operations. The general methodology comprises the steps shown in Figure 2.1. The first step involves a clear identification of the problem to be addressed. This included defining the proper decision variables and the data and parameters required to solve the problem. Finally, the problem definition encompasses identifying a proper set of alternatives that requires the utilization of a mathematical optimization model to provide an indication of an optimal solution. This set of alternatives is represented in the form of a superstructure. A mathematical model that describes the superstructure is then formulated. The mathematical model constitutes unknown decision variables (i.e. positive, integer, binary, etc.) and data (i.e. scalars, parameters, etc.). The required data is gathered and the mathematical model is programmed in an optimization-software, such as the General Algebraic Modelling Software (GAMS) [8]. The data gathered is dependent on the case studies investigated, which illustrate the applicability of the formulated mathematical model, and includes obtaining values of parameters incorporated in the formulated model. These include, for example, future projections of bitumen and SCO production levels, forecasts of fuel prices, lead time for construction of new plants, etc. The results obtained are then analyzed and sensitivity analyses are conducted when appropriated to provide an indication of the optimal solution.

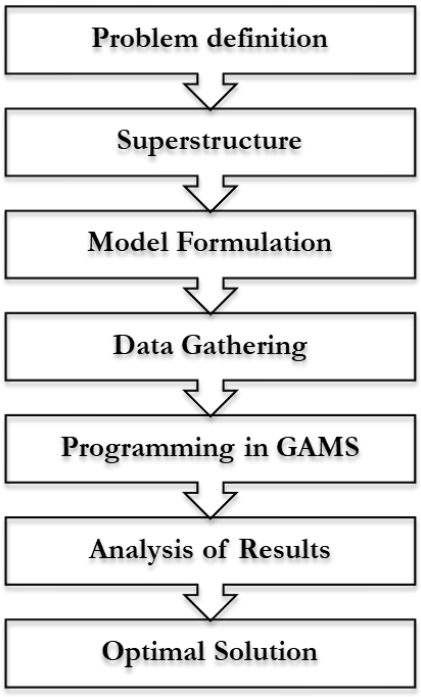

Figure 2.1 General methodology utilized to achieve the contributions of the thesis

In this thesis several single and multi-period mathematical programming models and solution strategies for planning and scheduling under carbon management have been developed. These models offer the appropriate scheme for selecting available reduction strategies while minimizing total investment and operating costs. In the area of energy production planning, a generalized modeling framework has been developed for assessing the feasibility of industrial networks in order to demonstrate environmental and economic benefits of industrial facilities working cooperatively to share energy and materials, including the production of hydrogen to support a future hydrogen economy. Multi-period optimization models and solution strategies that determine the optimal mix of energy supply sources that meet specified energy demands (i.e. heat, electricity, process fuels, etc.) and CO_2 emission targets have been developed. The models

considered the use of different CO_2 control strategies, employed fuel balancing, incorporated alternative energy sources, and advanced energy production technologies. In order to take further steps in integrating renewables, we focused on the transition from a fossil-based economy to incorporating various forms of energy produced from renewable energy. This includes bioenergy, wind-electrolysis for power-to-gas and power-to-gas-to-power, and geothermal energy. These have been incorporated in a robust mathematical programming based framework that incorporates the synergism, conflicts, and interdependence among feedstocks and which accounts for the simultaneous production of energy and fuels. To enable the exchange of power in energy infrastructures that can supply the various forms of energy services to industrial, commercial, and residential consumers, we embarked on the modeling of complex networks of energy hubs and provided financial viable solutions which have the potential to significantly reduce greenhouse gas emissions. We developed also generic mathematical models for the optimal energy management of future communities where hydrogen is used as an energy vector.

For the energy planning model the use of different CO_2 control strategies, which include making enhanced use of alternative energy and/or advanced technologies, and employing CO_2 removal technologies have been incorporated. Also, the model included the scheduling component or energy storage considerations. The model considers renewable energy integration and planning of the whole network including energy storage. Finally, also incorporated in the model was the conversion of electricity into hydrogen during price troughs and the possible use of the stored hydrogen to produce electricity during peak hours, for the hydrogen economy, or for power-to-gas. One common approach that

has been employed for integrated scheduling and planning problems is detailed scheduling whereby a small time step is employed for the entire planning horizon. In this fashion the planning decision variables are replaced by those of scheduling. Though such formulation ensures optimality, it usually leads to large scale models which are computationally expensive. In rolling horizon approaches the time frame is divided into serval subintervals. At every iteration, the early interval is represented in detail while the other intervals are aggregated. After that, the early interval is fixed, and the next interval will be in detail until all intervals are considered. The problems discussed involve making multiscale decisions of system components, interconnections of units, operating conditions, and interactions along supply chains. Furthermore, variabilities can be present at several levels such as prices, production rates and costs, labor, demand, and raw material availability and this will require the investigation of various scenarios. The planning and scheduling decisions will be integrated in order to obtain solutions pertaining the location and capacity of components such as renewable energy resources and energy storage, the charge/discharge of hydrogen tanks, energy resources commitment, and Power-to-X decisions. The overall objective will include installation, operation, reliability, and penalty costs. The installation cost includes the investment and replacement costs of all components. The operation cost includes the operation and maintenance cost of all energy system components, power purchased, and emission pollution credit cost. The reliability cost will be calculated based on energy not supplied by the energy system. Modeling will be based on the superstructures of alternatives developed and which account for alternative energy sources as well as for conventional sources and for pollution prevention technologies.

Chapter 3

Optimized Integration of Renewable Energy Technologies into Alberta's Oil Sands Industry[1]

3.1 Introduction

3.1.1 Alberta's oil sands industry – Current and future challenges

The majority of oil reserves in Canada are located in the Western Canada Sedimentary Basin, of which the oil sands in Alberta comprise the majority of reserves. The majority of Canadian oil sands are located in Alberta in three major deposits, which are Peace River, Cold Lake and Athabasca. The largest and most heavily developed among them is the Athabasca oil sands deposit, which includes deposits that can be surface mined and extensive in situ reserves. The Canadian Oil Sands is the third largest crude oil proven reserves in the world, which amount to proven reserves of about 168 billion barrels constituting approximately 97% of Canada's total oil reserves [9, 10].

The oil sands are a mixture of bitumen, sand, clay and water. Bitumen is a heavy viscous crude that requires significant amounts of energy for production, upgrading and transportation. Extracted bitumen can be diluted by solvents (e.g. naphtha) to reduce its viscosity for further transportation to be sold as commercial crude bitumen or to be upgraded to higher quality synthetic crude oil (SCO). Bitumen upgrading operations can be integrated with mining or steam assisted gravity drainage (SAGD) extraction operations, and they typically consist of hydrocracking or thermocracking processes to break the heavy hydrocarbon molecules into lighter ones. Mining extraction is typically

[1] A variant of this chapter is published: M. Elsholkami, A. Elkamel, F. Vargas, Computers and Chemical Engineering, 2016, 90(1), 1-22.

employed for bitumen deposits located at depths up to 75 meters. The Oil Sands are mined by electric and hydraulic shovels, which are then transported by trucks to separation units in which hot water and solvents are used to extract the bitumen from the Oil Sands mixture. In-situ methods are used for deep bitumen deposits that are located more than 75 meters below the earth's surface, and they have been employed to recover deposits at depths within the range of 350 – 600 meters below the surface. In-situ methods rely on the use of steam, solvents or thermal energy to extract the bitumen from the oil sands in order to enhance its flow, which is then pumped to the surface. The two prominent production technologies are mining and in-situ, the latter being more economically and environmentally preferable and will account to approximately two-thirds of future oil sands production capacity. Mining extraction is currently the dominant method used for bitumen extraction [10, 11, 12].

Continued reliance on crude oil is expected to persist in future years and dominated the world's energy supply. Global oil demand is expected to reach 111 million barrels per day by 2040 [13], and approximately one fourth of this oil will be supplied by Canada and the United States. The continuing decline of conventional crude oil resources is increasing the reliance on unconventional crude oil production (e.g. bitumen).

The significant drop in oil prices that occurred in 2014 has a major negative impact on Canada's economy. By taking into consideration the forecasted oil price profiles, it is estimated that the damage to Alberta's gross domestic product will be around 0.8 parts per thousand in 2015, which would eliminate the chance of falling into a recession with a growth rate maintained at 2.7% [14]. Therefore, it is expected that development of oil sands projects will continue as planned and the production of Canadian unconventional

oil will continue on an increasing trend. The situation is likely to resemble that of the recession in 2008-2009, in which oil production of Alberta continued to rise steadily as oil sands producers adopted the view of long term market conditions [15, 16, 17]. However, there are uncertainties associated with the further development of the oil sands industry as a result of the concerns associated with the availability of energy commodities (e.g. power, steam, etc.). Moreover, environmental issues regarding the greenhouse gas (GHG) emissions associated with the production of the energy commodities required for oil sands operations represent a major concern for Alberta provincial and Canadian federal governments, and their management is essential for sustaining the further development of oil sands operations [18].

The availability of energy commodities (i.e. power, hydrogen, steam, etc.) and managing the environmental impacts of production while maintaining economic feasibility is a crucial factor to the further development of the oil sands industry. Under the United Nations Framework and Kyoto protocol Canada is obligated to reduce GHG emissions to achieve international environmental standards. This in return has focused efforts of research on the development of sustainable energy pathways that impose minimum environmental burdens [19, 20].

Operations of oil sands require significant amounts of energy, which are derived from burning natural gas, making the industry the largest contributor to the growth of GHG emissions in Canada, and an increase in production offsets achieved reductions in their intensity [10]. The natural gas supporting the energy production for the oil sands industry is obtained from the Mackenzie Basin south through the Mackenzie Valley Pipeline, which is currently in regulation processes. It is projected that by 2025 the oil sands

operations will require 1.6-2.3 billion cubic feet of natural gas daily, which is equivalent to the maximum capacity of the Mackenzie pipeline that also provides natural gas used for heating Canadian homes. All of these factors contribute to the requirement of diversifying the energy infrastructure of the oil sands industry [21]. A potential alternative source of energy for the Oil Sands industry is nuclear energy, which was recently considered to provide steam and electricity for bitumen extraction and upgrading operations. Nuclear based technologies have near zero emissions associated with their operations, and the commodities produced can replace natural gas based plants significantly reducing emission intensity. The environmental impacts and public perceptions of the risks associated with employing nuclear technologies present a major resistance to their penetration in the energy infrastructure mix. There are various challenges associated with the introduction of nuclear based technologies in Alberta's energy infrastructure, which include public and government acceptance, environmental concerns associated with radioactive waste storage, water consumption, and very long construction times [22].

Efficient and robust mathematical models that describe the operations of the Canadian oil sands industry are useful tools that can be used to assess current and future production scenarios, and their associated environmental impacts. These models are useful in order to determine the energy infrastructure required to meet the oil production demands projected over the upcoming years, which will be of great assistance as a decision making tool in planning future operations of the industry. Variability and uncertainties in key process operational parameters, such as natural gas prices, GHG emission targets, etc., can be evaluated easily using these modeling tools. Several models have been developed

in previous studies to describe the operations of the oil sands industry. Ordorica et al. modeled the energy demands and GHG emission of the oil sands industry [4]. They formulated a mathematical model referred to as the oil sands operations model in order to estimate the energy requirements associated with SCO and bitumen production. Their formulations were based on production data available from current commercial oil sands operators. The production schemes incorporated in their model include integrated mining and upgrading, integrated in-situ extraction and upgrading, and diluted thermal bitumen production. In addition, they considered three different upgrading routes based on hydrocracking and thermocracking processes. The computation of GHG emissions associated with supplying the energy requirements (i.e. power, hydrogen, steam, hot water, natural gas, and diesel) for oil sands producers is also considered. They later developed a mixed integer linear programming optimization model that determines the optimal infrastructure required to meet the energy demands modeled in their previous work with an objective of minimizing total annual costs of energy supply that is subject to CO_2 emission constraints [5]. In their model, only conventional power and hydrogen plants within the energy infrastructure. They illustrated the applicability of the energy optimization model by investigating a case study of the oil sands operations for the year 2003. Their results included the quantified energy costs and emissions associated with bitumen and SCO production.

Betancourt-Torcat et al. [6] later developed an optimization model that simultaneously determines the optimal energy infrastructure and oil sand production schemes, and referred to it as the integrated oil sands energy optimization model. In comparison to the work done by Ordorica et al. [5] the energy demands are not determined a priori, instead

they are calculated internally in the optimization model since both energy and oil producers are set as decision variables. Their model was also formulated with the objective of minimizing total annual cost subject to CO_2 emission constraints. They applied the model on two case studies for the operational years 2003 and 2020. In a later work they incorporated nuclear energy for power and steam production, and also imposed an additional environmental constraint (i.e. water withdrawal limits from the Athabasca River) [7]. The model was formulated as a mixed integer non-linear programming model and was applied for a case study for the oil sands 2030 operational year. In a later study they investigated the effect of varying key environmental and operational parameters on the oil sands operations. These are CO_2 capture levels, natural gas prices, and steam-to-oil ratios (SOR) [27]. The CO_2 emission targets are expected to become increasingly stringent in order to satisfy emissions policies set by the government of Alberta. Natural gas prices and SOR are the two parameters that have the most significant impact on the total annual costs of producing SCO and commercial bitumen. They later extended their work to develop a stochastic optimization model that accounts for the uncertainty in natural gas prices and SOR [28]. They also offered a comparison of the results of their deterministic and stochastic optimization models.

To the authors' knowledge all of the optimization models developed for the modeling of oil sands operations up to this point do not incorporate capacity expansion decisions, or incorporate renewable energy technologies in the proposed energy infrastructure. This paper introduces a new capacity expansion energy optimization model for the Canadian oil sands industry. It also presents an approach for the integration of renewable energy technologies in the Alberta oil sands energy infrastructure, and illustrates the effect of

incorporating renewable energy production on reducing the reliance of the oil sands industry on fossil fuel resources (i.e. natural gas). A feature of the proposed model is the incorporation of capacity expansion decisions. A rolling horizon approach is implemented, in which the results obtained for a certain planning period are used as input for the following planning step. This allows for determining the effect of the existing energy infrastructure on new investment decisions, and allows for optimizing the capacity expansion decisions of both renewable and conventional energy production technologies. The key aspect in the proposed optimization model is the inclusion of renewable energy technologies as potential resources to provide energy for oil sands producers.

3.1.2 Renewable energy potential in Alberta

Renewable energy production can provide significant potential in reducing GHG emissions in Alberta. An assessment of selected renewable energy technologies that was conducted by the government of Alberta provides insight on the potential of renewable energy production in Alberta. The criteria used to conduct the assessment included applicability to Alberta, level of commercialization, environmental footprint and cost [29].

The potential of integrating renewable energy technologies depends significantly on their applicability to Alberta's physical characteristics. The results obtained indicated that Geothermal, Enhanced Geothermal Systems (EGS), Hydropower and Wind are the most complimentary to Alberta's physical environment. On the other hand, Concentrated Solar Power technologies required minimum direct normal irradiance values that are higher than the average available in Alberta. Solar PV showed strong compatibility with Alberta; however, their potential is only limited to small scale applications (e.g.

residential). Over the past few decades wind and hydropower had high levels of commercialization in various European countries and over Canada. Technologies, such as EGS have low levels of commercialization and their implementation is not considered to be viable in the near future. Geothermal and EGS systems have GHG emissions relatively higher than those of other renewable technologies considered in the conducted evaluation. However, these emissions are negligible in comparison with fossil-fuel based energy production technologies. For example, geothermal plants emissions range from near-zero emissions to 5% of the CO_2, 1% of the SO_2, and less than 1% of the N_2O emitted by coal-fired plants of a similar size [29].

Geothermal

There are two major incentives for utilizing geothermal energy in oil sands operations, which are natural gas cost, and reduction in GHG emission intensity. Most of the energy utilized for heating water for oil sands operations is obtained from natural hydrocarbons or by heat recovery techniques in cogeneration technologies. Significant efforts are being made to implement alternative sources of thermal energy. Low-grade geothermal heat can economically compete with burning natural gas and reduce the overall demand for it [30].

In the Athabasca region of Northern Alberta heat is present at depths within the earth, and to extract thermal energy in such a region requires artificially created porosity (i.e. fractures) and fluids injected into the hot dry rocks. This is referred to as an engineered geothermal system. Northern Alberta is characterized by having low thermal gradient and geothermal energy is unsuitable for electricity production applications. However, it is applicable for direct heating, producing hot water for oil sands operations. Bitumen extraction in oil sands mining operations requires significant volumes of water at

temperatures within the range of 50 – 60^{o}C. Critical environmental concerns are associated with these operations, including significant fresh water consumption and GHG emissions, in addition to concerns associated with the availability of the large volume of natural gas required. Geothermal energy provides the potential of mitigating two of these issues to significant extents [31].

Table 3.1 Characteristics of a geothermal plant producing hot water for oil sands operations

Geothermal system	One injection and two production wells
Temperature increase ΔT	35^{o}C
Water flowrate	100 kg s^{-1}
Project lifetime	30 yr.
Capital cost (i.e. drilling, fracturing, and pumps and surface installations)	$33 million
Operating cost (i.e. pumping, water treatment, transportation, etc.)	$2 million yr^{-1}
Total cost of EGS	$0.013 per kWh thermal

The extraction of bitumen from oil sands requires significant volumes of hot water, which are provided by burning natural gas. Approximately 80% of oil sands reserves are located at great depths and require SAGD extraction methods, which mostly utilize steam in their operations. Geothermal energy has the potential to provide heat for bitumen extraction and upgrading operations, which would significantly reduce GHG emission levels. Geothermal resources are classified according to their subsurface temperatures as high (> 150^{o}C), medium (50 ^{o}C – 150 ^{o}C) and low (< 50^{o}C). Low temperature resources are found within the upper 2 km of the Western Canadian Sedimentary Basin, which are suitable for direct heating applications. Power generation using geothermal technologies requires very high temperatures (>150^{o}C), which to obtained requires drilling at great depths.

Majorowicz et al. conducted a research focused on evaluating potential heat sources that can be implemented for supporting oil sands operations in areas with existing leases. Their study was based on a detailed fracture modeling of the proposed geothermal system, in which they took into account the sensitivity of energy recovery to various well properties (e.g. fracture dimensions), the effect of reservoir temperatures and well spacing and sustained water flow rates and temperatures, and determined the optimal design of the EGS for the proposed location. The main area of interest for geothermal applications in the oil sands industry is located in the Athabasca region. The extraction of heat for power production applications would require the development of EGS. The heat is produced by circulating fluids at depths after creating artificial porosity zones. Temperatures greater than 80^{o}C are typically required for EGS electricity production applications. High temperatures can be found in the deep Alberta basin within sedimentary aquifers and requires drilling to the depth of several kilometers. However, temperatures in Northern Alberta are considerably low to be suitable for electricity production and the main focus is to utilize geothermal resources to provide heat for oil sands operations [31].

Majorowicz et al. conducted an economic analysis of utilizing geothermal energy for heat and power production for oil sands operations in Alberta. For direct heating applications the calculations were done for drilling a well doublet up to 6 km in depth, in which the flow rate of water is sustained for 10 years and production temperature is maintained at 60^{o}C. At a sustained flowrate of 40 – 60 L/s the cost of direct geothermal heating is similar to the cost range of burning natural gas ($3 – 6/GJ at 50% boiler efficiency). The results they obtained were used as input for the techno economic data of geothermal

systems in the optimization model (Table 3.1). It was concluded from their results that direct geothermal heating is economic in comparison with burning natural gas considering expected future increases in natural gas prices and significant incurred carbon mitigation costs associated with the increasingly stringent environmental constraints. The total cost of burning natural gas to provide the same amount of hot water for oil sands operations costs approximately $0.012 per kWh. Considering future increases in natural gas prices and added cost of mitigating the associated GHG emissions, it can be concluded that geothermal energy production has an economic advantage [32]. The utilization of geothermal heat for the production of electricity requires the use of an Organic Rankine Cycle, which is characterized with efficiency levels in the range of 8 – 12%. For a system of one injection and two producing wells at a rate of 50 L/s and temperatures in the range of 50 – 150 ^{o}C will require a cost of approximately $22 million per MW. Great drilling depths will be required as the temperature gain with depth in crystalline rocks of the Athabasca region is considerably low. As a result electricity production from EGS for oil sands operations is considered uneconomic [32, 33].

Wind power-to-hydrogen via electrolysis

The oil sands industry in Alberta is highly dependent on hydrogen for the upgrading of bitumen, for which the demand is expected to reach approximately 3.1 million tonnes per year by 2023. This translates to a significant projected increase in hydrogen requirement since hydrogen production for Canada as a whole was approximately 2 million tonnes per year in 2004. This in return will require an increased reliance on renewable alternatives in order to maintain or achieve higher GHG emission reduction levels. Hydrogen used for

oil sands upgrading processes is mostly produced using steam methane reforming, which contributes significantly to increase in GHG emissions associated with oil sands operations. The production of hydrogen from wind energy can contribute to considerably reduce GHG emissions associated with bitumen upgrading operations [34].

Hydrogen production from renewable energy sources is considered the long-term goal for the hydrogen economy. Hydrogen production from wind energy via electrolysis has received global recognition as a potentially viable hydrogen production pathway among renewable resources. It is also considered to be one of the hydrogen production pathways that imposes the least environmental impact based on life cycle assessment analysis studies. The production of hydrogen from wind energy has received little attention in Canada, and its employment is typically in conjunction with other renewable energy sources or a part of an energy mix. Other than utilization in the automobile industry, the production of hydrogen from renewable sources for other industrial sectors in Canada is rarely investigated [35].

Alberta's installed wind capacity is currently determined to be 1,434 MW, which accounts to approximately 9% of total electricity generation capacity, and is expected to increase by 58% by 2024. There has been a considerable increase in installed wind capacity over the base decade by seven-fold, and considering the required abatement of GHG emissions the installed capacity of wind power is expected to further increase. Therefore, increasing utilization of wind power is an attractive solution to decrease reliance on fossil-fuel based technologies for both power and hydrogen production, which will allow significant reductions in GHG emissions [34, 35].

Electrolysis of water is mature technology that generates hydrogen with very high purity (>99.9%), which is highly desirable for bitumen upgrading operations to produce synthetic crude oil. The wind hydrogen plant incorporated in the proposed energy model is based on the expansion of an existing wind farm (i.e. Summerview wind farm) in Pincher Creek, Alberta. Currently the wind farm has an installed capacity of 134 MW. In 2010 the Summerview wind farm has undergone a capacity expansion where they approximately doubled their power production capacity, which was established in the Summerview 2 wind farm located adjacent to Summerview 1. This provides plausibility for the further expansion of the wind farms to accommodate for the production of hydrogen given the entailed environmental benefits. A proposed expansion project of a wind hydrogen plant in such a location will reduce the cost of hydrogen production due to the eliminated costs of land purchase, grid connections, infrastructure, etc. This can facilitate a cost effective approach for hydrogen production.

Southern Alberta is the primary area with significant wind resources in the province, in which all wind farms of Alberta are currently allocated. The transmission infrastructure in this region requires significant improvements to transport wind power to large load centers. Therefore, the wind hydrogen plant will incorporate electrolyzers to be installed in conjunction with wind turbines at Pincher Creek, and the produced hydrogen is then transported to bitumen upgraders in Fort McMurray [35].

Due to the variability of wind power resources, it is necessary to quantify the available wind energy potential by accounting for the average hourly wind speed variation in Pincher Creek (Fig. 1) [36]. A Vestas V-90 1.8 MW wind turbine is used for the wind hydrogen plant, which is the type of wind turbine currently used in the Summerview

wind farm. The power curve for the selected wind turbine is shown in Figure 3.1 [37]. The power characteristics of a wind turbine are defined in their associated power curve. These include cut-in and cut-out speeds, rated power, efficiency and power coefficient. The power curve can be used to translate a certain wind speed to the amount of power that can be generated, and considering the variability of wind speed in a certain region the capacity factor of the wind turbine can be calculated. Using the wind speed data for Pincher Creek and the Vestas power curve the annual energy yield and capacity factor can be calculated using the methodology outlined in Olateju and Kumar [38]. They are determined to be 7.4 MWh and 46.7%, respectively.

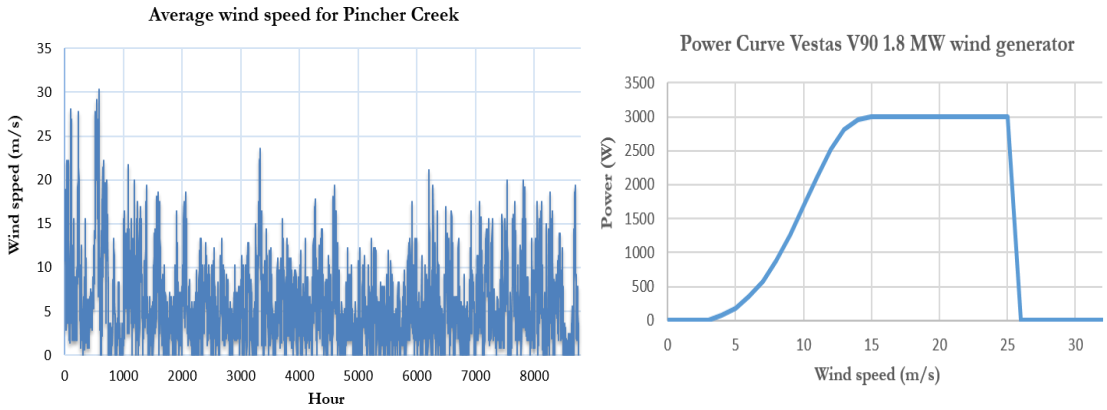

Figure 3.1 Average wind speed data for Pincher Creek and power curve for Vestas V90 wind turbine

There are three main types of electrolyzers, which are alkaline, proton exchange membrane and high-temperature electrolyzers. The scale of hydrogen flow rate is one of the most important factors influencing the selection of a suitable type of electolyzer for the wind power-to-hydrogen plant application. This is affected by achieving economies of scale reducing the capital cost of hydrogen production with the increase in production capacity. Moreover, maximizing the capacity factor of an electrolyzer considerably decreases the unit cost of hydrogen production; however, the capacity factor is also affected by the relative size of the electrolyzer and the wind

turbine. Alkaline electrolyzers are determined to be the most suitable for the considered application for their scale of hydrogen flow rate, efficiencies, and relatively low capital costs.

Olateju et al. [38, 39] conducted two studies on the techno-economic evaluation of electrolytic hydrogen production from wind energy for the upgrading operations of bitumen from oil sands. This system would have virtually no GHG emissions during operation. The wind-hydrogen plant they proposed has a capacity of 563 MW with the delivery of hydrogen to the bitumen upgraders via pipeline. They assessed several plant configurations to determine the optimum electrolyzer size and quantity. The optimal plant configuration they obtained consists of 80 electrolyzers with a production capacity of 760 Nm^3 h^{-1} each and a hydrogen production cost of \$8.43 kg^{-1}.

Running electrolyzers strictly from wind electricity can result in annual capacity factor as low as 30%, and in low wind electricity seasons the capacity factor of electrolyzers can be considerably lower (10% of high season). This requires significant amounts of hydrogen storage. Reducing hydrogen storage by relying on other sources of electricity production (e.g. fossil fuels, nuclear, biomass, etc.) will result in a considerably low capacity factors for these resources as well [34].

Hydropower

Oil Sands operators are allowed to withdraw up to 441 million m3 of water from the Athabasca River annually, which is expected to increase by as much as 200% over the upcoming few years. In addition, there are no regulations on freshwater withdrawal by oil sands operators even during low-flow periods, which represent the highest threats for downstream ecosystems. Less than 5% of the withdrawn water is returned to the river, and most of it ends up in toxic tailing ponds. Annual runoff in the Athabasca River has considerably declined over the past few decades by up to 30%, and a further 30% reduction in runoff is projected to occur in the future with the sustained water withdrawal. If the projected decline in river flowrates persists, then future water supplies may be insufficient to support future development of oil sands operations and sustain ecosystems [40, 41]. The river reach between Fort McMurray and Lake Athabasca was

considered to have low potential for the development of hydropower applications due to several factors. These include flat gradient, low banks, wide valley, and the considerable water resources assigned for bitumen extraction operations. Even though hydropower has significant potential in reducing GHG emission, the potentially threatened river ecosystems hinders their development to support oil sands operations. Therefore, hydropower production is disregarded in the proposed optimization model [42, 43].

Biomass

Western Canada hosts significant amount of forest and agricultural residues remaining from logging operation by pulp and lumber industries. These residues are abandoned on roadsides where they rot and release GHG emissions to the atmosphere. Agricultural residues in Western Canada also include straw from wheat and barley crops. Utilizing these agricultural residues for energy production can allow achieving reductions in GHG emissions and reliance of fossil-fuel sources of energy. The pulp and timber industry is where most of whole-forest biomass is allocated, which makes it unavailable for bioenergy production. However, most of the residues remain unused, which can be allocated for energy production to support the oil sands operations. Utilizing biomass for the production of energy will reduce the intensity of GHG emissions associated with oil sands operations. The emissions from bioenergy production include emissions from the production processes, biomass transportation, plant construction, and energy commodity transportation [43, 44].

Sarkar and Kumar [34] investigated the feasibility of incorporating biohydrogen production from forest and agricultural residues for upgrading of bitumen from oil sands. On average, there is approximately 6.48 million dry tonnes yr^{-1} of forest and agricultural residues for biohydrogen production, which can provide potential for reducing GHG emissions as well as dependence on hydrogen production from fossil fuels. They considered two types of gasifiers, which are the Battelle Columbus Laboratory (BCL) and the Gas Technology Institute gasifiers (GTI). The latter

is more preferable for large-scale biohydrogen production. The optimal plant sizes for BCL and GTI gasification technologies were determined to be approximately 3000 dry tonnes day^{-1} and 6000 dry tonnes day^{-1}, respectively. Both technologies were considered for the proposed energy optimization model [45]. Other options that were considered for the utilization of biomass as a source of fuel are for the production of SAGD steam using fluidized bed gasification boilers [46] and for power production [47]. On average, there is approximately 6.48 million dry tonnes yr^{-1} of forest and agricultural residues that could be utilized for producing energy for the oil sands industry [43]. The considered energy commodity producers that can utilize biomass as a fuel are biomass gasification boilers for the production of SAGD steam, biomass IGCC power plants, and biohydrogen gasification plants.

3.2 Optimization model formulation

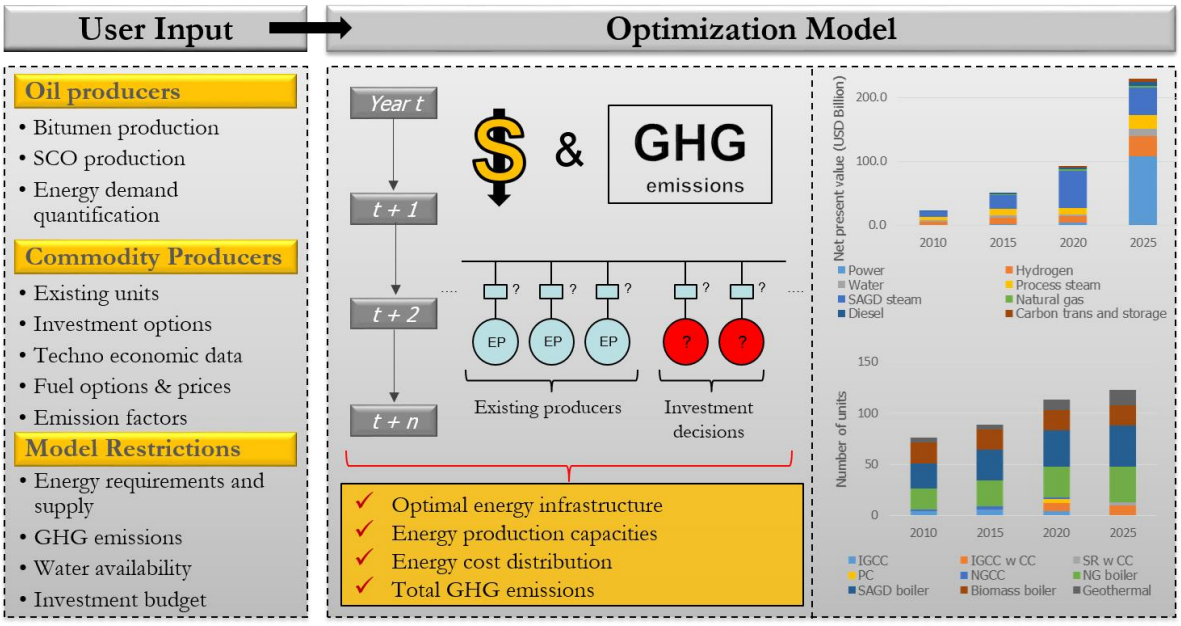

Figure 3.2 General structure of the renewable energy capacity expansion optimization model

The methodology used for the optimized integration of renewable energy technologies into the oil sands energy infrastructure is outline in Figure 3.2. After determining potentially viable renewable energy technologies that can provide adequate energy

supply, techno-economic data about different energy commodity producers are used as an input to the optimization model. The energy requirements of oil producers for steam, electricity, hot water, hydrogen and process fuels supplies from energy producers. Finally, the capacity expansion of conventional and renewable energy technologies is optimized using the developed model, which is the core of the methodology used to integrate renewable energy in the oil sands infrastructure.

This section presents the renewable energy and capacity expansion optimization model. The proposed model is used to select the optimal set of oil producers and quantify their energy requirements. Integrated extraction (SAGD or mining)/upgrading and SAGD extraction are considered for the production of SCO and commercial bitumen, respectively. Their energy requirements are supplied by power plants, hydrogen plants and steam boilers. Renewable energy technologies were also considered for power, hydrogen, steam and hot water production. Natural gas is also used in upgrading operations, and diesel is used to fuel trucks and shovels for mining operations. The model imposes CO_2 emission constraints on the energy infrastructure, which are met by integrating carbon capture and sequestration (CCS) technologies and producing energy through renewable systems. Figure 3.3 shows a schematic representation of the proposed energy optimization model. The optimization model is geared toward the minimization of the total cost (i.e. net present value) of producing energy, while being subject to energy commodity and oil producers' capacity, environmental, energy requirements and supply constraints.

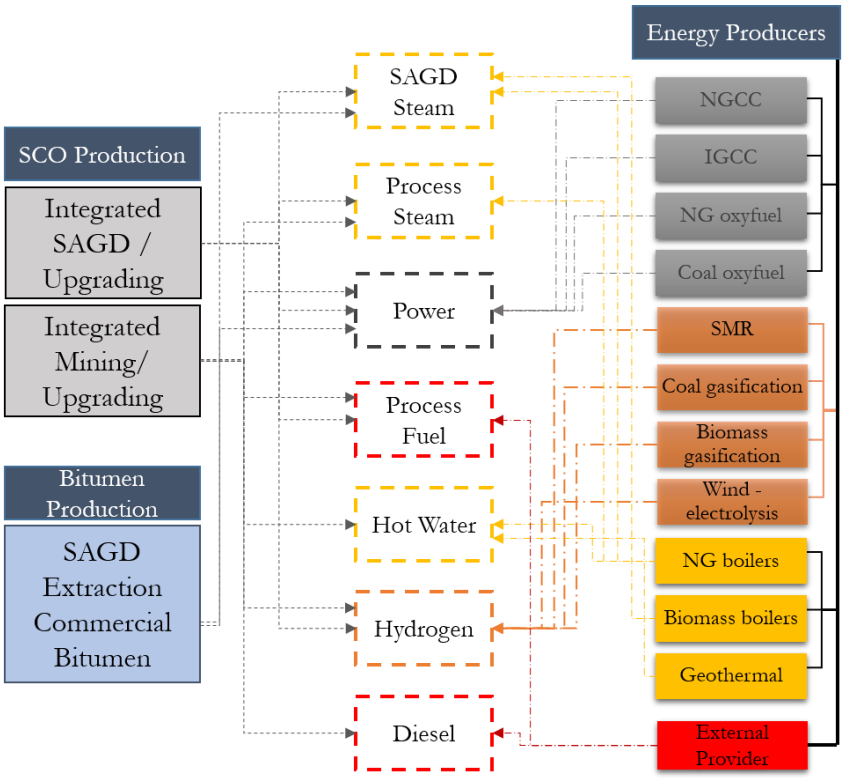

Figure 3.3 Schematic presentation of the energy optimization model

3.2.1 Energy commodity producers

Energy commodity producers are included in the proposed model to provide the energy requirements for oil sands operations. The energy commodities considered include power, hydrogen, steam and hot water that can be produced by non-renewable and renewable energy technologies. The energy producers used to satisfy the energy requirements include boilers and geothermal energy for the production of SAGD steam, process steam and hot water. Power plants are used to satisfy the electricity requirements of oil sands extraction and bitumen upgrading processes. Hydrogen plants are used to satisfy the hydrogen demands of bitumen upgrading operations.

Boilers

The proposed model considers two types of boilers, which are conventional natural gas boilers and biomass-fired boilers. The boilers are also classified based on the type of steam they produce. A set of natural gas and biomass boilers are defined for the production SAGD steam, which produce 80% quality steam at 8000 kPa. The amount of SAGD steam (SS_b) produced from natural gas and biomass boilers is calculated as follows [48]:

$$SS_b = \frac{HHV_b\, \eta_b}{\Delta HSS} XB_b \tag{3.1}$$

where HHV_b is the heating value (kJ/Nm^3 NG or kJ/tonne biomass) of the fuel used by boiler type b, ΔHSS is the change in enthalpy (kJ/tonne steam), η_b is the boiler efficiency, and XB_b is the amount of fuel consumed (Nm^3 of NG/h or tonne biomass/h).

Another type of steam considered in the optimization model is process steam, which is generated at 6300 kPa and 500^{o}C. Process steam is used in the mining extraction process of bitumen and in the upgrading process of bitumen to produce synthetic crude oil. The amount of process steam produced can be calculated as follows:

$$PS_b = \frac{HHV_b\, \eta_b\, \%S}{\Delta HPS} XB_b \tag{3.2}$$

Hot water is also used in the mining extraction process of bitumen, and it is produced at 35^{o}C. In the proposed model it is assumed that hot water is coproduced in the boiler dedicated for the production of process steam. The amount of hot water produced can then be calculated as presented in Eq. 3.3, where $\%S$ is the percentage of boiler capacity dedicated for the production of process steam.

$$HW_b = \frac{HHV_b\ \eta_b\ (1 - \%S)}{\Delta HHW} XB_b \tag{3.3}$$

The number of new natural gas boilers (NB_b) installed and existing boilers (ENB_{be}) must satisfy the total production requirements of SAGD steam (SS_b), process steam (PS_b) and hot water (HW_b). The maximum capacity of each boiler is defined by the parameter S_b^{max} (tonne steam/h). The capacity constraints for SAGD steam, process steam and hot water boilers are defined by Eqs. 3.4 – 3.6.

$$SS_b \leq \left(NB_b + \sum_{e \epsilon E_b} ENB_{be} \right) S_b^{max} \tag{3.4}$$

$$PS_b \leq \left(NB_b + \sum_{e \epsilon E_b} ENB_{be} \right) S_b^{max}\ \%S \tag{3.5}$$

$$HW_b \leq \left(NB_b + \sum_{e \epsilon E_b} ENB_{be} \right) S_b^{max}\ (1 - \%S) \frac{\Delta HPS}{\Delta HHW} \tag{3.6}$$

Power plants

The conventional power generation plants considered in the energy infrastructure are natural gas combined cycle (NGCC), oxyfuel, integrated gasification combined cycle (IGCC), and supercritical pulverized coal (SCPC) [49, 50]. Natural gas is used as a feedstock in NGCC and oxyfuel plants. Coal is used as a feedstock in IGCC, SCPC and oxyfuel technologies. For each technology integration with carbon capture and sequestration was also considered. Biomass gasification was considered as a renewable option for the production of power [47].

The production from natural gas and coal power plants can be modeled as presented in Eq. 3.7 [51 – 53], given the heating value of fuel utilized (HHV_p, NG: kJ/Nm^3 or coal and biomass: kJ/kg) and the heating rate (HR_p, kJ/kW) of power production technology p. The amount of power produced (PP_p) can then be calculated based on the amount of fuel consumed (FP_p, NG: Nm^3/h or coal and biomass: kg/h) as follows:

$$PP_p = \frac{HHV_p}{HRP_p} FP_p \qquad \forall p \tag{3.7}$$

The capacity constraint for each power production technology p is defined in Eq. 3.8. The amount of power produced (PP_p) must be less than or equal to the maximum capacity of technology p (PP_p^{max}) multiplied by the number of new (NP_p) and existing (ENP_{pe}) units selected by the optimization model.

$$PP_p \leq \left(NP_p + \sum_{e \epsilon E_p} ENP_{pe} \right) PP_p^{max} \qquad \forall p \tag{3.8}$$

Hydrogen plants

Steam methane reforming and coal gasification [54 – 56] are the two conventional hydrogen production technologies considered within the energy infrastructure for the oil sands operations. Biomass gasification is also considered as a renewable hydrogen production technology. For each type of fossil-fuel based hydrogen production plant integration with carbon capture and sequestration was also considered. The amount of hydrogen produced by each technology can be modeled based on Eq. 3.9 [57, 58], given the heating value (HHV_h, NG: kJ/Nm^3 or coal and biomass: kJ/kg) of the fuel utilized and the heating rate required to produce one tonne of hydrogen (HRH_h, kJ/tonne H_2) for each

hydrogen production technology h. The amount of hydrogen produced can then be calculated based on the amount of fuel consumed (FH_h, NG: Nm^3/h or coal and biomass: kg/h).

$$HH_h = \frac{HHV_h}{HRH_h} FH_h \quad \forall h \tag{3.9}$$

Coal gasification hydrogen production plants are used to cogenerate electricity. Part of the synthetic gas that is produced from the gasification process is used to drive gas turbines for power generation. Cogeneration can be incorporated in the Oil Sands energy infrastructure as an option to increase energy efficiency. It is therefore necessary to quantify the net power (PH_h) required or produced by these technologies, which is assumed to be a factor (HP_h^{cogen}, kWh/tonne H_2) of the amount of hydrogen produced (HH_h) by technology h. This can be presented as follows:

$$PH_h = HP_h^{cogen} HH_h \quad \forall h \tag{3.10}$$

The capacity constraint for each hydrogen production technology h can be defined as illustrated in Eq. 3.11. The maximum capacity for technology h is defined by the parameter HH_h^{max} (tonne H_2/h). The total amount of hydrogen produced by technology h (HH_h) must be satisfied by the total number of newly installed (NH_h) and existing plants (ENH_{he}).

$$HH_h \leq \left(NH_h + \sum_{e \epsilon E_h} ENH_{he} \right) HH_h^{max} \quad \forall h \tag{3.11}$$

Geothermal

The geothermal heating system used in the proposed optimization model is based on the results obtained by Pathak et al. [33]. They determined that the optimum geothermal direct heating system is composed of three wells (one injector and two producers) with a horizontal spacing of 500 – 600 m. Compared to other systems this arrangement provided improved heat transfer due to the increase in contact between injected water and the hot dry rocks. Such a system is capable of providing a thermal power output as high as 29.4 MW [33].

The geothermal heating system is most suitable to provide the heating requirements for hot water production used in oil sands mining operations [33]. The amount of hot water produced from geothermal heating (*GW*, tonne/h) can be calculated as the ratio of the heating rate (*HRGEO*, MJ/h) of the geothermal system to the change in enthalpy of water (ΔHHW, MJ/tonne), and can be presented as follows:

$$GW = \frac{HRGEO}{\Delta HHW} \tag{3.12}$$

The total amount of hot water production (*GW*) must be less than or equal to the maximum capacity of a geothermal system ($HRGEO^{max}/\Delta HHW$, MJ hr^{-1} / MJ $tonne^{-1}$) multiplied by the number of new (*NGEO*) and existing ($EGEO_e$) units selected by the optimization model. The capacity constraint can be presented as follows:

$$GW \leq \left(NGEO + \sum_{e \epsilon E_{GEO}} EGEO_e \right) \frac{HRGEO^{max}}{\Delta HHW} \tag{3.13}$$

Wind power-to-hydrogen via electrolysis

Olateju et al. [38, 39] investigated the feasibility of integrating various electrolyzer capacities that can be integrated with wind power. According to their results the optimum size of the electrolyzer in the wind power-to-hydrogen plant is 3496 kW. This is the capacity of the electrolyzer considered in the proposed optimization model. The electrolyzer will utilize power from the Vestas V-90 1.8 MW turbines considered in this model, which is the type of turbine used in the Summerview wind farm in southern Alberta.

Power production from the wind turbines must satisfy the power requirements of the electrolyzers. The power produced from a wind turbine can be estimated by the product of its annual power yield (*AWP*, kW) and its capacity factor (*WTCF*). These were estimated by the methodology outlined by Olateju et al. [38, 39] based on the wind data available the Summerview wind farm in Southern Alberta [36], and were determined to be 7400 kWh and 46.7%, respectively. The total amount of power produced from the wind turbines can be estimated by multiplying the power yield of a turbine multiplied by the number of newly installed (*NWT*) and existing (EWT_e) units selected by the optimization model, which can be represented as follows:

$$PWT = \left(NWT + \sum_{e \epsilon E_{WT}} EWT_e \right) WTCF\ AWP \tag{3.14}$$

The yield of hydrogen from water electrolysis (EER^{-1}) is assumed to be 0.018 tonne H_2/MWh [39]. The total amount of hydrogen produced from newly installed and existing electrolyzers can therefore be calculated as follows:

$$HHE = PWT\ EER^{-1} \tag{3.15}$$

The number of electrolyzers selected depends on the maximum (HH_{elect}^{max}) allowable hydrogen flowrates produced. Eq. 3.16 presents the capacity constraint for newly installed and existing electrolyzers. NHE_{elect} is an integer variable representing the number of new electrolyzers selected by the optimization model during a certain time period. $ENHE_{elec}$ is a binary variable that determines whether an existing electrolyzer is operational during the investigated time period (i.e. 1 if the electrolyzer is operational or 0 otherwise).

$$HHE \leq \left(NHE + \sum_{e \epsilon E_{elec}} ENHE_e \right) HH_{elect}^{max} \tag{3.16}$$

3.2.2 Energy requirements

The calculation of energy demands for oil sands operations depends on the extraction method, as well as the upgrading route of bitumen to produce synthetic crude oil. The two extraction methods considered are oil sands mining and steam assisted gravity drainage (SAGD). The bitumen produced from the extraction processes is then upgraded to synthetic crude oil. The production schemes incorporated in the optimization model are integrated mining/upgrading, integrated SAGD/upgrading, and standalone SAGD extraction for the production of commercial diluted bitumen. The upgrading route can be based on a thermocracking process (delayed coking and hydrotreatment), a hydrocracking process (LC-fining and hydrotreatment), or a combination of both (LC-fining, fluid coking and hydrotreatment). All these stages require energy in the form of power, hydrogen, steam, heat and fuel (i.e. natural gas and diesel). The quantification of

these energy demands is explained in details in the following sections. The procedure used to model the energy requirements for the considered oil sands operations is based on the approach developed by Ordorica et al. [23].

Bitumen extraction

Oil sands that are within 75 m from the surface are recoverable through mining operations. However, deeper deposits are only recoverable through in-situ extraction methods. In the proposed optimization model, it is assumed that only in-situ extraction methods are suitable for the production of commercial bitumen, whereas SCO can be produced through both integrated mining/upgrading and integrated SAGD/upgrading production schemes. The bitumen produced through mining operations typically contains high levels of solids and water, and therefore, it is usually upgraded to SCO on site instead of being marketed as it is unsuitable for shipping to conventional refineries.

Mining extraction

Mining extraction is a surface method used for the production of bitumen from oil sands. The energy commodities used in mining extraction operations are diesel, electricity, process steam and hot water. An energy resource that is extensively used in mining extraction is diesel. It is consumed by trucks and shovels used in mining operations. Diesel consumption depends on the specifications of the vehicles used and their number. A parameter is used to quantify the amount of diesel consumed per barrel of bitumen produced (MDC = 0.17 L diesel/bbl bitumen), which is based on a model of a typical Canadian Oil Sands mining operation [4]. The total amount of diesel consumed can be estimated from the amount of bitumen produced in the mining production routes as

illustrated in Eq. 3.17, where BIT_m is the amount of bitumen produced through integrated mining/upgrading route *m*, and $IMBIT_m$ representing the selection of route *m*.

$$MEDD = MDC\left(\sum_m IMBIT_m\, BIT_m\right) \tag{3.17}$$

The electricity demand for mining operations can be calculated as illustrated in Eq. 3.18. The power used is mostly required for driving pumps, and the pumping factors are adopted from Ordorica et al. [4], which were determine based on simulations conducted in Aspen Plus. The power demand for hydrotransport depends on the slurry rate in tonnes per year (SL_m), the distance from the mine to the extraction plant in meters d_m, and a pumping factor PF_m (0.0787 kWh /tonne slurry/m) that indicates the power requirements necessary to transfer oil slurry into the following stage [4].

The power demand for bitumen recovery is associated with the transportation of tailings and centrifugation stages. TPE_m and TSE_m are the tailings produced from primary and secondary extraction stages, respectively. The distance in meters between the extraction plant and the tailing ponds is defined by dT_m. The electricity requirement is defined by the pumping factor PFT_m (0.0016 kWh /tonne/m) [4]. The amount of diluted bitumen transferred to the centrifugation stages is defined as DBC_m (m^3/hr) and *ECR* is the power requirement for centrifugation (kWh /m^3).

$$MEPD = \sum_m (SL_m d_m PF_m + (TPE_m + TSE_m) dT_m PFT_m + DBC_m ECR)\; IMBIT_m \tag{3.18}$$

Process steam is required for conditioning and bitumen recovery stages. The amount of process steam can be calculated as presented in Eq. 3.19. MO_m is the oil sands mining

rate (tonne oil sand/hr) and SC_m is the steam requirement for the conditioning stage (0.036 tonne steam/tonne oil sand [59]). Some of the mining production routes *m* do not incorporate a conditioning stage, therefore, the parameter SC_m takes the value of zero in these routes. BMF_m is the bitumen froth produced in primary extraction (tonne froth/hr) and *SF* is the steam requirement in bitumen extraction (0.04 tonne steam/tonne froth) [59].

$$MEPSD = \sum_m (SC_m MO_m + SF\ BMF_m)\ IMBIT_m \tag{3.19}$$

The hot water demand for mining operations includes consumption in the conditioning, hydrotransport and bitumen recovery stages. Eq. 3.20 illustrates the calculation of the total water demand for mining operations. The water requirements for these stages are defined by the parameters WC_m (0.333 tonne water/tonne oil sand and zero for route *m* that does not include a conditioning stage), *WH* (0.30 tonne water/tonne oil sand) and *WR* (0.41 tonne water/tonne oil sand extraction wash water requirement), respectively [59].

$$MEWD = \sum_m (WC_m + WH + WR)\ MO_m\ IMBIT_m \tag{3.20}$$

SAGD extraction

The two energy commodities required for SAGD extraction operations are steam and electricity. The demand for SAGD steam (SSD) can be calculated as illustrated in Eq. 3.21. The *SOR* is the steam to oil ratio parameter, which is assumed to be 2.4 tonnes of steam per tonne of bitumen extracted [60]. The amount of commercial crude bitumen extracted is presented by the term *CB* (tonne bitumen hr^{-1}), and BIT_s is the amount of bitumen considered for SCO production by each considered route (*s*).

$$SESD = SOR\left(CB + \sum_{s} ISBIT_s\, BIT_s\right) \tag{3.21}$$

The power required for the production of commercial bitumen and bitumen used for the production of SCO through integrated SAGD/upgrading operations can be calculated as presented in Eq. 3.22. *ECB* is a parameter that represents the electricity requirement for the production of bitumen by SAGD extraction (3.1 kW/tonne bitumen) [61].

$$SEPD = ECB\left(CB + \sum_{s} BIT_s\, ISBIT_s\right) \tag{3.22}$$

Upgrading operations

Energy is required for the upgrading stages that are integrated with SAGD and mining extraction processes in order to convert the bitumen extracted to synthetic crude oil (SCO). There are three upgrading routes that are considered in the presented model, and each of them can be integrated with the mining or SAGD extraction methods. The three upgrading routes considered are: 1) LC-fining and hydrotreatment; 2) delayed coking and hydrotreatment; 3) LC-fining, fluid coking and hydrotreatment. LC-fining is a hydrocracking based process, and delayed coking and fluid coking are thermocracking based processes. There are significant amounts of energy required for these upgrading processes. The energy consumed is in the form of hydrogen, electricity, process steam, and process fuel (i.e. natural gas) for heating.

The first step in all upgrading routes is the diluent recovery unit (DRU), which involves the recovery of the diluent (i.e. naphtha) used to dilute the crude bitumen to facilitate its transportation by pipelines. The products generated in the first stage are naphtha, light

gas oil (LGO), and atmospheric topped bitumen (ATB). The naptha is recycled, and the LGO and ATB are sent for further treatment to produce SCO.

The LGO is transferred to the hydrotreatment unit for sulfur and nitrogen removal. The ATB is sent to the vacuum distillation unit (VDU), or is split between the VDU and the LC-finer unit. LGO and heavy gas oil (HGO) are products from the VDU, which are sent to the hydrotreatment unit. The second upgrading stage involves mixing the bottom products of the VDU, which is known as the vacuum topped bitumen (VTB), with any residual ATB generated from the DRU. The mixture is then sent to LC-finers or delayed cokers. In delayed cokers the heavy hydrocarbons are cracked to lighter compounds using thermal energy, whereas in LC-finers they are cracked using hydrogen. There are two types of LC-finers considered in the proposed model, which are low and high conversion. The products from LC-finers and delayed cokers, which include LGO, HGO and naphtha are treated with hydrogen for the removal of impurities. For the low conversion LC-finers, the bottom products are further treated in fluid cokers to yield additional light hydrocarbons. The products remaining from the final upgrading stages are SCO from hydrotreatment and petcoke residue from LC-finers and cokers.

The upgrading units (i.e. LC-finers, cokers and hydrotreatment) included in the proposed model are modeled according to the approaches proposed in [59 – 65]. The parameter representing the power, hydrogen and thermal (i.e. process steam and fuel) requirements of bitumen upgrading operations were obtained from these studies.

Power demand

The power demand for the upgrading stages can be quantified as presented in Eq. 3.23. VTB_o represents the amount of vacuum topped bitumen sent to the LC-finers or delayed

cokers in the hydrocracking and thermocracking routes, respectively. For the upgrading route of LC-fining plus fluid coking an additional stream is sent to the LC-fining unit, which is a fraction of the atmospheric topped bitumen ($ATBF_o$). For this upgrading route the bottom oil from the LC-fining is sent to the fluid coker, which is presented by the variable BF_o. The power requirement of the LC-fining for each upgrading route is presented by the parameter EL_o, which is 23.3 kWh/tonne, 99.8 kWh/tonne for the delayed coker and LC-finer, respectively [59, 61]. The power requirement of the fluid coker is presented by the parameter ED_o, which is 36.3 kWh/tonne [62].

$$UPD = \sum_{o \in (S \cup M)} EL_o(VTB_o + ATBF_o) + ED_o\, BF_o \tag{3.23}$$

Process steam demand

Process steam is required for diluent recovery, vacuum distillation and fluid coking. The total process steam demand for bitumen upgrading can be calculated as illustrated in Eq. 3.24. *DR* is the parameter that defines the fraction of diluent, and *SRD* (0.30 tonne steam/tonne feed) is the steam requirement for the DRU. The steam requirement in the VDU is presented by the parameter *SRV* (0.07 tonne steam/tonne feed) [61], and the ATB recovered from the DRU that is transferred to the VDU is presented by the variable ATB_o (tonne/hr), which excludes the fraction of ATB that is sent to the low conversion LC-finers ($ATBF_o$, tonne/hr). The steam requirement for the fluid coker unit is *SRF* (0.308 tonne steam/tonne feed [61]) and the amount of bottom oil from the LC-finer sent to the fluid coker is BF_o (tonne/hr).

$$UPSD = \sum_{o \in (S \cup M)} BIT_o\,(1 + DR)\,SRD + (ATB_o - ATBF_o)\,SRV + BF_o\,SRF \qquad (3.24)$$

Hydrogen demand

The total hydrogen demand for the upgrading stages in integrated SAGD/upgrading and mining/upgrading operations is calculated as illustrated in Eq. 3.25. Hydrogen is consumed in two stages, which are hydrocracking and hydrotreatment. The hydrogen requirement for hydrocracking is defined by the parameter HRU_o. For the hydrocracking based route the hydrogen requirements for the LC-finer is 0.020 kg H_2/tonne feed [54 – 56]. For the LC-finer plus fluid coking upgrading route, the hydrogen requirement of the LC-finer is 0.014 kg H_2/tonne feed [59]. The hydrogen requirements for the hydrotreatment of naphtha, LGO and HGO are presented by the parameters *HN* (0.0185 tonne H_2/tonne naphtha), *HL* (0.0186 tonne H_2/tonne LGO) and *HHG* (0.0175 tonne H_2/tonne HGO), respectively [52, 54].

$$UHD = \sum_{o \in (S \cup M)} HRU_o\,(VTB_o + ATBF_o) + HN\,N_o + HLG\,LGO_o + HHG\,HGO_o \qquad (3.25)$$

Fuel demand

The total requirement of natural gas for oil sands upgrading operations can be calculated as shown in Eq. 3.26. Natural gas is required for operating both hydrocracking (LC-fining) and thermocracking (delayed coking) based upgrading routes. The natural gas fuel requirements for LC-fining and delayed coking is presented by the parameter FR_o (LC-fining: 0.562 GJ/tonne; Delayed coking: 0.911 GJ/tonne) [62], where *o* is the sub index representing the integrated mining or SAGD/upgrading route. *HNG* represents the heating value of natural gas (0.038 GJ/Nm^3).

$$UFD = \frac{1}{HNG} \sum_{o \in (S \cup M)} (VTB_o + ATBF_o)\ FR_o \tag{3.26}$$

Additional energy requirements

The hydrogen production technologies have electricity requirements to drive pumps and compressors. Power is required for the operation of steam methane reforming plants that are utilized for hydrogen production. This energy requirement (*SMPRD*) can be calculated as illustrated in Eq. 3.27, where *ESMR* represent the electricity requirement (kW/tonne H_2).

$$SMRPD = HH_{SMR} ESMR \tag{3.27}$$

Power consumption takes place during the transportation of CO_2 to sequestration sites, which is calculated as illustrated in Eq. 3.28. C_i (tonne CO_2/hr) represents the amount of CO_2 captured in power and hydrogen plants, ECC_i (1.34 kWh/tonne CO_2/km) is the electricity requirement for compressing CO_2 for transport, and L (km) is the length of the CO_2 pipeline connecting Fort McMurray and the depleted oil fields located near Edmonton, which is approximately 600km [6]. The sub index i represents the set of energy producers and commodities that are incorporated in the oil sands optimization model, which include power plants, hydrogen plants, steam and hot water producers, diesel and natural gas.

$$CCPD = \sum_{i \in (P \cup H)} C_i ECC_i L \tag{3.28}$$

3.2.3 Environmental restrictions

The CO_2 emissions associated with energy commodity producers is determined by multiplying the CO_2 emission factor (Table 3.3) of each producer by its total production capacity. As shown in Eq. 3.29 the total CO_2 emissions (tonne CO_2/hr) associated with energy production for the oil sands industry can be calculated as the sum of emissions of energy producers (CO_2e_i).

$$CO_2T = \sum_i CO_2e_i \tag{3.29}$$

The CO_2 emission constraint incorporated in the model is shown in Eq. 3.30. The CO_2 emission target is set by the right hand side of the inequality equation. CO_2E (tonne/hr) is an input parameter to the model the maximum allowable emission level for a certain operational year, and the *%RED* is a parameter that indicates the percentage emissions reduction that is required to be achieved.

$$CO_2T \leq CO_2E\ (1 - \%RED) \tag{3.30}$$

3.2.4 Objective function

The NPV is used to facilitate incorporation of capacity expansion decisions. This facilitates the comparison between existing and newly established facilities. The annuity costs (*A*) are converted to NPV by using the following general formula:

$$NPV = A\ PVF \tag{3.31}$$

The present value annuity factor (*PVF*) is defined by the following formula:

$$PVF = \frac{1 - (1 + i)^{-(L - \Delta T)}}{i} \tag{3.32}$$

where i is the annual interest rate, which is assumed to be 15%. L is the life of plant for which the NPV is calculated. ΔT is the time difference between the current year of operation and the year at which the plant was established.

The individual cost of each commodity is calculated by multiplying the number of newly established and existing units of each commodity producer by the capital and operating cost factors associated with each technology. The capital cost factors represent the amortized investment cost over the plants operating lives. The total cost of commodity production also depends on the fuel (i.e. natural gas, coal, etc.) consumption and the price of fuel. The production costs of power, hydrogen, steam and hot water are represented as follows.

Power cost

The net present value of the cost of power production (PC, \$) can be calculated as illustrated in Eq. 3.33. NP_p is an integer variable that indicates the number of new plants installed from each power production technology. EP_{pe} is a binary variable that indicates whether or not an existing plant is operational during an investigated year. CCP_p (\$/yr) and OMP_p (\$/yr) are the amortized capital cost and operating and maintenance cost factors, respectively, for each power production technology p. FP_p (GJ/hr) is the amount of fuel consumed by production technology p, and PF_p (\$/GJ) is the associated fuel price.

$$PC = \sum_{p} NP_p\left(CCP_p + OMP_p\right)\ PVF_p + \sum_{p}\sum_{e\epsilon E_p} EP_{pe}\left(CCP_p + OMP_p\right) EPVF_{pe} + FP_p\ PF_p\ t\ PVF_p \tag{3.33}$$

Hydrogen cost

The cost of hydrogen production (*HC*, $) can be determined as defined in Eq. 3.34. NH_h and EH_{he} are integer and binary variables that indicate the number of new hydrogen plants to be installed and existing plants operating in the investigated year, respectively. The capital cost hydrogen plants is represented by the parameter CCH_h ($/yr) and the operating and maintenance cost by OMH_h ($/yr). Fuel consumption by each hydrogen production technology is presented by the variable FH_h (GJ/hr) and the associated fuel cost is accounted for by the parameter PF_h ($/GJ).

$$HC = \sum_h NH_h(CCH_h + OMH_h)\, PVF_h + \sum_h \sum_{e \epsilon E_h} EH_{he}(CCH_h + OMH_h)\, EPVF_{he} + FH_h PF_h\, t\, PVF_h + NHE(CCHE + OMHE)\, PVF_{elec} + \sum_{e \epsilon E_{elec}} EHE_e(CCHE + OMHE)\, EPVF_{elec} \quad (3.34)$$

Steam and hot water cost

The cost of producing SAGD and process steam is calculated as illustrated in Eq. 3.35. NB_b is the integer variable representing the number of boiler of type *b* (i.e. natural gas or biomass fueled) producing SAGD extraction and process steam. ENB_{be} is the binary variable representing the operation of an existing boiler during an investigated year. CCB_b and OMB_b are the associated capital and operating cost factors for each type of boiler. XSB_b is the amount of fuel consumed by newly installed and existing boilers, and PFB_b is the associated fuel price.

$$SC = \sum_{b} NB_b(CCB_b + OMB_b)PVF_b + \sum_{b}\sum_{e\epsilon E_b} ENB_{be}(CCB_b + OMB_b)\, EPVF_{be} + XSB_b PFB_b\, t\, PVF_b \quad (3.35)$$

Process hot water is also produced using geothermal heating. The cost of production associated with this technology is estimated as illustrated in Eq. 3.36, where the capital (*CCGEO*) and operating (*OMGEO*) cost factors account for the cost of drilling, sustaining the flow rate of water for a period of 10 years, and providing water at 60^{o}C and a flow rate of 50 L/s [33].

$$HWGC = NGEO(CCGEO + OMGEO)\, PVF_g + \sum_{e\epsilon E_{GEO}} EGEO_e(CCGEO + OMGEO)\, EPVF_{ge} \quad (3.36)$$

Extraction fuel (Natural gas and Diesel) cost

Diesel and natural gas are consumed in bitumen extraction operations. Diesel is consumed by the trucking and shoveling fleet used in oil sands mining operations and its total cost is calculated by multiplying the total diesel requirements *MEDD* (L/hr) by the price of diesel (*PD*, $/L). Natural gas is consumed in hydrocracking and thermocracking upgrading operations for SCO production. Total natural gas requirement for integrated SAGD/upgrading and mining/upgrading operations is expressed by the variable *UFD* (GJ/hr), respectively. *PNG* is the price of natural gas ($/GJ).

$$EFC = [MEDD\ PD\ +\ UFD\ PNG]\, t\, PVF_f \quad (3.37)$$

Carbon transportation and sequestration cost

The transportation and sequestration cost of captured CO_2 from power and hydrogen plants is calculated as illustrated in Eq. 3.38. *TC* ($/tonne/km) and *SC* ($/tonne) are the unit transportation and sequestration costs of CO_2, respectively. $CSCP_p$ and $CSCH_h$ are the amounts of CO_2 captured by power and hydrogen plants (tonne/hr)), respectively.

$$CCSC = (TC\ L + SC)\left(\sum_{p} CSCP_p + \sum_{h} CSCH_h\right) PVF_{ccs} \tag{3.38}$$

The formulated optimization model is directed towards the minimization of the total cost of energy production. It incorporates the individual costs of producing each energy commodity (i.e. power, hydrogen, SAGD steam, process steam, hot water, and fuel). The objective function also incorporates the carbon capture and sequestration costs. The optimization model searches for the set of energy commodity producers, as well as bitumen and SCO producers that minimize the total cost of oil sands operations while being subject to CO_2 emission constraints.

$$Minimize\ NPV = PC + HC + SC + HWGC + EFC + CCSC \tag{3.39}$$

3.2.5 Energy supply

The total energy commodity requirements for oil sands extraction and upgrading operations must be satisfied by the supply from the energy producers. The supply constraints defined in Eq. 3.40 – 3.44 specify that the total amounts energy commodities produced from newly established and existing energy producers must be greater than or equal to that required by oil sands operations.

$$\sum_{p} PP_p + \sum_{h \epsilon H_{CO}} PH_h \geq MEPD + SEPD + UPD + SMRPD + CCPD \quad (3.40)$$

$$\sum_{h} HH_h + HHE \geq UHD \quad (3.41)$$

$$\sum_{b} SS_b \geq SESD \quad (3.42)$$

$$\sum_{b} PS_b \geq MEPSD + UPSD \quad (3.43)$$

$$\sum_{b} HW_b + GW \geq MWD \quad (3.44)$$

3.3 Case Study

The developed renewable energy capacity expansion optimization model for the oil sands industry was applied to consecutive operational periods (i.e. 2010, 2015, 2020 and 2025). The results of one operational period was used as an input for the following periods, for which capacity expansion decisions were optimized. Data for oil sands production levels (i.e. bitumen and SCO), producers' capacities, techno-economic data of energy producers, fuel prices, and environmental regulations for these operational years are readily available in the literature. Different scenarios were considered to illustrate the benefits of incorporating renewable energy technologies and capacity expansion decisions in the oil sands energy optimization model. The sequential approach is applied, in which the results of one operational year are used as an input for the following investigated period, and was investigated with and without the incorporation of renewable energy technologies [66, 67]. In the sequential approach the existence of a mix of energy infrastructure influences investment decisions in the following investigated

period. The preference of the model to incorporate new technologies (e.g. renewable energy) in the new energy mix is dependent on the technologies in the existing infrastructure. The production capacity of oil producers is also affected by the energy production technologies included. An increment of five years is considered between the investigated operational years, which is used by decision makers to review investment decision in the oil sands industry [68].

Table 3.2 lists the oil and energy producers incorporated in the model. The oil producers included in the investigated case study depend on the oil sands extraction method and upgrading route. The two considered extraction methods are oil sands mining and in-situ SAGD. Each extraction method can be possibly integrated with any of the three considered upgrading routes. The upgrading routes can be based on hydrocracking, thermocracking, or a combination of both. The technology considered for the hydrocracking only route is high conversion LC-fining. Delayed coking was the technology considered for the thermocracking upgrading route. Low-conversion LCF plus fluid coking was considered for the combined hydrocracking and thermocracking. Hydrotreatment is a required stage in all upgrading routes. The energy producers incorporated include technologies for the production of SAGD steam, process steam, hot water, hydrogen, and power.

Table 3.2 Oil and energy producers considered in the optimization model

Oil producers
MP1 – Mined bitumen + Conditioning upgraded by LCF + FC + HT
MP2 – Mined bitumen upgraded by LCF + FC + HT
MP3 – Mined bitumen upgraded by DC + HT
MP4 – Mined bitumen upgraded by LCF + HT
SP1 – SAGD bitumen upgraded by LCF + FC + HT
SP2 – SAGD bitumen upgraded by DC + HT
SP3 – SAGD bitumen upgraded by LCF + HT

SAGD commercial diluted bitumen production
Energy producers
Steam and hot water producers
S1 – NG at 6300 kPa and 500^{o}C steam w/o CO_2 capture [42]
S2 – NG 80% steam at 8000 kPa w/o CO_2 capture [42]
S3 – Biomass Fluidized Bed Gasification Steam Plant 1250 psig steam [37]
S4 – Geothermal System for Direct Heating of Water [24]
Power producers
P1 – NGCC w/o CO_2 capture [41]
P2 – Supercritical coal w/o CO_2 capture [41]
P3 – IGCC w/o CO_2 capture [40]
P4 – IGCC with 88% CO_2 capture via Selexol [40]
P5 – IGCC with 88% CO_2 + H_2S co-capture via Selexol [40]
P6 – NGCC with 90% CO_2 capture via MEA [41]
P7 – NG Oxyfuel with CO_2 capture [41]
P8 – Coal Oxyfuel with CO_2 capture [41]
P9 – Pulverized coal with 90% capture via Selexol [41]
P10 – Wind turbines Vestas V90 1.8MW [29]
P11 – Biomass IGCC plant [38]
Hydrogen producers
H1 – SMR w/o CO_2 capture [45, 46]
H2 – SMR with 90% CO_2 capture via MEA [47]
H3 – Coal gasification w/o CO_2 capture [45, 46]
H4 – Coal gasification with 90% CO_2 capture via Selexol [47]
H5 – Coal gasification with 90% CO_2 + H_2S co-capture via Selexol [47]
H6 – Electrolyzer Indutstrie Haute Technologie (IHT) Type S-556 [29, 30]
H7 – BCL Biomass gasification [34]
H8 – GTI Biomass gasification [34]

The individual cost parameters, fuel rates and emission factors for each energy commodity producer are summarized in Table 3.3, and other key economic parameter required for the model are summarized in Table 3.4.

Table 3.3 Techno-economic parameters of energy producers

Technology	Capacity	Capital Cost	O&M Cost	Fuel Rate	Emission factor	Reference
Boiler	Tonne hr^{-1}	\$ / tonne hr^{-1}	% Capital Cost	MJ tonne^{-1}	tonne CO_2 Nm^{-3} NG	
S1	340	376,576	0.006	3,415	1.72e-3	[60]
S2	340	376,576	0.006	2,470	1.72e-3	[60]
S3	117	336,410	0.0323	2,469	7.13e-5	[37]
S4	920	\$922 kW^{-1}	0.06	115	0	[24]
Power	kW	\$ kW^{-1}	% Capital Cost	MJ kWh^{-1}	Tonne CO_2 kWh^{-1}	
P1	507,000	570	0.018	7.17	3.67e-4	[41]

P2	524,000	1,230	0.038	9.16	8.11e-4	[41]
P3	539,000	1,760	0.026	8.76	8.00e-4	[40]
P4	448,000	2,400	0.025	11.06	1.31e-4	[40]
P5	513,000	1,890	0.026	10.17	1.18e-4	[40]
P6	432,000	930	0.037	8.41	4.3e-5	[41]
P7	492,000	1,980	0.049	12.04	1.07e-4	[41]
P8	440,000	1,250	0.086	7.70	1.20e-5	[41]
P9	532,000	1,950	0.076	9.72	8.4e-5	[41]
P10	1,180	785	0.25	0	0	[29]
P11	50,000	3,542	0.034	13.2	4.6e-5	[38]
Hydrogen	Tonne H_2 h^{-1}	M$/tonne H_2	% Capital cost	MJ $tonne^{-1}$ H_2	Tonne CO_2 $tonne^{-1}$ H_2	
H1	6.25	1,113	0.060	174,900	8.992	[45, 46]
H2	6.25	1,776	0.060	204,200	1.050	[47]
H3	32.09	2,378	0.036	209,000	18.732	[45, 46]
H4	32.09	2,507	0.036	209,000	1.502	[47]
H5	32.09	234	0.036	209,000	0.810	[47]
H6	760	145,220	0.000117	4.8	1.05	[29, 30]
H7	10.5	3,079	0.096	0.0834	1.355	[34]
H8	20.85	4,578	0.0434	0.0834	1.355	[34]

Table 3.4 Key techno-economic parameters [14 – 18]

Parameter	**Value**
Boiler feed water cost ($ $tonne^{-1}$)	1.5
Coal cost ($ GJ^{-1})	3.0
Diesel cost ($ L^{-1})	1.5
Natural gas cost ($ GJ^{-1})	7.3 – 9.6
CO_2 transport cost ($ 100km $tonne^{-1}$)	1.4
CO_2 injection cost ($ $tonne^{-1}$)	8.0
Natural gas heating value (MJ Nm^{-3})	38.05
Coal heating value (MJ kg^{-1})	24.05
Biomass heating value (MJ kg^{-1})	20.5
Biomass availability (tonne hr^{-1})	740
Annual operating hours (hours yr^{-1})	8,760
Boiler's capacity for process steam (%)	0.82
CO_2 emission base case (tonne hr^{-1})	9,195

The input data dependent on the specific operation period investigated include total bitumen and synthetic crude oil production levels, fuel prices, and emission targets. The values for these inputs for the operational periods investigated are summarized in Table 3.5.

Table 3.5 Data for the investigated periods [61, 62]

	2010	2015	2020	2025
SCO production (bbl d^{-1})	570,000	943,471	1,490,000	1,900,000
Bitumen production (bbl d^{-1})	400,000	566,082	1,290,000	1,480,000
Natural gas price ($ GJ^{-1})	7.3	8.0	9.0	9.6
CO_2 emission target (%)	0	15	30	52

3.4 Results and Discussion

A stepwise capacity expansion optimization for the Alberta oil sands energy infrastructure has been conducted for a time frame of ten years (i.e. 2015 to 2025). For the planning steps 2015, 2020 and 2025, the capacity expansion of the energy infrastructure was optimized. Two scenarios were considered for the planning period investigated. The first scenario involved the inclusion of renewable technologies in the energy infrastructure, while the second only incorporated conventional fossil fuel based technologies. The input data to the optimization model include the total production rates of bitumen and synthetic crude oil, techno-economic data of existing and new energy production technologies, CO_2 emission constraints, and fuel prices (i.e. natural gas, coal and diesel). The results for the year 2010 were used as the initial energy infrastructure and used as an input for the following year. This was assumed to be the existing energy production capacity. The model simultaneously selects the optimal set of SCO and bitumen producers, quantifies their energy requirements, and selects a set of energy commodity producers that will meet the energy demands at minimum costs while complying with the imposed CO_2 emission constraints. In the capacity expansion model the results of one planning step was used as input for the next planning step. This data includes the number of units and techno-economic data of energy production plants installed (i.e. existing technologies). It also includes the production capacities of oil

producers, which is used as a lower bound for the production capacities of producers in the following period.

Table 3.6 shows a summary of the total production volumes of mined and SAGD produced synthetic crude oil and the total energy requirements over the planning period (2015 – 2025) for both the renewable and conventional energy scenarios. For the renewable energy scenario the total integrated SAGD upgrading capacity is higher for the entire planning period in comparison to the scenario in which only fossil fuel-based technologies are considered. On the other hand, integrated mining upgrading capacity constitute a higher share of total synthetic crude oil production in the conventional energy scenario. The total production of commercial bitumen is achieved through only SAGD extraction as its production route in both the renewable and conventional energy scenarios. The total requirements for each energy commodity depends on the total production capacities of integrated mining/upgrading, integrated SAGD/upgrading and SAGD extraction for commercial bitumen. For example, the higher production level of integrated SAGD/upgrading for the renewable energy scenario results in a higher amount of SAGD steam requirements over the planning in comparison to the conventional energy scenario. Similarly the requirement of hot water, process steam and diesel, which are extensively used in mining extraction, are higher for the conventional energy scenario due to the higher production capacity of integrated mining/upgrading.

Table 3.6 Total production from mining and SAGD oil producers, and their energy requirements for both the renewable and conventional energy scenarios over the planning period (2015 – 2025)

	Renewable			**Conventional**		
	2015	**2020**	**2025**	**2015**	**2020**	**2025****
Total mined SCO (TB d^{-1})	500	691	910	500	794	965
Total SAGD SCO (TB d^{-1})	443	799	990	443	696	935
Total SCO (TB d^{-1})	943	1,490	1,900	943	1,490	1,900

Total bitumen (TB d^{-1})	567	1,290	1,480	567	1,290	1,480
Energy demand						
Power (MWh)	817	1,215	1,450	817	1,323	1,687
SAGD steam (kt h^{-1})	16	36	38.9	16	33	37.7
Water (kt h^{-1})	24	29	42	24	31	44
Process steam (kt h^{-1})	3.8	5.3	7.4	3.8	5.6	7.9
Diesel (kL h^{-1})	37	42	66.8	37	48	67.9
Hydrogen (t h^{-1})	149	253	305	149	235	323
Natural gas (Mm^3 h^{-1})	1.1	2.3	3.1	1.5	2.5	2.9
Coal (kt h^{-1})	1.3	2.4	2.0	1.3	2.2	2.8
Biomass (kt h^{-1})	0.74	1.5	2.2	NA		

**The results shown for this scenario are those obtained for the maximum emission reduction target (37%) achieved by the conventional energy mix. This value is lower than the emission reduction target required for the year 2025 (52%)

The requirements for each energy commodity also depend on the type of upgrading route integrated with the extraction method. For integrated mining/upgrading four production routes have been considered, which include a combination of thermal and hydrogen cracking (MP1), a combination of thermal and hydrocracking and an additional conditioning stage for extraction (MP2), thermal cracking (MP3), and hydrocracking (MP4). For integrated SAGD/upgrading three upgrading routes were also considered, which include a combination of thermal and hydrogen cracking (SP1), thermal cracking (SP2), and hydrogen cracking (SP3). Figure 3.4 shows the distribution of synthetic crude oil production among the considered production routes over the planning period. The upgrading routes that contribute the highest share (up to 75%) of synthetic crude oil production are based on hydrocracking (MP2, MP4 and SP3). MP4 and SP3 were selected among the most suitable integrated mining/upgrading and SAGD/upgrading SCO producers, because they are based on the highest conversion hydrocracking production routes, which yield higher SCO conversion compared to thermocracking processes and other hydrocracking routes. The hydrocracking production routes are characterized by having higher conversion of bitumen to synthetic crude oil compared to

thermocracking-based bitumen upgrading routes. Hydrocracking is a process that involves the utilization of hydrogen to breakdown large molecules in the heavy oil feedstock to smaller molecules, whereas thermocracking relies on the utilization of heat for the cracking process, which is mostly produced from burning natural gas (i.e. process fuel).

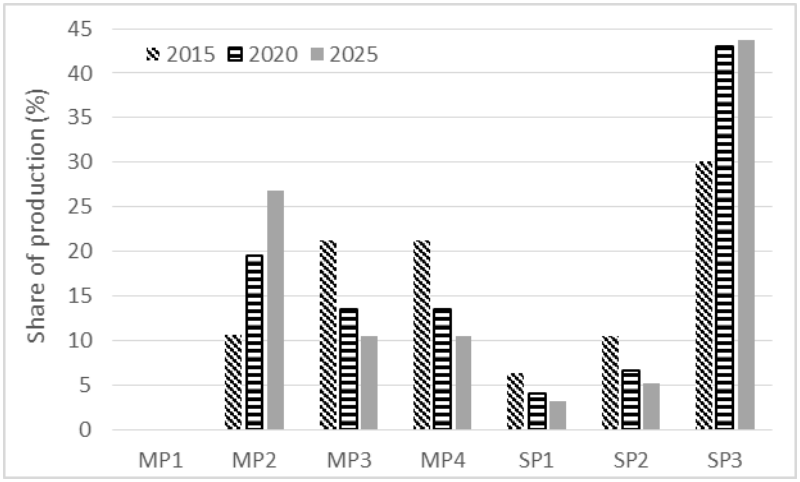

Figure 3.4 Distribution of oil proudction among mining and SAGD producers for the renewable scenario over the planning period (2015 – 2025)

Hydrogen can be inexpensively produced through coal gasification plants. Coal is an economical fuel and is considerably lower in cost compared to natural gas (Table 4). However, burning coal results in significantly higher CO_2 emissions compared to natural gas due to its higher carbon content. This tradeoff affects the selection of oil producers over the planning period, in which the emission reduction target becomes more stringent over the years, which in return requires cleaner methods of energy production. This can be a contributing factor to the reduction in the percentage share of some of the hydrocracking-based oil producers (i.e. MP4) over the planning period as shown in Figure 3.4. Even though the share of some hydrocracking upgrading routes in the total production of synthetic crude oil is decreasing, their total share in production is

considerably high. The integrated mining/upgrading routes MP1 and MP2 both have the same upgrading processes; however, MP1 incorporates an additional bitumen treatment stage during the extraction process, which is bitumen conditioning. This step requires the utilization of additional process steam and hot water. The additional requirements of energy commodities by this bitumen processing route reduces the likelihood of its selection by the optimization model.

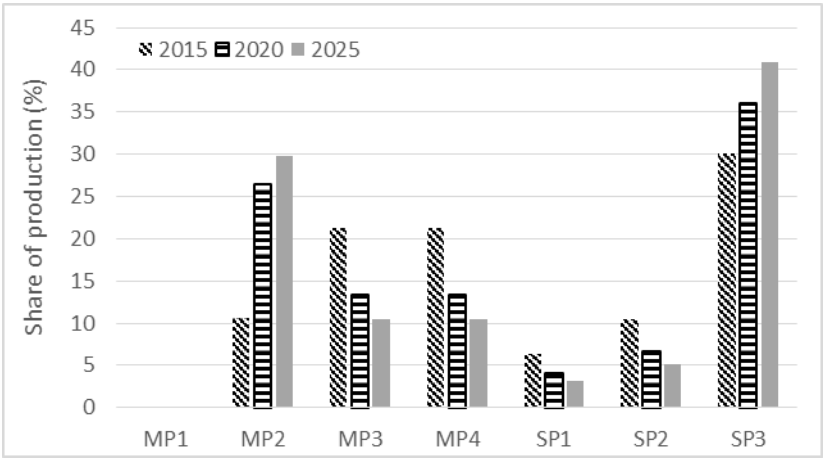

Figure 3.5 Distribution of oil proudction among mining and SAGD producers for the conventional scenario over the planning period (2015 – 2025)

Figure 3.5 shows the distribution of the percentage share of synthetic crude oil production among the oil producers for the conventional energy scenario. It can be observed that the distribution among the synthetic crude oil producers is similar to that obtained for the renewable energy scenario. The only difference that can be observed is in the total share of integrated mining/upgrading routes (MP1 – MP4) relative to integrated SAGD/upgrading (SP1 – SP3). The share of mining producers in the conventional scenario is higher than that in the renewable scenario. Moreover, the percentage increase in mining producers (MP2) is higher compared to that of SAGD producers (SP3). This is due to the significant steam requirements by SAGD producers, which can only be

produced by natural gas boilers in the conventional scenario. SAGD producers' consumption of natural gas is highly intensive compared to mining producers, which results in higher cost of energy production and CO_2 emissions. The second factor affecting the selection of oil producers is the type of upgrading route, which can be based on hydrocracking and thermocracking processes. Similar to the renewable energy scenario the largest share of synthetic crude oil production is contributed to by hydrocracking-based upgrading routes (MP2, MP4 and SP3). This is due to the availability of coal gasification in the optimization model, which results in hydrogen production being more economically attractive than utilizing natural gas for heat production in thermocracking upgrading processes.

The highest increase in the share of oil producers in the production capacity is attributed to mining production routes. The production of SCO through integrated mining/upgrading technologies represent a more preferable route compared to SAGD operations. This is due to the significant steam requirements of SAGD operations, which is mostly satisfied through the use of natural gas boilers. Another reason for favoring mining operations is due to the high steam to oil ratio (SOR) that is based on current SAGD operations, which is 2.4 tonne steam/tonne bitumen. However, with technological advances the SOR for SAGD extraction is expected to considerably decrease in the future. This is also evident in the comparison between renewable and non-renewable energy production scenarios. In the case were natural gas boilers are the only source of SAGD steam, the production from mining operations is preferred due to the lower process fuel requirements. This trend is likely to continue in the short-term future despite the fact that 80% of bitumen deposits are only recoverable through in-situ methods,

which are expected to contribute significantly to oil sands production given the expected technological advancements that will lead them to become the primary extraction processes. Even though SAGD extraction methods are expected to dominate oil sands operations in the future, a significant portion of their production is expected to be marketed as commercial bitumen instead of being upgraded to SCO. This is because crude bitumen produced through mining operations consists of significant amounts of water and suspended solids making its commercialization unfavorable. An increase in the production capacity of mining operations was accompanied by a significant increase in hot water demand, which can be attained through geothermal direct water heating that has a considerably lower carbon foot print compared to natural gas boilers.

It is important to note that the change in the environmental constraint affects the distribution of oil producers. As the environmental constraints become more stringent, the optimization model will require the selection of energy producers that minimize energy production costs for the imposed constraints. This is in agreement with data reported in the literature, which in indicated that in-situ production results in emissions that are on average 2.5 times higher than those associated with mining operations. Therefore, the model is gravitated towards increasing the capacity of integrated mining/upgrading schemes over integrated SAGD/upgrading schemes. This will in return affect the selection of oil producers, as it will increase reliance on mining based operations to reduce the steam requirements. Moreover, since the emissions from natural gas boilers are not controlled, and they are the only producers for steam and hot water for the scenario where no renewable technologies were considered, the emission constraint for the year 2025 was not met, and a lower emission reduction target was achieved

compared to the renewable scenario. However, with the incorporation of renewable technologies, particularly biomass boilers for SAGD steam production and geothermal energy for hot water production, significant GHG emission reductions were achieved. The higher production capacities available from geothermal sources increased the reliance on integrated mining/upgrading production operations.

Figure 3.6 shows the cost distribution of the net present value for each investigated scenario. The NPV was used in the cost analysis of the renewable capacity expansion optimization model. The existence of certain energy commodity producers in the oil sands energy infrastructure can affect investment decisions in future operational years. The major energy commodities that contribute to the total cost are hydrogen, SAGD steam production, and process steam production. Hydrogen is used extensively for the upgrading of bitumen to SCO in hydrocracking, which can comprise up to approximately 85% of total SCO production. Hydrogen is also extensively used in hydrotreatment processes for the removal of sulfur and other impurities. Since SAGD extraction is the only production route considered for commercial bitumen, SAGD steam represents the most important energy commodity for its production. SAGD steam is also extensively used in the production of SCO through integrated SAGD/upgrading routes considering the high SOR required for their operations. Moreover, process steam is also extensively utilized in oil sands operations as it is required for mining extraction processes, such as hydrotransport and bitumen recovery, as well as for upgrading stages. The total cost of energy production increases with the increase of the CO_2 emissions constraints. This is due to the inclusion of CO_2 capture technologies, which require an additional energy supply to compensate for the power consumption for the transportation of CO_2 through

pipelines to the underground sequestration sites. This imposes the requirement of additional independent power suppliers to satisfy the increased demand.

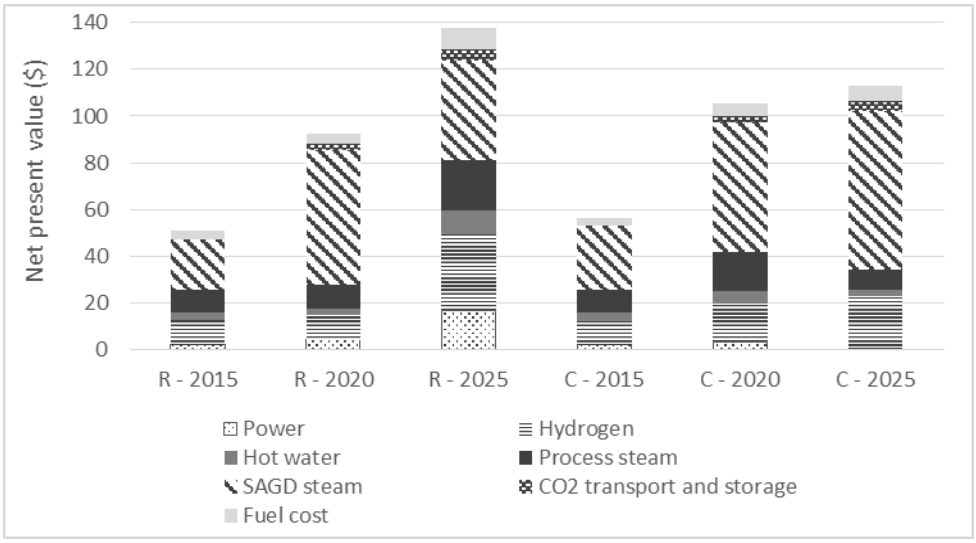

Figure 3.6 Cost distribution for the production of energy for both the Renewable (R) and Conventional (C) energy scenarios over the planning periods (2015 - 2025)

It can be observed from the results in Figure 3.7, which shows the total emissions for each operational year for both the renewable and conventional energy scenarios, that the incorporation of renewable technologies in the oil sands energy infrastructure facilitates the achievement of higher emission reductions in comparison to conventional energy technologies.

Moreover, the use of renewable energy technologies results in lower total cost of energy production for the same level of emissions reduction. This is particularly evident from the results obtained for the operational year 2020, for which the total cost of energy production was 14% higher for the conventional energy scenario. For the conventional energy scenario SAGD steam can only be produced through natural gas boilers, while biomass-fired boilers are available for SAGD steam production in the renewable energy scenario. Biomass is considerably lower in cost compared to natural gas (Table 3.4). In

this study the consumption of biomass was assumed to be carbon neutral, from which emissions are considerably lower compared to the consumption of natural gas. Moreover, the availability of geothermal energy for hot water production also significantly contributes to the reduction of natural gas consumption. The unavailability of renewable technologies requires the integration of carbon capture and sequestration into the energy infrastructure in order to be able to comply with the imposed emission constraints. This translates to a substantial increase in the cost of energy production in the conventional energy scenario.

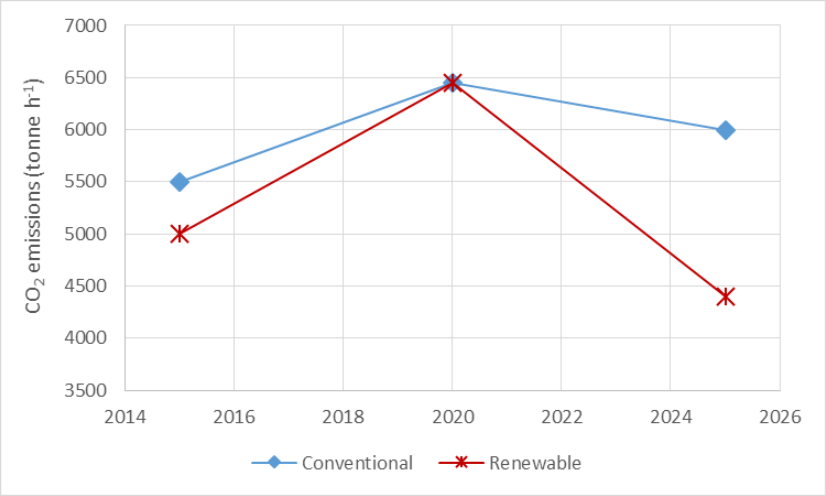

Figure 3.7 Carbon dioxide emissions for both the renweable and conventional energy scenarios over the planning periods (2015 - 2025)

The Alberta government plan to the Kyoto protocol requires the reduction of CO_2 emissions from the oil sands industry to a level of at least 50 million tonnes per year by 2020, which can be estimated as approximately 6000 tonnes per hour and will become more stringent in future years. The emission reduction constraint set for the year 2025 (50%) was not achievable through a fossil-fuel-based energy infrastructure and the optimization model returned an infeasible result. The maximum level of achievable emission reduction for the conventional energy scenario was determined to be 35%,

which is equivalent to a total emission level of 5976 tonne CO_2 h^{-1}. For the renewable energy scenario an emission reduction level of 52% was achieved, which corresponds to a total emission level of 4400 tonne CO_2 h^{-1}. The higher level of emission reduction achieved in the renewable energy scenario justifies the higher cost required for energy production during the operating year 2025. For the renewable energy scenario the cost of power is relatively high for the year 2025 as the production switches to the lowest emission technology (i.e. NG oxyfuel with CCS) included in the energy infrastructure, from which the majority of power is produced. The increase in the cost of power is driven by a substantial increase in the power demand combined with the higher capital and operating cost of the low-emission technology. The selection of biomass fired boilers for SAGD steam production and geothermal energy for the heat requirements of mining extraction played a significant role in achieving the required emission reduction levels.

Table 3.7 summarizes the set of energy commodity producers selected by the optimization model and the capacity expansion decisions for both the conventional and renewable energy scenarios over the investigated time period (2015 – 2025). The majority of hydrogen produced for both the renewable and conventional energy scenarios is achieved through coal gasification plants. Coal is a relatively economical fuel, particularly in comparison with natural gas. Moreover, this type of hydrogen plants can cogenerate electricity, which contribute in providing the electricity requirements of oil sands operations. This makes the production of hydrogen through coal gasification more efficient and economically attractive compared to other options considered in the optimization model. Cogeneration is currently incorporated in the Oil Sands energy infrastructure as an option to increase energy efficiency by using the output of one

technology (e.g. hydrogen) to drive turbines for power generation. As the GHG emission constraint becomes more stringent, the hydrogen production fleet switches to IGCC with integrated carbon capture and sequestration technologies. The incorporation of renewable energy technologies facilitates the utilization of existing-fossil fuel based producers without the requirement of emission mitigation options as overall emissions do not exceed the imposed constraint. For example, for the operational year 2020 lower capacities for CCS are required for power and hydrogen production and there is decreased reliance on less CO_2 intensive fossil-fuels (i.e. natural gas), which translates to lower production costs of these commodities.

Table 3.7 Distribution of energy producers and their production capacities (existing and newly installed) for both the conventional and renewable energy scenarios over the planning period (2015 – 2025)

Energy Producers	Renewable			Conventional		
	2015	2020	2025	2015	2020	2025
Hydrogen (tonne h^{-1})	**149**	**253**	**331**	**149**	**235**	**301**
Existing IGCC	80	80	0.0	80	53	0.0
New IGCC	70	0.0	0.0	70	0.0	0.0
Existing IGCC wCC	0.0	0.0	186	0	0.0	235
New IGCC wCC	0.0	173	42	0	182	44
Existing SR wCC	0.0	0.0	0.0	0.0	0.0	0.0
New SR wCC	0.0	0.0	102.5	0.0	0.0	22.5
Power (MWh)	**817**	**1,240**	**2,409**	**817**	**1,231**	**1,449**
Existing PC	0.0	0.0	0.0	0.0	0.0	0.0
New PC	0.0	472	0.0	0.0	472	0.0
Existing NGCC	452	363	0.0	452	409	0.0
New NGCC	0.0	0.0	0.0	0.0	0.0	0.0
New NG Oxyfuel	0.0	0.0	2,160	0.0	0.0	0.0
IGCC co-gen	365	195	0.0	365	130	0.0
IGCC w CC co-gen	0.0	210	277	0.0	220	1,449
Steam and Hot water (tonne h^{-1})	**44,140**	**73,924**	**105,810**	**44,339**	**75,913**	**91,874**
Process Steam – existing NG boilers	3,063	3,899	5,570	3,063	4,177	5,848
Process Steam – new NG boilers	798	1,451	2523	998	2228	3,013
Existing NG SAGD boilers	10,200	10,540	21,573	10,200	16,320	33,320
New NG SAGD boilers	321	19,720	0.0	6,054	15,300	4,919

Existing Biomass SAGD boilers	0.0	5,733	5,751	NA	NA	NA
New Biomass SAGD boilers	5,733	18	0.0	NA	NA	NA
Water – Existing NG boilers	18,120	23,062	14,921	18,120	24,709	34,593
Water –New NG boilers	4,723	8,581	32,946	5,904	13,178	17,822
Existing geothermal	0.0	920	1,841	NA	NA	NA
New Geothermal	1,181	0.0	20,687	NA	NA	NA

For the operation year 2025 the majority of hydrogen is still produced through coal gasification integrated with carbon capture. However, the stringent emissions constraint for this operational year requires the utilization of a cleaner fuel (i.e. natural gas). In order to comply with the imposed emissions constraints a portion of hydrogen is produced through steam methane reforming integrated with carbon capture, which is observed for the results obtained for both the renewable and conventional energy scenarios. The utilization of wind power for the production of hydrogen through water electrolysis was not selected by the optimization model. The hydrogen production capacity of the integrated wind power and electrolysis system is relatively low compared to other hydrogen production technologies in the optimization model. Moreover, the unit cost of hydrogen is considerably high due to the transportation costs from the wind-electrolysis facility in southern Alberta to the bitumen upgrading facilities. The low-emission technology does not justify the high unit production and transportation cost of hydrogen.

The power plants selected by the optimization model for the renewable scenario are natural gas gasification combined cycle (NGCC), pulverized coal (PC) and natural gas oxyfuel technologies. The power infrastructure switches from NGCC and PC to natural gas oxyfuel in order to reduce the total CO_2 emissions. Natural gas oxyfuel is the lowest emission power production technology in the energy production mix used in the

optimization model. Other economical and environmentally friendly options are available for power production, such as biomass gasification. However, the utilization of biomass for power production is limited due to its availability. The biomass feedstock available for energy production for oil the sands operations is used for the production of SAGD steam. For the conventional energy scenario the electricity requirements are mostly satisfied by the power cogenerated from coal gasification plants integrated with carbon capture.

It is evident from the results that the use of renewable energy is important in providing the heat requirements for oil sands operations. A significant portion of SAGD steam is provided by biomass fired boilers and hot water for mining extraction is provided by geothermal energy. These sources of energy were used to replace natural gas boilers in order to achieve the required emission reduction targets. The incorporation of renewable energy technologies plays a vital role in satisfying emission constraints for the year 2025, and their elimination from the energy infrastructure reduces the maximum achievable emission reduction target. For the conventional energy scenario the maximum reduction of CO_2 emissions was determined to be 35%. However, the use of renewable energy facilitates an emission reduction target of 52%.

The developed mathematical models was solved using an Intel Core 2 Duo, 2.33 GHz machine running the DICOPT solver accessed via the general algebraic modelling software [8]. The corresponding computational statistics are summarized in Table 3.8. The resulting computational times and optimality gaps for the simulation runs are satisfactory.

Table 3.8 Model computational results for all the investigated scenarios

Configuration	Renewable			Conventional		
	2015	2020	2025	2015	2020	2025
Optimality gap (%)	0	0	0	0	0	0
CPU time (s)	280	260	280	290	265	296

3.5 Conclusions

An energy optimization model that can be used to determine a well-balanced mix of renewable and conventional energy technologies that can provide the significantly increasing energy demands of Alberta's oil sands industry without increasing reliance on fossil-fuel based and nuclear energy production. The optimization model selects the optimal set of oil sands producers and energy commodity producers that minimizes the total net present value of the oil sands industry. By the large-scale introduction of renewable energy into the oil sands energy infrastructure, considerably higher emissions reductions can be achieved without being offset by the rapidly increasing energy production required to support the developments in the industry.

The model was applied to a case study to illustrate its capability using data for various years of oil sands operations (i.e. 2010, 2015, 2020 and 2025). The results were compared for the sequential (i.e. the results of one year are used as an input for the following) and the non-sequential model approaches. The sequential approach was investigated for both the incorporation and elimination of renewable technologies in the energy infrastructure. The results from the sequential approach indicate that the existing infrastructure has an impact on new investment decisions. Due to the lower cost of existing technologies, the model is more reluctant to switch to cleaner alternatives (i.e.

less carbon intensive fuels and renewables). However, the sequential approach provides a more realistic presentation of the oil sands operations.

The results also show that renewable energy technologies have significant potential in reducing emissions from energy production for the oil sands operations. The incorporation of these technologies allowed achieving the same or higher emission reductions at lower total cost of energy production. Moreover, for the year 2025 the emission constraints were considerably high to be achievable using only fossil-fuel based technologies, which resulted in the model becoming infeasible. However, including renewables in the energy mix facilitated the achievement of the required emission reduction levels.

In all the investigated scenarios the model preferred the selection of upgrading routes that are based on hydrocracking processes. This is because hydrogen can be inexpensively produced through coal gasification technologies in addition to coproducing power to be supplied to other oil sands operations. Integrated mining/upgrading production routes were generally favored by the optimization model, which is a trend that is expected to prevail in the short-term future. This is due to the lower steam requirement by these production routes compared to SAGD operations. These production routes require significant amounts of hot water; however, this can be provided by geothermal plants, which are economically attractive and have low carbon emissions associated with them. However, based on oil production forecasts in the literature it is expected that in the long-term future SAGD production routes will be dominant in the production of commercial bitumen and SCO. The provision of steam to support these operations was unfavorable based on the results of the optimization model. Besides the limited resources of steam

production from biomass, natural gas boilers were the only other production routes for which carbon mitigation options were not incorporated. This will hinder the achievement of the desirable emission reductions, and therefore, in future work it is important to consider other less carbon intensive alternatives for steam production in the energy infrastructure (e.g. steam production from nuclear energy).

The results obtained indicate that the proposed energy optimization model is a powerful tool that allows the scheduling and planning of future production scenarios of oil sands operations. However, the disadvantage of the proposed model is that it does not involve the optimization of the entire planning time frame at once. The results obtained from optimizing the entire time frame are expected to be different from the sequential approach used in this paper. This can be accounted for by the incorporation of a time index in the energy optimization model, which will be addressed in future work. This will also facilitate the incorporation of time variable parameters, such as oil production levels, fuel prices, government emission regulations, construction lead times, etc. Accordingly, the authors developed the multi-period energy optimization model to represent the operations of the Canadian oil sands industry, which is studied in Chapter 4.

Chapter 4

General optimization model for the energy planning of industries including renewable energy: A case study on oil sands[2]

4.1 Introduction

After fossil fuel and electricity production, Canada's most energy-intensive industries (e.g. industrial chemicals, cement, smelting, etc.) are considerably large and typically represent the mainstay of their regional and local economies. The industries are an important and defining element of the Canadian economy [68]. However, their energy production costs can represent more than 20% of the value added, and up to 60% of the operating costs. The cost of production from these industries is expected to significantly increase in the future due to the expected continuous increase in the prices of the fuels used to provide their energy requirements, as well as the governmental legislations to achieve GHG emission reductions [69]. Therefore, it can be deduced that the integration of clean energy production technologies to reduce GHG emissions in the context of any energy-intensive industry is a challenging problem, considering the uncertainty revolving around future environmental legislation, fuel supply and prices, and future production levels and their associated energy intensities. This is particularly evident for the oil sands industry, which is the most energy-intensive industry and the largest contributor to the growth of GHG emissions in Canada.

The province of Alberta is currently facing a significant challenge in balancing the development of the growing oil sands industry and the reduction in the provincial annual

[2] A variant of this chapter is published: M. Elshokami and A. Elkamel. AIChE J, 2017, 63(2), 610-638.

greenhouse gas (GHG) emissions. In the Climate Change Strategy of Alberta in 2008 the province committed to reducing its 2005 GHG emissions levels by 50 megatonne per year by 2020, and achieve a reduction of 200 megatonne per year by 2050 [70]. The production of unconventional fossil fuels such as bitumen extraction from oil sands is facing challenges due to the energy-intensive nature of their production, from which emissions are expected to increase by threefold by the year 2030. As a result, in order to achieve the required emission targets, the province will have to reduce the production of emissions from oil sands operations, which have contributed to making it the most GHG intensive province in Canada. In the future the contribution of oil sands extraction operations to the production of emissions in the province will be largely dictated by the supply of energy required to support them [71].

The Alberta Oil Sands are the third largest crude oil proven reserves in the world after Saudi Arabia and Venezuela, which amount to 168 billion barrels constituting approximately 97% of Canada's total oil reserves [72]. Approximately 20% of these reserves are shallow enough to be recovered through mining operations. However, the remaining volumes are only recoverable through in situ techniques, in which the oil sands formations are heated in order to enhance the flow of bitumen to the surface [73]. The exploitation of oil sands reserves is dependent on their Energy Return on Investment (EROI), which is the ratio of the energy in the extracted bitumen or produced synthetic crude oil to the energy used for their production. The EROI has a significant impact on the long term viability of oil sands operations, and it is affected by several factors which include the bitumen extraction and upgrading processes selected and the type of energy

(i.e. electricity, heat, hydrogen, etc.) production technologies used to satisfy their energy requirements [74].

The oil sands are a mixture of bitumen, sand, clay and water, from which bitumen (a heavy viscous form of crude oil) is extracted and upgraded to a refinable form of oil (i.e. synthetic crude oil). A significant amount of energy is required for these operations, which makes the Canadian oil sands one of the most energy intensive crude oil production industries in the world [75]. The most prominent bitumen extraction techniques are surface mining and steam assisted gravity drainage (SAGD), and the most prominent upgrading processes are based on thermocracking and hydrocracking technologies. In these processes energy is consumed in the form of electricity, steam, hydrogen, and fuel (i.e. heating and transportation). Currently, this energy is mostly provided by burning natural gas, in which the energy production mix for it is constituted by grid electricity, stand-alone steam generation, on-site cogeneration, steam methane reforming, and natural gas furnaces [76].

Natural gas was initially utilized as a measure to reduce the GHG emissions associated with energy production for oil sands operations. However, the continuously increasing oil sands production levels are offsetting the achieved emission reductions [71]. GHG emissions associated with oil sands operations accounted for approximately 12% of Canada's total emissions in 2014, and represent the mostly rapidly increasing source of GHG emissions in the country [77]. In addition, further restrictions are imposed on the lifecycle GHG emissions of transportation fuels, such as California's Low Carbon Fuel Standard. All of this provide an incentive for oil sands operators to implement measures for further reduction in GHG emissions associated with bitumen extraction and upgrading

processes. Moreover, there are growing concerns regarding the resource availability and price volatility of natural gas, which have prompted industries to consider alternative fuels and options for energy production. The oil sands industry utilized approximately 3,400 million cubic feet per day (MMcf/day) of natural gas in 2015, and the industry's consumption rate of natural gas is expected to reach up to 5,800 MMcf/day by 2030 [78].

According to Reilly et al. [79], global climate policies have a significant impact on the development of the oil sands industry in Alberta. This indicates that it is in the interest of oil sands operators and developers to reduce the GHG emissions associated with their bitumen extraction and upgrading processes. The oil sands industry considered numerous options to reduce the utilization of natural gas. Several studies in the literature have proposed less carbon-intensive energy production methods for the Alberta oil sands, which include nuclear energy for power and heat production [80-85], integrated wind-electrolysis for hydrogen production [86, 87], bioenergy [88], and geothermal energy [89-93]. Several studies also investigated the possibility of utilizing alternative fuels, such as bitumen, asphaltenes, petroleum coke and coal, which are readily available fuels in Alberta. These alternative fuels have variable properties (e.g. carbon content, energy density, cost, etc.) and, therefore, they have different life cycle effects [94 -96]. Other studies considered reducing the consumption of natural gas by improving the efficiency of energy production, for example, through increasing the capacity of combined heat and power generation instead of the currently utilized standalone systems [76, 97]. Moreover, the government of Alberta is expecting significant reductions in CO_2 emissions to be achieved through the integration of carbon capture and sequestration technologies with the large emitters in the province [81]. In each of these studies a potential alternative is

compared to the currently utilized energy mixture using a scenario-based analysis in terms of factors such as cost, environmental impacts, accessibility, system reliability, energy use, etc.

Based on the above considerations, it is important to develop reliable modeling tools that can be utilized to estimate the production and environmental costs for providing energy for the Canadian oil sands operations. Optimization mathematical modeling tools can be used for the planning and scheduling of the energy production requirements of the Canadian oil sands, which can provide an indication of the potential optimal energy infrastructure that can be utilized by the industry. Similarly, these tools facilitate the investigation of the effects of uncertainty in key techno-economic parameters, such as natural gas prices, CO_2 emission targets and credits, oil sands production levels and their energy intensities, etc., on the selection of energy production technologies and the cost of energy production. Mathematical optimization models describing the Canadian oil sands operations have been recently introduced in the literature [98 – 104]. In these studies, the most suitable energy infrastructure is selected for a given oil production infrastructure. They only considered fossil fuel-based (natural gas and coal) and standalone energy production technologies. However, there have been various studies proposing the possibility of including less carbon intensive technologies in the oil sands energy infrastructure, such as nuclear energy, renewable energy (i.e. wind, bioenergy, and geothermal), and cogeneration (power, heat and hydrogen) energy systems [82 – 96]. Moreover, the mathematical models proposed in these studies adopt a deterministic snapshot approach, in which the operations of oil sands are investigated only for a given

point in time without considering the variability of parameters over a long-term planning horizon that would lead to a phased infrastructure development.

There are various factors that have a significant impact on planning the energy infrastructure of the oil sands industry that are variable with time. These include the continuously increasing CO_2 emission reduction targets required in order to achieve international environmental standards as per the United Nations Framework and Kyoto protocol [105, 106]. Moreover, emitters in Alberta that are unable to meet the emission reduction targets will be required to pay a carbon tax, which was CAD 15 per tonne of CO_2 in 2015 and is expected to considerably increase in the future [107, 108]. A major driver for the cost of natural gas energy production systems that constitute the majority of oil sands energy infrastructure is the fuel price, for which there are concerns regarding its volatility over the next few decades [76]. Other time-dependent parameters include forecasted energy demand intensities and oil sands production levels, construction lead time, capital and operating costs, etc. Although the above issues can be addressed individually, a comprehensive approach that integrates their interaction is currently lacking. Based on these considerations, it is important to develop a mathematical model that optimizes the development of the energy infrastructure over an entire planning time frame (e.g. 20 – 30 years).

Several studies have been published on using multi-period optimization methods for energy planning purposes. Numerous works have been published on optimizing the power generation planning of electric systems in the power sector [68, 108-115]. The models are typically geared towards minimizing the cost of electricity production to meet specified energy demands subject to a set of emission constraints. The time dependent

parameters considered include forecasts of energy demand, lead time and costs of energy systems, conservation initiatives, fuel prices, etc. Several studies have also considered the incorporation of multiple energy carriers as well as different forms of energy demands, particularly electricity and heat (i.e. space and water heating). The models developed in these studies are formulated to incorporate regional energy demands, some of which incorporate industrial energy requirements. However, models that focus on incorporating the needs of energy intensive industries (e.g. chemical, steel, cement, pulp and paper, etc.) to integrate energy efficiency performance in production management are scarce. This necessitates the development of an optimization based approach to apply the current knowledge of clean energy production technologies with an emphasis on energy-intensive industrial operations to achieve CO_2 emission reductions in an emission-constrained environment considering variability in time-dependent parameters.

Within the above context, this study proposes a generalized multi-period mathematical optimization model that is geared towards minimizing the costs of supplying the energy requirements of an energy-intensive industry, such as the oil sands industry in Alberta, subject to various CO_2 mitigation policies. The formulated mixed integer linear programming (MILP) model considers multi-period factors, low-carbon intensive energy production, and CO_2 abatement technologies. Moreover, the implementation effects of different carbon mitigation policies are investigated and compared quantitatively. The results obtained can provide an indication of the optimal configuration of the energy infrastructure that will meet the current and future energy requirements and the required emission reduction targets over the specified planning period. This is accomplished by selecting the types, number and production capacities of energy production technologies

and carbon mitigation options. To the author's knowledge, generalized multi-period mathematical optimization models used for the energy planning of energy-intensive are not available in the literature. Moreover, the application of the proposed model is novel, as there have been no multi-period energy planning optimization models applied to the case study based on the energy intensive oil sands operations in Alberta over a long time horizon (i.e. 2015 – 2050), in order to examine the economical and structural impact on the energy production fleet when considering variability in oil sands production levels, energy demand intensities, carbon mitigation policies, and fuel prices, as well as variability in time-dependent parameters. This will assist governmental or industrial policy makers in making decisions of the energy planning for oil sands operations. It is important to note that the superstructure-based optimization energy planning model built is generalized, and is suitable to be utilized to determine the optimal energy infrastructure required for any energy-intensive industry.

4.2 Optimization model formulation

The proposed optimization model is based on the superstructure shown in Figure 4.1. The energy requirements for an energy intensive industry is supplied by a set of energy commodity producers. These include fossil-fuel based (i.e. coal and natural gas), combined heat and power, renewable, nuclear, and polygeneration gasification of alternative fuels (i.e. coal, bitumen, asphaltene, petcoke, and biomass) technologies. These producers are used to generate electricity, heat (i.e. steam, hot water, etc.), fuels (e.g. hydrogen, synthetic gas, synthetic diesel, etc.). The model also consider the possibility of integrating carbon capture and sequestration as an emission mitigation

option. The energy optimization model will be used to estimate the cost of energy production subject to a carbon mitigation policy.

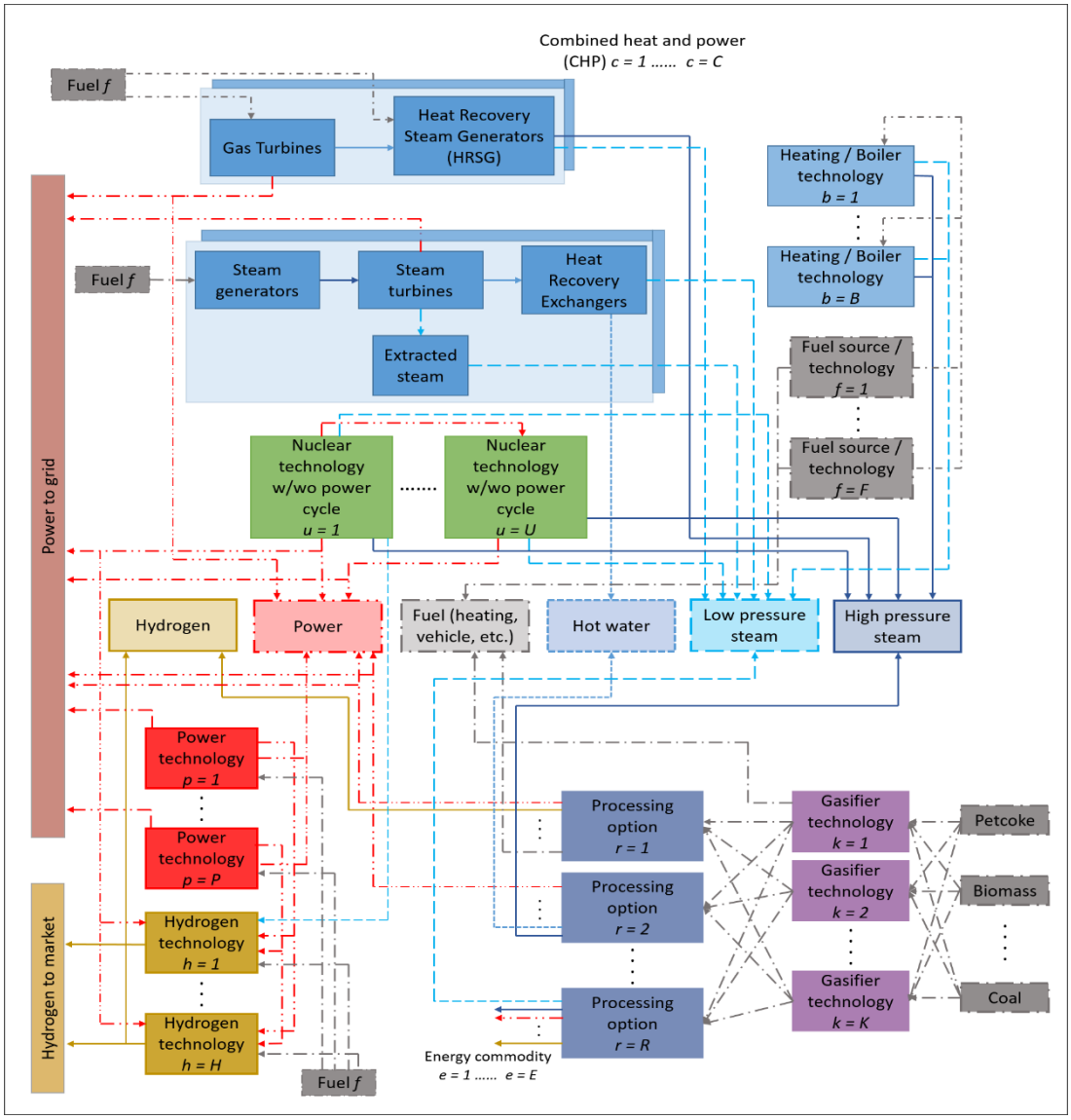

Figure 4.1 Superstructure of the proposed energy optimization model

The carbon mitigation constraint consists of an emission cap, an allocated carbon credit/tax, carbon credit buying (i.e. agents can buy a required amount of carbon credits from global carbon markets or carbon exchanges to offset their emissions), and carbon credit selling (i.e. an additional incentive to reduce their emissions; agents can earn

revenue by selling their surplus carbon credits) [115]. The results of the optimization model include the capacity of energy producers, the cost of energy production, and the total annual emissions generated. Each of the modeling aspects included in the formulation of the mathematical optimization model are discussed below. The indices, sets, variables, and parameters used in the proposed energy planning model are presented in Appendix A. The time scale of this energy planning model is annual.

4.2.1 Energy requirements

In the proposed mathematical model the inputs are represented by the required annual total production of the final products (e.g. synthetic crude oil and commercial bitumen), the carbon dioxide emission targets, and the type and number of energy producers available over the planning period. The production data and the emission targets are either obtained from forecast data or are specified by the user.

The amount of energy required is represented by an energy-intensity factor, which can be defined as energy consumption per unit of production. The total amount of each energy commodity required for the production of each final product can be calculated as follows.

$$DEC_{et} = \sum_{q} \sum_{j \in J_q} EI_{eqj} QP_{qjt}^{T} \qquad \forall\, e, t \tag{4.1}$$

where EI_{eqj} is the energy intensity of each energy commodity e (e.g. electricity, heat, steam, hydrogen, etc.) per each product q (e.g. synthetic crude oil, commercial bitumen, etc.) produced through production route j, QP_{qjt} is the production rate for each product via production route j during time period t, and DEC_{et} is the total amount of each energy commodity required. The production capacity for each product (e.g. SCO) from all

production routes *j* must satisfy the production requirements for each operational year, which can be presented by the following constraint.

$$\sum_{j \in J_q} QP_{qjt}^{T} \leq QPR_{qt} \qquad \forall\, q, t \tag{4.2}$$

It is also important to ensure that the production capacity for each production route added during a certain time period is carried over for the following time periods, which is enforced by the following constraint.

$$QP_{qjt}^{T} = QP_{qj,t-1}^{T} + QPCE_{qjt} \qquad \forall\, q, t \tag{4.3}$$

where $QPCE_{qjt}$ is the capacity added during time period *t*. Finally it is important to limit the capacity added during each time period *t* to the maximum available capacity expansion, which is presented by the following constraint.

$$QPCE_{qjt}^{MIN}\ ze_{qjt} \leq QPCE_{qjt} \leq QPCE_{qjt}^{MAX}\ ze_{qjt} \qquad \forall\, q, t \tag{4.4}$$

4.2.2 CO_2 mitigation constraint

In order to not exceed the emission cap imposed on an industry, the following constraint on CO_2 emissions is incorporated.

$$\sum_{i} \sum_{n \in N_i} \left(ECO2_{int}^{new} + ECO2_{int}^{exist}\right) - Creditbuy_t + Creditsell_t \leq CO2_t^{limit} \quad \forall\, t \tag{4.5}$$

where the amount of CO_2 produced from the all newly established ($ECO2_{int}^{new}$) and existing ($ECO2_{int}^{exist}$) energy producers must not exceed the imposed emission cap ($CO2_t^{limit}$) for each time period *t*. The CO_2 constraint presented in Eq. 3.5 also considers the potential reduction of CO_2 by means of purchasing carbon credits ($Creditbuy_t$). The carbon emissions produced by the entire energy production fleet can be reduced by

purchasing CO_2 credits for that year in order to satisfy the emission cap. An additional incentive is also added in order to encourage industries to further reduce their emissions, in which they can earn revenue by selling their surplus carbon credits ($Creditsell_t$). This is achieved if their emissions are lower than the imposed cap for any of the investigated years.

4.2.3 Power module

In this section, only standalone power plants are discussed, which are defined to be energy producers from which the net energy output is only in the form of electricity. These include fossil-fuel based technologies and renewable technologies (e.g. hydropower and wind turbines). The fossil-fuel based standalone power plants considered in this optimization model include natural gas combined cycle (NGCC), supercritical pulverized coal (SCPC), and oxyfuel. The technologies are considered with and without carbon capture, which could either be post-combustion or oxy-combustion. The first is utilized in integration with NGCC and SCPC power plants and the latter is integrated with oxyfuel plants. The oxyfuel plants considered can utilize either natural gas or coal as a fuel [116-120]. Other standalone power production options considered in the model include renewable options such as wind turbines, solar panels, hydropower, etc. The production of power from technologies that can produce multiple energy commodities (e.g. nuclear, gasification, and combined heat and power) will be discussed later in the upcoming sections. The total cost of power production from standalone plants can be calculated as follows.

$$PC_t^{total} = \sum_p \sum_{n \in N_p} CCP_{pt}\, PMAX_{ptt'}\, np_{pnt'} + \sum_p \sum_{n \in N_p} FOP_{pt}\, PMAX_p\, yp_{pnt} \quad (4.6)$$

$$+ VOP_{pt}\ PP_{pnt} TT + \sum_{p \in P^F} \sum_{n \in N_p} CFP_{pt}^F FCP_{pnt}^F TT$$

where np_{pnt} is a binary variable that indicates if unit *n* of power plant type *p* is constructed during period *t*, CCP_{pt} is the capital cost, yp_{pnt} is a binary variable that indicates if the power plant is operational during time period *t*, PP_{pnt} is the amount of power produced from each unit, FOP_{pt} and VOP_{pt} are the fixed and variable operation and maintenance costs, respectively, FCP_{pnt}^F is the amount of fuel consumed by each fossil-fuel based power plant, and CFP_{pt}^F is the cost of fuel utilized by technology *p*. The amount of fuel consumed (FCP_{pnt}^F) by each fossil-fuel based power plant can be calculated as follows.

$$FCP_{pnt}^F = \frac{HRP_p^F\ PP_{pnt}^F}{HVP_p^F} \qquad \forall\, p \in P^F, n \in N_p\,, t \quad (4.7)$$

where HRP_p^F is the heating rate (MJ/kWh) and HVP_p^F is the heating value of the fuel utilized. Power production from renewable technologies can be estimated by using the production potential of a production unit (e.g. wind turbine) and the capacity factor, which is estimated based on the renewable energy potential for the location of interest. For example, a wind turbine with a rated power of 1800 kW located in Pincher Creek Alberta will have a nominal annual energy yield of 15,768,000 kWh, which is the amount of power produced if the wind turbine is operated at maximum capacity (i.e. depicts the ideal scenario in which the wind speed is maintained at the rated turbine wind speed). The capacity factor can then be defined as the ratio of the actual annual energy yield to the nominal energy yield. The annual energy yield is determined based on the variability

of the wind resource over a particular year, and can be estimated using various methods in the literature [86, 87]. Therefore, the amount of power produced (PP_{pnt}^{R}) from renewable technologies can be estimated as follows.

$$PP_{pnt}^{R} = CF_{pt}^{R}\, NPY_{pt} \qquad \forall\, p \in P^{R}, n \in N_{p}\,, t \tag{4.8}$$

where CF_{pt}^{R} is the estimated annual capacity factor and NPY_{pt} (kWh) is the nominal power yield for each technology. The total power produced from each unit can potentially be directed towards satisfying the power requirements of the industry (e.g. oil sands operations), exported to the grid, and used to satisfy the power requirements of other energy production technologies (e.g. power for electrolytic hydrogen production). It is assumed that only power from fossil-fuel based plants integrated with carbon capture and from renewable plants can be exported to the grid or utilized to produce clean hydrogen via electrolysis. This is illustrated in Eq. 4.9 as follows.

$$PP_{pnt} = PP_{pnt}^{GRID} + PP_{pnt}^{DEM} + PP_{pnt}^{H} \qquad \forall\, p \in (P^{F-CCS} \cup P^{R}), n \in N_{p}\,, t \tag{4.9}$$

where PP_{pnt}^{DEM} is the power used to satisfy the demand of the industrial operations, PP_{pnt}^{GRID} is the excess power exported to the grid, and PP_{pnt}^{H} is the power exported to hydrogen production facilities to satisfy their electricity requirements.

4.2.4 Hydrogen module

In this section, only standalone hydrogen plants are discussed, which are defined to be energy producers from which the net energy output is only in the form of hydrogen. For standalone hydrogen production plants, the proposed superstructure considers fossil-fuel based technologies, such as steam methane reforming (SMR). These plants are modeled according to [121 – 125], and are considered with and without CO_2 capture. Another

option considered for hydrogen production involves the use of water electrolysis utilizing power from the grid, nuclear energy and renewable power. The electrolyzers considered in this study are modeled according to the approach in Olateju et al. [86, 87]. The total cost of hydrogen production from these options can be estimated as follows.

$$HC_t^{total} = \sum_h \sum_{n \in N_h} CCH_{ht}\, HMAX_{htt'}\, nh_{hnt'} + \sum_h \sum_{n \in N_h} FOH_h\, HMAX_h\, yh_{hnt} + VOH_h\ HP_{hnt} TT + \sum_h \sum_{n \in N_h} CFH_{ht} FCH_{hnt} TT \quad (4.10)$$

where nh_{hnt} is a binary variable that indicates if unit n of hydrogen plant type h is constructed during period t, CCH_{ht} is the capital cost, yh_{hnt} is a binary variable that indicates if the hydrogen production unit is operational during time period t, HP_{hnt} is the amount of hydrogen produced from each unit, FOH_{ht} and VOH_{ht} are the fixed and variable operation and maintenance costs, respectively, FCH_{hnt}^F is the amount of fuel consumed by each fossil-fuel based hydrogen plant, and CFH_{ht}^F is the cost of fuel utilized by technology h. The production of hydrogen might require the consumption of other energy commodities. For example, SMR requires the consumption of fuel (i.e. natural gas) for the chemical reaction of generating hydrogen from methane, and for heat production through combustion that is required for the endothermic reaction to occur. In this model the heat required for hydrogen production can be produced from fuel combustion or from nuclear energy [83, 84]. Moreover, the production of hydrogen through water electrolysis requires the consumption of power, which is imported from the grid or from renewable and nuclear energy. The fuel, power and heat requirements for hydrogen production can be modeled according to Eq. 4.11 – 4.13.

$$FCH_{hnt}^{F} = FRH_{h}^{F}\, HP_{hnt}^{F} \quad \forall\, h \in H^{F}, n \in N_h\,, t \tag{4.11}$$

$$HPC_{hnt} = PReq_{h}^{H} HP_{hnt} \quad \forall\, h \in H^{ELEC}, n \in N_h\,, t \tag{4.12}$$

$$HHC_{hnt}^{H} = Heat_{h}^{H} HP_{hnt} \quad \forall\, h \in H^{SMR}, n \in N_h\,, t \tag{4.13}$$

The amount of heat required for hydrogen production must be equal to the amount of heat produced specifically for hydrogen production that is obtained from fuel combustion and nuclear plants as presented in the following equation.

$$\sum_{u}\sum_{n\in N_u} HeatU_{unt}^{H} + \sum_{h}\sum_{n\in N_h} FCH_{hnt}^{heat} HVH_{h}^{F} = \sum_{h}\sum_{n\in N_h} HHC_{hnt}^{H} \quad \forall\ t \tag{4.14}$$

where $HeatU_{unt}^{H}$ is the amount of heat available from nuclear energy, and FCH_{hnt}^{heat} is the amount of fuel consumed for the production of heat. Moreover, the amount of power consumed by hydrogen production plants must be equal to the amount of power imported from the grid, and the amount of power from standalone power plants and nuclear plants produced specifically for hydrogen production, which is presented by the following constraint.

$$\begin{aligned}\sum_{h}\sum_{n\in N_h} HPC_{hnt} \\ = \sum_{p\in\left(P^{F-CCS}\cup P^{R}\right)}\sum_{n\in N_p} PP_{pnt}^{H} + \sum_{u}\sum_{n\in N_u} PowU_{unt}^{H} \\ + PGrid_{t}^{ELEC} \quad \forall\ t\end{aligned} \tag{4.15}$$

where PP_{pnt}^{H} and $PowU_{unt}^{H}$ are the amounts of power available for export from standalone power plants and nuclear plants, respectively, and $PGrid_{t}^{ELEC}$ is the amount of power exported from the grid to by utilized by electrolyzers. Finally, the amount of

hydrogen produced via electrolysis can be used to satisfy the demand of industrial operations or sold to the market, which is illustrated as follows.

$$HP_{hnt} = HP_{hnt}^{DEMAND} + HP_{hnt}^{MARKET} \qquad \forall\, h = Electrolyzers, n \in N_h, t \qquad (4.16)$$

4.2.5 Boilers

In the proposed model any technology utilized to heat water to generate high pressure steam, low pressure steam and hot water is classified under the set of boilers. For example, natural gas boiler and any preheating technology (e.g. geothermal energy, solar energy, waste heat recovery) utilized to heat feed water sent to boilers or heat recovery steam generators are classified under the set of boilers. The total cost of producing steam and hot water from boilers can be calculated as follows.

$$\begin{aligned} BC_t^{total} = & \sum_b \sum_{n \in N_b} CCB_b\, BMAX_{bt\prime t}\, nb_{bnt\prime} \\ & + \sum_b \sum_{n \in N_b} (FOB_b\, BMAX_b\, yb_{bnt} + VOB_b\, BP_{bnt} TT) \\ & + \sum_b \sum_{n \in N_b} CFB_{bt} FCB_{bnt} TT \\ & + \sum_{b\prime \in B_{PH}} \sum_{n \in N_{b\prime}} CCB_{b\prime}^{PH}\; HRMAX_{b\prime t t}^{Preheat}\, nb_{b\prime nt\prime}^{PH} \\ & + \sum_{b\prime \in B_{PH}} \sum_{n \in N_{b\prime}} \big(FOB_{b\prime}^{PH} HRMAX_{b\prime}^{Preheat}\, yb_{b\prime nt}^{PH} \\ & + VOB_{b\prime}^{PH}\, HRX_{b\prime nt}^{Preheat} TT\big) \end{aligned} \qquad (4.17)$$

where nb_{hnt} is a binary variable that indicates if unit *n* of boiler type *b* is constructed during period *t*, CCB_{bt} is the capital cost, yb_{bnt} is a binary variable that indicates if the boiler unit is operational during time period *t*, BP_{bnt} is the amount of steam or hot water

produced from each unit, FOB_{bt} and VOB_{bt} are the fixed and variable operation and maintenance costs, respectively, FCB^{F}_{bnt} is the amount of fuel consumed by each boiler, and CFB^{F}_{bt} is the cost of fuel utilized by boiler b.

Boilers convert energy from fuel or electricity to produce heat. The heat is utilized to generate high pressure steam, low pressure steam, and hot water. The efficiency of the boiler determines the energy loss and is specific to each type of boiler. This has an effect on the actual amount of energy input consumed. Moreover, the feed water to the boiler can be preheated through various options. For example, renewable energy sources, such as solar and geothermal energy, could be integrated with conventional boilers and steam cycles to preheat the feed water to the system. Also, preheated water can be utilized directly by end users (e.g. hot water used in the bitumen extraction process from oil sands). In many industrial applications it is also possible to recover waste heat streams for preheating water [126 – 128]. For example, Butler and Dwa [129] investigated various possibilities to capture low grade heat from existing plants (e.g. coal power plants) and potential benefits of utilizing the heat in low grade thermal energy applications (e.g. preheating boiler feed water), which provides significant potential in reducing fuel consumption and emission intensity in heavy industrial applications (e.g. pulp and paper industry). It will be assumed that the change of enthalpy achieved in the boiler is equal to the total amount of heat produced from fuel combustion, as well as the amount of heat obtained from the preheating sources. This is expressed by the following constraint.

$$BP^{G}_{bnt}\,\Delta HB_{b} = \left(HV^{NG}FCB^{G}_{bnt} + HV^{syn}SynS^{G}_{bnt}\right)\eta^{G}_{b} + \sum_{b\prime}\sum_{n\prime\in N_{b\prime}} HRX^{Preheat}_{b\prime n\prime t}\,\eta^{preheat}_{b\prime} \quad \forall\, b, n \in N_{b}\,, t \tag{4.18}$$

where BP_{bnt}^{G} is the amount of steam or hot water produced from boiler type b, ΔHB_b is the required change in enthalpy per unit mass of steam or hot water, FCB_{bnt}^{G} is the amount of fuel consumed, $SynS_{bnt}^{G}$ is the amount of syngas exported from gasification facilities and consumed by each boiler, HV^{NG} and HV^{syn} are the heating values of fuel and syngas, respectively, $HRX_{b\prime nt}^{Preheat}$ is the amount of heat available from each preheating option *b'*, and η_{b}^{G} and $\eta_{b\prime}^{preheat}$ are the efficiencies of boiler and preheating technologies, respectively. The feed water entering each boiler from which steam or hot water is produced is written as the sum of water flowrate coming from all preheating options associated with boiler type *b*. This is presented as follows.

$$BP_{bnt}^{G} = \sum_{b\prime} \sum_{n' \in N_{b\prime}} BP_{bnb\prime n\prime t}^{GtoP} \qquad \forall\, b, n \in N_b\,, t \tag{4.19}$$

Similarly, the amount of feed water entering each preheating option must be equal to the sum of flowrates to each boiler, and is presented as follows.

$$BP_{b\prime n\prime t}^{Pre} = \sum_{b} \sum_{n \in N_b} BP_{bnb\prime n\prime t}^{GtoP} \qquad \forall\, b', n' \in N_{b\prime}\,, t \tag{4.20}$$

The flow of water from preheating option *b'* to boiler *b* should not exceed the maximum capacity of the boiler or the preheating option. This is presented by the following constraints.

$$BP_{bnb\prime n\prime t}^{GtoP} \leq BMAX_{b}^{G}\, bp_{bnb'n't} \quad \forall\, b, n \in N_b, b', n' \in N_{b\prime}\,, t \tag{4.21}$$

$$BP_{bnb\prime n\prime t}^{GtoP} \leq BMAX_{b\prime}^{Pre}\, bp_{bnb'n't}\ \forall\, b, n \in N_b, b', n' \in N_{b\prime}\,, t \tag{4.22}$$

where $bp_{bnb'n't}$ is a binary variable that indicates the existence of the interconnection between a boiler and a preheating technology. Moreover, it is assumed that each boiler

technology can only be connected to one preheating option, which is presented by the following constraint.

$$\sum_{b'} \sum_{n' \in N_{b'}} bp_{bnb'n't} \leq 1 \qquad \forall\, b, n \in N_b\,, t \tag{4.23}$$

The heat rate from each preheat option can raise the enthalpy of feed water by a certain amount, which can be expressed as a percentage of the total enthalpy change. This constraint is imposed in order to ensure that the preheating results only in a certain change in the specific enthalpy, and is expressed as follows.

$$HRX_{b'n't}^{Preheat} \eta_{b'}^{preheat} = BP_{b'n't}^{Pre}\, \Delta HB_{b'}^{Preheat} \qquad \forall\, b, b' \in B'_{PH}, n \in N_b\,, t \tag{4.24}$$

4.2.7 Industrial combined heat and power system

The industrial natural gas combined heat and power system consists of gas turbines and/or extraction condenser steam turbines that are used for power generation. The steam turbines might be fed by high pressure steam produced by boilers or from heat recovery steam generators, which recover heat from the exhaust of gas turbines. Supplementary fuel might be combusted in addition to the heat recovered in order to raise the enthalpy of steam to a desired state. The gas turbines utilize natural gas and syngas from gasification facilities as fuel in the combustion chambers, and the high pressure steam generators can utilize various fuels (Figure 4.2). The industrial cogeneration system is modeled according to the approaches in [76, 112, 130, 131]. It is assumed that the system consists of depressurizing valves to control the pressures of steam to the desired levels.

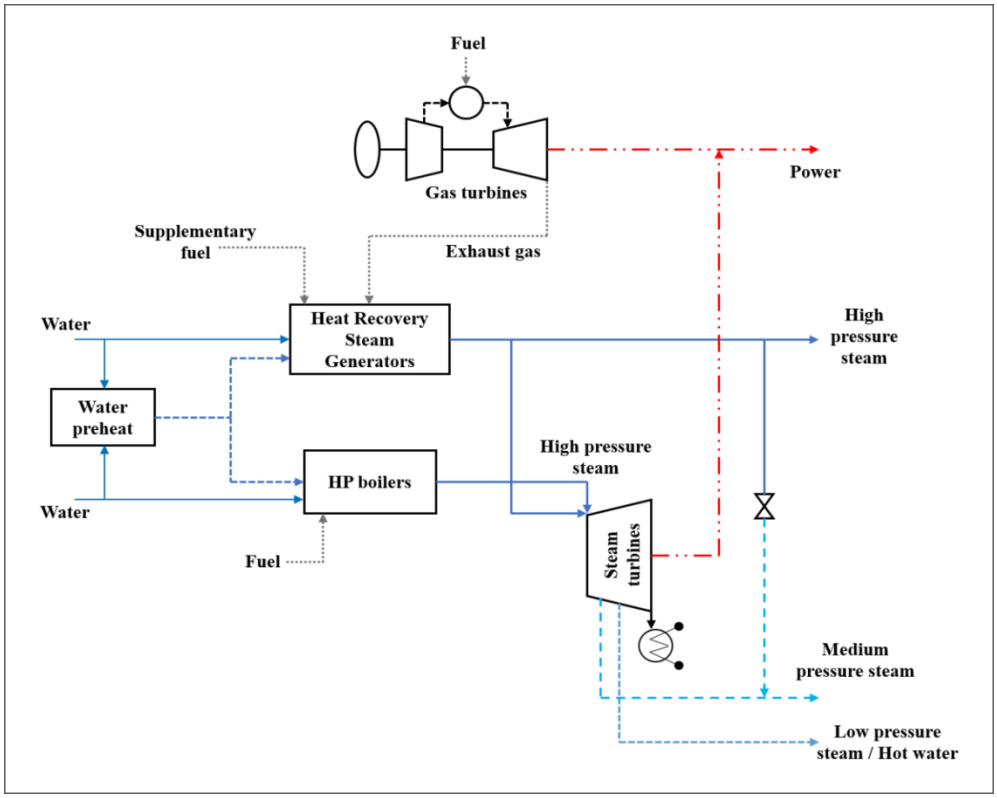

Figure 4.2 Schematic representation of an industrial combined heat and power system

The cost of cogeneration facilities can be calculated as follows.

$$COC_t^{total} = \sum_c \sum_{n \in N_c} CCO_{ct}^{GT}\ COMAX_{ct't}^{GT}\ nc_{cnt'}^{GT} \tag{4.25}$$

$$+ \sum_c \sum_{n \in N_c} (FCO_{ct}^{GT}\ COMAX_c^{GT}\ yc_{cnt}^{GT} + VCO_{ct}^{GT}\ PPC_{cnt}^{GT} TT)$$

$$+ \sum_c \sum_{n \in N_c} CCO_{ct}^{ST}\ COMAX_{ct't}^{ST}\ nc_{cnt'}^{ST}$$

$$+ \sum_c \sum_{n \in N_c} (FCO_{ct}^{ST}\ COMAX_c^{ST}\ yc_{cnt}^{ST} + VCO_{ct}^{ST}\ PPC_{cnt}^{ST} TT)$$

$$+ \sum_c \sum_{n \in N_c} CFCO_{ct} FCC_{cnt}^{Tot} TT \qquad \forall\, t$$

The amount of fuel (i.e. natural gas) consumed in the combustion chambers of gas turbines and supplementary fuel consumed in the heat recovery steam generator can be calculated as illustrated in Eq. 4.26 and Eq. 4.27, respectively.

$$FCC_{cnt}^{GT} = \frac{3.6\ PPC_{cnt}^{GT}}{\eta_c^{GT}} \quad \forall\ c, n \in N_c, t \tag{4.26}$$

$$FCC_{cnt}^{GR-post} \tag{4.27}$$

$$= \frac{SP_{cnt}^{GR}\Delta HS_c - (1-\eta_c^{GT})FCC_{cnt}^{GT}\eta_c^{GR} - \sum_{b\prime}\sum_{n\in N_{b\prime}} HRX_{b\prime nt}^{GR-pre}\eta_{b\prime}^{preheat}}{\eta_c^{GR}} \quad \forall\ c, n$$

$$\in N_c, t$$

where PPC_{cnt} is the power generated from the gas turbine and SP_{cnt}^{GR} is the amount of high pressure steam produced from the heat recovery from exhaust gases, which can be sent to steam turbines to produced power or used for the high pressure steam requirements of the industrial operations.

$$SP_{cnt}^{GR} = SPD_{cnt}^{HP} + SPC_{cnt}^{G-S} \quad \forall\ c, n \in N_c, t \tag{4.28}$$

The amount of steam produced from high pressure boilers used in steam turbines can be calculated as follows.

$$SPC_{cnt}^{HPB}\ \Delta HSS = HV^{NG}FCS_{cnt}^{ST}\eta_c^{G} + HV^{syn}SynSS_{cnt}^{ST}\eta_c^{G} + \sum_{b\prime}\sum_{n\in N_{b\prime}} HRX_{b\prime nt}^{SR-pre}\eta_{b\prime}^{preheat} \quad \forall\ c, n \in N_c\ , t \tag{4.29}$$

where FCS_{cnt}^{ST} and $SynSS_{cnt}^{ST}$ are the amounts of natural gas and syngas from gasification facilities consumed, respectively. The power produced in steam turbines can then be calculated as follows.

$$PPC_{cnt}^{ST} = \eta_c^{ST}(SPC_{cnt}^{HPB}h_1 + SPC_{cnt}^{G-S}h_{G-S} - SPC_{cnt}^{EXT2}h_2 - SPC_{cnt}^{EXT3}h_3)\ \forall\ c, n \in N_c\ , t \tag{4.30}$$

where SPC_{cnt}^{HPB} and SPC_{cnt}^{G-S} are the amounts of high pressure steam produced in high pressure boilers and steam produced from heat recovery from exhaust gas, respectively. SPC_{cnt}^{EXT2} and SPC_{cnt}^{EXT3} are the amounts of steam extracted from the steam turbine at the required pressure levels. The total amount of fuel consumed in the industrial cogeneration facility is calculated as follows.

$$FCC_{cnt}^{Tot} = FCC_{cnt}^{GT} + FCC_{cnt}^{GR-post} + FCS_{cnt}^{ST} \quad \forall\, c, n \in N_c\,, t \tag{4.31}$$

4.2.8 Nuclear energy system

In the proposed model nuclear energy can be used to cover the energy requirements of industrial operations in the form of power and heat. The heat generated can be used to produce high, medium and low pressure steam, and/or used for other heating applications for which typically fuel combustion is used. For example, in the oil sands industry, nuclear energy can be used to produce power, SAGD steam, process steam, hot water, upgrading heat, and heat utilized by SMR plants for hydrogen production. The excess power produced from nuclear facilities can also be sold to the grid or used in electrolyzers for hydrogen production, which can also be used to satisfy the hydrogen requirements of bitumen upgrading operations or sold to the market (Figure 3.3). Nuclear energy is a low-carbon footprint technology, which make it an attractive alternative to the reduction of emission from energy intensive industries. Moreover, a carbon emission trading and tax system is being considered to control and penalize industries that do not meet their GHG emission requirements. Therefore, nuclear energy can play a significant role in the energy infrastructure of these industries.

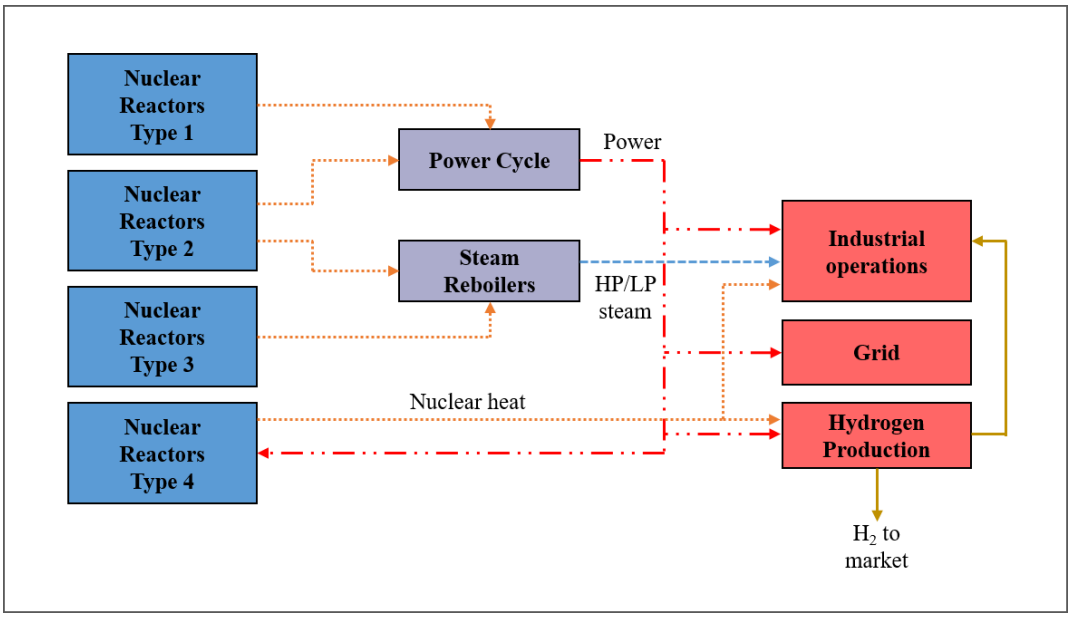

Figure 4.3 Schematic representation of the nuclear energy system

The cost of nuclear energy production can be estimated as follows.

$$NUC_t^{total} = \sum_u \sum_{n \in N_u} \sum_{t'} CCNU_u NUMAX_{ut't} \, nu_{unt'} \tag{4.32}$$

$$+ \sum_u \sum_{n \in N_u} (FONU_u \, NUMAX_u \, yu_{unt} + VONU_u \, HRU_{unt}^{NU} TT)$$

$$+ \sum_u \sum_{n \in N_u} CNA \, PNA \, RAF \, yu_{unt} \quad \forall \, t$$

where nu_{unt} is a binary variable that indicates if unit n of nuclear facility type u is constructed during period t, $CCNU_{ut}$ is the capital cost, yu_{unt} is a binary variable that indicates if the nuclear facility is operational during time period t, HRU_{unt}^{NU} is the heat rate produced from each unit, $FONU_{ut}$ and $VONU_{ut}$ are the fixed and variable operation and maintenance costs, respectively, CNA is the cost incurred as a result of a nuclear accident, PNA is the probability of a nuclear accident occurring during time period t, and RAF is a factor associated with the individual-risk perception. The yield of producing energy

commodities from a nuclear plant are expressed per MWth of nuclear energy. The amount of each energy commodity produced can therefore be calculated as follows

$$EPU_{uent}^{NU} = \delta YU_{ue}^{E} HRU_{unt}^{NU} \qquad \forall\, u, e, n \in N_u, t \tag{4.33}$$

where δYU_{ue}^{E} is the yield of energy commodity *e* generated from nuclear technology *u* (units of *e*/MWth). The amount of heat produced from nuclear facilities can be used to satisfy the heating requirements of downstream industrial operations (e.g. bitumen upgrading heat) and could be also utilized for providing heat for energy production plants (e.g. SMR for hydrogen production). This can be expressed by the following constraint

$$EPU_{uent}^{NU} = HeatU_{unt}^{UPG} + HeatU_{unt}^{H} \qquad \forall\, u, n \in N_u, e = Heat, n \in N_u, t \tag{4.34}$$

The power produced from nuclear plants can be used to provide the electricity requirements of industrial operations, exported to the grid, or sent to satisfy the energy requirement of other energy production facilities, such as electrolyzers or other nuclear facilities dedicated only for heat production. This can be written as follows

$$EPU_{uent}^{NU} = PPU_{unt}^{DEM} + PPU_{unt}^{GRID} + PPU_{unt}^{H} + PPU_{unt}^{NU} \qquad \forall\, u \in U^{P} \cup U^{CHP}, n \in N_u, e = Power, n \in N_u, t \tag{4.35}$$

4.2.9 Gasification polygeneration system

Polygeneration gasification systems that can utilize various fuels are considered in the proposed optimization model. Petcoke, asphaltenes, coal, bitumen, biomass or a combination of these can be utilized as alternative fuel inputs into the gasification reactor. Therefore, it is assumed that the different types of gasification and synthetic gas cleaning technologies considered depend on the type of fuel used as an input to the gasification process. The synthetic gas (syngas) produced is rich in hydrogen and carbon monoxide,

which can then be combusted to generate steam and/or electricity, or it can be purified to produce hydrogen. The effluent gas stream from the process of hydrogen purification can also be combusted to generate heat. Heat can also be recovered from waste heat streams to generate additional steam and/or hot water. The syngas produced can be used to generate synthetic natural gas, which can be exported to natural gas fueled facilities (e.g. boilers, furnaces, etc.) requiring little or no retrofit for their combustion chambers. Transportation fuels is a commonly required energy commodity in industrial operations. For example, oil sands mining operations require significant amounts of fuel to operate vehicles and trucks, for which diesel is currently used. Switching to low carbon intensive fuels can be achieved through the conversion of biomass to biofuels. The syngas produced from gasification can be purified and transformed into fuels (e.g. synthetic diesel, synthetic gasoline, etc.) (Figure 4.4).

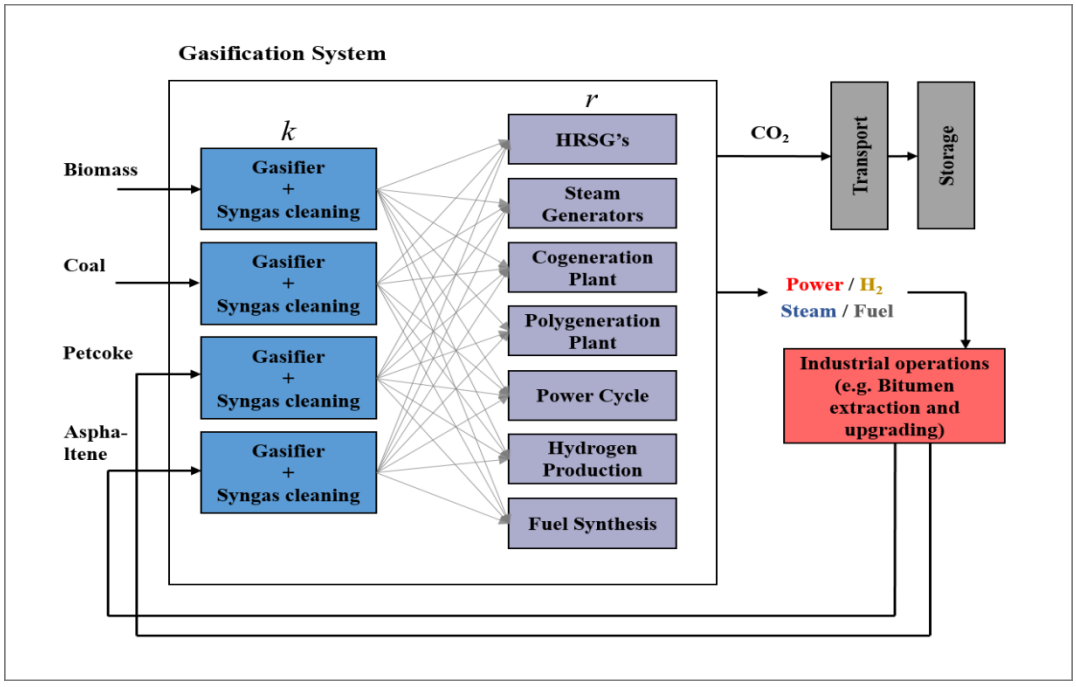

Figure 4.4 Schematic representation of the proposed gasification system

Accordingly, five types of processing options are considered for the produced syngas, which include GPR1: hydrogen, GPR2: power and hydrogen, GPR3: power, steam and hydrogen, GPR4: power and steam, and GPR5: fuel production (e.g. synthetic natural gas, biofuels, etc.). The gasification system is modeled according to [131 – 134]. The cost of polygeneration gasification facilities can be calculated as follows.

$$GASC_t^{total} = \sum_k \sum_{n \in N_k} \sum_{t'} CCK_k KMAX_{kt't} \, nk_{knt'} \tag{4.36}$$

$$+ \sum_k \sum_{n \in N_k} (FOK_k \, KMAX_k^T \, yk_{knt} + VOK_k \, SYN_{knt}^{KT} TT)$$

$$+ \sum_k \sum_{n \in N_k} CFK_k \, FCG_{knt}$$

$$+ \sum_r \sum_{n \in N_r} \sum_{t'} CCR_r RMAX_{rt't} \, nr_{rnt'}$$

$$+ \sum_r \sum_{n \in N_r} (FOR_r \, RMAX_r^T \, yr_{rnt} + VOR_r \, SYN_{rnt}^{RT} TT) \quad \forall \, t$$

The amount of syngas produced from a certain gasification technology depends on the type of fuel utilized and can be calculated as follows.

$$SYN_{knt}^{KT} = \delta YK_k^{syn} FCG_{knt} \quad \forall \, k, n \in N_k, t \tag{4.37}$$

where $FCPC_{knt}$ is the amount of fuel (i.e. coal, biomass, asphaltene, petcoke) utilized, δYK_k^{syn} is the yield of syngas, and SYN_{knt}^{KT} is the amount of syngas produced. The amount of syngas produced can be distributed among the available gas processing options to produce energy or to be exported to other energy commodity producers (e.g. natural gas boilers). This constraint is represented as follows.

$$SYN_{knt}^{KT} = \sum_r \sum_{n' \in N_r} SYN_{knrn't} + SYN_{knt}^{exp} \quad \forall \, k, n \in N_k, t \tag{4.38}$$

The amount of syngas produced from gasification that is available for export is distributed among natural gas combined heat and power and boilers as follows.

$$\sum_{k}\sum_{n\in N_k} SYN_{knt}^{exp} = \sum_{c}\sum_{n\in N_c} SynSS_{cnt}^{ST} + \sum_{b}\sum_{n\in N_b} SynS_{bnt}^{G} \quad \forall\ t \tag{4.39}$$

Also, the amount of syngas entering a processing option must be equal to the amount of syngas sent to it from all gasification technologies, which is presented as follows.

$$SYN_{rnt}^{RT} = \sum_{k}\sum_{n\in N_k} SYN_{knrn't} \quad \forall\, r, n \in N_r, t \tag{4.40}$$

where SYN_{rnt}^{RT} is the amount of syngas sent from gasification technology *k* to gas processing option *r*. The flow of syngas from gasification technology *k* to processing options *r* should not exceed the maximum capacity of gasification technology *k* or the maximum capacity of processing option r. This is presented by the following constraints.

$$SYN_{knrn't} \le SYNK_{k}^{MAX} kr_{knrn't} \quad \forall\, k, n \in N_k, r, n' \in N_r, t \tag{4.41}$$

$$SYN_{knrn't} \le SYNR_{r}^{MAX} kr_{knrn't} \quad \forall\, k, n \in N_k, r, n' \in N_r, t \tag{4.42}$$

Moreover, it is assumed that each gasification technology can only be connected to one gas processing options, which is presented by the following constraint.

$$\sum_{r}\sum_{n'\in N_r} kr_{knrn't} \le 1 \quad \forall\, k, n \in N_k, t \tag{4.43}$$

The amount of each energy commodity produced from each syngas processing option can be calculated as follows.

$$EC_{rent}^{PCK} = \delta YR_{re}^{EC} SYN_{rnt}^{RT} \quad \forall\, r, e, n \in N_r, t \tag{4.44}$$

where δYR_{re}^{EC} is the yield of energy commodity *e* from processing option *r*, and EC_{rent}^{PCK} is the amount of energy commodity *e* produced from each unit n of processing option *r*.

4.2.10 Capacity constraints

A feature of the developed multi-period model is the consideration of construction lead time for new energy producers, which is important because energy cannot be supplied until the construction of the plant is complete. The variation in construction lead time depends on the type of energy production technology considered. Therefore, in order to ensure that during the construction phase of energy production technology no energy is provided by it, a capacity constraint that takes into account construction lead time is formulated. This constraint is formulated according to the matrix method provided in Sirikitputtisak et al. [114]. The maximum capacity of an energy production plant is defined by two time indices. One time index represent the construction year *t'*, and the other time index *t* refers to years of regular operation, which can be presented as follows.

$$CMIN_{iet't}^{LT} n_{int'}^{new} \leq EC_{inet}^{new} \leq CMAX_{iet't}^{LT} n_{int'}^{new} \quad \forall\, i, e, n \in N_i, t, t' \tag{4.45}$$

where $n_{int'}^{new}$ is a binary variable that indicates if unit *n* of plant type *i* is constructed during time period *t'*, and $CMIN_{iet't}^{LT}$ and $CMAX_{iet't}^{LT}$ are the minimum and maximum capacities, respectively. Moreover, the capacity constraints accounts for limits on energy production from renewable energy sources (heat and power) as they have limits on their potential. In other words, limitations are imposed on the output of hydropower, solar, geothermal, wind, etc. The capacity constraint for existing and new energy production technologies can be presented as follows.

$$CMIN_{iet}y_{int} \leq EC_{inet} \leq CMAX_{iet}y_{int} \quad \forall\, i, e, n \in N_i, t \tag{4.46}$$

where y_{int} is a binary variable that represents if unit *n* of plant type *i* is operations during time period *t*. Moreover, the construction of any energy production unit can only take place during a certain time period, which is enforced by the following constraint.

$$\sum_{t} n_{int}^{new} \leq 1 \quad \forall\, i, n \in N_i \tag{4.47}$$

Moreover, a limit can be set on the number of energy production units installed during a certain time period for each technology, which is illustrated as follows.

$$\sum_{n \in N_i} n_{int}^{new} \leq NMAX_{it}^{new} \quad \forall\, i, t \tag{4.48}$$

4.2.11 Fuel availability constraint

Limits on energy production from available fuels (e.g. biomass, natural gas, petcoke, etc.) are accounted for by incorporating maximum thresholds on fuel consumption. Fuel consumption is related power, hydrogen, thermal (i.e. boilers), gasification plants, and other needs (e.g. vehicles, furnace heating, etc.). The entire sum of the contribution of these energy suppliers to fuel consumption for a certain type of fuel *f* during time period *t* has to be comprised to an upper bound, which is illustrated by the following constraint.

$$\sum_{n \in N_p} FCP_{pnt}^{F} + \sum_{n \in N_h} FCH_{hnt}^{F} + \sum_{n \in N_b} FCB_{bnt}^{F} + \sum_{n \in N_c} FCC_{cnt}^{Tot} + \sum_{n \in N_k} FCG_{knt} + Fuel_{ft} \leq Fuel_{ft}^{available} \quad \forall\, p \in P_f, h \in H_f, b \in B_f, c \in C_f, k \in K_f, t \tag{4.49}$$

4.2.12 Demand constraints

The total energy requirements of the industrial operations in the model must be satisfied by the proposed energy commodity producers. Therefore, the total amount of energy commodities produced by the energy technologies considered must be greater than or equal to the amount of energy required, which is presented by the following constraints.

$$\sum_{p}\sum_{n\in N_p} PP_{pnt}^{DEM} + \sum_{u}\sum_{n\in N_u} PPU_{unt}^{DEM} + \sum_{c}\sum_{n\in N_c} PPC_{cnt}^{DEM} + \sum_{r}\sum_{n\in N_r} EC_{r,e=pow,nt}^{PCK} \geq DEC_{e=pow,\ t} \quad \forall\ t \tag{4.50}$$

$$\sum_{h}\sum_{n\in N_h} HP_{hnt} + \sum_{r}\sum_{n\in N_r} EC_{r,e=H2,nt}^{PCK} \geq DEC_{e=H2,\ t} \quad \forall\ t \tag{4.51}$$

$$\sum_{b\in B^{HP}}\sum_{n\in N_b} BP_{bnt}^{G} + \sum_{c}\sum_{n\in N_c} SPD_{cnt}^{HP} + \sum_{r}\sum_{n\in N_r} EC_{r,e=HP\ steam,nt}^{PCK} \geq DEC_{e=HP\ steam,\ t} \quad \forall\ t \tag{4.52}$$

$$\sum_{b\in B^{LP}}\sum_{n\in N_b} BP_{bnt}^{G} + \sum_{c}\sum_{n\in N_c} SPC_{cnt}^{EXT2} + \sum_{r}\sum_{n\in N_r} EC_{r,e=LP\ steam,nt}^{PCK} \geq DEC_{e=LP\ steam,\ t} \quad \forall\ t \tag{4.53}$$

$$\sum_{b\in B^{HW}}\sum_{n\in N_b} BP_{bnt}^{G} + \sum_{c}\sum_{n\in N_c} SPC_{cnt}^{EXT3} + \sum_{r}\sum_{n\in N_r} EC_{r,e=Hot\ water,nt}^{PCK} \geq DEC_{e=Hot\ water,\ t} \quad \forall\ t \tag{4.54}$$

$$Fuel_{ft} + \sum_{r}\sum_{n\in N_r} EC_{r,e=Syn\ fuel,nt}^{PCK} \geq DEC_{e=Fuel,\ t} \quad \forall\ t \tag{4.55}$$

4.2.13 Objective function

The objective of the proposed deterministic multi-period MILP model is to minimize the total present value of the cost of energy production over a specified planning period, which is presented as follows.

$$min \quad Cost^T = \sum_t (PC_t^{total} + HC_t^{total} + BC_t^{total} + COC_t^{total} + NUC_t^{total} + GASC_t^{total}) \tag{4.56}$$
$$+ \sum_i \sum_{n \in N_i} \sum_t (CostCT\ PKM + CostCS) TT\ ECO2_{int}\ \varepsilon_i$$
$$+ \sum_t CostCredit_t TT(Creditbuy_t - Creditsell_t) + \sum_t \sum_f FC_f\ Fuel_{ft}$$
$$+ \sum_t PowPrice_t\ TT(PurGrid_t - SellGrid_t) - \sum_t H2Price_t\ H2Sell_t$$

The total cost function is estimated by the cost of individual energy commodities required for industrial operations. The objective function also incorporates the environmental costs associated with carbon capture and sequestration, and the purchase of carbon emission credits. Finally, the possibility of buying energy commodities (e.g. power from grid) or selling excess energy commodities produced, such as selling excess power to the grid or excess hydrogen to the market, is incorporated in the proposed objective function.

4.3 Case Study

In order to investigate its applicability, the formulated model is applied to a case study based on the oil sands operations in Alberta. This is an active area for recovering and upgrading bitumen, where significant quantities are transported to refineries in Canada and the United States. Energy consumption data and factors affecting the operations of the industry that are required to complete the evaluation of the application of the energy production technologies are readily available in the public domain.

The oil sands industry is one of the biggest contributors to the production of primary energy in Canada, and it is also one of the largest end-users of energy. The oil sands industry consumes thermal energy (i.e. steam, hot water, and heat) and hydrogen, which are currently produced from natural gas, electricity from the grid, and diesel fuel. Continued growth in oil sands production levels and the associated increase in energy use will result in a substantial increase in GHG emissions produced from fuel combustion. In 2014, the oil sands operations accounted for approximately 21% of the electricity demand in the province, 30% of natural gas demand (excluding the production of electricity), and 20% of diesel fuel demand. Various projections of bitumen and synthetic crude oil production are provided in the literature. Moreover, various scenario based estimates of the energy requirements associated with the oil sands production levels are also available in the literature. These scenarios include the business as usual scenario that provides the energy estimates expected to unfold based on historical trends, the increased energy efficiency scenario that assumes technology learning and innovation that reduces energy consumption, and the decreased reservoir quality scenario in which the reservoir quality deteriorates resulting in an increase in the energy intensity of bitumen extraction [135]. Based on these scenarios, six demand levels for the various energy commodities required for oil sands operations were developed (Fig. A1 in Appendix), reflecting the different levels of energy intensities associated with oil sands operations.

Although Canada has withdrawn from the Kyoto Protocol in late 2011, and there are concerns among political parties about carbon mitigation policies that will be adopted in the future, in order to evaluate the impact of a carbon mitigation policy on the operations of the oil sands industry, it will be assumed that the emission targets once proposed are

still going to be applied by the government of Alberta. In 2013, the GHG emissions from the oil sands sector accounted for 23% of the provincial emissions and 8.5% of national emissions of 726 million tonnes CO_2, which represented a 94% increase from the 2005 levels of 32 million tonnes CO_2. This called for a reduction in emissions from the 2005 levels by 20% and 60% - 70% by 2020 and 2050, respectively. In addition, it is expected that the oil sands industry will account for 12% of Canada's total emissions by 2020. Therefore, the proposed emission target can be presented as shown in Figure A2 (Appendix) for the planning period 2015 – 2050. These reduction targets are large on paper only, since oil sands operators are permitted to comply by these emission target through purchasing offset carbon emission credits from projects in Alberta, and by making payments of CAD 15/tonne CO_2 into the Climate Change and Emissions Management Fund. However, tougher governmental regulations are expected to take place in the future were Alberta's Environment Minister announced an increase in the province's carbon tax, which is expected to increase from the current price of CAD 15/tonne CO_2 to CAD 20/tonne CO_2, and possibly further to CAD 30/tonne CO_2 by 2017. Accordingly, a carbon credit/tax profile is used as an input for the optimization model over the investigated planning period (Figure A2 in the Appendix). Six scenarios for the carbon mitigation policies are considered for this case study, which are the business as usual emission targets and the proposed emission targets, each accompanied with high, low and no carbon credit/tax costs [79, 105 – 108].

In order to meet the forecasted energy demand requirements for the different CO_2 mitigation policies investigated, several energy supply sources are considered. The technologies considered include nuclear (PBMR, ACR-700, ACR-1000, CANDU, and

HTGR) for power and heat production, natural gas combined cycle and oxyfuel for power production, pulverized coal and coal oxyfuel for power production, steam methane reforming for hydrogen production, gasification (coal, petroleum coke, biomass, and asphaltenes) for power, hydrogen and thermal energy production, industrial natural gas combined heat and power production, natural gas boilers, integrated wind power, nuclear power and water electrolysis for power and hydrogen production, biodiesel, and geothermal energy. Each fossil-fuel based technology considered can be integrated with carbon capture and sequestration. The renewable energy (i.e. wind, biomass, and geothermal) production technologies considered were selected based on an evaluation of Alberta's renewable energy potential [136]. The supply technologies' techno-economic data, as well as factors required for the implementation of these technologies (e.g. fuel prices) are presented in the appendix [76, 80-97, 116-151]. The model is solved using the CPLEX solver in the General Algebraic Modeling System (GAMS) [8].

4.4 Results and discussion

This section summarizes the outcomes of the model's decisions on the construction of energy production technologies required for the oil sands industry over the considered planning period (2015 – 2050).

4.4.1 Scenario I: Variability in energy demands

Figure 4.5 shows the distribution of the energy production from the technologies selected over the planning period. It can be observed that the level of demand intensity has a significant effect on the types of energy production technologies selected by the optimization model. Since the lower range of annual CO_2 emission limits were imposed for this scenario, the selection of the energy production technologies by the optimization

model is more influenced by economic factors (i.e. capital and operating cost, and fuel price forecasts). This is particularly evident at low energy demand levels. However, as the energy demand levels increase, which have higher emission levels associated with their production, the selection of energy production technologies is more geared towards low-emission technologies in order to minimize the purchase of carbon credits.

At the lowest demand level the majority of energy produced is derived from fossil fuel based technologies. During the first few years the existing energy production technologies provide the energy requirement for oil sands operations. Hydrogen is produced from existing steam methane reforming plants, heat is produced from burning natural gas in dedicated boilers, and power is supplied from the grid. However, these alternatives are later replaced by more economically and environmentally favorable technologies. Hydrogen production is later replaced with petcoke gasification integrated with carbon capture. Petcoke is a byproduct of bitumen upgrading that is considered as waste by oil sands operators, and ends up stockpiled next to upgrading facilities. Petcoke is a low-cost fuel compared to natural gas.

The gasification of the high-sulfur and high-carbon waste provides significant potential in reducing the natural gas requirements when integrated with carbon capture and sequestration. The production of heat (i.e. SAGD steam, process steam and hot water) and power is achieved through dedicated natural gas boilers and natural gas combined heat and power cogeneration facilities. Around the middle of the planning period, the cogeneration facilities are integrated with carbon capture technologies in order to achieve the emission requirements and reduce the cost of emission credits. The upgrading heat and diesel requirements are also provided by bioheat and biodiesel production.

It can also be observed from Figure 4.5 that for higher energy requirements the share of natural gas cogeneration integrated with carbon capture increases in the energy infrastructure, as well as the capacity of nuclear energy. The majority of nuclear energy production capacity selected is used to satisfy the power and SAGD steam requirements of oil sands operations. For example, more than 50% of the energy production for the highest energy demand level is accounted for by nuclear cogeneration facilities and natural gas combined heat and power by the year 2050. Due to the considerably low fuel cost, and the advantage of no carbon emissions, nuclear energy production has a cost advantage for higher energy demand requirements.

Standalone natural gas fired boilers required for SAGD steam, process steam and hot water account for a significant share of total energy production. At the low range of natural gas prices considered for this scenario, the production of heat from burning natural gas in dedicated boilers represents the most economical option, which is supported by the low capital and operating cost associated with this energy production alternative.

It can be observed that it is uneconomical to produce power from any of the considered standalone power production technologies, and that it is more favorable to be produced from cogeneration facilities. Despite the higher onsite fuel use, cogeneration facilities have a higher operating efficiency on the order of 70 – 80% when compared to standalone electricity or heat (e.g. steam) production. The main requirement to justify the incorporation of cogeneration facilities is the steady availability of thermal energy demand. Due to the significant heating requirements of oil sands operations, the power production from a cogeneration facility will typically exceed the onsite electricity

requirements. This excess power might be sold to the Alberta grid, which would provide an additional benefit of reducing the emissions of the most carbon intensive power system in Canada that mostly relies on coal and natural gas for power generation.

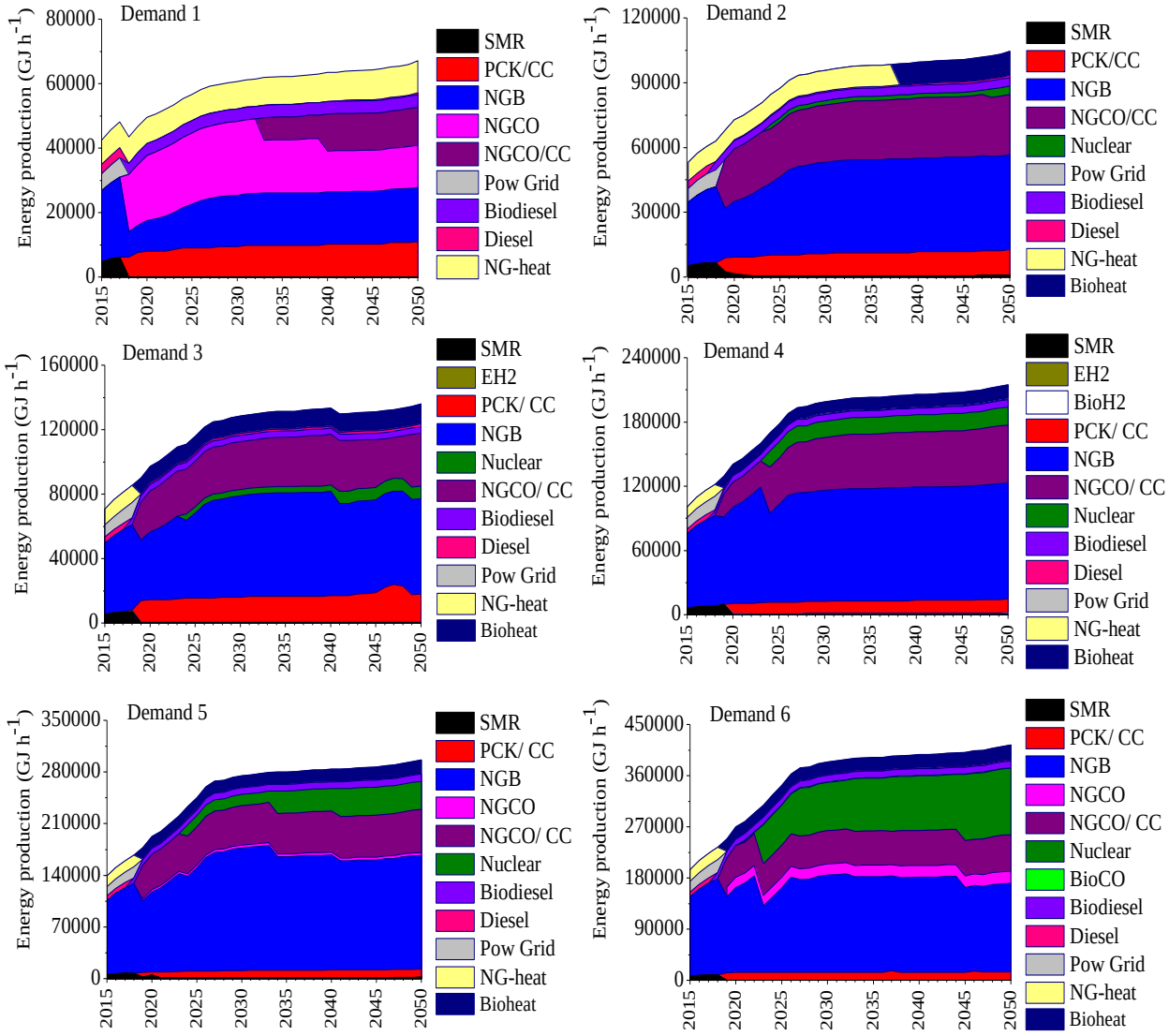

Figure 4.5 Energy generation composition for the optimal pathways under the investigated six demand levels. SMR: Steam methane reforming, PCK/CC: petcoke gasification, NGB: natural gas boiler, NGCO: Natural gas cogeneration, EH2: Electrolytic hydrogen, BioCO: Biom

Bioheat and biodiesel production contributed significantly to providing the upgrading heat and diesel requirements for all the demand levels over the entire planning period.

Their inclusion in the energy infrastructure contributes significantly in reducing the total carbon emissions, which minimizes the purchase of emission credits. The synthetic natural gas produced from biomass has a very high energy content, and it can be used in existing natural gas-fired infrastructure, which is the current technology used to provide heat for thermal upgrading operations, without retrofitting requirements.

Figure 4.6 shows the annual CO_2 emissions over the planning period for all the demand levels. The emission cap that was imposed for all scenarios is shown by the red line in the figure. The model has an option of selecting low-carbon emission technologies or purchasing carbon credits in order to satisfy the emission constraints for each operational year. It can be observed that for low demand scenarios (Demand 1 – 3), the selected energy mix (Figure 4.5) is capable of satisfying the imposed emission constraints. The selected energy production technologies for these scenarios are capable of minimizing the total cost of energy production, while satisfying the emission constraints without the requirement of purchasing carbon credits. However, as the demand level increases (Demand 4 – 6), it becomes more economical to purchase carbon emission credits at the proposed rate (i.e. 15 CAD/tonne CO_2) than to increase the capacity of lower carbon emission technologies and carbon mitigation options (e.g. nuclear and carbon capture). This is mainly due to the substantial heat requirements in oil sands operations in the form of SAGD steam, process steam and hot water that are used for oil sands extraction, recovery and upgrading processes, and are mainly produced by standalone natural gas boilers that have low capital and operating costs. However, as will be observed from the following scenarios changing the natural gas price forecasts, the imposed emission limits,

and the cost and availability of carbon emission credits have a major impact on the energy mix distribution and the annual emissions generated.

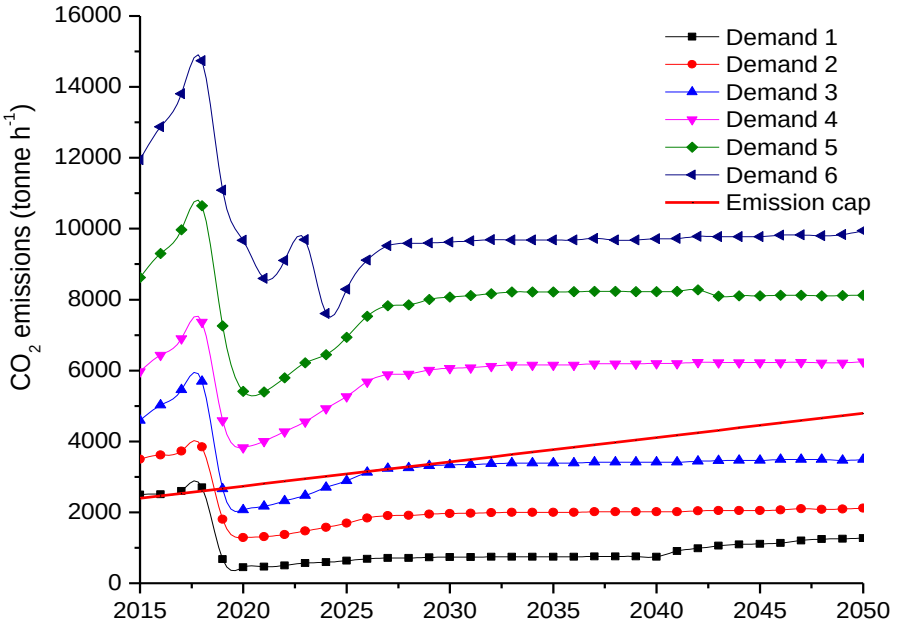

Figure 4.6 CO_2 emission level of the energy infrastructure for the optimal pathways under the six investigated energy demand levels for the assigned carbon emissions cap

Figure 4.7 presents a comparison of the total expenditure for all the demand levels for the entire study period of 2015 – 2050. It can be observed that the total cost of energy production increases with the increase in energy demand levels. In addition to the increase of the required energy production capacity, the increase in total cost is also attributed to by the increase of the share of low-CO_2 emission technologies, such as NG-cogeneration integrated with carbon capture and nuclear energy facilities. The increase in fuel costs is due to the increase in utilization of natural gas in dedicated boilers and combined heat and power cogeneration facilities. A significant increase is observed for the cost of carbon capture and carbon credits for the higher demand levels (Demand 4 – 6).

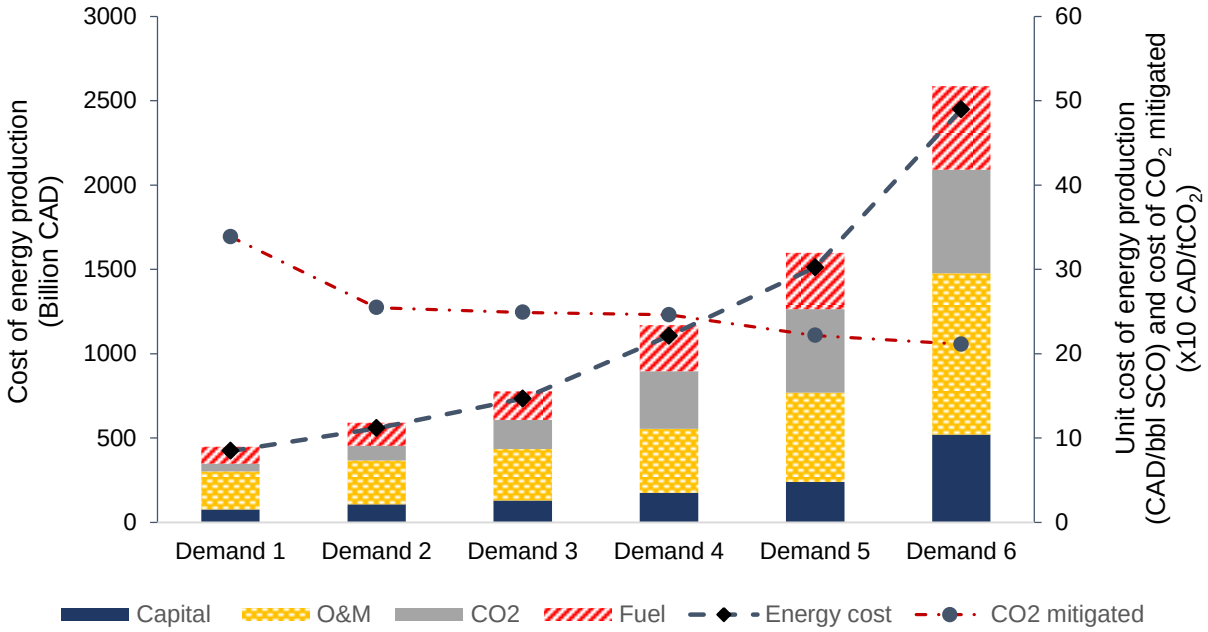

Figure 4.7 Total net present value of the cost of energy production and the unit cost of energy production over the entire planning period under the six investigated demand levels

4.4.2 Scenario II: Variability in carbon mitigation policy

In this scenario the demand level was fixed (Demand 5), and the carbon mitigation policy was varied in order to determine its effect on the results of the optimization model. In this scenario two different sets of emission limits over the planning period were considered, and for each set two different ranges of carbon credit prices were considered (i.e. low and high) (Figure A2 in the Appendix). Moreover, the possibility of carbon emission credits being unavailable was also modeled for each set of emission limits. Figure 8 shows the distribution of the energy production mix over the planning period for the investigated carbon mitigation scenarios. It can be observed that increasing the carbon emission constraint results in significant changes in the energy infrastructure, which is expected due to the increase in the cost of carbon emission credits that would occur if the energy production mix remains unchanged.

As can be observed from the results in Figure 4.8, for the lower emission limit, the majority of the thermal energy is produced by standalone natural gas boilers with a low contribution of carbon mitigation options. As the emission constraint is increased, a significant increase in the production capacity of natural gas combined heat and power, nuclear energy, and geothermal energy is observed. However, standalone thermal energy production still contributes to a noticeable share of the energy mix.

From Figure 4.8 it can also be observed that the price of carbon emission credits has a significant effect on the energy production mix. As the price of credits is increased the majority of the energy infrastructure switches to low-carbon emission technologies, such as natural gas cogeneration with carbon capture and nuclear energy. It can also be observed that the capacity of renewable energy production considerably increases. The capacity of standalone thermal energy production is substantially reduced. For example, for the low emission limit and high carbon credit price scenario, the energy production mix is accounted for by approximately 30% natural gas cogeneration with carbon capture, 23% nuclear energy and 23% renewables (geothermal, bioheat, biodiesel and biohydrogen) by the year 2050.

The remaining production capacity is produced by standalone thermal energy production technologies. However, their production is completely diminished for the higher emission limit scenario by the year 2050, and the production mix is accounted for by approximately 60% nuclear energy, 26% natural gas cogeneration, and the remaining capacity is produced from bioenergy and petcoke gasification with carbon capture. The significant share of nuclear production plants is attributed to their cost advantage that is due to their long operating life time, low fuel cost, and the advantage of no carbon

emissions, which justifies its fast development in the energy infrastructure over the planning period.

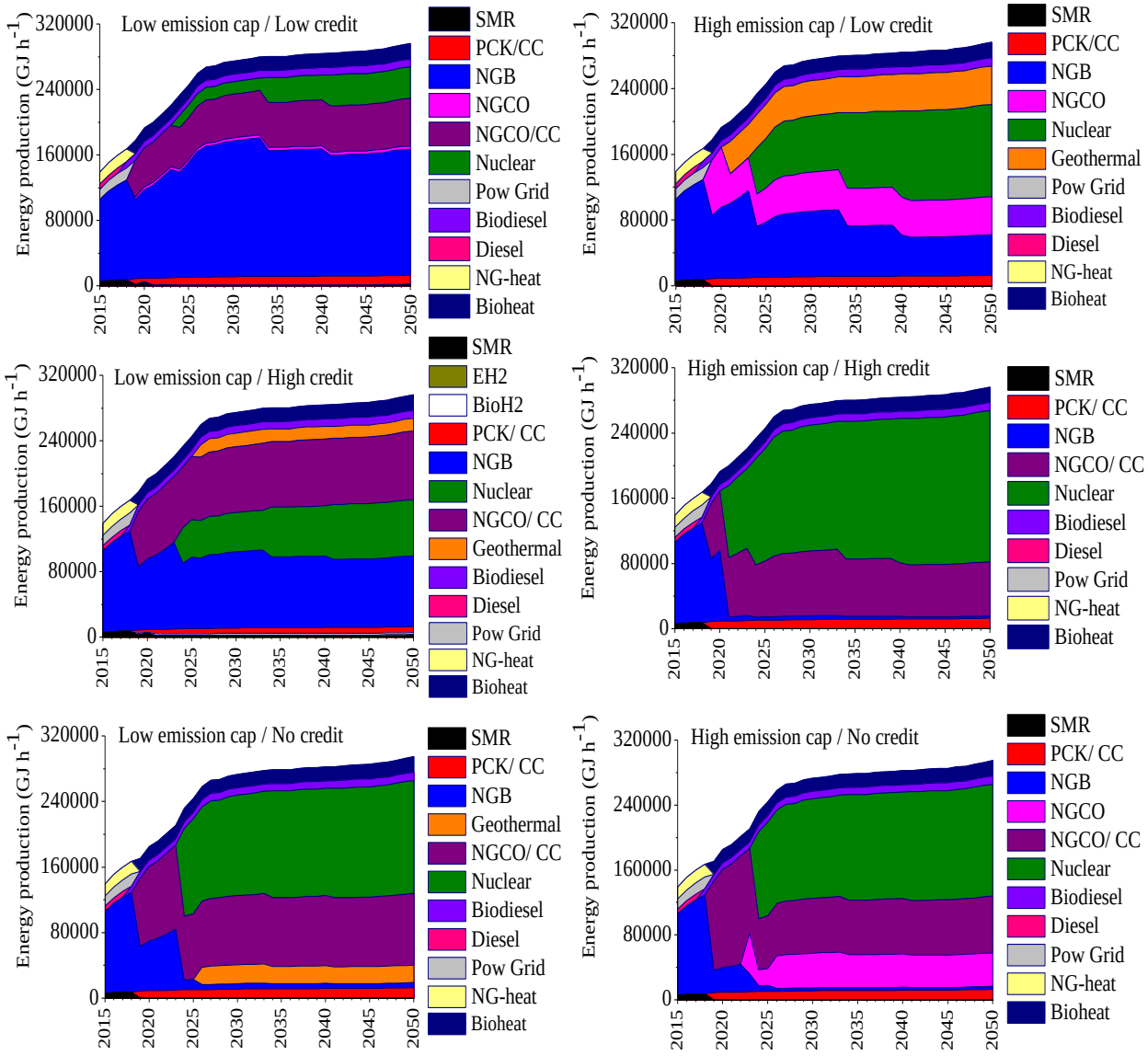

Figure 4.8 Energy generation composition for the optimal pathways under the six investigated carbon mitigation policy scenarios using demand level 5. SMR: Steam methane reforming, PCK/CC: petcoke gasification, NGB: natural gas boiler, NGCO: Natural gas cogeneration

The elimination of the possibility of purchasing carbon credits requires the energy infrastructure to be able to satisfy the emission constraints over all the years in the planning period. In this case the CO_2 emitted by the entire fleet for a particular year

cannot be reduced by purchasing CO_2 credits. It can be observed from Figure 8 that for the no carbon credit scenario the production of thermal energy (i.e. steam and hot water) from natural gas boilers is diminished towards the end of the planning period. Instead thermal energy is coproduced with power in nuclear plants and natural gas cogeneration plants with carbon capture. A considerable share of the thermal energy requirements is also produced from geothermal energy. The production of hydrogen is mainly from petcoke gasification with carbon capture. Diesel and upgrading heat requirements are satisfied from biodiesel and bioheat energy production.

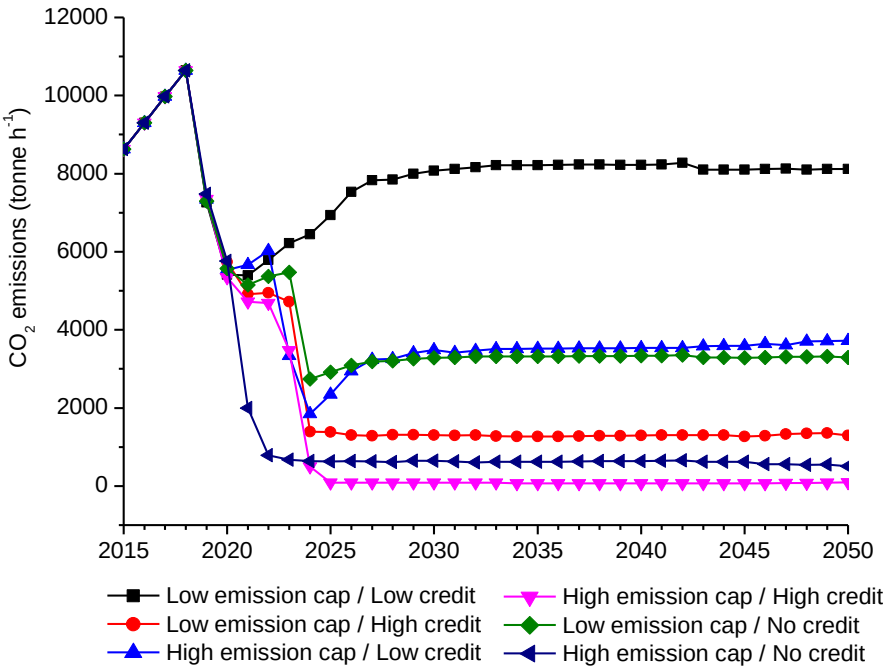

Figure 4.9 CO_2 emissions of the energy production infrastructure for the optimal pathways under the six investigated carbon mitigation policy scenarios for demand level 5

Figure 4.9 shows the annual emissions for the various carbon mitigation policies considered for this scenario over the planning period. As can be observed both carbon emission targets were not met at the low range of carbon credit prices. In other words, it is more economical to purchase carbon emission credits, which is presented as the gap

between the emission levels and the emission targets, than to produce energy from low-carbon intensive technologies. The low price range of carbon credits was assumed to be the price level currently used in Alberta, which is CAD 15 – CAD 50 per tonne CO_2. However, as observed from the results this price range is not sufficient to provide an incentive for oil sands operators to reduce their emission levels to the imposed targets. However, at a higher price range of carbon credits (CAD 15 – CAD 70 per tonne CO_2) the developed energy infrastructure is mainly composed of low-carbon intensive (e.g. natural gas cogeneration with carbon capture) and non-emitting technologies (e.g. nuclear energy), which results in achieving emission levels that are well below the set emission targets. The emission levels achieved are actually lower than those achieved for the no carbon credit scenarios. This is mainly due to the added incentive of selling the excess offset carbon emissions as carbon credits to neighboring industries.

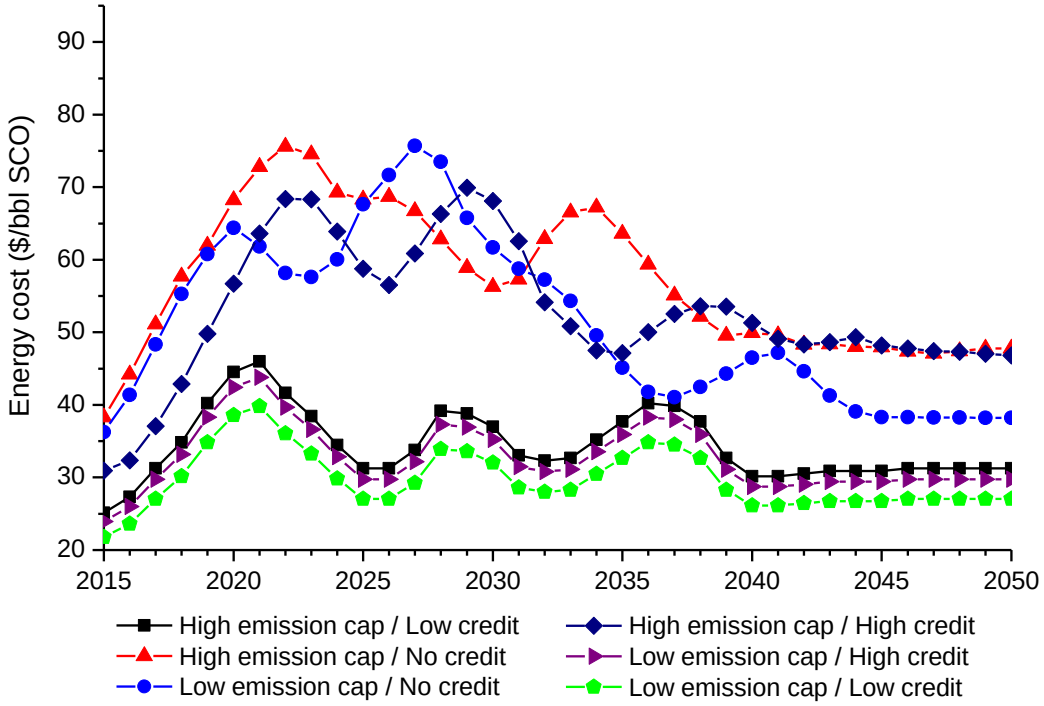

Figure 4.10 Annual unit cost of energy production over the planning period under the six investigated carbon mitigation policy scenarios for demand level 5

Figure 4.10 shows the cost profile of energy per unit barrel of oil sands produced for all the carbon mitigation policy scenarios over the planning period. In all scenarios the majority of new units are installed within the first 10 – 15 years. This results in a trough forming during this time period in the cost of energy plot, which is a results of the high capital expenditure relative to the amount of energy and oil sands production. As the energy infrastructure is established and the oil sands production and their energy requirements increase, the cost of energy production decreases until it reaches a steady value. The rise in cost in the first few years is also due to the purchase of carbon credits required to satisfy the emission constraints until the low-carbon emission technologies come into operation after their construction (i.e. construction lead time). As can be observed from the results in Figure 4.10, a higher emission constraint will result in a higher cost of energy production, which is due to the utilization of the low-carbon intensive and/or non-emitting energy production technologies that are characterized by having higher capital and operating costs in comparison with the more mature and existing fossil fuel based technologies. For example for the low range of carbon credit price the average cost of energy production was determined to be 32.7 CAD/bbl and 54.9 CAD/bbl for the low and high emission constraints, respectively. A similar effect is observed when the price range of carbon credits is increased, which for the high range the average cost was determined to be 45.8 CAD/bbl and 68.5 CAD/bbl, respectively. However, the scenarios in which carbon credits are incorporated result in a lower cost of energy production than scenarios in which they are eliminated from the model.

Figure 4.11 shows the total cost and the unit cost of energy production over the entire planning period for the investigated carbon mitigation policies. It can be observed that the

total cost and unit cost of energy production are considerably higher for the scenarios in which the purchase of carbon credits is eliminated and for the higher emission reduction target and carbon credit price. The increase in cost is significantly accounted for by the increase in total capital investment. This is due to the higher nuclear energy production capacity. The cost of CO_2 mitigation is considerably high for the scenarios in which carbon credits are eliminated due to the increased requirement of carbon capture and sequestration and investment in low-carbon emitting energy production technologies. A similar behavior was observed for the case of a high emission cap and a high cost of carbon credit, in order to avoid purchasing a considerably higher amount of the more expensive carbon credits.

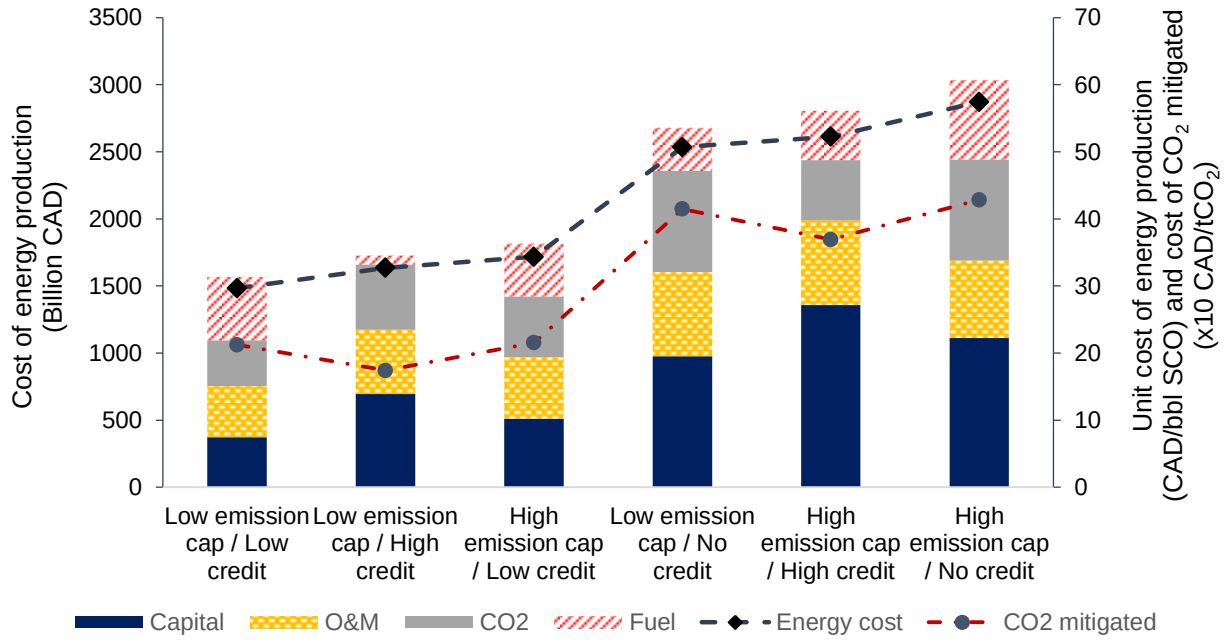

Figure 4.11 Total net present value of the cost of energy production and the unit cost of energy production for the optimal pathways under the six investigated carbon mitigation policy scenarios for demand level 5

4.4.3 Scenario III: Variability in fuel prices

The fuel with the highest expected variability in its price and availability is natural gas. Due to the considerably high demand for natural gas in the future, it is expected that its price will steadily increase over the next few decades. There are various forecasts of the natural gas prices in Alberta available in the literature (Figure A3 in the Appendix). The base case demand level at high emission reduction target and low credit price was investigated for the various forecasts of natural gas prices. Figure 4.12 shows the consumption of natural gas over the planning period for various natural gas prices. It can be observed that as the natural gas price increases its consumption decreases, and the energy infrastructure switches to alternatives of natural gas. For example, from Figure 4.13 it can be observed that for a higher natural gas price the capacity of natural gas standalone boilers and cogeneration, and their preheat options (i.e. geothermal) are considerably reduced. On the other hand, the capacity of energy production from petcoke gasification (i.e. hydrogen, power and heat) and nuclear energy are significantly increased over the planning period. For brevity, only the results for the case in which the average natural gas price over the planning period is $9.6/GJ are shown for the distribution of the energy infrastructure, as the results for the other fuel prices show a similar comparison with the base case.

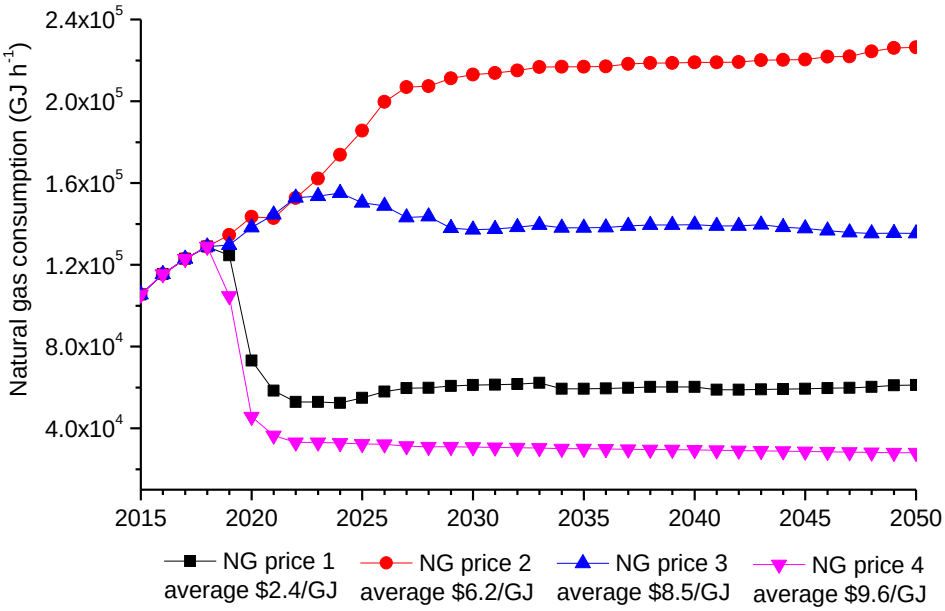

Figure 4.12 Annual natural gas consumption at various fuel prices over the entire planning period (Demand level 5, high emission cap, low credit price)

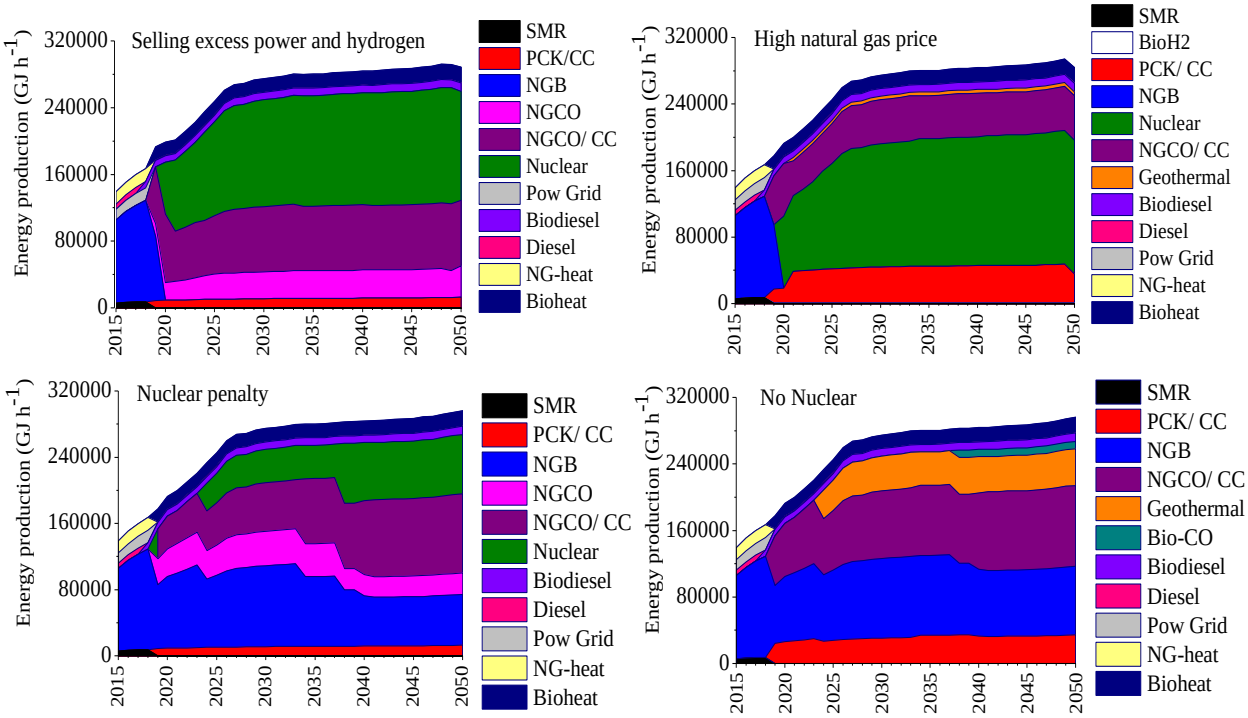

Figure 4.13 Energy production composition for the base case scenario (demand level 5, high emission cap, and low carbon credit price) compared with the scenarios in which excess power and hydrogen sold to the market (at H_2 selling price of \$5/kg), the natural gas price is increased (at NG price 3: \$8.4/GJ), the incorporation of external nuclear penalty cost, and the elimination of nuclear energy from the energy infrastructure. SMR: Steam methane reforming, PCK/CC: petcoke gasification, NGB: natural gas boiler, NGCO: Natural gas cogeneration, EH2: Electrolytic hydrogen, BioCO: Biomass cogeneration

Figure 4.14 shows the total costs and unit costs of energy production over the entire planning period for the different natural gas prices. It can be observed that there is a generally increasing trend in the cost of energy production. However, this increase is mainly contributed to by the increase in nuclear energy production capacity, which is observed in the increase in capital cost. The cost of fuel, on the other hand, slightly decreases, which is explained by the considerable decrease in fuel consumption. From this scenario it can be observed that nuclear energy and alternative fuels, such as petcoke gasification, play a significant role in replacing the utilization of natural gas as a fuel in the operations of the oil sands industry.

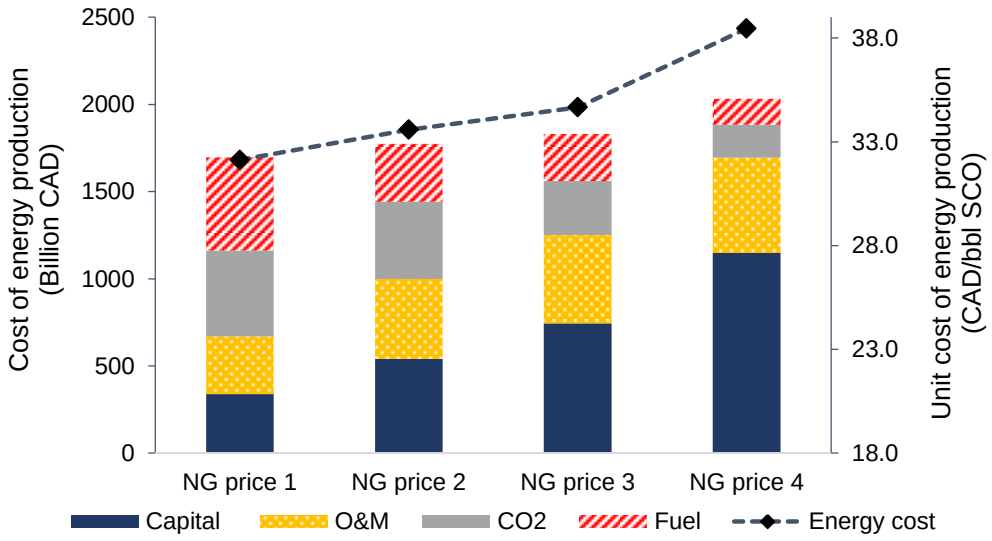

Figure 4.14 Total net present value of the cost of energy production and unit cost of energy production for the entire planning period for various fuel prices (Demand level 5, high emission cap, low credit price)

4.4.4 Scenario IV: Selling excess power and hydrogen

The incorporation of cogeneration and polygeneration facilities might result in one of the energy commodities to be produced in excess. Considering the high ratio of heat to power demand for oil sands operations, electricity is one of the energy commodities that is most likely to be produced in excess from these facilities. Electricity in Alberta is mostly produced from coal, which provides an incentive for the grid to purchase clean power produced from nuclear, wind and fossil-fuel based technologies integrated with carbon capture. Another options considered was utilizing the excess power from nuclear and renewable technologies for the production of hydrogen via water electrolysis, which can be used to satisfy the hydrogen demand of oil sands operations or sold to the market. It was observed that the amount of excess electricity sold to the grid and the production of hydrogen through water electrolysis are highly sensitive to the selling price of hydrogen. Figure 4.15 shows the amounts of hydrogen produced via electrolysis that are sent to satisfy the demand and sold to the market. It can be observed that the hydrogen to demand and hydrogen to market follow opposite trends over the planning period, in which the former increases and the latter decreases. Moreover, the total amount of hydrogen production via electrolysis is higher at higher hydrogen selling prices. At hydrogen selling prices below $2.3/kg, production via electrolysis is not economically attractive.

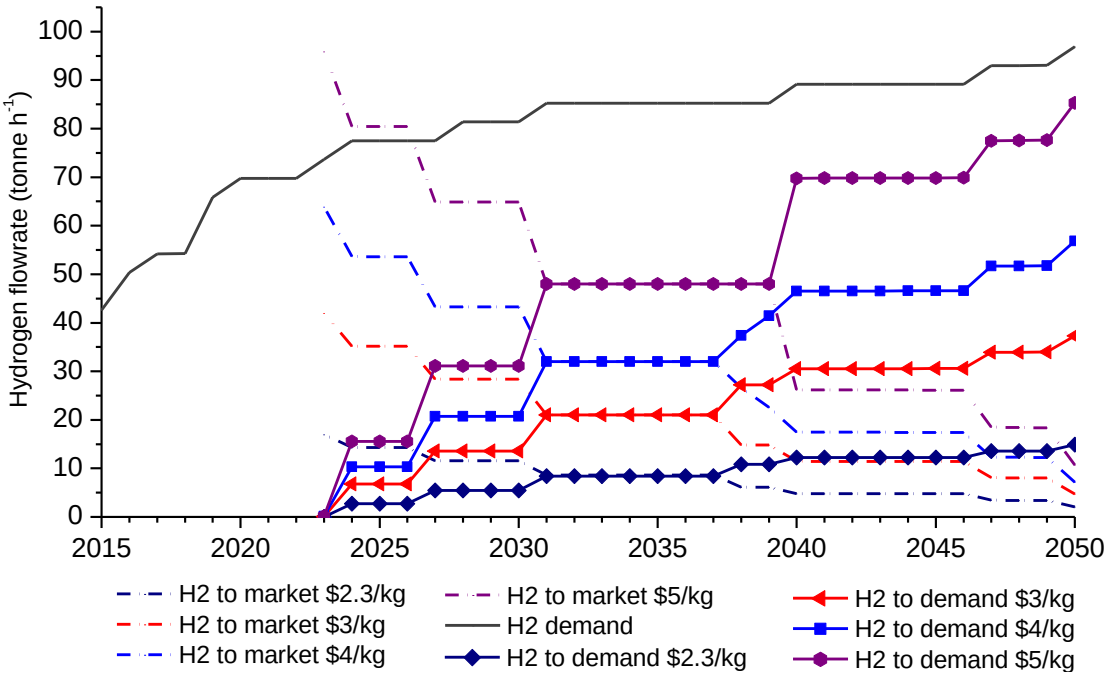

Figure 4.15 Electrolytic hydrogen produced to satisfy the demand for upgrading operations and hydrogen sold to the market at different hydrogen selling prices (Demand level 5, High emission cap, low carbon credit price)

It was also observed that the amount of excess electricity sold to the grid increases as the selling price of hydrogen increases. Figure 4.16 shows the amount of power exported to the grid at different hydrogen selling prices. This indicates that the additional power production capacity and electrolyzers capacity is justified by the additional revenue obtained from selling hydrogen and electricity to the market. The higher selling price of hydrogen provides an incentive to sell more hydrogen to the market, which will require a higher amount of excess power production to be used by electrolyzers. Figure 4.13 shows the distribution of the energy infrastructure for the scenario in which excess electricity is sold to the grid and excess hydrogen is sold to the market. It can be observed that selling the excess from these commodities provides an incentive to install a higher capacity of cogeneration facilities, such as nuclear and natural gas combined heat and power. For brevity, only the results for the case in which the hydrogen price is $5/kg are shown for

the distribution of the energy infrastructure, as the results for the other hydrogen prices show a similar comparison with the base case.

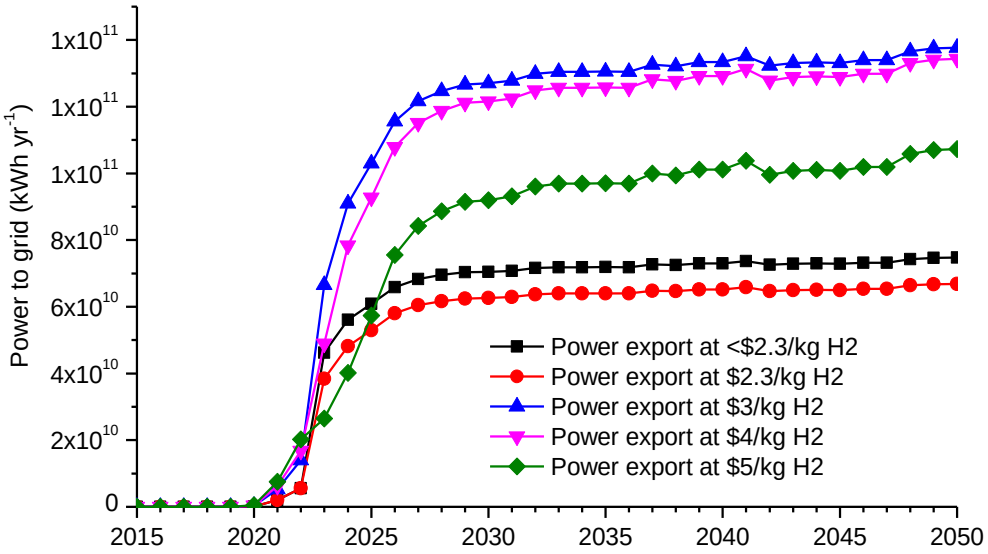

Figure 4.16 Excess power sold to the grid at various hydrogen selling prices (Demand level 5, high emission cap, low carbon credit price)

Figure 4.17 shows the total and unit cost of energy production for the different levels of hydrogen selling prices. It can be observed that selling excess power and hydrogen has a significant impact on reducing the unit cost of energy production. The increase in the production capacity of nuclear energy, which is utilized to provide power, heat and hydrogen (i.e. via electrolysis) requirements, will significantly reduce fuel consumption, and in return will reduce fuel costs. Moreover, the cost of CO_2 mitigation is significantly reduced due to the higher capacity of clean energy production.

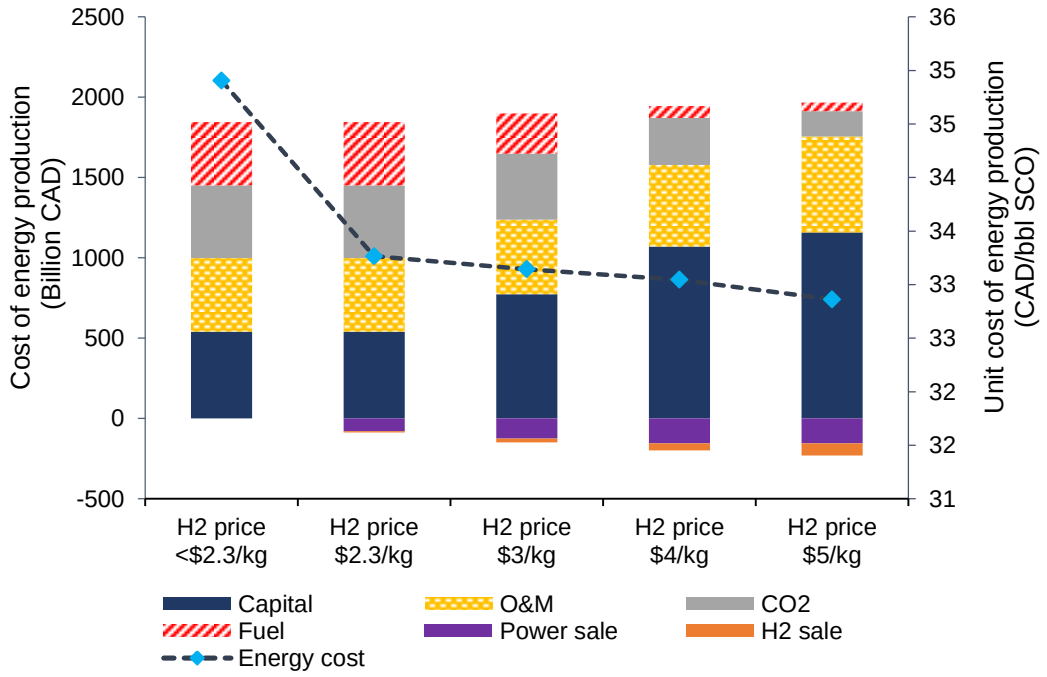

Figure 4.17 Total net present value of the cost of energy production and unit cost of energy production for the entire planning period at various hydrogen selling prices (Demand level 5, high emission cap, and low carbon credit price

4.4.5 Scenario V: Nuclear external penalty cost

An important aspect of using nuclear energy technologies for the production of power and heat is associated with the social, political and environmental impacts involved with their construction and operation. In this scenario the penalty cost factor that determines the effect of the environmental and social implications of nuclear accidents on the selection of these technologies is investigated. Accounting for the costs associated with nuclear accidents involves the incorporation of the cost of environmental and social damage incurred due to a nuclear accident and the probability of occurrence of a nuclear accident per reactor based on historical data of the operation of these facilities in Canada[70]. The remaining inputs to the optimization model are the same as those used for the base case scenario. Based on the results shown in Figure 4.13, it can be observed that the incorporation of nuclear penalty costs has a slight effect on the distribution of energy

production technologies over the planning period. A small percentage of the nuclear production capacity is replaced by natural gas cogeneration facilities with carbon capture. These results show that the penalty factors considered do not represent a significant burden on the economic performance of energy production for oil sands operations, which can be attributed to the assumed low probability of a nuclear accident occurrence. Moreover, these results were obtained for the lowest price of natural gas considered. Based on the results obtained from the sensitivity analysis of the variability in natural gas price, the selection of natural gas based technologies was considerably reduced at higher price levels. This indicates that the effect of nuclear penalty costs might have an even lower impact at higher natural gas prices.

Figure 4.18 compares the CO_2 emission levels of the scenarios in which the natural gas prices are increased, excess power and hydrogen are sold, and nuclear penalty cost are incorporated to the base case scenario (i.e. demand level 5, high emission reduction cap, low carbon credit price, and $2.4/GJ of natural gas). It can be observed that increasing the natural gas price and selling excess power and hydrogen will result in considerably lower annual emissions compared to the base case scenario. This is due to the increased production capacity of nuclear generation facilities. The emission levels in the scenario in which nuclear penalty cost is incorporated is slightly lower compared to the base case scenario. This is due to the higher capacity of natural gas combined heat and power integrated with carbon capture.

4.4.6 Scenario VI: Elimination of nuclear energy

It was observed from the previous results that nuclear energy plays a significant role in providing energy for oil sands operations and reducing the total emissions associated with

providing these energy requirements. Nuclear energy accounts to approximately 15% of Canada's energy mix, and several Canadian provinces have experience in nuclear energy production. However, with respect to Alberta, there has been no experience with the production of nuclear energy in the province, which indicates the existence of significant uncertainties in the licensing process and provincial legislation regarding nuclear facilities. Even though other Canadian provinces have experiences with the licensing process, which might provide guidance in licensing Alberta's first nuclear facilities, provincial governments adopt different positions. Moreover, based on licensing experiences in other provinces, licensing new nuclear projects are typically faced with the challenge of divided powers involved in conducting their environmental impact assessment, which results in uncertainty in redefining the terms of the licensing process [153]. As a result, it is important to consider the effect of the possibility that nuclear reactors cannot be incorporated in the energy production portfolio for oil sands operations.

It can be observed from the results in Figure 4.13 that the technologies that contribute significantly to the energy production mix for this scenario include natural gas cogeneration with carbon capture and boilers for the production of SAGD steam, process steam and power, petcoke gasification for the production of hydrogen, steam and power, bioenergy (heat, diesel and cogeneration), and geothermal energy. Figure 18 shows the total emissions generated for this scenario. The total emissions generated were considerably higher compared to the other scenarios in which nuclear energy was incorporated. Moreover, even with applying the higher carbon tax (Figure A2 in the appendix), the emission cap imposed (high emission cap) was not achieved. This is

because it was more economical to purchase carbon credits than to significantly increase the capacity of technologies integrated with carbon capture and renewable technologies. The total cost of energy production for this scenario over the entire planning period was determined to be CAD 5,890 billion, which corresponds to a cost of carbon mitigated of CAD 1,214 per tonne of CO_2.

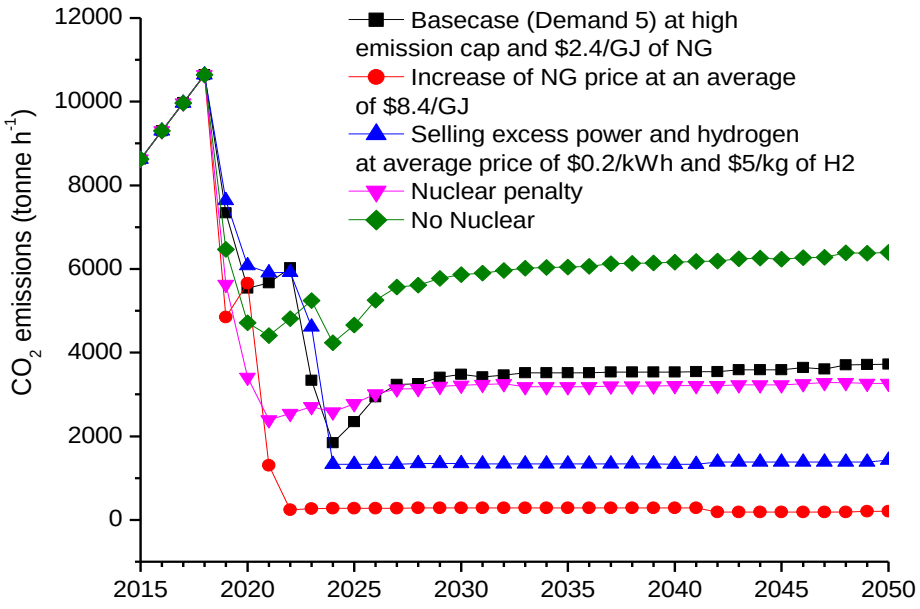

Figure 4.19 CO_2 emission level over the entire planning period of the base case scenario compared with the scenarios in which excess power and hydrogen sold to the market (H_2 selling price of $5/kg), the natural gas price is increased (at NG price 3: $8.4/GJ), the incorporation of external nuclear penalty cost, and elimination of nuclear energy

The cost of carbon mitigated for this scenario is considerably higher than that obtained for the scenario in which nuclear energy was incorporated. Achieving the significant required emission reductions is difficult without the introduction of nuclear facilities in the oil sands energy infrastructure. This supports the renewed interest of Alberta's Provincial Energy Strategy in nuclear energy as a low-emission source for the growing demands of heat and electricity of oil sands operations. The government of Alberta has been striving to achieve emission reductions in the power sector and heat generation for

oil sands operations (main source of oil sands CO_2), for which nuclear energy can be a strong candidate, based on experience in other Canadian provinces (e.g. Ontario) [154]. The efforts of the government of Alberta has been mainly focused on developing carbon capture and sequestration projects, which might be more uneconomic when integrated with the dominantly utilized coal-based power plants in Alberta and natural gas boilers utilized for heat production of oil sands operations. This is due to the difficult and expensive chemistry of the process that involves the separation of CO_2 from nitrogen, which is present in significant amounts as air is used as the oxygen source for the combustion of these fuels [154, 155].

4.5 Conclusions

In this paper a deterministic multi-period mixed integer linear programming model for the planning of energy production for energy intensive industrial operations was described and evaluated. The optimization model is developed with the objective of identifying the optimal mix of energy supply and CO_2 emission mitigation options to satisfy a set of energy demands (e.g. power, heat, hydrogen, etc.) and emission targets at minimum cost. In order to accomplish this, an objective function is formulated that is geared towards the minimization of the net present value of the total cost of energy production over the entire planning period. Moreover, the model formulation incorporated time dependent parameters in order to account for the variability in major factors affecting the operations of the industry. These include energy demands, fuel prices, CO_2 emission reduction targets, CO_2 credit/tax cost, construction lead time, and techno-economic parameters of energy production technologies. In order to illustrate the applicability of the proposed mathematical model, it was applied to a case study based on

the energy-intensive oil sands operations in Alberta over the planning period 2015 – 2050. The application of the proposed model on the oil sands operations in Alberta addresses potential long term issues associated with extracting and upgrading bitumen, which include GHGs emission and instability in fuel prices associated with the continuously increasing quantities of natural gas consumed as the main energy source. The energy supply technologies considered include nuclear (PBMR, ACR-700, ACR-1000, CANDU, and HTGR) for power and heat production, natural gas combined cycle and oxyfuel for power production, pulverized coal and coal oxyfuel for power production, steam methane reforming for hydrogen production, gasification (coal, petroleum coke, biomass, and asphaltenes) for power, hydrogen and thermal energy production, industrial natural gas combined heat and power production, natural gas boilers, integrated wind power, nuclear power and water electrolysis for power and hydrogen production, biodiesel, and geothermal energy. Carbon mitigation options also included carbon capture and sequestration, and purchase of carbon credits to satisfy emission targets. In addition, the model incorporated the possibility of selling excess power production to the Alberta grid, and excess hydrogen to the market. Several scenarios were investigated in order to account for the variability in time dependent parameters. These include variability in energy intensities, carbon mitigation policies, fuel prices, and price of energy commodities (e.g. H_2 selling price).

In the first investigated scenario, in which six demand levels were investigated based on variability in energy intensities for a certain oil production level, the optimal energy infrastructure switched from mostly natural gas based production (i.e. boilers, CHP and SMR) at low demand levels to nuclear, renewable and alternative fuels at higher demand

levels. For example, at demand level 1 the energy production mix consisted of newly installed NG-boilers and NG-CHP for power, steam and hot water production, SMR and petcoke gasification with carbon capture for hydrogen production, biodiesel, and natural gas combustion for upgrading heat. During the middle of the planning period, the NG-CHP were integrated with carbon capture. However, at demand level 6 a considerable portion of the energy production mix was contributed to by nuclear energy production and NG-CHP with carbon capture, and bio-SNG for upgrading heat. For the demand level 1 – 6, the total and unit energy production costs ranged from CAD 446 – 2586 billion and 8.45 – 48.9 CAD/bbl SCO, respectively. The average annual emissions generated ranged from 1100 – 12000 tonne h^{-1} for demand levels 1 – 6. The currently applied \$15/tonne CO_2 carbon tax in Alberta was not sufficient to achieve the required emission reductions. Moreover, an average price of natural gas of \$2.48/GJ was assumed for this scenario, which is actually expected to considerably increase in the future, explains the high dependency on natural gas-based energy production.

In the second scenario, the carbon mitigation policy was varied. A high and low range of emission reduction targets was considered. For each, a low and high range of carbon credit prices was considered, as well as the unavailability of carbon credits. The results of this scenario showed that increasing the emission reduction target at the low range of carbon tax caused the model to increase the production capacity of clean energy production technologies (e.g. nuclear, renewables, and carbon capture). However, the average annual emissions were still considerably high at 3200 tonne CO_2 h^{-1}. At both a high emission reduction target and carbon tax, the average annual emissions achieved was less than 1000 tonne CO_2 h^{-1}, which is well below the imposed emission target. For

the cases in which the availability of purchasing carbon credits is eliminated, the annual emissions achieved were approximately equal to the imposed targets. However, the cost of energy production were the highest for these scenarios due to the high cost of carbon capture and sequestration.

Other scenarios were investigated in order to examine the effect of the variability in fuel prices, the possibility of selling excess energy commodities (i.e. hydrogen and power), and the incorporation of factors such as the social effect of utilizing nuclear energy on the selection of the optimal mix of energy production technologies. At higher prices of natural gas, the capacity of nuclear, combined heat and power, renewables (geothermal), and alternative fuels (petcoke and biomass) increases. The use of these technologies resulted in a considerable reduction in the consumption of natural gas. For example, at an average natural gas price of \$2.4/GJ the natural gas consumption continuously increases over the planning period reaching levels of 2.4×10^5 GJ h^{-1} by 2050. However, at average natural gas prices in the range of \$8/GJ – \$9/GJ, the consumption of natural gas drops to levels of $3.1 \times 10^4 – 7.0 \times 10^4$ GJ h^{-1}, which translates to a considerable decrease in the cost of fuel consumption. The lowest range of the unit cost of energy production was obtained for the scenario in which excess power is sold to the grid and excess hydrogen is sold to the market, which was in the range of \$32.9/GJ – \$34.9/GJ. The hydrogen selling price was found to have an effect on the amount of power and hydrogen sold. The higher hydrogen selling price justified the investment in electrolyzers that utilized excess power produced from nuclear facilities. This provided an incentive to increase the capacity of clean energy producers, resulting in a considerable reduction of CO_2 emissions, which reached average annual levels of 1100 tonne CO_2 h^{-1} that are well below the imposed

emission targets. The final scenario investigated involved the eliminations of nuclear energy from the energy infrastructure, which clarified their significant contribution in achieving high emission reductions in oil sands operations.

Based on the results obtained, it can be observed that the proposed model provides potential benefits as a tool to study future production scenarios for oil sands operations over a long planning period. Moreover, the model can be employed for the planning and scheduling of future configurations of oil sands producers and energy commodity producers in the Canadian oil sands. However, it is important to note that the results obtained might considerably vary depending on the values of the input parameters. For example, if emission factors of energy production technologies that are based on detailed life cycle assessment analyses are incorporated, they can considerably affect the results obtained from the model, and hence the conclusions drawn. This is because there are various concerns that are associated with upstream emission of various energy production technologies (e.g. natural gas based, nuclear, biomass-based, etc.) that depend on their location and source of fuel[89-91]. These indirect emissions might render a low-carbon emitting (i.e. direct emissions) technology to be considered carbon intensive for the specified location and fuel source, which might affect the selection of these technologies by the model. Moreover, even though the proposed model takes into account the time variability in various parameters affecting the operations of oil sands over a long planning period, it does not account for the uncertainty in these parameters at a certain time period. These uncertainties arise in the energy demand intensities, fuel prices, selling prices of energy commodities, etc. For example, a more realistic scenario would consider a user defined probability distribution of the natural gas prices. Accordingly, the

proposed deterministic multi-period model will be adjusted into a stochastic energy optimization model. A stochastic energy optimization model will help to provide an indication of the most suitable configurations given the probability distribution in key input parameters.

Chapter 5

Multi-objective integrated planning and scheduling of the energy infrastructure of the oil sands industry incorporating intermittent renewable energy[3]

5.1 Introduction

The Canadian Oil Sands represent the third largest crude oil proven reserves in the world, and they account for approximately 97% of Canada's total oil reserves. Bitumen extraction from oil sands and its upgrading to higher quality crude (i.e. synthetic crude oil; SCO) requires significant amounts of energy [163]. The energy required is in the form of steam, hydrogen, power, and operating fuel that are mostly derived from burning natural gas, which was initially utilized instead of more carbon-intensive fuels in order to achieve reductions in total greenhouse gas (GHG) emissions from the industry's operations [164]. However, the increase in the production levels from the industry over the past decade had offset the achieved emissions reductions, resulting in the industry becoming the largest contributor to the growth of GHG emissions in Canada. Moreover, the majority of this natural gas is obtained via the Mackenzie Valley pipeline, which has a capacity that will not be capable of supporting the natural gas requirements of oil sands operations by 2030 (5800 million cubic feet/day) [165, 166].

Further governmental and global climate policies (e.g. California's Low Carbon Fuel Standard) are imposed on the lifecycle GHG emissions of transportation fuels and are

[3] A variant of this chapter has been accepted: M. Elsholkami and A. Elkamel. Industrial & Engineering Chemistry Research, 2018.

becoming increasingly strict, which has a significant impact on the development of the oil sands industry [167, 168]. All of these factors provide an incentive for oil sands operators to implement measures for achieving further reductions in their total GHG emissions. Moreover, there are rising concerns regarding the resource availability and price volatility of natural gas, which has prompted the industry to consider alternative options for energy production (e.g. alternative fuels, renewables, etc.) [169, 170]. As a result, oil sands operators are progressively interested in utilizing technologies and implementing operational techniques that allow further reductions in the GHG emissions associated with bitumen extraction and upgrading operations [171, 172], as well as reducing the reliance on natural gas for providing their energy requirements [173, 174]. Several studies in the literature have investigated the utilization of less-carbon intensive technologies and alternative fuels for natural gas for the production of energy for oil sands operations. These include nuclear energy for the cogeneration of heat and power [175, 176], electrolytic hydrogen production from wind power [177], bioenergy [178], geothermal energy [179, 180], and alternative fuels that are widely available in Alberta (e.g. bitumen, asphaltenes, coal [181, 182], petroleum coke [183], etc.). Other studies have investigated increasing the efficiency of energy production from natural gas, such as the capacity expansion of facilities for the cogeneration of heat and power [184, 185].

In each of the studies previously mentioned, the scenario-based analyses of comparing the alternative energy production technologies to the currently existing energy infrastructure incorporate economic, environmental, and sustainability (e.g. accessibility, reliability, etc.) factors. There are models that have been developed to assess the total energy demands of the oil sands industry [185]. Moreover, there have been studies that

proposed mathematical optimization models that take into account these factors simultaneously in order to support the decision making process for the planning and scheduling of energy production required for the Canadian oil sands operations [186, 187]. In the development of these models various energy production technologies were considered, including conventional fossil-fuel based, nuclear, renewable (i.e. wind, bioenergy, and geothermal), and petroleum coke-fired energy production units, which were also integrated with carbon capture technologies [188, 189]. These models generated solutions that provide an indication of the optimal energy infrastructure required to meet the energy demands (i.e. steam, hydrogen, power, etc.) for a given oil production infrastructure.

The mathematical models proposed in these studies address the optimization of the energy infrastructure of oil sands operations using a deterministic snapshot approach or multi-period models that are geared towards long-term planning (i.e. annual), in which average annual estimates of input parameters (e.g. fuel prices, electricity prices, etc.) are used. Moreover, these proposed models assumed that the production infrastructure that provides the energy requirements for oil sands operations is stand-alone. However, in reality the energy infrastructure of the industry interacts with the local grid in several ways [190]. For example, the natural gas combined heat and power units that generate a significant share of the steam required for bitumen extraction and upgrading supply more than 50% of Alberta's cogeneration electrical capacity. It is estimated that if cogeneration is used within oil sands operations to its full potential, the technology can contribute to a reduction of more than 40% of the emissions of the power sector in Alberta [191]. Another example is the penetration of wind power that is part of the potential wind-

electrolysis system that can provide a portion of the hydrogen requirements of bitumen upgraders [176], which will have an effect on the unit commitment operations of the grid's existing power generation units. Similarly, this interaction must be accounted for with the introduction of any multi-commodity generation capacity (e.g. nuclear heat and power, petcoke gasification, etc.) into the energy infrastructure of oil sands operations.

There are numerous studies in the literature that focus on the optimization of distributed energy systems. These systems can be viewed as a network of nodes comprising energy generation suppliers, storage, and consumers that are connected via energy carrier lines (e.g. electricity transmission lines, water pipes, hydrogen pipelines, etc.). The energy generation, storage, and consuming components are commonly connected to the local grid. The optimization of the investment planning and operations management of these systems is typically carried out using multi-objective optimization techniques in order to account various energy efficiency and sustainability measures. Somma et al. [192] and Majewski et al. [193] investigated exergy in distributed energy systems design using a multi-objective optimization approach, in which economic and sustainability measures are incorporated. Falke et al. [194] applied multi-objective optimization approaches to the planning of residential energy systems that supply heat and power, in which various economic, environmental and energy efficiency measures are incorporated. Haikarainen et al. [195] provided a generalized approach for the optimization of distributed energy systems. Barbato et al. [196] developed an energy management framework that integrates local renewable energy sources and facilitates power management and scheduling in smart campuses. Another area of interest in the literature involves the performance analyses (i.e. economic, environmental, etc.) of unit commitment with distributed energy

systems, particularly in the presence of intermittent renewable energy resources. These models focus on the scheduling of the concerned energy infrastructures [197, 198]. Yang et al. [199] further incorporated uncertainties associated with renewable energy generation sources. Gamage [190] proposed a unit commitment mathematical model in order to investigate the effect of wind power penetration on the operations of the existing power generation units in the Alberta grid. The model was geared towards the minimization of total grid cost and the results outlined the performance of the grid's units with increased penetration of wind generation capacity. Integrated planning and scheduling is receiving increased interest in the literature, as the problem regularly arises in the process industry and supply chain. The problem has been approached by developing multi-scale mathematical optimization models that can facilitate the integration of decisions over a wide range of time scales [200, 201]. Hemmati et al. [202] later incorporated stochastic optimization techniques for the short-term scheduling and long-term planning of microgrids, and Vahid-Pakdel et al. [203] incorporated them using the energy hub approach in demand response markets. The models can serve as tools in the decision making process of policy makers and industrial operators that can assist in simultaneously determining long-term (e.g. monthly, annually, etc.) planning decisions including facilities' (i.e. production, storage, transportation, etc.) technologies, capacities and locations, as well as medium and short-term (e.g. weekly, daily, hourly, etc.) decisions including the assignment and sequence of production, storage and transportation tasks among the established entities.

Within the above context, this study proposes a mathematical programming model for the integrated planning and scheduling of the energy infrastructure of the oil sands industry.

The developed model is multi-period with an hourly increment over an annual span that can capture details in the variability of input parameters (e.g. electricity prices and demand, wind speed, etc.). The energy production units incorporated in the infrastructure of the industry are grid-connected, from which electricity can be sold to the grid. A unit-commitment model is incorporated to schedule the operations of the existing units of the grid and the newly installed technologies. Multiple objectives are incorporated in the model, which are the system cost, grid cost, and total GHG emissions. These distinctive features of the proposed model were not addressed before in the literature of oil sands operations. The model is applied to a case study for the year 2017 to illustrate its applicability.

5.2 System description and Problem Statement

The current energy infrastructure that provides the energy requirements (i.e. steam, hydrogen, heat, and power) is composed of natural gas boilers, natural gas combined heat and power plants, steam methane reformers, and power imported from the grid [189]. Figure 5.1 shows the superstructure of alternatives based on which the optimization model is developed. The energy requirements for the oil sands industry are assumed to be supplied by a set of energy commodity producers. These include fossil-fuel based (i.e. natural gas), combined heat and power, renewable, and nuclear technologies. These producers are used to generate electricity, heat (i.e. steam, hot water, etc.), and hydrogen.

Two new subsystems are introduced into the energy infrastructure, which are the wind-electrolysis and nuclear energy systems. The wind-electrolysis system consists of wind turbines, electrolyzers, and hydrogen storage tanks. Southern Alberta is the primary area with significant wind resources in the province, in which all wind farms are currently

allocated. The transmission infrastructure in this region requires significant improvements to transport wind power to large load centers, which hinders the possibility of sending electricity to oil sands operators in the north-eastern region of the province [204].

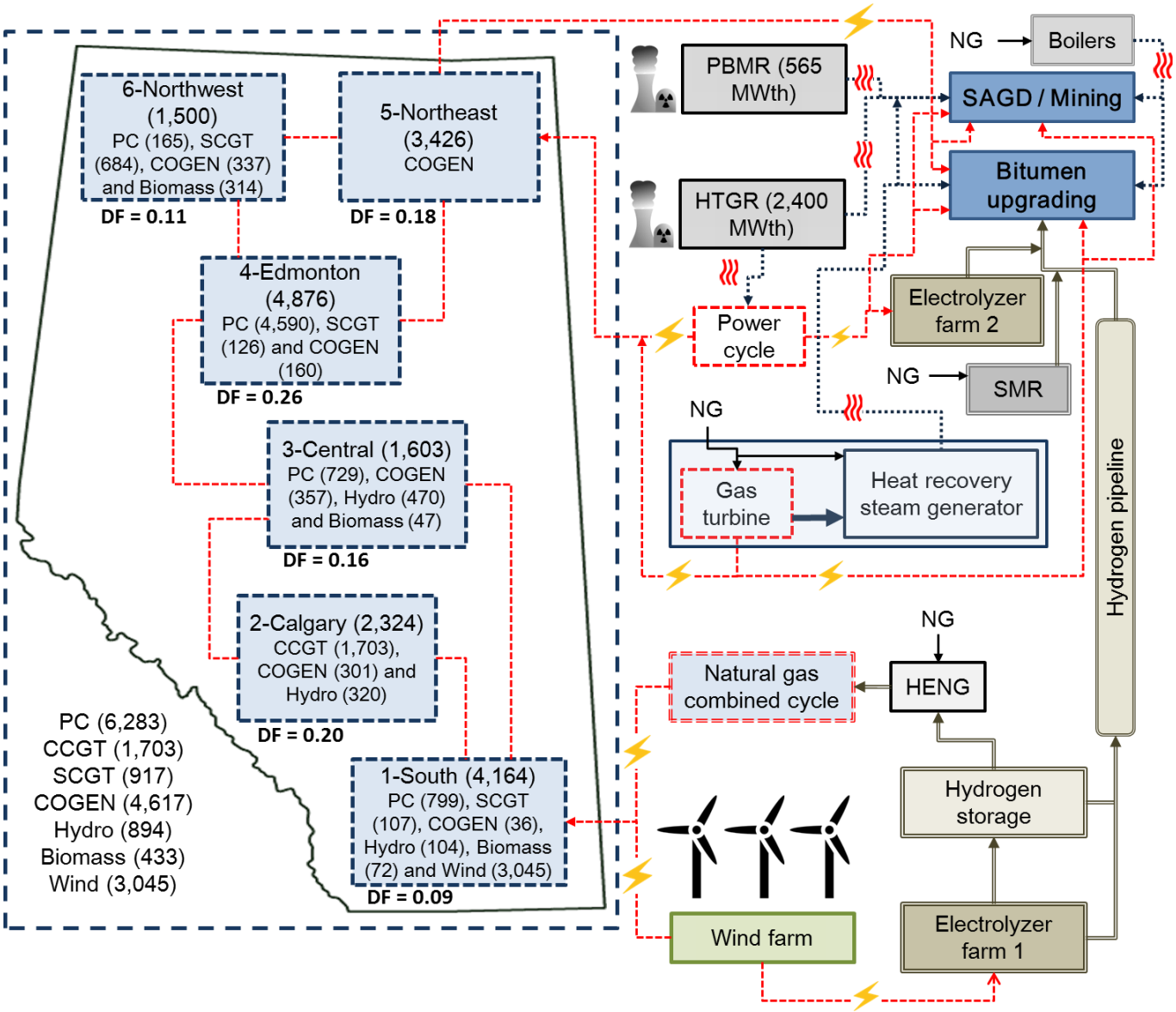

Figure 5.1 Superstructure representation of the proposed energy system for the oil sands industry (right) and its interaction with the local Alberta grid (left) [190]. The Alberta grid is divided into six regional buses. The power generation technologies connected to each bus and its total capacity is shown in brackets. The demand fraction (DF) for each bus is also shown. PC: Pulverized coal; SCGT: Simple cycle gas turbine; COGEN: Natural gas cogeneration; Biomass: Biomass; Hydro: Hydro power; CCGT: Combine cycle gas turbine; HENG: Hydrogen enriched natural gas; NG: Natural gas; SMR: Steam methane reforming; SAGD: Steam assisted gravity drainage; PBMR: Nuclear pebble bed modular reactor; HTGR: Nuclear high temperature gas reactor.

The wind power generated can be sent to electrolyzers for the production of hydrogen or sold to the grid. The electrolytic hydrogen produced can be sent directly via pipelines to bitumen upgraders, and the excess can be stored to be retrieved for later use. Hydrogen retrieved from storage tanks can be sent to bitumen upgraders or used in hydrogen enriched natural gas used as a fuel in natural gas combined cycle (NGCC) power generation units. The power produced can be sold to the grid. The nuclear energy system consists of nuclear reactors (i.e. Pebble bed modular reactor; PBMR and high temperature gas-cooled reactor; HTGR), power cycle, and electrolyzers. The heat generated from the nuclear reactors provides the heat requirements of oil sands operations, particularly steam for steam assisted gravity drainage (SAGD) bitumen extraction. The electricity generated from the power cycle provides the power requirements for the operators in the vicinity, sold to the grid, or sent to electrolyzers to produce hydrogen for bitumen upgraders.

Based on Gamage [190] the Alberta grid can be represented by six regional buses with transmission lines among them as shown in Figure 5.1. The total installed power generation capacity in Alberta currently amounts to 16,661 MW, of which approximately 38% is coal-based generation capacity. The peak demand of the system is estimated to be approximately 12,523 MW with an annual load factor of approximately 80% [205, 206]. The Alberta Electric System Operator (AESO) is an independent system operator in Alberta, in which the electricity market is deregulated and power production is considered to be a competitive business. The transmission system is composed of a high voltage power line (240 kV) that is connected to four capacities of low voltage regional transmission centers (69 kV, 72 kV, 138 kV, and 144 kV) [190, 204]. The Alberta power system is considered to be the most carbon intensive power generation system in Canada.

This is attributed to significant share of electricity produced from coal-based generation units, which annually accounts to approximately >60%. As shown in Figure 5.1 the model developed in this study depicts the Alberta power system to consist of six regional buses and seven transmission lines connecting them. The generation capacity of each generation technology and the demand fraction for each bus is also shown. Based on Gamage [190], this representation provides satisfactorily accurate results for the operations of the power system as validated by actual historical operating data [190].

There are various configurations and tradeoffs that can be realized from the proposed energy system as well as the scheduling of the operations of the existing production units, for which it is required to apply integrated planning and scheduling optimization tools in order to determine the optimal set of decision variables in the system. The planning variables include the capacity of energy producers and carriers (i.e. NG cogeneration, NGCC, wind turbines, nuclear reactors, electrolyzers, hydrogen storage tanks, and hydrogen pipeline capacity), energy flows between energy producers, energy flows between energy producers and end users. It is assumed that there exists sufficient capacity of natural gas boilers and SMR units to meet the energy demands of oil sands operators. Scheduling decisions will determine the hourly dispatch of the existing power generation units of the grid, as well as the newly installed plants. Exogenous parameters such as hourly power demand, hydrogen demand, fuel prices, electricity prices, and techno-economic data are considered. To the author's knowledge there is no work available in the literature that focus on the optimized planning of a grid-connected energy infrastructure for oil sands operations using mathematical optimization techniques. The

distinctive features of the optimization model presented in this work can be summarized as follows:

- A multi-objective and multi-period mixed integer linear programming (MILP) model that minimizes the total system cost, total grid cost, and total GHG emissions with the consideration of grid interactions (i.e. grid connected). The total system cost comprises the capital and operating costs associated with providing and managing the generators of multiple energy commodities (i.e. heat, power and hydrogen) for oil sands operators. The Alberta grid operating cost comprises the cost of managing power generation and distribution facilities, which are owned by various companies. Minimizing the grid cost can be of interest to the Alberta Electric System Operator (AESO), which is a non-profit organization that works with industrial partners to manage and distribute power sold by generators in a competitive electricity market. The electricity generated with the lowest cost is sold first, followed by higher cost electricity until the total demand is satisfied. Another reason the system and grid operating costs have been separated into two different objective functions is because they have considerably different orders of magnitude (the system cost is at least an order of magnitude higher). This is a necessary step, as otherwise the optimization model results would have been dominated by the objective function with the higher order of magnitude.
- Incorporates a unit commitment model to determine the effect of the penetration of new power production technologies, including renewables (i.e. wind), on the dispatch of the existing grid units and newly installed units.

- The developed model allows for the integrated planning and scheduling of the proposed energy system for the oil sands industry (Figure 1).
- Considers the development of potential energy hubs that incorporates hydrogen economy to manage the off-peak surplus of intermittent renewables, for which multiple recovery pathways are considered (i.e. power-to-gas-to-users and power-to-gas-to-power). The model considers the sizing of the electrolyzers and hydrogen storage farms.

5.3 Optimization model formulation

The mathematical model proposed in this study for the integrated planning and scheduling of the energy infrastructure of the oil sands industry is presented as multi-period and multi-objective mixed integer linear programming model (MILP). Three objective functions are incorporated, which are the total system cost, grid cost, and total GHG emissions. Interactions with the grid are accounted for by unit commitment constraints for the existing grid power generation units. Each of the modeling aspects included in the formulation of the mathematical optimization model are discussed below. The indices, sets, variables, and parameters used in the proposed integrated planning and scheduling model are presented in Appendix B. The time scale of the model is annual planning with hourly scheduling over a single year.

5.3.1 Objective functions

The objective functions, which are the total energy system cost, grid operating cost, and total GHG emissions, are presented below. The epsilon constraint method is used as the solution method to address the multi-objective aspect of the proposed model. The total

system cost and grid operating cost have been separated into two different objective functions because they have considerably different order of magnitudes.

5.3.1.1 System Cost

Eq. 5.1 shows the first objective function, which is the total cost of the energy system. It determines the total system cost for the selected planning year, for example, the year 2020. The total system cost is composed of the capital, operating and fuel costs of the new and existing (if not yet depreciated) fossil-fuel based generating units, as well as renewable technologies (e.g. wind, biomass, geothermal, etc.) and nuclear technologies. In addition, costs for the transport of energy commodities (e.g. hydrogen) among the nodes of the system are included. Finally, the cost of importing of energy commodities, and the revenues earned from exports are part of the total system cost.

$$
\begin{aligned}
TC^{SYSTEM} = Objective_1 = z_1(x) \\
&= \sum_{p\in P^F}\sum_{n\in N} C_{capex}{}_{pn}^{FF_{exist}} + \sum_{p\in P^F}\sum_{n\in N}\sum_{t\in T} C_{opex}{}_{pnt}^{FF_{exist}} + \sum_{p\in P^F}\sum_{n\in N}\sum_{t\in T} C_{fuel}{}_{pnt}^{FF_{exist}} \\
&+ \sum_{p\in P^F}\sum_{n\in N} C_{capex}{}_{pn}^{FF_{new}} + \sum_{p\in P^F}\sum_{n\in N}\sum_{t\in T} C_{opex}{}_{pnt}^{FF_{new}} + \sum_{p\in P^F}\sum_{n\in N}\sum_{t\in T} C_{fuel}{}_{pnt}^{FF_{new}} \\
&+ \sum_{p\in P^{SW}}\sum_{n\in N} C_{capex}{}_{pn}^{Solar\&Wind} + \sum_{p\in P^{SW}}\sum_{n\in N}\sum_{t\in T} C_{opex}{}_{pnt}^{Solar\&Wind} \\
&+ \sum_{p\in P^{NU}}\sum_{n\in N} C_{capex}{}_{pn}^{Nuclear} + \sum_{p\in P^{NU}}\sum_{n\in N}\sum_{t\in T} C_{opex}{}_{pnt}^{Nuclear} + \sum_{p\in P^{NU}}\sum_{n\in N}\sum_{t\in T} C_{accid}{}_{pnt}^{Nuclear} \\
&+ \sum_{q\in Q}\sum_{e\in E}\sum_{n'\in N, n\neq n'} C_{capex}{}_{qenn'}^{Transport} + \sum_{d\in D}\sum_{e\in E}\sum_{n'\in N, n\neq n'}\sum_{t\in T} C_{opex}{}_{denn't}^{Transport} \\
&+ \sum_{e\in E}\sum_{t\in T} C\_system_{et}^{Import} - \sum_{e\in E}\sum_{t\in T} C\_system_{et}^{Export}
\end{aligned}
\tag{5.1}
$$

5.3.1.2 Grid Cost

Eq. 5.2 shows the total operating cost of the grid [190]. The objective function incorporates the operating costs, startup costs, and fuel costs of the grid's operating units, as well as the cost of the unserved demand for all the regional buses. In this study, the import cost shown in the objective function is only for the cost of power that is imported from the energy infrastructure of the oil sands industry, and the export revenue is from the power sent to the energy system.

$$\begin{aligned} TC^{Grid} = Objective_2 = z_2(x) \\ = \sum_{i\in I}\sum_{t\in T}\left[C_{opex}{}_{it} + C_{startup}{}_{it}\right] + \sum_{i\in I^{FF}}\sum_{t\in T} C_{fuel}{}_{it}^{FF} \\ + \sum_{k\in K}\sum_{t\in T} C_{unserved\_demand}{}_{kt} + \sum_{t\in T} C\_grid_{e=power,t}^{Import} \\ - \sum_{t\in T} C\_grid_{e=power,t}^{Export} \end{aligned} \tag{5.2}$$

5.3.1.3 GHG emissions

Eq. 5.3 represents the total GHG emissions from the energy system, which is mainly generated from the combustion of fuels consumed from fossil-fuel based technologies. Emissions can be generated from the transportation of energy commodities among the nodes of the energy system. For example, power consumed by compressors of hydrogen pipelines is obtained from the grid, which has an average emission factor associated with it. Eq. 5.4 represents the total GHG emissions generated from operating the power generation units of the grid, which is associated with the fuel consumed for operation and fuel consumed during the startup of the units.

$$TEC^{SYSTEM} = \sum_{p\in P^F}\sum_{n\in N}\sum_{t\in T}\left[ECO2_{pnt}^{FF_{exist}} + ECO2_{pnt}^{FF_{new}}\right] + \sum_{q\in Q}\sum_{e\in E}\sum_{n'\in N, n\neq n'}\sum_{t\in T} ECO2_{qenn't}^{Transport} \quad (5.3)$$

$$TEC^{Grid} = \sum_{i\in I}\sum_{t\in T}\left[ECO2_{it}^{operation} + ECO2_{it}^{startup}\right] \quad (5.4)$$

Eq. 5.5 shows the third objective function incorporated in the optimization model, which represents the total GHG emissions generated from the energy infrastructure of the oil sands industry and the Alberta grid. The system and grid emissions have the same order of magnitudes, and can be added together to represent the total GHG emissions objective function. The possibility of incorporating different weights for the grid and system emissions was incorporated in order to provide flexibility for the user of the mathematical model. For example, if the users of the mathematical model are companies in the oil sands industry, then they might be interested in only taking into account reductions in GHG emissions associated with their facilities as taking into account both the system and grid emissions will have a considerable impact on the economic objective function and investment decisions. In order to take into account the possibility of setting different weights on the emissions from the energy system and the emissions from the grid, the approach outlined in Fakhfakh et al. [207] is adopted. The approach involves determining the ranges (i.e. minimum and maximum values) of the system (Eq. 5.3) and grid emissions (Eq. 5.4), which are then normalized. The normalized values of emissions are then multiplied by their desired weights (between 0-1), similar to the weighted sum approach.

$$Objective_3 = z_3(x)$$

$$= \phi_{emissions}^{SYSTEM}\left(\frac{TEC^{SYSTEM} - TEC_{MIN}^{SYSTEM}}{TEC_{MAX}^{SYSTEM} - TEC_{MIN}^{SYSTEM}}\right) + \phi_{emissions}^{GRID}\left(\frac{TEC^{Grid} - TEC_{MIN}^{Grid}}{TEC_{MAX}^{Grid} - TEC_{MIN}^{Grid}}\right) \quad (5.5)$$

`

The proposed multi-objective MILP formulation considers Eqs. 5.1, 5.3 and 5.5 as the objective functions, which are labelled z_1, z_2 and z_3, respectively. The multi-objective optimization problem can then be represented as shown in Eq. 5.6.

$$\underbrace{min}_{x \in F} \{z_1(\boldsymbol{x}), z_2(\boldsymbol{x}), z_3(\boldsymbol{x})\} \quad (5.6)$$

where $\boldsymbol{x}$ is the vector of decision variables in the space of feasible region F. The solution approach of the proposed multi-objective mathematical model is the epsilon-constraint method adopted from Liu and Papageorgiou [208]. The objective functions can be represented as follows.

$$\begin{aligned} &\underbrace{min}_{x \in F}\ z_1(\boldsymbol{x}) \\ s.t.\ \ &z_2(\boldsymbol{x}) \leq \varepsilon_2 \\ &z_3(\boldsymbol{x}) \leq \varepsilon_3 \end{aligned} \quad (5.7)$$

Two sub-problems are solved individually in order to determine the minimum and maximum values of ε_3. These are represented in Eqs. 5.8 and 5.9.

$$\begin{aligned} &\underbrace{min}_{x \in F}\ z_1(\boldsymbol{x}) \\ s.t.\ \ &z_2(\boldsymbol{x}) \leq \varepsilon_2 \end{aligned} \quad (5.8)$$

$$\underbrace{min}_{x \in F} z_3(\boldsymbol{x}) \quad s.t. \;\; z_2(\boldsymbol{x}) \leq \varepsilon_2 \tag{5.9}$$

In both sub-problems the objective z_2 is constrained by ε_2, which is a predetermined value of the objective function. The highest possible value of z_2 is determined from the problem defined in Eq. 5.8, in which z_1 is the objective, while z_3 is eliminated. The least possible value of z_2 is determined from the problem defined in Eq. 5.8, in which z_2 is the objective, while z_1 is eliminated. The problem defined in Eq. 5.7 can then be solved by defining ε_3 as represented in Eq. 5.10.

$$\varepsilon_3 = \omega z_3^{max} + (1 - \omega) z_3^{min} \tag{5.10}$$

where $\omega \in [0,1]$ indicates the weight set on the emissions objective function. For each selected value of ε_2, the value of ε_3 is obtained by varying $\omega \in [0,1]$ with an increment of 0.1.

5.3.2 Energy production technologies

The energy production technologies incorporated in this study include fossil-fuel based facilities, particularly natural gas cogeneration units for the cogeneration of power and heat, and natural gas combined cycle power generators. Included in the energy system is wind power production integrated with water electrolysis for hydrogen production. To manage the intermittent behavior of wind power, hydrogen storage is included with two recovery pathways, which are power-to-gas (i.e. hydrogen sent to bitumen upgraders) and power-to-gas-to-power (i.e. hydrogen in HENG used as fuel in natural gas generators). Finally, nuclear energy for power and heat production is included, from which excess

power can be utilized to produce electrolytic hydrogen for bitumen upgrading. The constraints that define the operations of each of these technologies are represented below.

Natural gas combined heat and power

The industrial natural gas cogeneration units included consist of gas turbines that are used for power generation. The steam used to satisfy the heat requirements of oil sands operations is produced by heat recovery steam generators, which recover heat from the exhaust of gas turbines [209, 210]. Supplementary fuel might be combusted in addition to the heat recovered to raise the enthalpy of steam to a desired state. The gas turbines and the high pressure steam generators utilize natural gas as fuel in the combustion chambers. The industrial combined heat and power system is modeled according to the approaches in [211, 212]. The constraints representing the operations of the system are shown in Eqs. 5.11-5.22. The amount of fuel consumed by the gas turbines is calculated based on the amount of power generated and the efficiency of the turbines (Eq. 5.11). The power generated is used to satisfy the power requirements of the host facility, and the excess is sent to the Alberta grid (Eq. 5.12). The amount of supplementary fuel required to achieve the heat demand of the host facility is calculated as shown in Eq. 5.13, which depends on the efficiencies of generation and recovery of the heat recovery steam generator. The total fuel consumed in the cogeneration units is the sum of fuel consumed in the gas turbines and supplementary fuel consumed in heat recovery steam generators (Eq. 5.14). The decision to install cogeneration unit g is determined by the binary variable $YNCO_g$ (Eq. 5.15). The operation of each cogeneration unit g is constrained by Eqs. 5.17 – 5.22. The operations of the gas turbines and heat recovery steam generators are limited by their minimum and maximum operating capacities (Eqs. 5.16-5.17). The startup and shutdown

of each cogeneration unit g during each hour t are defined by the binary variables zco_{gt} and yco_{gt}, respectively (Eqs. 5.18-5.19). After startup during a certain hour t, the cogeneration unit g must operate for a minimum number of hours before shutdown, which is defined in Eq. 5.20. Similarly, after shutdown there is a minimum down time for each unit g before startup (Eq. 5.21). The ramping of each cogeneration unit is limited by the constraint in Eq. 5.22.

$$Fuel\_T_{gt} = 0.0036\, EC_{gt}/\eta_{turbine} \tag{5.11}$$

$$EC_{gt} = P\_EC_{gt}^{grid} + P\_EC_{gt}^{demand} \tag{5.12}$$

$$Fuel\_G_{gt}\, \eta_{generation} = Heat\_cogen_{gt} - \eta_{recovery}(1 - \eta_{turbine}) Fuel\_T_{gt} \tag{5.13}$$

$$Fuel\_cogen_{gt}^{total} = Fuel\_T_{gt} + Fuel\_G_{gt} \tag{5.14}$$

$$EC_{gt} \leq Max\_CR^{cogen} YNCO_g \tag{5.15}$$

$$Min\_CR^{cogen} uco_{gt} \leq EC_{gt} \leq Max\_CR^{cogen} uco_{gt} \tag{5.16}$$

$$Heat\_cogen_{gt} \leq Max\_HRSG^{cogen} uco_{gt} \tag{5.17}$$

$$zco_{gt} \geq uco_{gt} - uco_{g,t-1} \tag{5.18}$$

$$yco_{gt} \geq uco_{g,t-1} - uco_{gt} \tag{5.19}$$

$$\sum_{\tau=t-Min\_uptime_{cogen}}^{t} zco_{gt} \leq uco_{gt} \tag{5.20}$$

$$\sum_{\tau=t-Min\_downtime_{cogen}}^{t} yco_{gt} \leq 1 - uco_{gt} \tag{5.21}$$

$$-Ramp^{cogen} \leq EC_{gt} - EC_{g,t-1} \leq Ramp^{cogen} \tag{5.22}$$

Natural gas combined cycle

The natural gas combined cycle (NGCC) units are used as highly dispatchable power generation facilities in the proposed model. The power plant consists of a gas turbine generator fueled by natural gas or a mixture of natural gas and hydrogen (i.e. hydrogen enriched natural gas; HENG), a heat recovery steam generator, and a triple pressure, reheat and full condensing steam turbine generator. The hourly fuel consumption and power generated by NGCC units is calculated as shown in presented in Eq. 5.23, which depends on the efficiency of power production. As previously mentioned, the fuel supplied to the NGCC units might incorporate hydrogen retrieved from the power-to-gas system, which is presented by Eq. 5.24. Based on various sources in the literature [211], the share of hydrogen that can be safely used in NG-fired facilities without significant retrofits is 5%. This is represented in the constraint shown in Eq. 5.25, in which the share of hydrogen in the HENG cannot exceed the maximum allowable limit ($\varphi_{H_2}^{HENG}$). The selection of each NGCC unit *f* is determined by the binary variable $YNGCC_f$ in Eq. 5.26. The binary variable u_ngcc_{ft} determines if unit *f* is operational during hour *t* in Eq. 5.27, which also limits the operation of each unit between its maximum and minimum capacities. The startup, shutdown and ramping constraints (Eqs. 5.28-5.32) are similar to those of the natural gas cogeneration units.

$$Fuel\_NGCC_{ft} = 3.6\, Power\_NGCC_{ft}/\eta_{NGCC} \tag{5.23}$$

$$\sum_{f} Fuel\_NGCC_{ft} = NG\_NGCC_{t} + H\_to\_NGCC_{t} \tag{5.24}$$

$$\frac{H\_to\_NGCC_{t}}{\rho_{H_2}\, HV_{H_2}} \leq \varphi_{H_2}^{HENG}\left(\frac{H\_to\_NGCC_{t}}{\rho_{H_2}\, HV_{H_2}} + \frac{NG\_NGCC_{t}}{\rho_{NG}\, HV_{NG}}\right) \tag{5.25}$$

$$Power\_NGCC_{ft} \leq Max\_CR^{ngcc} YNGCC_{f} \tag{5.26}$$

$$Min\_CR^{ngcc} u\_ngcc_{ft} \leq Power\_NGCC_{ft} \leq Max\_CR^{ngcc} u\_ngcc_{ft} \tag{5.27}$$

$$z\_ngcc_{ft} \geq u\_ngcc_{ft} - u\_ngcc_{f,t-1} \tag{5.28}$$

$$y\_ngcc_{ft} \geq u\_ngcc_{f,t-1} - u\_ngcc_{ft} \tag{5.29}$$

$$\sum_{\tau=t-Min\_uptime_{ngcc}}^{t} z\_ngcc_{ft} \leq u\_ngcc_{ft} \tag{5.30}$$

$$\sum_{\tau=t-Min\_downtime_{ngcc}}^{t} y\_ngcc_{ft} \leq 1 - u\_ngcc_{ft} \tag{5.31}$$

$$-Ramp^{ngcc} \leq Power\_NGCC_{ft} - Power\_NGCC_{f,t-1} \leq Ramp^{ngcc} \tag{5.32}$$

Wind-electrolysis system

The considered on-shore wind turbines have an average capacity of 1.91 MW, which is the average nameplate capacity installed in Pincher Creek in Alberta. The location of Pincher Creek, Alberta is selected to install the wind turbines used in the energy system

due to the high wind speed potential and its close proximity to nearby on-shore wind farms. The expected wind speed in this location varies on average from 5.81 m/s during the summer to 9.02 m/s during the winter, and the average annual wind speed is estimated to be approximately 6.5 m/s [213, 214]. The power generated from wind energy is sent to electrolyzers for hydrogen production (i.e. power-to-gas), or sold to the Alberta grid. The hydrogen is sent to bitumen upgraders, and excess hydrogen can be stored in storage tanks, which can be retrieved and sent to upgraders or used in HENG utilized in natural gas power generators (i.e. power-to-gas-to-power). The advantage of electrolyzers over other methods for producing hydrogen is the suitability of the technology to adjust to variable energy inputs, such as intermittent wind energy. This is due to their wide operational range, in which they respond quickly to variations in input power [215]. Therefore, they have the potential to increase the availability and reliability of wind energy sources incorporated in the proposed distributed energy system. Alkaline electrolyzers are selected for this study, as they have high efficiencies that can reach values >70% [216]. Six capacity levels were considered for the electrolyzer sizes included in this study, which have different operational ranges. This was included in order to improve the operational range and capacity factor of the total electrolyzer capacity installed. The electrolyzer capacity factor is defined as the ratio of the actual total annual production of hydrogen to the maximum possible annual production level (i.e. total installed capacity of electrolyzers for all operational hours in a year).

The total amount of power generated from wind turbines each hour was estimated as the available wind potential multiplied by the installed number of turbines (Eq. 5.33). The wind potential in megawatts was estimated as shown in Eq. 5.34; it depends on the air

density (kg/m^3), rotor area (m^2), wind speed (m/s) and wind turbine efficiency. It is important to note that the effect of rising extremes, which instantaneously shuts down wind plants by turning the blades into neutral position for operational safety, is not incorporated in Eq. 5.34. Extension of the model in future work can allow for the implementation of alternative input data sets that take into account climate models and forecasts of more frequent storm events simultaneously. The power generated from wind turbines is sent to electrolyzers or sold to the grid (Eq. 5.35). The electrolytic hydrogen produced depends on the electrolyzers' power constant ($AELZ$), which is on average 53.4 kWh/kg H_2 (Eq. 5.36). The total amount of electrolytic hydrogen produced from wind power is divided among the different capacity levels of electrolyzer farm-1 to determine its size (Eq. 5.37). In Eq. 5.38, the number of electrolyzers selected from each electrolyzer capacity level *c* depends on its operational range (i.e. maximum and minimum flowrates when operational). The total electrolytic hydrogen produced is sent to bitumen upgraders in the Alberta Industrial Heartland, and the excess is sent to storage tanks (Eq. 5.39). The material balance on the total hydrogen storage capacity during each hour *t* is shown in Eq. 5.40. The number of hydrogen storage tanks installed depends on the maximum capacity level of a single tank (Eq. 5.41). In Eq. 5.42, the hydrogen stored can be retrieved for two purposes: 1- sent to bitumen upgraders during hours of low electrolytic hydrogen production (i.e. low wind potential), 2- used in HENG utilized in natural gas generators (i.e. power-to-gas-to-power). The electrolytic hydrogen produced and hydrogen retrieved from storage is sent to bitumen upgraders via the available pipeline capacities (Eq. 5.43). Only one pipeline capacity level is selected (Eq. 5.44)

$$Wind\_P_{\ t} = Wind\_Potential_{\ t}\ NWT \tag{5.33}$$

$$Wind\_Potential_{\ t} = 0.5\rho_{air} A_{rotor}\ V_h^3\ \eta^{WT}/1{,}000{,}000 \tag{5.34}$$

$$Wind\_P_{\ t} = Wind\_P_t^{electrolyzers} + Wind\_P_t^{grid} \tag{5.35}$$

$$H\_electrolyzer_t^{wind} = Wind\_P_t^{electrolyzers}/AELZ \tag{5.36}$$

$$H\_electrolyzer_t^{wind} = \sum_{c1} CH_{c1t} \tag{5.37}$$

$$CH\_MIN_{c1}\ N\_electrolyzer_{c1}^{farm1} \le CH_{c1t} \le CH\_MAX_{c1}\ N\_electrolyzer_{c1}^{farm1} \tag{5.38}$$

$$H\_electrolyzer_t^{wind} = H\_input_{\ t} + EH\_to\_upgrader_t^{wind} \tag{5.39}$$

$$H\_storage_t = H\_input_{\ t} - H\_output_{\ t} + H\_storage_{t-1} \tag{5.40}$$

$$H\_storage_t \le H\_storage\_MAX\ \ NHT \tag{5.41}$$

$$H\_output_{\ t} = SH\_to\_upgrader_t + H\_to\_NGCC_t \tag{5.42}$$

$$EH\_to\_upgrader_t^{wind} + SH\_to\_upgrader_t \le \sum_d H\_Transport_d^{MAX} Y\_Hpipe_d \tag{5.43}$$

$$\sum_d Y\_Hpipe_d \le 1 \tag{5.44}$$

Nuclear energy system

In the proposed model nuclear energy can be used to contribute to the energy requirements of the oil sands industry in the form of power and heat. The heat generated can be used to produce steam at different pressure levels, and used for other heating applications. For example, nuclear energy can be used to produce SAGD steam, process steam, and heat utilized by SMR plants for hydrogen production. The power generated can also be used to satisfy the electricity requirements of the host facility, sold to the grid, or used in electrolyzers for hydrogen production for bitumen upgraders. Nuclear energy is a low-carbon intensive technology, which makes it an attractive alternative for the reduction of emission from oil sands operations. The amount of each energy commodity produced can be calculated as presented in Eq. (5.45), where δP_{ue}^{NU} is the yield of each energy commodity e generated from nuclear technology u (units of e/MWth). The power produced from each nuclear plant u during hour t can be used to provide the electricity requirements of oil sands operators, sent to the grid, or sent to electrolyzers for the production of hydrogen for bitumen upgrading (Eq. 5.46). The number of nuclear reactors installed from each nuclear technology *u* depends on its maximum capacity and the total energy requirements (Eq. 5.47). Similar to the wind-electrolysis system, the size of electrolyzer farm-2 that is located in the Alberta Industrial Heartland in the vicinity of bitumen upgraders is determined by the set of constraints in Eqs. 5.48-5.50.

$$EPU_{uet}^{NU} = \delta P_{ue}^{NU} HRP_{ut}^{NU} \tag{5.45}$$

$$EPU_{u,e=power,t}^{NU} = P\_NU_{ut}^{grid} + P\_NU_{ut}^{electrolyzers} + P\_NU_{ut}^{demand} \tag{5.46}$$

$$HRP_{ut}^{NU} \leq \xi_u^{NU} HR\_MAX_u^{NU} NNU_u \tag{5.47}$$

$$H\_electrolyzer_t^{NU} = \left(\sum_u P\_NU_{ut}^{electrolyzers} \right) / AELZ \tag{5.48}$$

$$H\_electrolyzer_t^{NU} = \sum_{c2} CH_{c2t} \tag{5.49}$$

$$\begin{aligned} CH\_MIN_{c2}\, N\_electrolyzer_{c2}^{farm2} \leq CH_{c2t} \\ \leq CH\_MAX_{c2}\, N\_electrolyzer_{c2}^{farm2} \end{aligned} \tag{5.50}$$

5.3.3 Demand constraints

The total energy requirements of the oil sands operators (i.e. power, heat and hydrogen) in the model must be satisfied by the incorporated energy providers. Therefore, the total amount of energy produced by the energy producers included in the energy system must be greater than or equal to the total energy demand for each commodity, which is presented by the set of constraints in Eqs. (5.51-5.53). It is assumed that the existing capacity of natural gas boilers (for heat requirements) and steam methane reforming plants (for hydrogen production) is sufficient to meet any heat and hydrogen requirements that are not fulfilled by the newly installed energy producers.

$$\sum_g P\_EC_{gt}^{demand} + \sum_u P\_NU_{ut}^{demand} + Grid\_to\_OS_t \geq DEC_{e=power,t} \tag{5.51}$$

$$\begin{aligned} EH\_to\_upgrader_t^{wind} + SH\_to\_upgrader_t + H\_electrolyzer_t^{NU} + H\_SMR_t \\ \geq DEC_{e=hydrogen,t} \end{aligned} \tag{5.51}$$

$$\sum_{u} EPU_{u,e=heat,t}^{NU} + \sum_{g} Heat\_cogen_{gt} + Heat\_boiler_{t} \geq DEC_{e=heat,t} \quad (5.53)$$

5.3.4 Grid constraints (unit commitment)

One of the objective functions incorporated in the proposed optimization model is the minimization of total grid cost and grid emissions are also incorporated in the emissions objective function. This affects the operations of the grid's power generation units, which are subject to the unit commitment constrains outlined in Eqs. 5.54-5.68, which are based on the methodology proposed by Gamage [190].

For each regional bus *k*, the power generation units *i* connected to it must satisfy the sum of demand for that bus during hour *t*, as well as the power flow in transmission lines between this bus *k* and other buses *k'*, which is presented by the power balance constraint in Eqs. 5.54-5.56. A variable is incorporated in the power balance constraints to account for any unserved demand, for which their cost is included in the objective function. For regional buses 1 and 5, power is sent to them from generation units in the energy system of the oil sands industry. New wind turbines are installed in regional bus 1, as well as natural gas generators that utilize HENG. Power generated from these units is assumed to be connected to bus 1 (Eq. 5.54). Similarly, natural cogeneration facilities and small-scale nuclear reactor used to produce power and heat requirements for oil sands operators are installed in the Alberta Industrial Heartland. Therefore, excess power generated from these units is assumed to be connected to regional bus 5 (Eq. 5.55). Power generated by the units connected to bus k that is in excess to the total demand at the bus is limited to a percentage of the total demand ($\emptyset^{TE}$), which is set to zero in this study (Eq. 5.57).

The total power flow in transmission lines among buses is calculated as represented in Eq. 5.58, which is based on the DC power flow method that incorporates that susceptance of the transmission lines ($\beta_{kk'}$) and the voltage angles among the buses ($\delta_{kt},\ \delta_{k't}$) at a certain time [190]. This is limited by the transmission capacity (Eq. 5.59). Eq. 5.60 is a capacity constraint on each generation unit *i* during time *t*, in which its power output and the amount of spinning reserves provided by it are within its operational capacity. The binary variable u_gu_{it} represents the commitment of unit *i* during hour *t*. The total amount of spinning reserves generated by all the generation units must satisfy the total spinning reserves of the system (Eq. 5.61), and the spinning reserves generated by a certain unit is limited by its reserve capacity (Eq. 5.62). Eq. 5.63 ensures that the generation of wind and hydro power is below the resource availability in hour *t*. The constraints in Eq. 5.64 and Eq. 5.65 are state transition constraints, in which the binary variables z_gu_{it} and y_gu_{it} indicate the startup and shutdown of generation unit *i* during hour *t*, respectively. The unit commitment constraints in Eq. 5.66 and 5.67 control the amount of time during which a unit must run after startup before the next shutdown (i.e. minimum up-time) and the amount of time a unit must remain off after shutdown before startup (i.e. minimum down-time). Eq. 5.68 represents the ramping control constraint of the grid's units.

$$\sum_{i \in I\_bus1} pp_{it} + Wind\_P_t^{grid} + \sum_n Power\_NGCC_{nt} = Grid\_demand_{bus1,t} - P_{unserved_{bus1,t}} + P_{excess_{bus1,t}} + P_{trans_{bus1,t}} \quad (5.54)$$

$$\sum_{i \in I\_bus5} pp_{it} + \sum_g P\_EC_{gt}^{grid} + \sum_u P\_NU_{ut}^{grid} = Grid\_demand_{bus5,t} + Grid\_to\_OS_t - P_{unserved_{bus5,t}} + P_{excess_{bus5,t}} + P_{trans_{bus5,t}} \quad (5.55)$$

$$\sum_{i \in I\_busk} pp_{it} = Grid\_demand_{kt} - P_{unserved_{kt}} + P_{excess_{kt}} + P_{trans_{kt}} \quad \forall k \in \{k2, k3, k4, k6\}, t \quad (5.56)$$

$$\sum_k P_{excess_{kt}} \leq \emptyset^{TE} Grid\_Demand_t^{Total} \quad \forall t \quad (5.57)$$

$$P_{trans_{kt}} = \sum_{k' \in K} -\beta_{kk'}(\delta_{kt} - \delta_{k't}) \quad (5.58)$$

$$-Trans_{kk'}^{Max} \leq -\beta_{kk'}(\delta_{kt} - \delta_{k't}) \leq Trans_{kk'}^{Max} \quad (5.59)$$

$$Min\_CR^{gu} u\_gu_{it} \leq pp_{it} + sr_{it} \leq Max\_CR^{gu} u\_gu_{it} \quad (5.60)$$

$$\sum_i sr_{it} \geq SR_t \quad (5.61)$$

$$sr_{it} \leq SR\_lim_i^{MAX} \tag{5.62}$$

$$pp_{it} \leq RA_{it}^{hydro\&wind} \quad \forall i \in I^{Hyd\&Wind}, t \tag{5.63}$$

$$z\_gu_{it} \geq u\_gu_{it} - u\_gu_{i,t-1} \tag{5.64}$$

$$y\_gu_{it} \geq u\_gu_{i,t-1} - u\_gu_{it} \tag{5.65}$$

$$\sum_{\tau=t-GU\_Min\_uptime_i}^{t} z\_gu_{it} \leq u\_gu_{it} \tag{5.66}$$

$$\sum_{\tau=t-GU\_Min\_downtime_i}^{t} y\_gu_{it} \leq 1 - u\_gu_{it} \tag{5.67}$$

$$-P\_Ramp_i^{gu} \leq pp_{it} - pp_{i,t-1} \leq P\_Ramp_i^{gu} \tag{5.68}$$

5.4 Data and Assumptions

To investigate the applicability of the proposed optimization model, it is applied to a case study based on the oil sands operations in Alberta, which is one of the major contributors to the production of primary energy in Canada. The extraction and upgrading of bitumen that is sent in significant quantities to refineries in Canada and the United States requires substantial amounts of energy making the industry one of the largest end-users of energy. The energy consumption data attributed to the industry is readily available in the public domain. The energy consumed by the oil sands operations is mainly in the form of power, hydrogen and heat, particularly steam for SAGD bitumen extraction. These energy commodities are currently produced from natural gas, and obtained as electricity from the grid. The continuous development of oil sands extraction and upgrading processes will

further increase the energy requirements and the associated GHG emissions resulting from fuel consumption. The current average requirements of these energy commodities (i.e. power, heat and hydrogen) are quantified to be approximately 1,460 MWh, 163,853 GJ/h, and 81 t/h, respectively [217]. With the current energy infrastructure, the emissions generated from the production of these commodities are on average 72.1 $MtCO_2$. By 2020 the energy requirements are projected to be approximately 2,718 MWh, 266,990 GJ/h, and 105 t/h, respectively, which correspond to an emission level of approximately 91.6 $MtCO_2$ accounting to approximately 12% of Canada's projected total GHG emissions. Even though Canada has withdrawn from the Kyoto Protocol in 2011, there are still growing concerns among political parties about the mitigation policies that will be adopted in the future [218]. Moreover, tougher environmental regulations are expected to take place in the future, which is evident from the continuous increase in the price of the carbon tax, which is currently valued at 20 CAD/tCO_2 [219, 220]. In a previous work [189], the carbon tax was incorporated in the cost objective function. However, it was concluded that the currently utilized carbon tax was not sufficient to provide an incentive for investment in new low carbon intensive technologies from an economic standpoint. Therefore, the total GHG emissions were accounted for in a separate objective function, and the effect of their reduction on the total system and grid costs were investigated in this work. It is in the interest of oil sands operators to adopt measures that will facilitate reductions in emissions associated with their operations. In order to be able to achieve lower emission levels, carbon mitigation measures should be incorporated in the energy infrastructure of the industry.

To achieve reductions in total GHG emissions, several low-carbon intensive energy supply sources are considered, which include natural gas combined heat and power, nuclear (PBMR and HTGR) for power and heat production, natural gas combined cycle for power production, and integrated wind power, nuclear power and water electrolysis for power and hydrogen production. It is important to note that different capacity levels of electrolyzers were incorporated were the model can select a mix of them in order to provide a wider range of operation for electrolytic hydrogen production. Four scenarios are investigated in this study, in which each energy supply technology is added to the potential energy production mix to investigate its effect on the energy infrastructure of the oil sands industry and on the Alberta grid operations. These scenarios are outlined as follows:

- Scenario 1: Wind-electrolysis for electrolytic hydrogen production is incorporated. Hydrogen storage is included to store hydrogen produced from excess wind power generated. The hydrogen can be retrieved to be sent to bitumen upgraders in the Alberta Industrial Heartland or utilized in HENG for power production from NGCC units.
- Scenario 2: In addition to the wind-electrolysis system in scenario, the capacity expansion of natural gas combined heat and power generation capacity of the oil sands industry is incorporated. Realizing the full potential of this technology can allow the achievement of emission reductions of up to 46% from the power sector. However, increasing its capacity will affect the planning and scheduling of the wind-electrolysis system, which is investigated in this scenario.

- Scenario 3: In the first two scenarios equal weights were set on the total GHG emissions from the energy infrastructure of the oil sands industry and the grid units. In this scenario, a higher weight is set on the total GHG emissions from the energy infrastructure of the oil sands industry relative to the grid in the objective function. The energy production technologies included are the same as in scenario 2.
- Scenario 4: In this scenario the effect of incorporating nuclear energy is incorporated. Nuclear energy has significant potential in providing a substantial share of the heat requirement for SAGD extraction, which contributes to a significant share of the energy requirements and emissions of the oil sands industry. Combined heat and power production from nuclear energy can provide additional benefits, in which the power co-produced can be sold to the grid or sent to electrolyzers to production hydrogen for bitumen upgrading.

The supply technologies' techno-economic data, as well as factors required for the implementation of these technologies (e.g., fuel prices) are presented in Table 5.1 and Table 5.2. It is assumed that the operating cost factors of nuclear facilities include the cost of fuel. The data for the grid generation units required as an input for the unit commitment submodule are readily available in the public domain. The current generation fleet for the year 2017 will be used as a baseline for this study.

Table 5.1 Techno-economic data for the energy production technologies included in the energy infrastructure of the oil sands industry. This includes the maximum capacity, capital and operating costs, and heat rate or yield. NGCC: Natural gas combined cycle; COGEN: Natural gas cogeneration; WT: Wind turbine; SMR: Steam methane reformer.

Technology	Capacity	Capital	F-O&M (%)	V-O&M	Heat rate/Yield	Reference
Electrolyzer	E1:0-50; E2:50-150; E3:150-300; E4:300-377;	$7895(Elec\_capacity)^{-0.439}$	1	0.0019 CAD/kWh	53.4 kWh/kg	[14, 59]

	E5:300-485; E6:190-760 $Nm^3\ h^{-1}$					
WT-Vestas 1.8	1.8 MW	1,443 CAD/kW	1	0.011 CAD/kWh	-	[60, 61]
Nuclear HTGR	2,400 MWth	1,887K CAD/MWth	1.5	62 CAD/MW	0.11 Mwe/MWth	[62, 63]
NG COGEN	85 MW 1600 GJ h^{-1}	1,491 CAD/kW	4	0.02 CAD/kWh	-	[22, 64]
SMR	6.25 t h^{-1}	11.2M CAD/t h^{-1}	4	76 CAD/t	174,886 MJ/tH_2	[65, 66]
NG boilers	340 GJ h^{-1}	377K CAD/t h^{-1}	4	9.8 CAD/t	-	[27, 67]
Nuclear PBMR	565 MWth	771K CAD/MWth	1.5	54 CAD/MW	0.096 Mwe/MWth	[68, 69]
NGCC	100 MW	567 CAD/kW	5	0.002 CAD/kWh	7.17 MJ/kWh	[27, 70]
H_2 storage	0 – 240 kg	$471(Storage\ capacity)^{-0.0896}$	1	0.00315 CAD/kg h^{-1}	-	[71, 72]
H_2 pipeline	196,250 kg h^{-1}	$23{,}823(Pipe\_capacity)^{-0.4142}$	1.5	0.7 kWh\kg	-	[72, 73]

Table 5.2 Important techno-economic parameters used as an input in the optimization model.

Hydrogen pipeline distance between Pincher Creek and Alberta Industrial Heartland (km)	480	[14]
Emission factor for natural gas (tCO_2/Nm^3 NG)	0.00179	[74, 75]
Emission factor for coal (tCO_2/t coal)	1.702	[75]
Heating value of process fuel natural gas (MJ/kg)	48	[27, 54]
Heating value of process fuel coal (MJ/kg)	24	[27, 55]
Boiler supplementary boiler efficiency	85%	[27, 67]
Gas turbine electricity generation efficiency	30%	[22, 27]
HRSG heat recovery efficiency	50%	[22, 27]
HRSG supplemental firing efficiency	95%	[22, 27]
NGCC thermal efficiency	52%	[27, 70]
Total cost of a nuclear accident (CAD)	1.28e11	[27]
Probability of occurrence of a nuclear accident (reactor yr^{-1})	0.000001	[27]

As was shown in the superstructure in Figure 5.1, the Alberta grid was divided into six regional buses, which was adopted from Gamage [190], and as described by the AESO long-term transmission plan [205]. The total generation capacity of each generation technology belonging to the grid, the total generation capacity of each bus, and the demand fraction of each regional bus from the total power demand is illustrated in the superstructure in Figure 5.1. Detailed information for each unit used as an input in the optimization model is included in Table B1 in the Appendix. This includes parameters for the heat rate, start-up fuel consumption, minimum up-time, minimum down-time, ramping rate, and minimum and maximum operating capacity for the generation units [204, 205, 190]. The hourly energy demand [228, 229], wind speed data [213], electricity price, and natural gas price in Alberta [189, 229] were obtained from public databases and are depicted in Figure B1 in the Appendix. It is important to note that the cost of fuel of other energy production technologies, such as coal and nuclear were assumed constant. However, their variability can affect the outcome of the model. The model is solved using the CPLEX solver in the General Algebraic Modeling System (GAMS) [8].

5.5 Results and Discussions

In this section the results obtained from applying the proposed optimization model to a case study based on the energy system for oils sands operations and its interaction with the Alberta Electric System Operator are presented. Several scenarios have been generated and investigated in this study including the integration of renewables (i.e. wind energy) into the energy infrastructure of oil sands operations and utilizing hydrogen as an energy carrier. The hydrogen produced can be sent via pipelines to bitumen upgraders and/or stored in hydrogen tanks to be utilized later in HENG that is injected into NGCC

units, from which the power generated can be sold to the grid. Moreover, the role of incorporating natural gas combined heat and power and nuclear energy is also investigated. These technologies mainly provide the heat requirements of oil sands operations, which constitutes a significant portion of their energy requirements. Power is produced as a byproduct from these technologies, which will be mainly supplied to the Alberta grid or used to produce hydrogen via electrolysis for bitumen upgrading. Finally, a scenario is investigated in which the emphasis on the emissions generated from providing energy for oil sands operations and grid emissions is varied (i.e. a lower weight is set on grid emissions in Eq. 5.5). The consideration of multiple objectives (i.e. system cost, grid cost and emissions) in the optimization model generates different results at different weight factors, which is also presented. The results presented include the Pareto front plots for each investigated scenario, as well as the energy infrastructure proposed by the model and the dispatch of energy production among the different technologies.

5.5.1 Pareto fronts and energy infrastructure planning

Figure 5.2 shows the Pareto optimality front for the four investigated scenarios, which presents the relationship among the three objective functions incorporated in the proposed optimization model (i.e. the annual total system cost, total grid cost, and total GHG emissions). A similar trend is exhibited in the four investigated scenarios. It can be observed that the lowest attainable emissions can only be achieved at a high system cost and only the lower range of the total grid cost. Increasing the grid cost translates to an increase in the total operation of its units, which is majorly constituted of fossil-fuel based technologies particularly coal generation units. This in return results in a significant increase in total emissions. Similarly, the lowest attainable values of the total

system cost can only be achieved at the highest emission levels and total grid cost values. However, at the highest range of the grid cost, lower emission levels can be achieved. This is because of the increase in operation of less carbon intensive generation technologies, mainly natural gas cogeneration facilities, as well as natural gas combined cycle and biomass facilities.

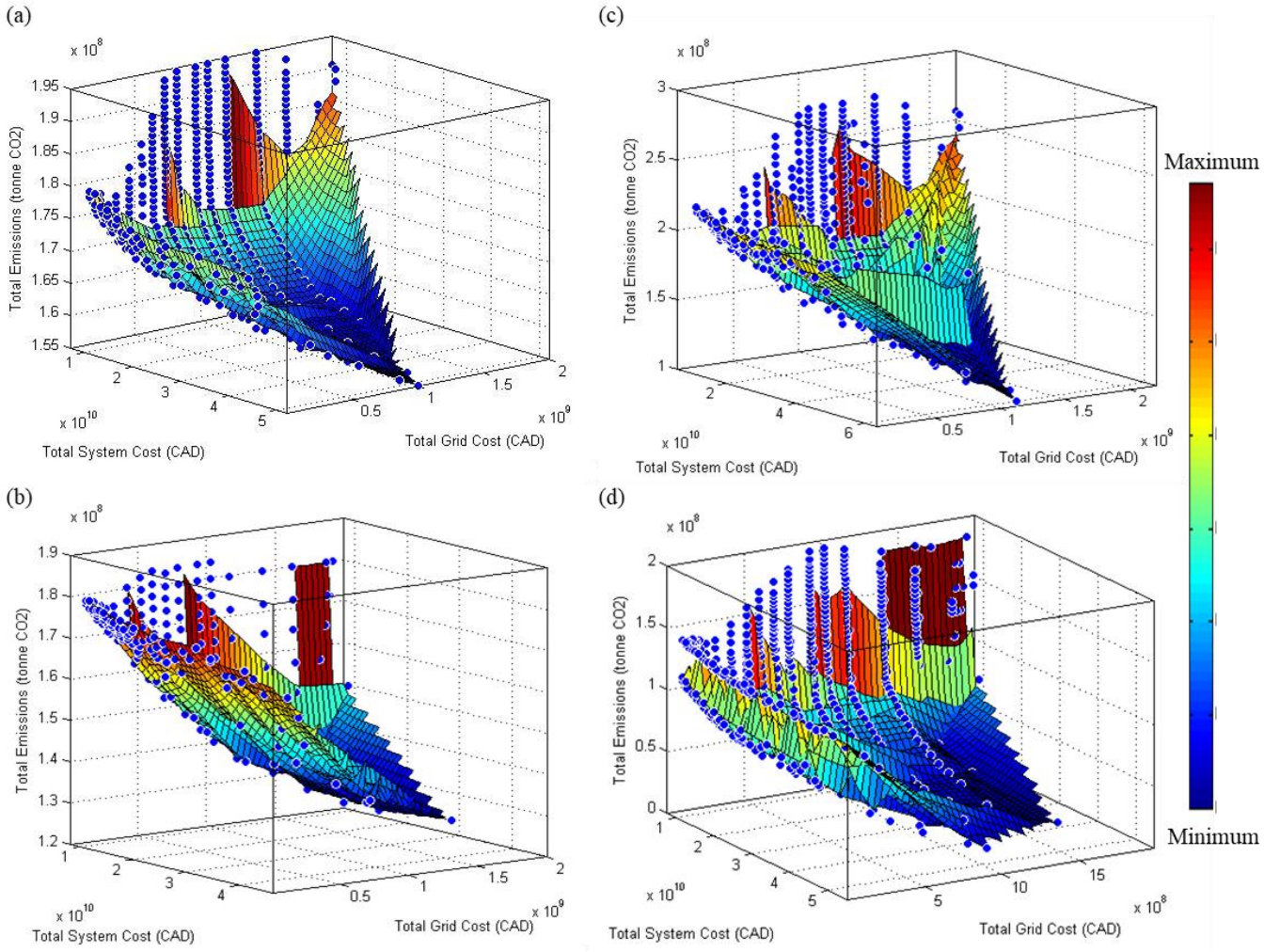

Figure 5.2 Pareto optimality fronts of the four investigated scenarios. The horizontal x and y-axes show the total system cost and total grid cost, respectively, and the vertical z-axis shows the total emissions. (a) Scenario 1: Wind-electrolysis and NGCC; (b) Scenario 2: Wind-electrolysis, NGCC, and cogeneration; (c) Scenario 3: Variable weights on the system and grid emissions; (d) Scenario 4: Wind-electrolysis, NGCC, cogeneration, and nuclear energy.

However, decreasing the system cost at the high range of grid cost, results in a significant increase in total emissions. This is because of the lower availability of new installations

of wind energy, lower carbon intensive fossil-fuel based technologies (i.e. CHP and NGCC), and nuclear facilities. The higher availability of these generation units decreases the total load on higher carbon intensive units of the grid (i.e. coal). Similarly, at a certain total system cost, increasing the operation of natural gas based and biomass generation facilities of the Alberta grid will facilitate achieving lower emissions, but at a higher grid cost due to the increase of fuel cost. Even though the Pareto optimality front plots for the four investigated scenarios exhibit a similar trend as can be observed from Figure 5.2, there are key differences among them to be noted. First, the lowest attainable value of total emissions generated is lower for the scenario in which cogeneration facilities are incorporated (Figure 5.2-b) and considerably lower when nuclear facilities are included (Figure 5.2-d). The incorporated cogeneration and nuclear facilities provides a significant portion of the energy requirements of oil sands operations, which displaces the current carbon-intensive conventional technologies, particularly natural gas boilers, steam methane reforming and power from the grid. In addition, the excess power generated as a byproduct is sent to the grid. Moreover, it can be observed that the same emission level can be achieved at a lower total system cost and grid cost with the incorporation of more low-carbon intensive technologies (i.e. CHP and nuclear). For the scenario in which a higher weight is set on the total emissions from the energy infrastructure of oil sands operations (Figure 5.2-c) it can be observed from the vertical axis that a wider range of total emissions is attainable. Moreover, lowering the weight on the grid's total emissions increases the availability of its carbon-intensive generation technologies (i.e. coal), which constitutes a significant share of its infrastructure. This translates to a significant increase in the total operation of the grid's units, which increases the total emissions generated

and the grid cost. Even though the range of total emissions is wider in comparison to the other scenarios, a lower total system cost can be achieved for a particular emission level due to the higher flexibility of grid operations.

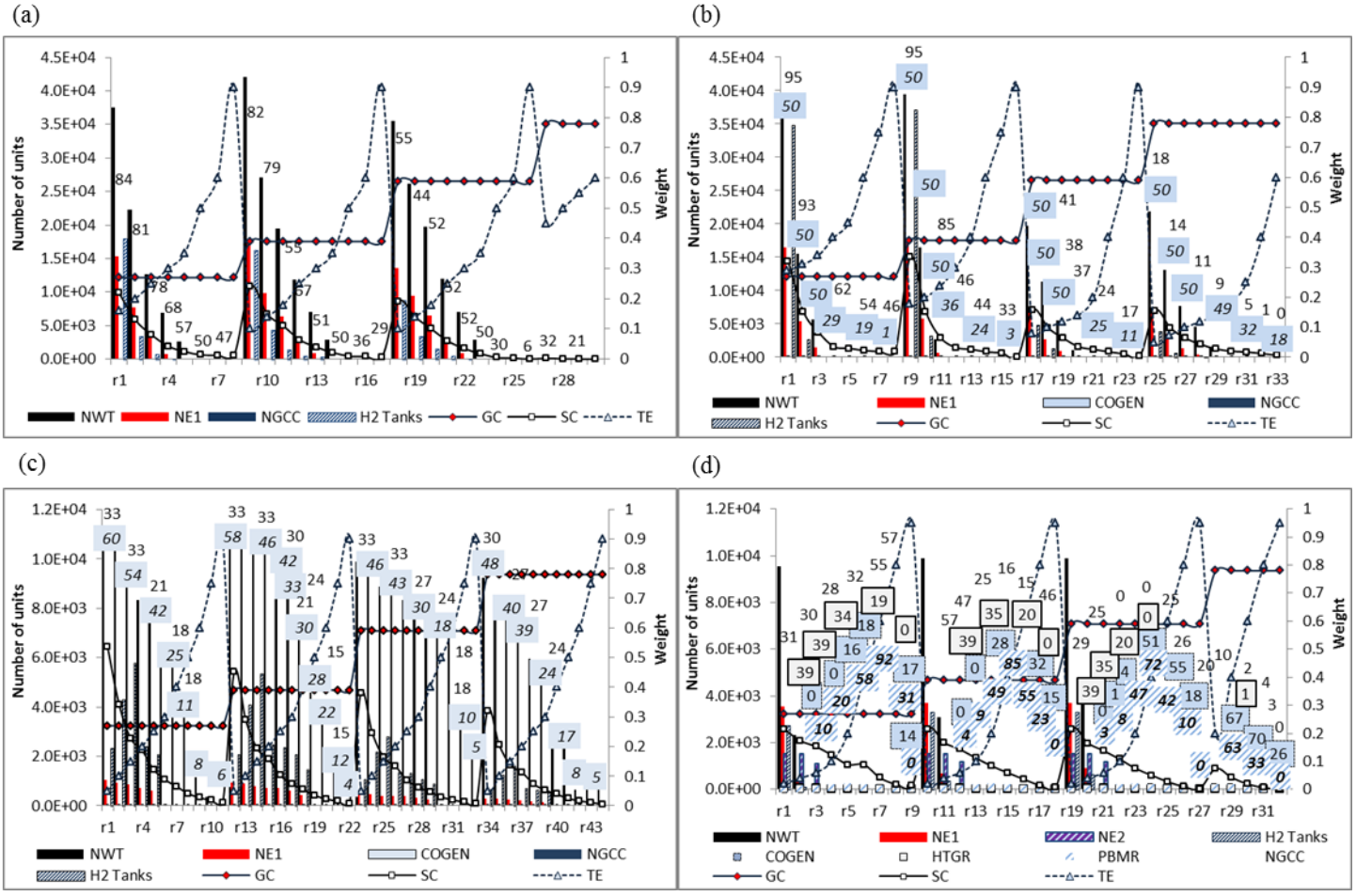

Figure 5.3 The optimal planning of the energy infrastructure for the investigated scenarios for each run. Primary axis: Number of units from each technology selected, which is also indicated by the numbers on top of the bars for clarity. Secondary axis: Normalized value of each objective function (i.e. system cost (SC); grid cost (GC); total emissions (TE)). (a) Scenario 1: SC (7.92 – 105 billion CAD), GC (0.005 – 2.04 billion CAD), and TE (153.6 – 202.7 $MtCO_2$); (b) Scenario 2: SC (7.66 – 86.4 billion CAD), GC (0.005 – 2.02 billion CAD), and TE (127.1 – 202.7 $MtCO_2$); (c) Scenario 3: SC (6.02 – 63.2 billion CAD), GC (0.060 – 2.21 billion CAD), and TE (103.2 – 276.3 $MtCO_2$); (d) Scenario 4: SC (7.66 – 127 billion CAD), GC (0.005 – 2.02 billion CAD), and TE (7.16 – 202.5 $MtCO_2$).

The Pareto optimality front plots shown in Figure 5.2 were created by performing various runs of the optimization model for each scenario. Based on the epsilon constraint method the grid cost and total emissions objectives were set as constraints, and the system cost

objective is minimized. First the grid cost is fixed at a certain value, at which the epsilon constraint of the emissions objective is varied, and the system cost is minimized. This procedure is then repeated for various grid cost values. This is illustrated in Figure 5.3, which presents a few selected runs for each scenario. For these selected runs, the normalized curves of the system cost, grid cost and total emissions are shown, as well as the optimal mix of the energy production technologies incorporated for each scenario.

From Figure 5.3, it can be observed that the system cost, grid cost, and total emissions follow a similar trend for the four investigated scenarios. For a particular grid cost, as the epsilon constraint on the emission objective is relaxed, which translates to a higher value of the emissions objective, the total system cost decreases. This is shown in the plot for each scenario, in which a cyclic behavior is observed for the total emissions and the system cost as the grid cost is increased. In other words, for a particular grid cost the minimum achievable value of emission and the highest system cost occur at the beginning of the cycle, and the highest value of emissions and the least achievable system cost occur at the end of the cycle. As the grid cost is increased, two things can be observed. First, a lower value of the minimum total emissions can be achieved. Second, the system cost required to achieve a certain emissions value decreases in comparison to the lower grid cost. This is because relaxing the epsilon constraint on the grid cost allows for the operation of more expensive technologies in the grid's infrastructure (i.e. biomass, and natural gas fueled technologies). Further increase in the grid cost translates to an increase in the operation of all the power production units that constitute the grid, which include carbon-intensive technologies (e.g. coal generation units). This combined with a strict constraint on excess power generation (i.e. power generation from all production

technologies including new installments should not exceed the total demand) will limit the installation of new low-carbon intensive technologies. This as a result increases the value of the minimum achievable total emissions, and decreases the total system cost.

For the first scenario, as the epsilon constraint on the emissions objective is relaxed the capacity of installed wind turbines, electrolyzers, hydrogen storage tanks and NGCC decrease. Moreover, the ratio of the installed capacity of electrolyzers to wind turbines, and hydrogen storage to electrolyzers also decrease. Relaxing the epsilon constraint on the emissions objective allows for an increase in the operation of the more carbon intensive and less expensive energy production technologies (e.g. hydrogen production from SMR and power generation from coal). Moreover, at a higher grid cost, fewer installations of new technologies are required to achieve a certain level of emissions. In addition, a higher grid cost translates to an increase in the operation of the grid's existing technologies over the year's span, which reduces the capacity available for new installations. For the second scenario, in which natural gas cogeneration facilities are incorporated, the penetration of wind power occurs only at points of very low emission factors. Moreover, a higher hydrogen storage capacity is required to alleviate the intermittency of the installed wind power production capacity. The incorporation of cogeneration facilities plays a significant role in reducing the total emissions. This is because a major energy requirement for oil sands operations is in the form of SAGD steam, and the power that is produced as a byproduct is utilized to satisfy their electricity demand and the remaining is sent to the grid. Increasing the cogeneration capacity hinders the penetration of wind power in order to avoid excess power generation (i.e.

difference between total electricity generation and total demand) and increases the requirement of energy storage (i.e. hydrogen storage).

Placing different weights on the emissions generated from oil sands operations and that from the grid had a significant impact on the optimal energy infrastructure as can be observed from the results of the third scenario. Setting a higher weight on reducing emissions from oil sands operations in comparison to the grid gears the model towards selecting an optimal energy infrastructure that emphasizes reducing emissions from oil sands operations. For example, the installed capacity of wind power is significantly lower than that obtained for the second scenario as can be observed from the magnitude of the vertical axis. Moreover, the ratio of the installed capacity of electrolyzers to wind turbines is higher. In addition, the production of electrolytic hydrogen occurs over a wider range of emission reduction. This is indicative of less wind power being sent to the grid. For the fourth scenario, combined heat and power from nuclear energy plays a significant role in achieving very high emissions reductions. This is because they fulfill the heat requirements of oil sands operations mainly in the form of steam, and the electricity generated from the power cycle is utilized to produce hydrogen via electrolyzers for bitumen upgraders or sent to the grid. As a result, they dominate the energy infrastructure selected by the optimization model. However, as the epsilon constraint on the emissions objective is relaxed the capacity of natural gas cogeneration facilities increases to achieve lower system costs. The incorporation of combined heat and power technologies (i.e. natural gas based and nuclear) is restricted by the total power demand of oil sands operations and the grid. Therefore, small nuclear reactors (i.e. PBMR) utilized for the production of SAGD steam only play a significant role in

reducing total emissions from oil sands operations, especially with the increase in the operation of the grid's units.

5.5.2 Cost distribution and CO_2 abatement cost

Figure 5.4 shows the total system cost distribution as well as the CO_2 abatement cost for the four investigated scenarios. It can be observed that the investment cost accounts for the highest share (>60%) of the total system cost for the points at which high emissions reductions is achieved. This is expected due to the high penetration of low-carbon intensive technologies in the energy infrastructure. As the epsilon constraint on the emissions objective is relaxed, the operating and fuel cost becomes more dominant. This is due to the increase in operation of the existing conventional technologies (i.e. natural gas boilers, SMR, etc.). The large share of operating cost in the fourth scenario is attributed to the high operating cost factor of the incorporated nuclear technologies.

The CO_2 abatement cost is calculated as the ratio of the total additional cost to the total emissions reduction achieved (i.e. (Total cost – Minimum cost) / (Maximum emissions – Total emissions)). It can be observed from Figure 4 that for a particular grid cost value at first there is a significant decrease in CO_2 abatement cost as the epsilon constraint on the emissions objective is relaxed. This provides an indication of the major additional cost required to be imposed with the installation of new low carbon intensive technologies in order to achieve a reduction of a ton of CO_2. It can be observed then that the CO2 abatement cost reaches a minimum and then increases towards the point of maximum value of emissions. This indicates that by imposing a reasonable increase in the total cost of operations, considerable reductions in emissions can be achieved from the point of maximum emissions. Further reductions in emissions will require considerable

investment, which is indicated by the increase in the CO_2 abatement cost towards the point of minimum achievable emissions. As the grid cost is increased the overall CO_2 abatement cost decreases. This is because an increase in grid cost translates to an increase in the operation of existing grid technologies and fewer installations of new low-carbon intensive technologies.

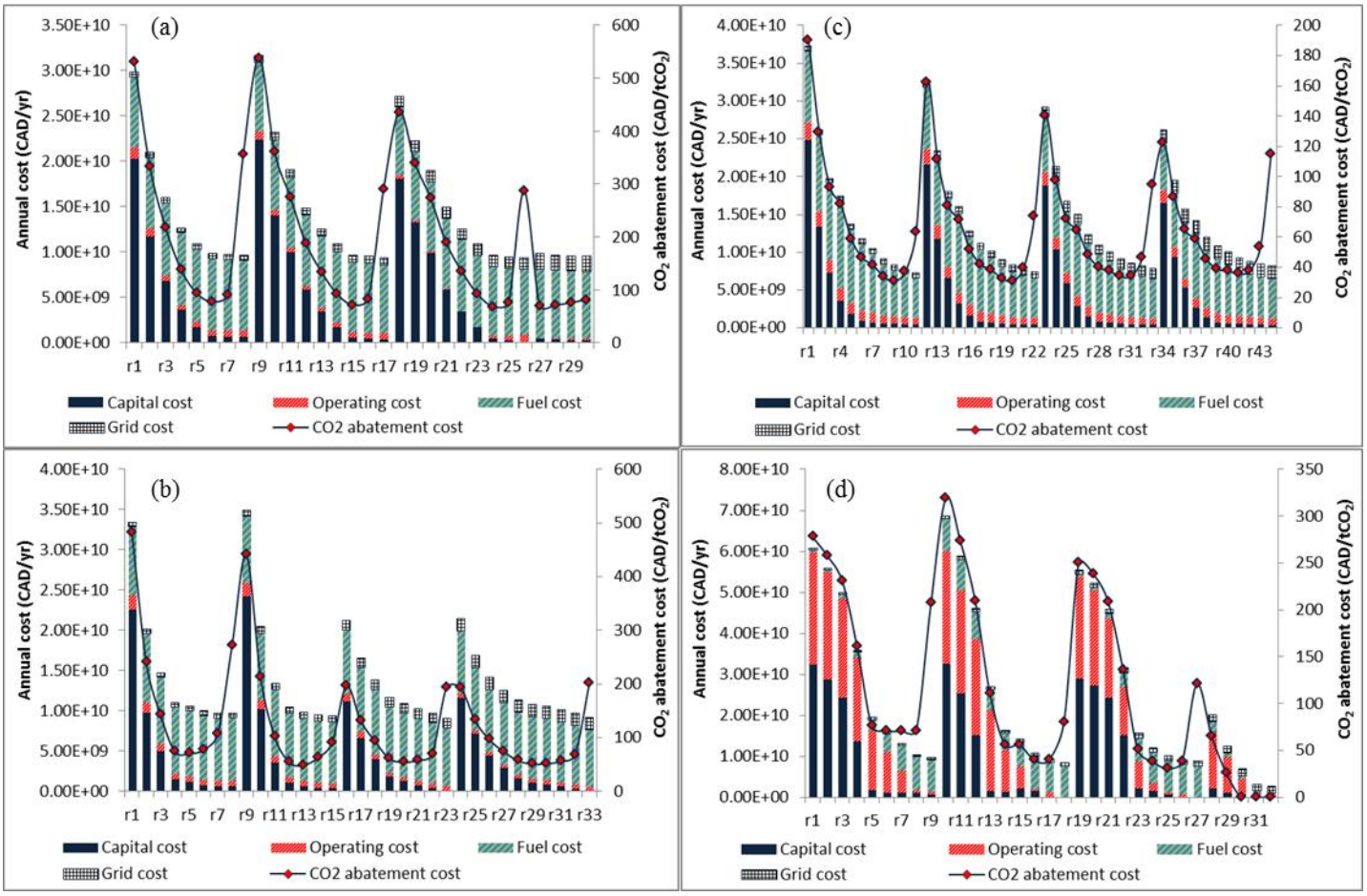

Figure 5.4 Breakdown of the total cost and the CO_2 abatement cost for (a) Scenario 1, (b) Scenario 2, (c) Scenario 3, and (d) Scenario 4.

It can be observed from Figure 5.4, that the highest CO_2 abatement cost (538 CAD/tCO_2) is attributed to the first scenario, in which emissions reductions are only achieved by the incorporation of wind power and electrolytic hydrogen production. The incorporation of natural gas cogeneration units can significantly lower the CO_2 mitigation cost as can be observed from Figure 5.4-b and Figure 5.4-c. The CO_2 abatement cost for the third

scenario (Figure 5.4-c) in which less emphasis was placed on grid emissions, is considerably lower compared to the other scenarios. This is because the grid emissions are generally higher for this scenario, and therefore, the values of the emissions reductions achieved from the point of maximum emissions are also higher. However, this does not translate to the lowest emissions achieved as was previously discussed for the Pareto optimality front (Figure 5.2). The lowest emissions were achieved in the scenario in which nuclear facilities were incorporated. Moreover, to achieve a certain level of emissions, the CO_2 abatement cost for this scenario is considerably lower than the other scenarios. This is because the incorporation of nuclear facilities plays a significant role in reducing emissions associated with the production of heat for oil sands operations, particularly in the form of SAGD steam, which accounts for the highest share of emissions associated with bitumen production and upgrading. Moreover, the power produced as a byproduct from the cogeneration nuclear plants can be sent to the grid or utilized to produce electrolytic hydrogen for upgrading operations with significant reductions in hydrogen transportation costs.

5.5.3 Energy production dispatch and unit commitment

Figure 5.5 shows the total power demand and the share of electricity produced by the different generation technologies considered. Also, the behavior of the energy production infrastructure for the oil sands operations and its interaction with the Alberta grid is depicted for the four investigated scenarios. For the first scenario, it can be seen that for a high weight on the epsilon constraint of the emissions objective the penetration of wind power is substantial and displaces coal generated electricity. At these points, a significant amount of power is sent to electrolyzers for the production of hydrogen, a large share of

which is sent to bitumen upgraders. The remaining hydrogen is stored and utilized later in HENG sent to NGCC for electricity generation. As the epsilon constraint on the emissions objective is relaxed electricity generation from coal facilities increases. Similarly, hydrogen production from SMR increases, eventually providing all the hydrogen requirements of bitumen upgraders. For the first scenario, the production of heat and electricity from natural gas cogeneration facilities remains fairly constant for the majority of runs. This is expected as the cogeneration facilities mainly follow the thermal energy demand of oil sands operators. Their operation decreases and the operation of natural gas fired boilers increases as the weight on emissions is reduced and cost of operation is emphasized. For the second scenario, the increase in the capacity of cogeneration facilities limits the penetration of wind power in comparison to the first scenario, which occurs in order to avoid wastage of power generated. Moreover, the ratio of power sent to electrolyzers for hydrogen production to the power sent to the grid is higher, which further reduces emissions from bitumen upgraders. For the third scenario, one observation that must be noted is that an increase in grid cost results in an overall reduction in power utilized from cogeneration facilities. This is because increasing the grid cost translates to an increase in the operation of its existing power generation units. This combined with a lower weight set on emissions generated from the grid, results in an increase in the operation of the existing high carbon intensive technologies, such as coal generation units. For the fourth scenario, it can be seen that nuclear facilities provides a significant share of the energy requirements of oil sands operations. A major energy requirement for oil sands operations is steam utilized for SAGD bitumen extraction. Nuclear facilities can provide the heat requirements of SAGD operators, and with the

incorporation of a power cycle, electricity can be cogenerated. The electricity generated is utilized to satisfy the power requirements of the host facilities, and the excess can be sent to the grid or utilized for the production of electrolytic hydrogen. The electrolyzers can be located in the vicinity of the bitumen upgraders, which considerably reduces the hydrogen cost by eliminating the requirement of hydrogen transportation (e.g. pipelines).

As was previously discussed and observed from previous results, the fossil-fuel based electricity generation units considered, particularly coal, NGCC, and NG cogeneration units, provide a significant share of electricity to the grid even at high penetration levels of non-conventional technologies. However, this indicates that these units will be often re-dispatched in order to manage for example the intermittency of wind power. The cyclical behavior of the dispatch of coal, NGCC, and NG cogeneration units is depicted in Figure 5.6 for the four investigated scenarios. The operational level of each type of technology is shown as a percentage of their maximum capacity rating (MCR). It can be observed that for the runs, in which there is a high penetration of wind power, the behavior of the conventional power generation units becomes increasingly cyclical. For the first scenario, the NGCC units operate cyclically to mitigate the intermittency of wind power and the variability of power demand, in order to achieve a lower total operational cost. This occurs because the operational and maintenance cost of coal generation units increases significantly at increasingly cyclical behavior.

Figure 5.5 Power production distribution among the different generation technologies satisfying the total grid demand (Left). Energy production dispatch satisfying the total energy (i.e. power, heat, and hydrogen) demand of oil sands operations. (a) Scenario 1, (b) Scenario 2, (c) Scenario 3, and (d) Scenario 4.

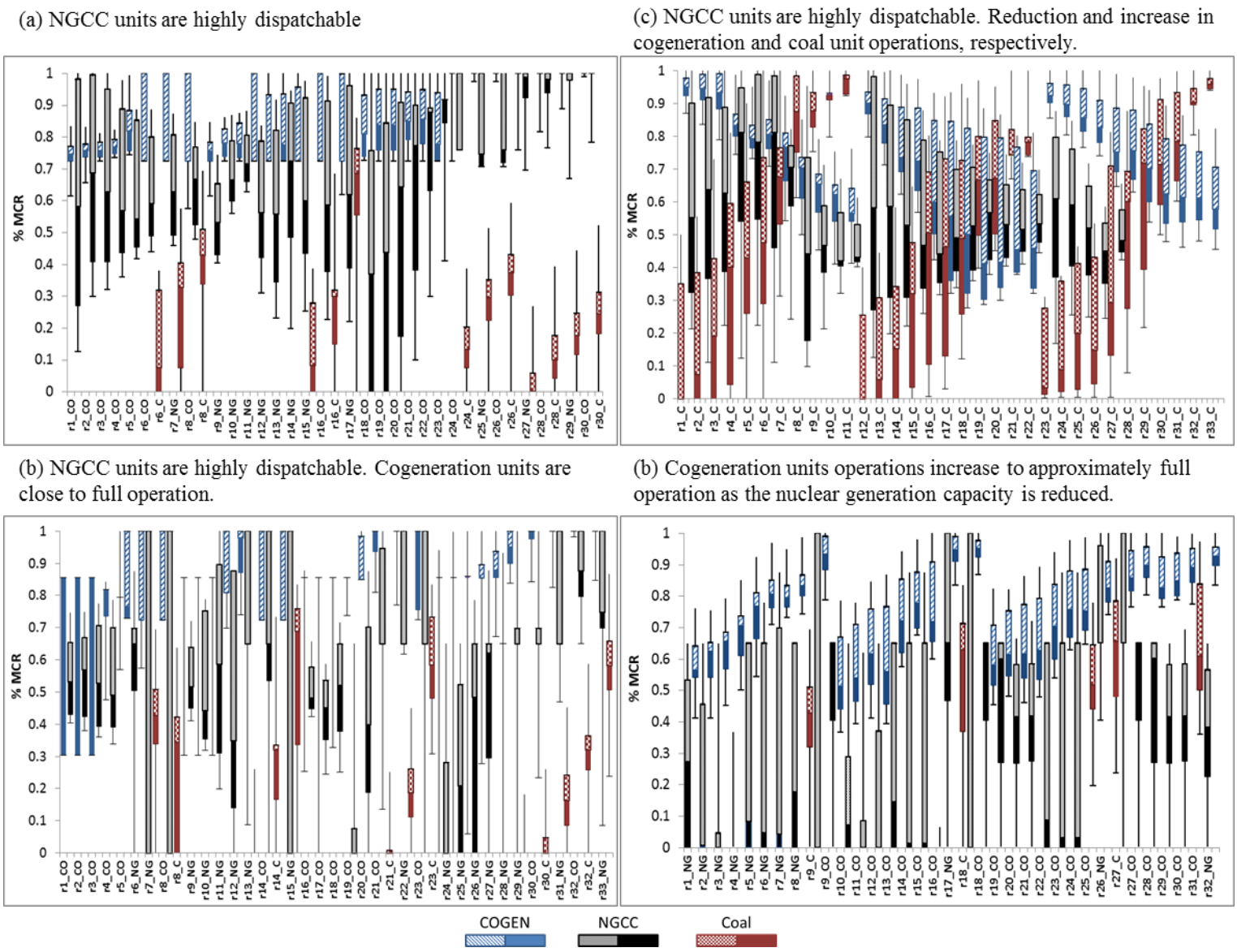

Figure 5.6 Box plots representing the unit operations of natural gas cogeneration (COGEN), natural gas combined cycle (NGCC) and coal generation units for all the runs for (a) Scenario 1, (b) Scenario 2, (c) Scenario 3 and (d) Scenario 4. The box plot are represented as a percentage of the maximum capacity rating (MCR) of the total production capacity of each technology.

Moreover, the cogeneration units follow the heat demand of their host facilities, and therefore, they operate in a narrow range of their MCR. At a specific grid cost, and at a high weight of the epsilon constraint on the emissions objective, the NGCC units operate over a wide range of their MCR, which becomes increasingly narrower as the epsilon constrain on emissions is relaxed due to the reduction in the penetration of wind power.

This is also accompanied with a start in the operation of coal generation units. The narrower range of operation of NGCC units also occurs due to a reduction in the production of electrolytic hydrogen and its utilization in the HENG feed. This behavior is also observed with an increase in grid operational cost, in which there is a reduction in the penetration of wind power.

A similar behavior is observed for the second scenario; however, the only difference is due to the considerable increase in the available capacity of cogeneration units, in which their operation takes place over a wider range of their MCR. This occurs in order to accommodate the variability in power demand as they provide a considerable share of the total power demand for this scenario as was previously discussed (Figure 5.5). For the third scenario, reducing the weight on the emission objective for the grid in comparison to the emission objective of oil sands operators had a significant impact on the operations of existing and new conventional units. It can be observed that there is an increasing trend in the range of the percentage of MCR at which the coal generation units are operational. In addition, the range of percentage of MCR becomes increasingly narrower. This indicates that the coal generation units are operating at a high share of their available capacity, without being frequently re-dispatched. This is also accompanied with a decrease in the range of percentage of MCR of the available cogeneration units. This is expected as the coal generation units provided a significant share of the total power demand as was previously discussed (Figure 5.5).

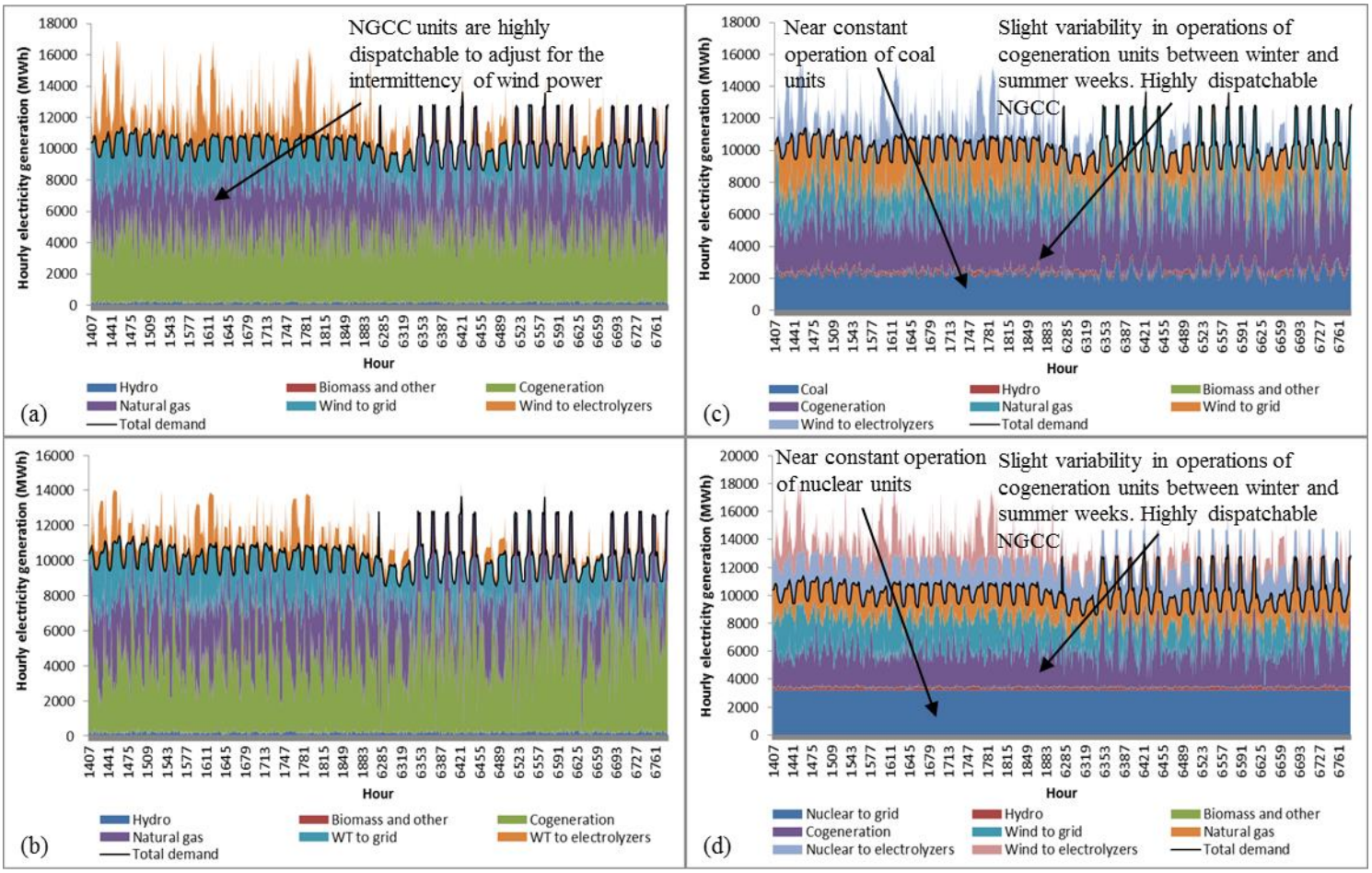

Figure 5.7 Hourly disptach of power generation units during winter (10^{th}-12^{th}) and summer (39^{th}-41^{st}) weeks for run 2 for (a) Scenario 1, (b) Scenario 2, (c) Scenario 3, (d) Scenario 4.

For the fourth scenario, nuclear units are not shown as it was assumed in the mathematical model that their operation cannot be re-dispatched over the 8760 hours of the time index. However, the decrease in their capacity that occurred as the epsilon constraint on the emissions objective was relaxed had an effect on the operation of the cogeneration units. As can be observed, there is an increasing trend in the percentage of MCR, and the range of operation is becoming narrower.

Figure 5.7 shows the hourly dispatch of power generation technologies for the four investigated scenarios during winter (10^{th}-12^{th}) and summer (39^{th}-41^{st}) weeks. For brevity

purposes, these results are shown for a single run of the optimization model for each scenario. It can be observed that during the hours of the winter weeks wind power represents a firm generation capacity providing a considerable share of the total power demand. Wind power in excess to the total demand is sent to electrolyzers to produce hydrogen that is utilized in HENG as a fuel for NGCC units during peak hours. The incorporation of the production of electrolytic hydrogen to be utilized for bitumen upgrading and in HENG contributes as a fossil fuel saver, and its introduction increases significantly the share of renewable energy (i.e. wind power) in the overall power generation infrastructure. During the hours of the summer weeks NGCC units plays an important role in mitigating the variability in demand in addition to the intermittency of wind power generation. This is attributed to their flexibility in operation, in which they can be re-dispatched without imposing significant additional operating costs in comparison to other available power generation units (e.g. coal and NG cogeneration). In the second and third scenarios, in which cogeneration units provided a considerable share of the total power demand, ramping of these units occurs in order to match, for example, the variability in demand associated with off-peak and on-peak hours. This is not observed for scenarios in which coal and nuclear generation units provide a firm share of the total demand, as they operate continuously at a steady load.

5.5.4 Wind-electrolysis performance

The incorporation of the wind-electrolysis system in the energy infrastructure for oil sands operations is an important component of the proposed optimization model. This is because, as previously discussed, the integration of renewable energy (e.g. wind power) is challenged by the geographic accessibility by oil sands operators. Utilizing hydrogen

as an energy carrier facilitates increasing the share of renewable energy in the energy infrastructure of oil sands operations, which in return will also increase its share in the overall power generation infrastructure in Alberta. The performance of the hydrogen production system is depicted in Figures 5.8 and 5.9.

Figure 5.8 shows the average capacity factor of electrolyzers and hydrogen storage, and the hydrogen production cost for the four scenarios. It is important to note that the production of electrolytic hydrogen is selected by the optimization model only when the weight on the emissions objective function is at its high range. At this range the normalized value of total emissions is within (0 – 0.3), which translates to achieving high emission reductions. At a specific grid cost it can be observed that a common trend among all scenarios is an increase in the capacity factor of electrolyzers accompanied with a decrease in the capacity factor of hydrogen storage as the epsilon constraint on the emissions objective is relaxed and the total emissions increase. Relaxing the epsilon constraint on the emissions objective will set a higher emphasis on decreasing the total cost of the energy system. The optimization model will try and minimize the number of energy production facilities installed, including electrolyzers. Therefore, as the weight on emissions is marginally reduced, instead of installing a high number of electrolyzers and wind turbines to utilize more wind power during hours of high wind energy potential, the optimization model selects a smaller total capacity of electrolyzers that utilizes a higher share of the total generated wind power. This in return increases the average capacity factor. However, the total amount of electrolytic hydrogen produced decreases as the weight on the emissions objective is reduced. As a result, less hydrogen is produced in excess to the total demand, which in return reduces the requirement for hydrogen storage

(i.e. a lower storage capacity factor). The installation of a smaller capacity of wind power generators and electrolyzers results in a reduction in the cost of electrolytic hydrogen production.

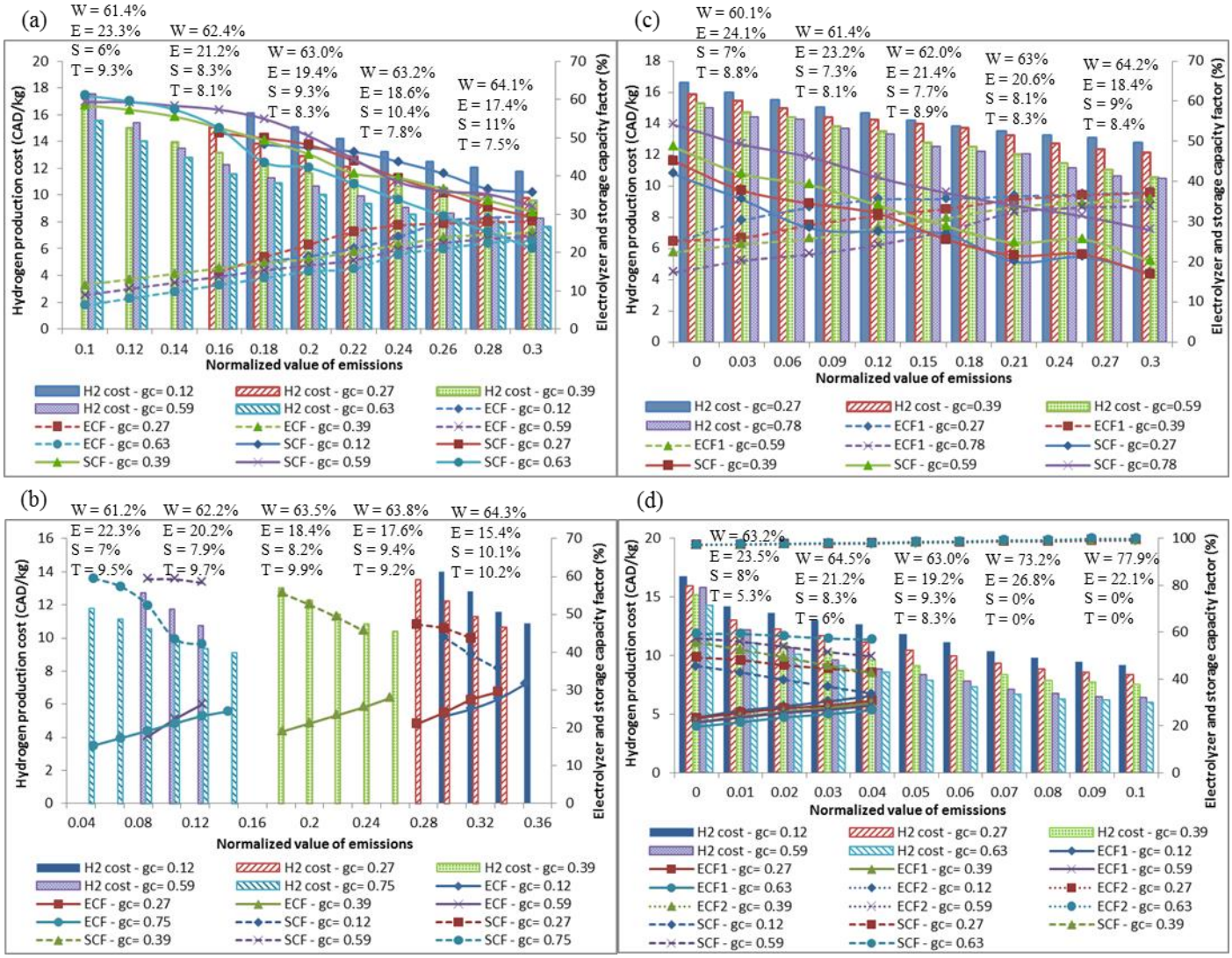

Figure 5.8 Total electrolytic hydrogen production cost and its distribution (Primary axis). Electrolyzer capacity factor (ECF) and storage capacity factor (SCF) (Secondary axis). (a) Scenario 1, (b) Scenario 2, (c) Scenario 3 and (d) Scenario 4. Cost distribution is shown in text in percentage of total cost (W = Wind and nuclear power cost; E = Electrolyzer cost; S = Storage cost; T = Transportation cost, GC = Normalized grid cost).

Moreover, the ratio of power sold to the grid to the power sent to electrolyzers increases, which increases revenue and contributes to the reduction in hydrogen cost. The average

capacity factor of electrolyzers, hydrogen storage, and the hydrogen production cost generally decrease as the grid cost is increased. This is as previously discussed, is due to the reduction in the installed capacity of wind turbines and electrolyzers.

The system components that constitute the total hydrogen production cost include the capital and operating costs of wind and nuclear power generating units, electrolyzers, storage tanks, and transportation pipeline. The hydrogen production cost was determined to be within the ranges of 7.64-17.5 CAD/kg, 9.1-14 CAD/kg, 7.64-16.6 CAD/kg, and 5.97-15.99 CAD/kg for the first, second, third and fourth scenarios, respectively. As can be observed, the cost of wind power constitutes the major share of the total cost of hydrogen production, which accounts to approximately >60%. In this analysis the minimum hydrogen production cost achieved is affected by the capacity of electrolyzers selected. Generally, the production cost of electrolytic hydrogen decreases as the capacity factor increases. The trend of the hydrogen production cost curve decreases until a minimum value is reached, after which the cost escalates with an increase in electrolytic hydrogen production capacity. This is because the grid electricity sales are not high enough to compensate for the high capital investment required, and the reduction in the electrolyzer farm capacity factor. The capacity factor of farms constituted of larger sized electrolyzers generally has a lower magnitude in comparison to farms consisting of smaller sized electrolyzers. This is due to the lower power requirements of farms constituted of smaller sized electrolyzers relative to the power available from the wind farms.

The cost competitiveness of an electrolyzer farm depends on the aggregate capacity factor of the wind farms providing the power requirements of the electrolyzer farm. For example, the average aggregate capacity factor of the Pincher Creek wind farm amounts to approximately 35%. Therefore, in order for the electrolyzer farm to be economically viable, it must have a capacity factor that is greater than that of the wind farm supplying its power requirements.

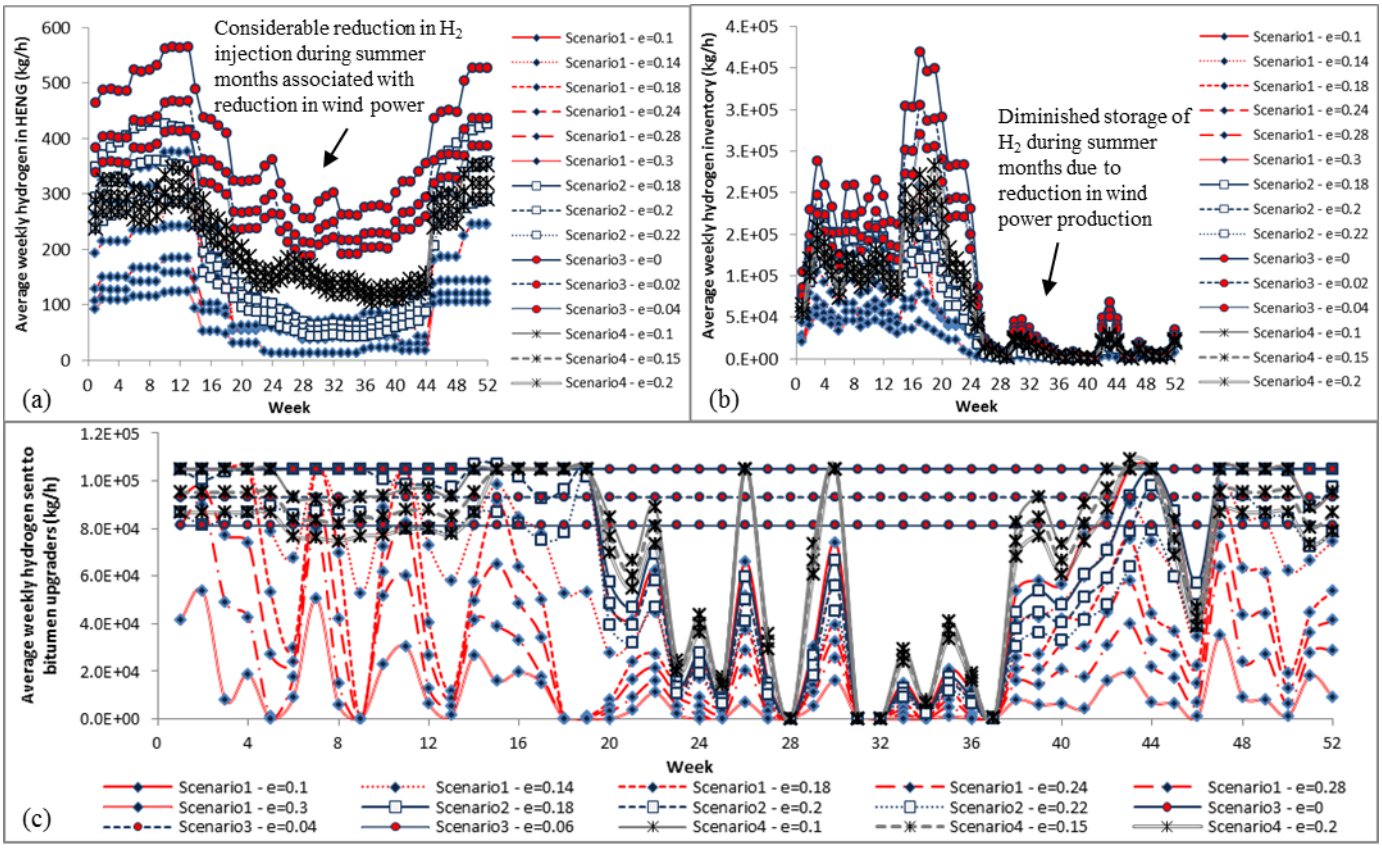

Figure 5.9 (a) Average weekly electrolytic hydrogen injected in hydrogen enriched natural gas sent to natural gas generators. (b) Average weekly electrolytic hydrogen held in hydrogen storage inventory. (c) Average weekly electrolytic hydrogen sent to bitumen upgraders. The results are shown for the four investigated scenarios at different normalized values of total emissions (e). Scenario 1: E (153.6 – 202.7 $MtCO_2$); Scenario 2: E (127.1 – 202.7 $MtCO_2$); Scenario 3: E (103.2 – 276.3 $MtCO_2$); Scenario 4: E (7.16 – 202.5 $MtCO_2$).

As a result, it can be observed that the lower hydrogen production costs are attributed to the scenarios in which the capacity factor is in the range of 35% - 45%. Another factor that plays a significant role in determining the capacity factor of the electrolyzer farm is

the operational range of individual units. The wider the range is (i.e. higher operational flexibility), the higher the number of hours during which the electrolyzers can be operational, and hence the higher the capacity factor of the electrolyzer farm. The hydrogen transportation cost decreases as the capacity of the hydrogen production plant increases, which is attributed to the economies of scale that can be achieved. The hydrogen transportation cost is considerably dependent on the scale of the electrolytic hydrogen production plant, and is unaffected by the amount of electricity sold to the grid. As a result, reducing the hydrogen transportation cost favors increasing the capacity of the electrolyzer farm, and hence the hydrogen flow rate, which facilitates the achievement of higher economies of scale. It is important to note that for the nuclear scenario the electrolyzers can operate at capacity factor >90%, and the transportation costs can be significantly reduced as the electrolyzers can be installed in the vicinity of bitumen upgraders.

Figure 5.9 shows the behavior of the operations of the electrolytic hydrogen production system, including the weekly average injection of hydrogen in HENG, hydrogen inventory in storage tanks, and hydrogen sent to bitumen upgraders. The trend of the hydrogen injection in HENG increases during the winter months, and then diminishes during the summer months, during which the hydrogen storage capacity is mostly utilized. A similar trend was observed for all the investigated scenarios, and for all the considered runs. It can be observed that for each scenario the curves of electrolytic hydrogen injection in HENG, hydrogen inventory, and hydrogen sent to upgraders are shifted upwards when the normalized emission level is decreased (i.e. high weight on the epsilon constraint of the emissions objective). The availability of hydrogen storage

contributes to the increase in the hydrogen injection levels into the natural gas sent to NGCC units. This is because the model provides flexibility for the power system, in which more of the surplus wind power can be used to produce hydrogen, and the excess hydrogen that is not injected is then stored in the available tanks to be retrieved later. For the fourth scenario, in which electrolytic hydrogen production from nuclear energy is considered, it can be observed that there is a constant supply of hydrogen is sent to upgraders. This is because the model selects a constant portion of the power generated from nuclear facilities to be sent to the electrolyzers, which considerably reduces the reliance on natural gas for SMR during the entire year of operation.

5.5.5 Computational results

The developed mathematical models was solved using an Intel Core 2 Duo, 2.33 GHz machine running the CPLEX solver accessed via the general algebraic modeling software [8]. The corresponding computational statistics are summarized in Table 5.3, including number of variables, computation time and optimality gap. The resulting computational times and optimality gaps for the simulation runs are satisfactory. However, it can be concluded that the model is computationally expensive as a result of using the fine mesh approach, and future work can incorporate methods in order to improve its tractability.

Table 5.3 Summary of computational results including number of equations and variables, computational time, and optimality gap.

Equations	5,334,881
Continuous variables	4,651,613
Discrete variables	1,708,209
CPU time (s)	23,100 – 28,000
Optimality gap (%)	0.0001

5.6 Conclusions

In this study an energy optimization model is developed for the integrated planning and scheduling of the decentralized energy infrastructure of the oil sands industry. Conventional, nuclear, and renewable energy production technologies are incorporated in the potential energy production mix. The proposed model incorporates power-to-gas for the management of the wind-electrolysis system. The model is presented as a multi-period and multi-objective MILP model that takes into account the total system cost, grid cost, and total emissions. Unit commitment constraints are incorporated to manage the operations of the existing and new grid power generation units to account for grid interactions with the energy infrastructure of the oil sands industry. The model is applied to a case study for the year 2020 in order to illustrate its applicability. For the first scenario, the planning of the wind-electrolysis and its effect on the operations of existing grid units was investigated. The ranges of total system cost, grid cost, and total emissions were determined to be 7.92 – 105 billion CAD, 0.005 – 2.04 billion CAD, and 153.6 – 202.7 $MtCO_2$, respectively. The cost of wind power production had the highest share of the cost of the wind-electrolysis system, and hence the highest share of the cost of electrolytic hydrogen production. It was concluded that in order for wind-electrolysis to be competitive with conventional SMR a high weight has to be set on the emissions objective function. The cost of hydrogen production was determined to be in the range of 7.64-17.5 CAD/kg H_2. The lower range of the hydrogen production cost was attributed to a high capacity factor of the electrolyzer farm and a high share of wind power sales to the grid.

For the second scenario, the ranges of total system cost, grid cost, and total emissions were determined to be 7.66 – 86.4 billion CAD, 0.005 – 2.02 billion CAD, and 127.1 – 202.7 $MtCO_2$, respectively. In comparison to the first scenario, significant emission reductions were achieved at lower system costs. This is due to the significant emission reductions associated with supporting the heat requirements of oil sands operators, particularly SAGD steam, and the power exported to the grid. However, high penetration levels of cogeneration units impede the penetration of wind power generation, as well as the production of electrolytic hydrogen. This increases the share of electricity sales of wind power to the grid, which reduces the electrolytic hydrogen production cost (9.1 – 14 CAD/kg H_2). For the third scenario, a higher weight was set on the emissions generated from energy system in comparison to the grid's emissions. The ranges for the objective function were determined to be 6.02 – 63.2 billion CAD, 0.060 – 2.21 billion CAD, and 103.2 – 276.3 $MtCO_2$ for the of total system cost, grid cost, and total emissions, respectively. Lower system costs were obtained for this scenario due to the increased commitment of the grid's existing units, which was accompanied with an increase in the total grid's operating cost and emissions. This facilitated increasing the capacity of the wind-electrolysis system for a higher range of weights on the emissions objective function. The cost of electrolytic hydrogen production was determined to be in the range of 7.64-16.6 CAD/kg H_2.

For the fourth scenario, nuclear energy had a significant impact on achieving further emission reductions. The ranges for the objective function were determined to be 7.66 – 127 billion CAD, 0.005 – 2.02 billion CAD, and 7.16 – 202.5 $MtCO_2$ for the of total system cost, grid cost, and total emissions, respectively. The nuclear energy system

covered a major share of the heat requirements of oil sands operators with the additional benefits of sending the byproduct power to the grid and electrolyzers that are in vicinity of the bitumen upgraders in the Alberta Industrial Heartland, which significantly reduces the wind-electrolysis hydrogen transportation cost from Pincher Creek. The hydrogen production cost for this scenario was determined to be in the range of 5.97-15.99 CAD/kg H_2. Moreover, in comparison to the other scenarios, the capacity factor of the electrolyzer farm supplied by nuclear power was >90% due to the constant available supply of power.

Based on the results obtained, it can be observed that the proposed model provides potential benefits as a tool to study future production scenarios for oil sands operations for the integrated planning and scheduling of its energy infrastructure. The strength of the model is that it provides an indication of the potential detailed interactions with the Alberta grid with the high penetration of new power production capacity (e.g. renewable, natural gas cogeneration, nuclear, NGCC, etc.), particularly in the presence of intermittent renewable energy. This provides the user of the model with a realistic overview of the impact of possible planning decisions on the operations of the energy infrastructure of the system and the local grid. However, this leads to large scale models, which are computationally expensive even with current computing resources. This is because the approach utilized is converting the different time scales in this multiscale model to the shortest planning period, which is hourly in this study. A potentially promising approach that has been receiving increased attention in the literature and will be utilized in future work is the use of a data clustering algorithm to reduce computational time.
This will allow the planning and scheduling of multiple operational years, possibly over a

time span of 15-25 years. This will allow the investigation of time dependent parameters, such as construction lead time, variability in carbon mitigation policies and fuel prices, etc. It will also allow for the investigation of situations in which uncertain input data are utilized that will require the incorporation of numerous scenarios to address the uncertainty using stochastic optimization techniques and perform sensitivity analyses. Another important aspect that will be addressed in future is the possibility of eliminating some of the objective functions (e.g. monetized emissions within total cost) to facilitate the addition of new objectives (e.g. system reliability).

Chapter 6

Design and operation of a sulfur supply chain for sour gas processing and bitumen upgrading operations[4]

6.1 Introduction

The rapid development of Canada's economy is accompanied by a sharp increase in energy demand. Sour gas and heavy oil deposits contribute to a significant proportion of the new petroleum production in Canada. This effect is related to the tightening of sweet crude supply, which has forced producers to resort to more sour petroleum despite the added cost of sulfur removal [237]. In Canada, by-product elemental sulfur is produced when sour gas is processed, and when bitumen is upgraded to synthetic crude oil. Sulfur is removed from gas and refined petroleum products to reduce sulfur dioxide emissions that occur when these products are used as fuel. In the last few decades, environmental concerns have resulted in increasingly stringent sulfur emission constraints. These constraints have stimulated the active management of industrial sulfur and its hazardous compounds in petroleum refineries and gas-processing plants. Significant volumes of sulfur are being involuntarily produced as a by-product of oil sands upgrading, oil refining and natural gas processing, which is utilized then for further industrial use, stockpiled beside gas plants and refineries, or sold for export. The main commercial use of the by-product is to produce sulfuric acid for use in fertilizer production and other industrial applications [238]. It is mostly shipped outside the province of Alberta, primarily to United States, Asia Pacific, and North Africa [239].The export demand for

[4] A variant of this chapter is published: M. Elsholkami and A. Elkamel. Energy & Fuels, 2014, 28, 7252 – 7267.

sulfur is expected to steadily increase [240].

With increased activity in the heavy oil sector production resulting in more produced sulfur, combined with an increase in demand for sulfur exports worldwide, there is a shortage of sulfur forming and handling capacity in Alberta. The sulfur is produced during oil and gas production and refining in Alberta in a molten form, manufactured into a dry product for handling, loaded to rail car for transport to Vancouver, stockpiled and eventually loaded on ships for further delivery to export markets. However, it is often looked upon as a waste by-product that usually ends up in storage facilities until its market price is high enough to justify its handling and distribution costs. In addition, the volatile nature of the sulfur market further complicates the effective usage of sulfur management options. It is expected that sulfur supply will considerably exceed its demand, which will result in piling it in the limited storage inventories of gas processing and petroleum refining plants and could possibly lead to shutdowns [241]. This will significantly impede the flow of petroleum and natural gas supply chains. There are considerably high cost-savings opportunities along the sulfur supply chain. The projected increase in sulfur production, an unpredictable future sulfur market, and the uncertain economic viability of transporting the by-product to market, are the driving needs for an effective sulfur management framework.

The government of Alberta is working to create a framework of sulfur management to provide improved environmental, social and economic sustainability [242]. Alberta Sulfur Research Ltd. is a non-profit research organization supported by petroleum-based industries and specialized sulfur production and handling businesses from Canada, USA, Europe and The Middle and Far East. Much of the research focus is on developing and

improving sulfur recovery processes in order to increase energy and environmental sustainability. As well as sulfur handling [243, 244, 245, 246], storage and transportation issues [247, 248, 249, 250], improvement of formed product quality and properties [251, 252, 253], and development of new uses and disposal methods for excess sulfur [254, 255, 256]. These will help in identifying the negative impacts associated with the handling of sulfur to reduce the potential for adverse effects, and developing measures to reduce the requirement of long-term handling and storage.

With the focus on the previously mentioned areas of research a lot of improvements are manifesting in the sulfur industry. However, many issues still exist within its supply chain causing significant costs to be incurred. For example, shipments costs could eliminate most of the potential profit that could be earned from selling sulfur due to difficulties of accessing the markets. Suncor and Syncrude plants located in Ft. McMurray are remotely accessible causing them to keep the sulfur in inventory or incur significant losses by sending it to the market due to the limited storage capacities. On the other hand, Shell Canada has several more strategic locations providing it with an accessibility advantage to the sulfur markets, which reduces its logistical costs and increases its profit gains [237].

A study has been conducted by Jula and Zschocke [237] that implements discrete event simulation to resolve some of the rail transportation issues faced by Sultran Ltd. in transporting elemental sulfur to the Pacific Coast Terminals (PCT) for export. Their simulation model helps to define operational and tactical decisions that address the challenges faced in the complex push-pull distribution system to provide opportunities for cost savings.

Several research works utilizing mathematical modeling techniques have been done to address issues associated with the operations of the Canadian Oil Sands industry in Alberta. Ordorica et al. [257] and Betancourt et al. [258] have developed MILP models to assist in determining strategic decisions regarding the optimal energy infrastructure used in the operation of the Oil Sands industry. In their work they account for changes in the energy infrastructure for future scenarios while considering greenhouse gas emission constraints and mitigation strategies. Their work is useful in assisting policy makers and oil producers in determining optimal strategic decisions for the continuing developments in the Oil Sands industry. However, the major concern of the associated unmanaged growing supply of sulfur could have a significant impeding impact on these developments.

With the expected increase of sulfur production, it will be required to increase sulfur forming, handling and storage capacities. Also with the increased quantities to be transported it will be required to reduce logistical costs. This problem could be approached using strategic supply chain network design to optimize investments in capital assets and reduce operational costs. Typical strategic supply chain design problems include capacity sizing, technology selection and facility allocation [259].

From the literature strategic network design has been widely implemented to improve the operations of various supply chains. AlMansoori and Shah [260] developed a single-period MILP to design hydrogen supply chains by integrating production, storage and distribution components. They determined the optimal allocation of production and storage facilities and their capacities, as well as the optimal configuration of transportation links among the nodes of the supply chain. Paquet et al. [261] incorporated

technology selection decisions in manufacturing network design. Their single-period MILP model determines the optimal structure for a manufacturing network, defining the required facilities and their technologies and capacities. The trade-off associated with the selection among the different technologies incorporated differences in fixed and variable costs, which manifested as differences in capacities and the associated economies of scale. The comparison was also based on the footprint area required to implement the different technologies.

Tsakis and Papageorgiou [262] developed an optimization model to determine the optimal production allocation and distribution network configuration subject to operational constraints, including quality, production, and supply and demand constraints. The single-period MILP model's objective function constituted of minimizing production, distribution center and transportation infrastructure costs, as well as material handling and operating costs. In their model the locations of production sites, distribution centers and customers are predefined, and the capacities and the connectivity of the nodes in the supply chain comprise the optimization problem.

You and Grossmann [263] develop an optimization model that determines strategic supply chain decisions, such as locations of distribution centers and customers assigned to them, shipment capacities among production plants, distribution centers and customers, as well as inventory and safety storage in the supply chain nodes. The formulated mixed-integer nonlinear program addresses the problem of designing multi-echelon supply chain networks of specialty chemicals and their associated inventory systems while considering demand uncertainty. Rodriguez et al. [264] extend this work to include more decisions on the strategic level, such as capacity expansion and elimination

of distribution centers allowing the redesigning of operating supply chains. They apply the proposed approach to a case study in an industrial context. Melo et al. [265] develop an MILP model to simultaneously consider the allocation of new facilities and relocation of existing facilities. Their problem also comprises capacity expansion and capacity reduction decisions.

Yan et al. [266] developed an MILP model that aims at selecting the locations of production plants and distribution centers, which are subject to capacity restrictions. Their model determines the optimal flow configuration of materials among the nodes of the supply chain with the objective of minimizing total cost, which is comprised of capital and operating costs. Sabri and Beamon [267] develop a multi-objective optimization model that simultaneously considers strategic and operational decisions while considering production and demand uncertainty. Tsou [268] generated an optimization model to minimize the total cost of the Chinese imported liquefied petroleum gas distribution system. The only variable was binary deciding the allocation of distribution centers. The objective was to minimize the total distance among the nodes of the supply chain and hence the transportation costs, as well as the cost of establishing and operating the distribution centers.

Up to now, there have been no studies that implement optimization techniques in mathematical modeling to describe the design and operation of sulfur supply chains. It could serve as a useful decision support system in the early stages of developing sulfur supply chains. The model will be used to estimate the total investments required to establish and operate sulfur forming and storage facilities and distribution networks. It will provide an indication about the optimal configuration of the sulfur supply chain,

which will assist governmental or industrial policy makers in making strategic decisions. These decisions include the number, location, type and capacity of sulfur forming plants and storage facilities, required transportation links among nodes in the network, and production rates of forming technologies and flowrates of sulfur. These will be presented as continuous and integer variables in the mathematical model geared towards minimizing capital and operating costs, which is described in the following sections.

6.2 Problem description

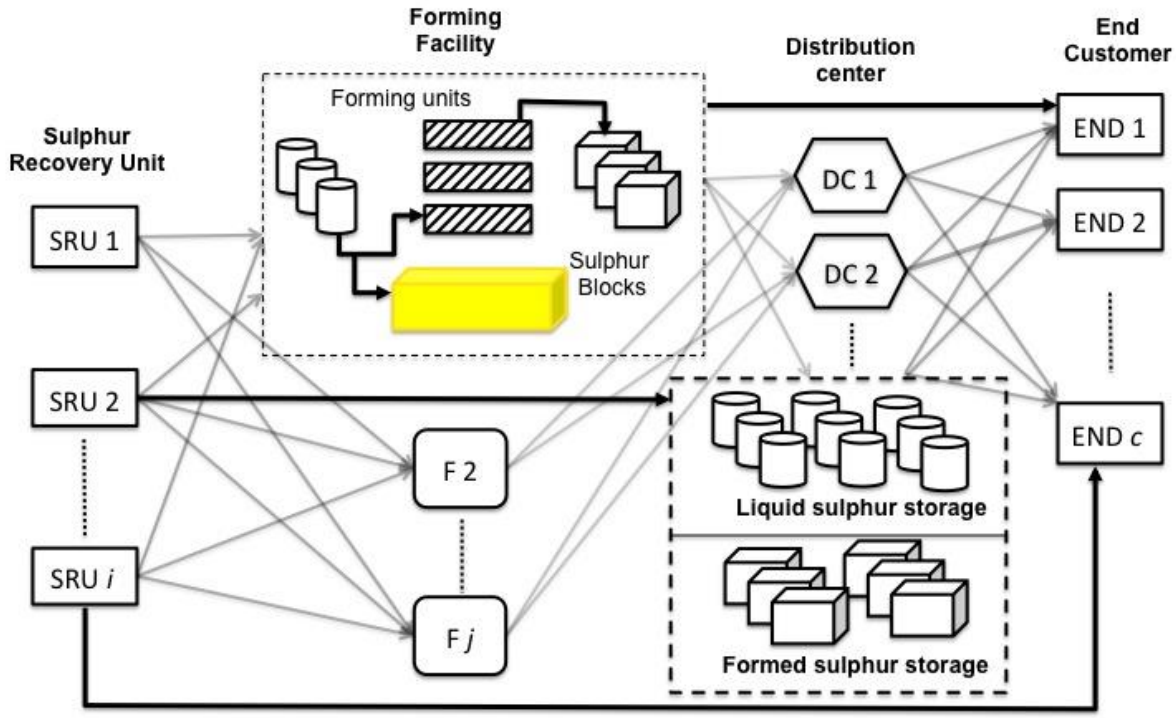

Figure 6.1 Sulfur supply chain superstructure

The problem addressed in this paper is based on the superstructure of sulfur supply chain shown in Figure 6.1. Sulfur is produced in sulfur recovery units as a by-product of oil sands upgrading, oil refining and natural gas processing. To avoid congestions in operations of these entities, the sulfur must be properly managed out of inventory. The

further processing of sulfur often requires it in liquid form, which makes it more convenient for transportation and storage. However, to maintain the high temperature requirements poses significant issues associated with economics and safety. Therefore, handling sulfur in liquid form can be suitable in the existence of certain factors, which are short transportation distances and storage cycles, and availability of adequate storage and transportation infrastructure [269].

In many situations it is required for sulfur to be transported in large volumes and for great distances, which created the need to convert sulfur into solid products that are easier and more economical to handle. Currently, sulfur is mainly formed into three types of products, which are granules, prills and pastille [239]. There are several patented technologies that produce each form in various capacity levels. Still in some cases transportation might be impossible due to the inexistence of sufficient infrastructure, or simply uneconomical due to low sulfur prices and long transportation distances. This imposes a significant challenge on many sulfur producers and causes them in some cases to resort to the third option of blocking sulfur. But these typically require significant space availability, which might not be feasible [237]. Sulfur is often retailed to offshore markets, which would require additional storage facilities outside the vicinity of sulfur producers and forming facilities. These export terminals will be regarded as the distribution centers in the supply chain.

A very simplified assumption that is incorporated is that the sulfur supply chain operates at steady state during which supply and demand are deterministic. However, these can considerably vary with time. The supply chain design problem is formulated as a single-period MILP model. For the investigated supply chain certain information will be

assumed given. This includes production rates of all sulfur recovery units, demand of all customers and the forms of sulfur they accept, and their locations. Also, given are the potential locations of forming facilities and distribution centers, and their space availability. Finally, available or feasible transportation links between nodes in the supply chain and their maximum and minimum capacity. Using the given information, the model will determine strategic decision variables including the number, location, type and capacity of sulfur forming plants and storage facilities, the production rates of all forming technologies and the average inventory of storage facilities, and the type and flowrates of transportation links between nodes in the supply chain.

6.3 Model components

6.3.1 Forming Facilities

Currently, three types of technologies have been considered for new installation of sulfur solid forming facilities. These are Enersul's GX^{TM} granulation process, Sandvik Rotoform® process, and the wet prilling process. The first two processes are the most popular and they produce products that meet the premium requirements set, for example, by the Sulfur Development Institute of Canada. During handling premium sulfur produces minimal amounts of fugitive dust compared to other forms. There are various environmental and safety concerns associated with sulfur fugitive dust [270]. Wet prilled sulfur does not meet premium requirements, and most of the older wet prill process designs are unavailable. However, several new installations of Devco and Enersul's wet prilling technologies took place recently, particularly in the United States after its entry to the sulfur export market. In the case studies to be investigated in this paper the only technologies that will be considered are the GX^{TM} granulation and the Sandvik

Rotoform® processes. Multiple units of each process can be installed to increase production capacity. The Enersul GX process is capable of processing large quantities of sulfur while occupying a smaller footprint area. The Rotoform® is most suitable for low capacity applications or in situations where space is not limited. In addition to cost, these are the factors that are going to be considered while selecting between the two technologies [239].

6.3.2 *Storage Facilities*

Liquid sulfur storage is important because it provides a buffer between the sulfur recovery units and any downstream systems, such as forming plants, liquid loading, blocking facilities, etc. This will help avoid interruptions in the operations of any of these units. Liquid sulfur is typically stored in insulated and heated carbon steel tanks, which can be heated using different methods. As long as the temperature of sulfur is maintained within the desirable temperature range ($125^{o}C – 145^{o}C$) [271], the selection among these typically depends on the unique requirements of each location. For example, two of the most common types of heating are steam jacketing and heat tracing. The former is more effective, but has a higher construction cost, while the later could be preferred in situations where steam is not readily available. Typically liquid storage is more expensive on a CAPEX per tonne basis and it is kept to a minimal, with sulfur remaining in inventory for a matter of days [249].

The storage of formed sulfur is required to account for inconsistencies in shipping rates from forming facilities and export terminals. They are also required to protect the quality of the formed products and to protect surrounding environmentally sensitive regions from fugitive dust. For large storage capacities indoor (e.g. linear sheds or geodesic domes) or

open stockpiles are typically used as they provide economies of scale. The former allows for lower fugitive dust emissions. For smaller volume applications, such as at forming facilities, hybrid tanks or silos are the preferred choice of storage [239].

As previously mentioned some sulfur producers might opt for long-term storage of sulfur, which is currently done in the form of blocks, instead of retailing it in domestic and international markets until more attractive prices prevail in the market. There are three main reasons for choosing to block sulfur, which are geographical isolation making transportation impossible or uneconomical due to low sulfur prices, emergency situations due to failure of forming and handling equipment avoiding congestions in the operation of the sulfur recovery unit, and they absorb inventory during uncertain market condition [272]. In this study the first reason mentioned for blocking is going to be considered in the formulation of the mathematical model. The last reason could be investigated in future work considering multiperiod stochastic optimization.

6.3.3 *Transportation Modes*

Transportation of liquid sulfur is achieved by using heated and insulated pipelines, tanker trucks, rail cars, or ships. Formed sulfur as well can be transported using trucks, rail, or ships. The cost of establishing and operating transportation links among nodes in the supply chain will have a significant effect on potential selected locations of forming facilities and distribution centers [239]. Whether or not a transportation link is established will involve a tradeoff between its cost and the cost of establishing a new forming facility or distribution center. All transportation links will involve a specific delivery distance, and maximum and minimum allowable carriage capacity.

6.4 Model Formulation

In this section the mathematical model that is proposed to solve the outlined problem is presented. The objective function and constraints of the formulated MILP model are described in detail.

6.4.1 Constraints

Sulfur recovery unit constraints

A total mass balance on each sulfur recovery unit is written to determine the amount of liquid sulfur flowing to each of the remaining nodes in the supply chain, which are the forming facilities, distribution centers, and consumers. Liquid sulfur can be transported directly to consumers if they are in the vicinity of the recovery units, for example, a sulfuric acid plant in a refinery. Therefore, the total amount of sulfur produced from a sulfur recovery unit i (RS_{ri}) must be equal to the total amount of sulfur transported to each of the remaining nodes e by transportation mode t (Q_{iert}).

$$RS_{ri} = \sum_{e \in E \setminus I} \sum_{t \in T_r} Q_{iert} \qquad \forall\, i, r \tag{6.1}$$

Forming facility constraints

The total amount of liquid sulfur transported from all recovery units i to forming facility j (Q_{ijrt}) using transportation modes t must be equal to the amount of sulfur formed into blocks for long-term storage (B_{jb}), and the amount of sulfur converted to the other solid forms that are suitable for further transportation using the forming technologies associated with each solid form (F_{jfn}):

$$\sum_{i}\sum_{t\in T_r} Q_{ijrt} = \sum_{f}\sum_{n\in N_f} g_{rfn}F_{jfn} + B_{jb} \qquad \forall\, j,r,f,b \tag{6.2}$$

The total amount of solid sulfur produced from any forming facility (F_{jfn}) must equal to the total amount of sulfur transported to distribution centers and consumers using transportation modes t ($Q_{jdft} + Q_{jcft}$):

$$\sum_{n\in N_f} F_{jfn} = \sum_{e\in D\cup C}\sum_{t\in T_f} Q_{jeft} \qquad \forall\, j,f \tag{6.3}$$

The amount of sulfur of a particular solid form f that can be produced using forming technology n (F_{gfn}) falls within upper and lower capacity limits. For each technology there are several capacity levels q, and for each capacity level there are upper and lower bounds of production, which are QF_{nq}^{max} and QF_{nq}^{min}, respectively. The total amount of sulfur of a particular form that will be produced in a newly established forming facility is constrained by the number of units (NF_{gnq}) installed of the associated forming technologies and their capacity levels:

$$\sum_{q\in Q_n} QF_{nq}^{min}\, NF_{gnq} \le F_{gfn} \le \sum_{q\in Q_n} QF_{nq}^{max}\, NF_{gnq} \qquad \forall\, g,f,n \in N_f \tag{6.4}$$

F_{jfn}^{max} and F_{jfn}^{min} also represent the upper and lower production limits in any forming facility. In addition to providing higher economies of scale, it is typically preferred that a single type of forming technology to be installed in any forming plant, because it will provide higher simplicity for operation. Therefore, the selection of technologies, which is presented by the variable X_{jn}, is limited to one for each of the newly established forming

facilities by the following constraints. X_{jn} also represents whether or not an existing forming facility is operated.

$$F_{jfn}^{min} X_{jn} \leq F_{jfn} \leq F_{jfn}^{max} X_{jn} \qquad \forall\, j, f, n \in N_f \tag{6.5}$$

$$\sum_{n \in N} X_{gn} \leq 1 \qquad \forall\, g \tag{6.6}$$

Storage constraints

As previously mentioned there are three types of storage facilities. The existence of a forming facility requires the presence of liquid sulfur storage to create a buffer for the forming units and the sulfur blocking facilities. The produced solid forms are required to be stored between consecutive shipments from the forming facilities. They are also required to hold the sulfur during periods of disruptions in supply or demand, which might also require the existence of blocking storage facilities. There are several storage technologies available for each of the liquid, formed and blocked sulfur. Therefore, the amount of liquid sulfur transported to the forming facilities (Q_{ijrt}), the amounts of transportable-formed sulfur produced (F_{jfn}), and the amounts sent for long-term storage in blocking facilities (B_{jb}) will be stored in their associated storage facilities. Storage facilities located outside the vicinity of the forming facilities are regarded as distribution centers. These typically require higher capacities and longer periods of storage. Similar to the storage facilities at the forming facilities, the amount of sulfur of each form transported to the distribution center from all sulfur recovery units (Q_{idrt}) and forming facilities (Q_{jdft}) must be stored in their associated storage facilities (ST_{es}) for a certain period of time (λ_{es}):

$$\sum_{s \epsilon S_R} (1/\lambda_{es}) ST_{es} = \sum_{i} \sum_{r} \sum_{t \in T_r} Q_{iert} \qquad \forall\, e \in (J \cup D) \tag{6.7}$$

$$\sum_{s \epsilon S_F} (1/\lambda_{js}) ST_{js} = \sum_{f} \sum_{n \in N_f} F_{jfn} \qquad \forall\ j \tag{6.8}$$

$$\sum_{s \epsilon S_B} (1/\lambda_{js}) ST_{js} = B_{jb} \qquad \forall\ j \tag{6.9}$$

$$\sum_{s \epsilon S_F} (1/\lambda_{ds}) ST_{ds} = \sum_{j} \sum_{f} \sum_{t \in T_f} Q_{jdft} \quad \forall\, d \tag{6.10}$$

For each type of storage technology there is an upper and lower limit on the amount of sulfur that can be stored, which are QST_{sq}^{max} and QST_{sq}^{min}, respectively. These will decide the number of units to be installed installed from each technology (NS_{esq}) to handle the storage requirements (ST_{es}) in the newly established facilities *g* or *u*:

$$\sum_{q \in Q_s} QST_{sq}^{min}\, NS_{esq} \leq ST_{es} \leq \sum_{q \in Q_s} QST_{sq}^{max}\, NS_{esq} \qquad \forall\, e \in (G \cup U), s \tag{6.11}$$

ST_{es}^{max} and ST_{es}^{min} represent the upper and lower storage limits in any storage facility. Z_{es} represents whether or not a storage technology is selected to be established in a new facility, or whether or not it is operated in an existing one.

$$ST_{es}^{min} Z_{es} \leq ST_{es} \leq ST_{es}^{max} Z_{es} \qquad \forall\, e \in (J \cup D), s \tag{6.12}$$

Moreover, all forms of product *p* transported to a particular distribution center *d* from sulfur recovery units *i* and forming facilities *j* using transportation modes *t* (Q_{idrt} + Q_{jdft}) must equal to all forms of products *p* flowing from that distribution center to customers (Q_{dcpt}):

$$\sum_{e\in I\cup J}\sum_{t\in T_p} Q_{edpt} = \sum_{c}\sum_{t\in T_p} Q_{dcpt} \qquad \forall\, d,p \tag{6.13}$$

Transportation constraints

To require the existence of a transportation link between two nodes in the supply chain imposes a lower limit (QT_t^{min}) for the quantity of sulfur flowing between them ($Q_{ee'pt}$). An upper limit (QT_t^{max}) represents the maximum capacity that could be handled by a particular transportation mode:

$$QT_t^{min} Y_{ee\prime t} \le \sum_{p} Q_{ee'pt} \le QT_t^{max} Y_{ee't} \qquad \forall\, e,e' \in E\backslash\{e\},t \tag{6.14}$$

Space constraints

The total area available in newly established forming facilities g and distribution centers u must be able to accommodate the required sulfur forming and storage facilities. The selection of establishing a potential forming or storage facility in a certain location is presented by the binary variables V_g and V_u, respectively.

$$\sum_{n}\sum_{q\in Q_n} \alpha n_{nq}\, NF_{gnq} + \sum_{s}\sum_{q\in Q_s} \alpha s_{sq}\, NS_{gsq} \le A_g^T V_g \quad \forall\, g \tag{6.15}$$

$$\sum_{s}\sum_{q\in Q_s} \alpha s_{sq}\, NS_{usq} \le A_u^T V_u \quad \forall\, u \tag{6.16}$$

Demand constraints

There is a set of consumers that utilize sulfur as a raw material for producing other commodities. Consumers can only accept sulfur in certain forms according to their preference, which is represented by the parameter (ρ_{cp}). The total flow of all acceptable

forms of sulfur by all transportation modes (Q_{ecpt}) must be greater than or equal to the total demand (D_c^T):

$$\sum_{e \in E \setminus C} \sum_{p} \sum_{t \in T_p} \rho_{cp} \, Q_{ecpt} \geq D_c^T \qquad \forall \, c \tag{6.17}$$

Non-negativity constraints

Positive values must be assigned to all continuous and integer variables:

$$RS_{ri} \geq 0 \quad \forall \, r, i \tag{6.18}$$

$$F_{jfn} \geq 0 \quad \forall \, j, f, n \tag{6.19}$$

$$B_{jb} \geq 0 \quad \forall \; j, b \tag{6.20}$$

$$Q_{ee\prime pt} \geq 0 \quad \forall \, e, e', p, t \in T_p \tag{6.21}$$

$$ST_{es} \geq 0 \quad \forall \, e \in (J \cup D), s \tag{6.22}$$

$$NF_{gnq} \geq 0 \quad \forall \, g, n, q \in Q_n \tag{6.23}$$

$$NS_{esq} \geq 0 \quad \forall \, e \in (G \cup U), s, q \in Q_s \tag{6.24}$$

$$X_{jn} \geq 0 \quad \forall \, e \in j, n \tag{6.25}$$

$$Y_{ee\prime t} \geq 0 \quad \forall \, e, e' \in E/\{e\}, t \in T_p \tag{6.26}$$

6.4.2 Objective function

The objective of the proposed model is to minimize the total annual cost of the sulfur supply chain. Capital and operating costs of the forming, storage and transportation facilities constitute the total annual costs. It is assumed that capital costs are amortized

over the lifetime of the project over an assumed period of 20 years with a compounded interest rate of 8%.

Facility capital and operating cost

The facility investment cost is calculated by multiplying the number of forming and storage technologies (NF_{gnq} and NS_{esq}) established by their associated capital costs. The capital cost coefficients depend on the type of technologies, capacity levels, and candidate locations:

$$FIC = \sum_{g}\sum_{n}\sum_{q\in Q_n} FFC_{gnq}NF_{gnq} + \sum_{e\in(G\cup U)}\left(LC_eV_e + \sum_{s}\sum_{q\in Q_s} FSC_{esq}NS_{esq}\right) + \sum_{j}\sum_{n} FCF_{jn}X_{jn} + \sum_{e\in J\cup D}\sum_{s} FCS_{es}Z_{es} \quad (6.27)$$

Facility operating costs include processing and maintenance costs of forming and storage facilities. They are obtained by multiplying unit production and storage costs by the corresponding amounts handled:

$$FOC = \sum_{j}\sum_{f}\sum_{n\in N_f} OFC_{jn}F_{jfn} + \sum_{e\in J\cup D}\sum_{s}\sum_{q\in Q_s} OSC_{es}ST_{es} \quad (6.28)$$

Transportation capital and operating cost

The cost of transportation is calculated as the summation of fixed and variable costs over all possible connections in the supply chain by all the feasible transportation modes. The components of fixed costs for rail, trucks or ships include land, construction, cargo handling equipment, rolling stock, and ships. Operating cost components for these modes

include maintenance, labor, and fuel. For heated transportation modes suitable for liquid there is an added cost for energy.

$$TTC = \sum_{e} \sum_{e' \in E \setminus \{e\}} \sum_{t \in T_p} \left(FIT_{ee't} Y_{ee't} + \sum_{p} \left(FTC_{ee'pt} + VTC_{ee'pt} D_{ee'} \right) Q_{ee'pt} \right) \quad (6.29)$$

The objective function aiming at minimizing the total cost can now be written as follows:

$$min(FIC + FOC + TTC) \quad (6.30)$$

6.5 Illustrative case study

Alberta Industrial Heartland (AIH) was chosen to illustrate the capability of the proposed model for several reasons. A considerable amount of sulfur is being produced in AIH, for which it is forecasted to reach 4 million tonnes per year by 2020, and will continue to increase over the following decades [273]. Most of the sulfur produced in AIH is from the oil sands upgrading industry, which is expected to significantly increase in activity in the following decades. This imposes the requirement of establishing and operating sulfur forming, handling and shipping facilities, for which there are several projects proposed [274]. Data regarding the detailed design of these projects was easily accessible from different authorities [275, 276]. This provides an adequate reference to which the results of the model could be compared. Figure 6.2 shows the map of AIH, and the locations of sulfur producers, consumers, and potential forming facilities.

To illustrate the versatility of the proposed model, a number of applicable production and storage technologies, and transportation modes were included in its components, which are listed in Table 6.1. They were used to outline all the possible structure of the sulfur

supply chain, from which the optimal configuration was determined. All the forming and storage technologies constituted the established forming facilities. Only formed sulfur storage technologies were considered for distribution centers, and the transportation links were used to establish the interconnections among the nodes of the supply chain.

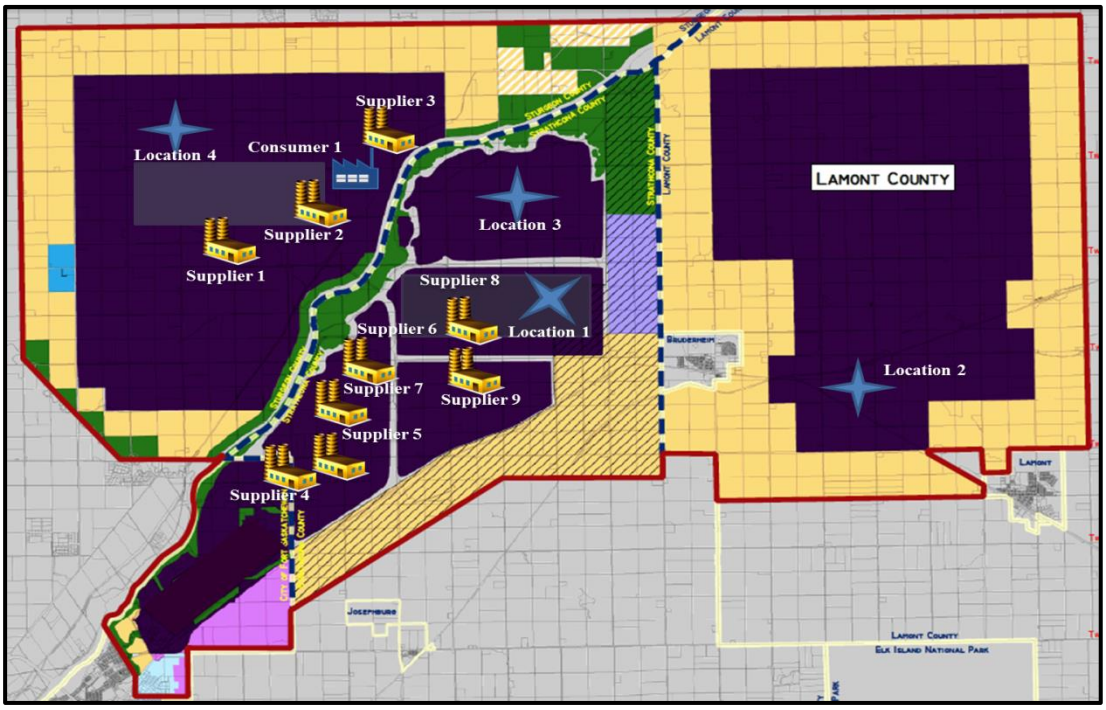

Figure 6.2 Map of Alberta's Industrial Heartland

Table 6.1 Forming, storage and distribution technologies included in the examined case study

Forming technology	• Sandvik Rotoform pastillation • Enersul GX granulation
Storage technology	• Liquid sulfur tanks • Formed sulfur sheds and silos • Emergency blocking facilities
Transportation mode	• Liquid sulfur tanker trucks, pipelines, tank cars, and tank ships • Formed sulfur trucks, rail cars, and ships

6.5.1 Sulfur supply and demand

Currently the total amount of sulfur produced from AIH is 1.8 million tonnes per year [277, 272]. The sulfur suppliers considered for this case study include Petro Canada

Sturgeon Upgrader, North West Upgrader, Synenco Upgrader, Petro Gas, Total Upgrader, Shell Canada Scotford Upgraders 1 and 2, BA Energy, and North American Oil Sands Upgrader, which are shown in Figure 6.2 as suppliers 1 – 9, respectively. The only consumer located in the heartland is Agrium Inc. (consumer 1), which is a fertilizer plant that sources sulfur for phosphate production. The remaining consumers are overseas including Australia, Brazil, China, New Zealand, South Africa, and USA, and their demands are listed in Table 6.2 as consumers 2 to 7, respectively. It is assumed in the case study that the consumers can accept all the sulfur forms taken into consideration in the model (i.e. ρ_{cp} = 1). Table 6.2 also lists all sulfur producers along with their production levels [273, 274, 275]. This is assumed to represent the current business as usual scenario. Other scenarios are considered to investigate the effect of varying supply and demand levels on the model's results. The assumed increases in supply and demand levels were based on the future sulfur market outlook [273, 277-283].

Table 6.2 Supply and demand of sulfur in thousand tonnes per year for the business as usual scenario

Supplier	Supply, kT yr^{-1}	Consumer	Demand, kT yr^{-1}
1	50	**1**	250
2	100	**2**	200
3	100	**3**	100
4	300	**4**	500
5	300	**5**	150
6	300	**6**	100
7	300	**7**	500
8	100		
9	250		

6.5.2 Forming facilities

Two types of the previously discussed forming technologies, which are currently the most commonly used for new establishments, were considered for this case study. For the granulation process, Enersul Inc. offers three capacity ranges, which are GXm1^{TM} (1,100 T day^{-1}), GXm2^{TM} (650 T day^{-1}), and GXm3^{TM} (350 T day^{-1}). The standard Sandvik Rotoform® has a capacity level of 5 T day^{-1}, and another available capacity level is the Rotoform® HS (10 T day^{-1}). These operating limits are defined as the maximum operating capacity levels[3]. The capacity levels of all the considered forming technologies are summarized in Table 6.2. The lower and upper limits for sulfur forming (i.e. F_{jfn}^{min} and F_{jfn}^{max}) were defined as the minimum and maximum flow rates of fully loaded unit of the considered transportation modes, respectively. The capital and operating costs of these technologies are listed in Table 6.4. The yield of all the forming technologies was assumed to be 1. The capital costs were estimated based on the investment costs of commercial sulfur forming plants implementing the technologies considered in this case study [273, 277-283]. The operating costs were estimated based on the utility requirements of these technologies [285, 286, 287] and the rates of industrial utilities and preliminary operating costs estimates given in Turton et al. [288].

6.5.3 Storage facilities

One of the major differences among the storage facilities is the amount of time the sulfur is typically held in stock, which was accounted for in the mathematical model by the parameter λ_{es}. The time period of which liquid sulfur is held in storage is minimized due to the associated high-energy requirement needed to keep the sulfur in molten state, which is typically 1-2 days [249]. During normal operation of the supply chain, formed

sulfur is held in storage at the forming facilities for a period of 10-20 days [276, 289]. The storage periods for silos and sheds were assumed to be two and three weeks, respectively. Holding periods that are longer than normal operation were assumed in the model in order to account for disruptions occurring due to operational bottlenecks. Blocking facilities typically used in emergency situations or to keep the sulfur off the market due to lower market prices are assumed to have a maximum holding period of two years. It is assumed that the storage facilities operate 365 days per year. Some of the most important economies of scale that exist within chemical supply chains are associated with storage facilities [290]. For example, a tank's variable cost could decrease by more than 50% if the capacity of the tank increases from 500 m^3 to 2000 m^3 [291]. For new establishments, it is preferred to install larger tanks rather than multiple smaller ones. Three capacity levels were assumed for each storage facility (i.e. small (S), medium (M), and large (L)). The intermediate storage capacities were assumed to be equal to that of currently existing or new sulfur forming facilities, and their capital and operating costs are listed in Table 4. The other capacity levels were determined by increasing and decreasing the intermediate capacity by a factor of two (Table 3). The sixth tenth rule [288] was then used to scale the associated capital and operating costs, which is a rule of thumb that can be used to provide satisfactory results when an approximate cost (±20%) is required. It is represented as the known cost of equipment of facility multiplied by a size factor (i.e. ratio of capacities) that is raised to the power of 1/6.

Table 6.3 Capacities of the considered forming and storage technologies

Technology	Minimum capacity	Maximum capacity
Forming unit (kT yr^{-1})		
Rotoform	M: 30, L: 60	M: 60, L: 110
GX	S: 30, M: 130, L: 240	S: 130, M: 240, L: 500
Storage unit (kT)		
Tank	S: 0.1, M: 0.4, L: 0.8	S: 0.4, M: 0.75, L: 1.5
Shed	S: 0.1, M: 2.6, L: 5.2	S: 9, M: 20, L: 40
Silo	S: 0.1, M: 0.3, L: 2.1	S: 0.3, M: 2.1, L: 4.4
Block	S: 500, M: 1300, L: 2600	S: 1300, M: 2600, L: 5200

L = Large, M = Medium, S = Small

Table 6.4 Capital and unit cost of sulfur forming and storage technologies

Technology	Capital cost (M$)	Units cost (k$ T^{-1})
Forming unit		
Rotoform	1.6	0.15
GX	2.3	0.21
Storage unit		
Tank	0.50	1.5
Shed	0.76	0.8
Silo	0.6	0.7
Block	0.20	0.05

6.5.4 Transportation modes

The maximum allowable limit for a liquid sulfur transportation mode is based on the assumption that it cannot transport more than the maximum production rate of sulfur suppliers, and the maximum capacity of a formed sulfur transportation mode cannot exceed the production rate of a large forming facility, which in this case could be estimated as the total consumers' demand. The minimum amount between nodes in the supply chain is assumed to be equal to a fully loaded transportation unit. The capital and

unit costs for each transportation mode are listed in Table 5 [281, 289, 292, 293, 294, 295]. The cost associated with establishing a transportation link between two locations, for example, rail line extension cost [296, 297] or tariff cost can be accounted for in the model as the parameter multiplied by the binary variable representing its existence in the objective function. The distances among the nodes of the supply chain were estimated using google maps (Table 6.6). Since most of the consumers considered in the case study are overseas, the sulfur will be distributed among them through export terminals, which are the only distribution centers considered in this case study. There are two export terminals that handle elemental sulfur in Canada and they are Pacific Coast Terminals and Vancouver Wharves, which have storage capacities of 220 KT and 175 KT, respectively. Their average annual capital and unit costs are $12K and $36.5/T, respectively [289].

Table 6.5 Capital and unit cost for sulfur transportation modes

Transportation mode	Capital cost ($ T^{-1})	Units cost ($ kg^{-1} hr^{-1} km^{-1})
Liquid sulfur		
Truck	100	0.83
Rail	280	0.1
Pipe	180	0.4
Ship	800	0.21
Formed sulfur		
Truck	20	0.34
Rail	80	0.025
Ship	680	0.01

Table 6.6 Delivery distances among nodes in the supply chain in km

Node	L1	L2	L3	L4	PCT	VW	C1	C2	C3	C4	C5	C6	C7
S1	10	20	12	3	255	335	3	16,473	24,428	22,925	22,280	10,550	9520
S2	11	23	15	4	252	342	4	17,118	24,570	23,570	26,796	10,250	9,520
S3	12	19	13	5	248	349	5	17,764	24,711	24,215	27,441	12,750	9,520
S4	10	15	12	15	245	356	18	18,409	24,853	24,860	28,086	20,344	9,500
S5	8	14	9	14	241	363	17	19,054	24,995	25,505	28,731	20,989	9,500
S6	6	12	7	14	238	370	15	19,699	25,137	26,151	29,376	21,635	9,500
S7	7	13	8	15	234	377	14	20,344	25,279	26,796	17,118	22,280	9,500
S8	3	8	6	16	231	384	9	20,989	25,420	27,441	17,764	26,796	9,500
S9	5	10	7	14	227	391	10	21,635	25,562	28,086	18,409	27,441	9,500
L1	-	-	-	-	280	320	24	22,280	25,704	28,731	10,550	28,086	9,466
L2	-	-	-	-	250	300	28	22,925	25,846	29,376	10,250	28,731	9,461
L3	-	-	-	-	260	310	5	23,570	22,280	30,022	12,750	29,376	9,456
L4	-	-	-	-	265	340	6	24,215	22,925	20,344	20,344	26,796	9,451
PCT	280	250	260	265	-	-	415	11,700	9,300	9,000	11,500	20,000	1,040
VW	320	300	310	340	-	-	490	12,950	10,550	10,250	12,750	21,250	1,800

S = Supplier, L = Forming facility location, C = Consumer

6.5.5 Facility location

The geographic area of AIH is managed by four municipalities, including Strathcona County, Lamont County, Sturgeon County, and the City of Fort Saskatchewan. These are responsible for the planning and development of environmentally sustainable industries in AIH. The land available is zoned to restrict the activities for which it is implemented for ranging from agricultural to heavy industrial use. This is achieved to preserve environmentally sensitive areas. All the potential locations for forming and blocking facilities identified on the map of AIH in Figure 6.2 are suitable for heavy industrial use. Locations one and two identified are those for the sulfur forming facilities projects

currently proposed for establishment in AIH [275, 276]. The other two locations identified are currently unoccupied and were included to provide more options for the investigated case study. Small-to-medium scale forming or blocking facilities can be established downstream of a sulfur recovery unit instead of large ones that server multiple sulfur producers. These were also included as options in the model, in which it was assumed that for each sulfur supplier a facility could be established within its proximity. The total area available for each potential location for a forming facility is listed in Table 6.7 along with the total area range required for the several forming and storage technologies considered for the case study. The cost of land was accounted for in the mathematical formulation, which was assumed to be $7K/acre [298].

Table 6.7 Area range for the considered forming and storage technologies, and potential locations

Facility / Location	**Area range (m^2)**
Forming unit	
Enersul GX	700 – 2,500
Sandvik rotoform	700 – 1,400
Storage unit	
Tank	400 - 700
Shed	12,000 – 48,000
Silo	400 - 700
Block	50,000 – 300,000
Location	
1	60,000
2	75,000
3	300,000
4	500,000
Supplier	10,000

6.6 Results and discussion

The previously outlined model was used to develop the structure of the sulfur supply chain of AIH. As previously mentioned, AIH's sulfur production is expected to significantly increase over the next few decades due to the considerable growth and development in the oil sands industry. The sulfur supply chain can operate in a steady state condition, in which the supply is equal to the demand. In this case an increase in the sulfur production levels will require increasing the sulfur forming capacity if it will be delivered to consumers in solid form. On the other hand, the supply of sulfur might exceed the demand, which will require the surplus to be stored in emergency blocking facilities. To account for these effects the case study was analyzed using a deterministic approach for different scenarios in supply and demand levels.

6.6.1 Steady-state operation

In years 2020 and 2030, the supply of sulfur from Alberta's Industrial Heartland is expected to increase by 100% and 200%, respectively, from the current production levels[63]. It is important to investigate the effect of these increases on the design of the sulfur supply chain. An assumption that was made is that there is market demand available for all the sulfur supply. Accordingly, the demand input to the model was increased by an amount equivalent to the supply increase. Three cases were investigated, which are the base case (i.e. current demand and supply), and the cases of 100% and 200% supply and demand increases. Figure 6.3 shows the optimal supply chain configurations for the three investigated scenarios.

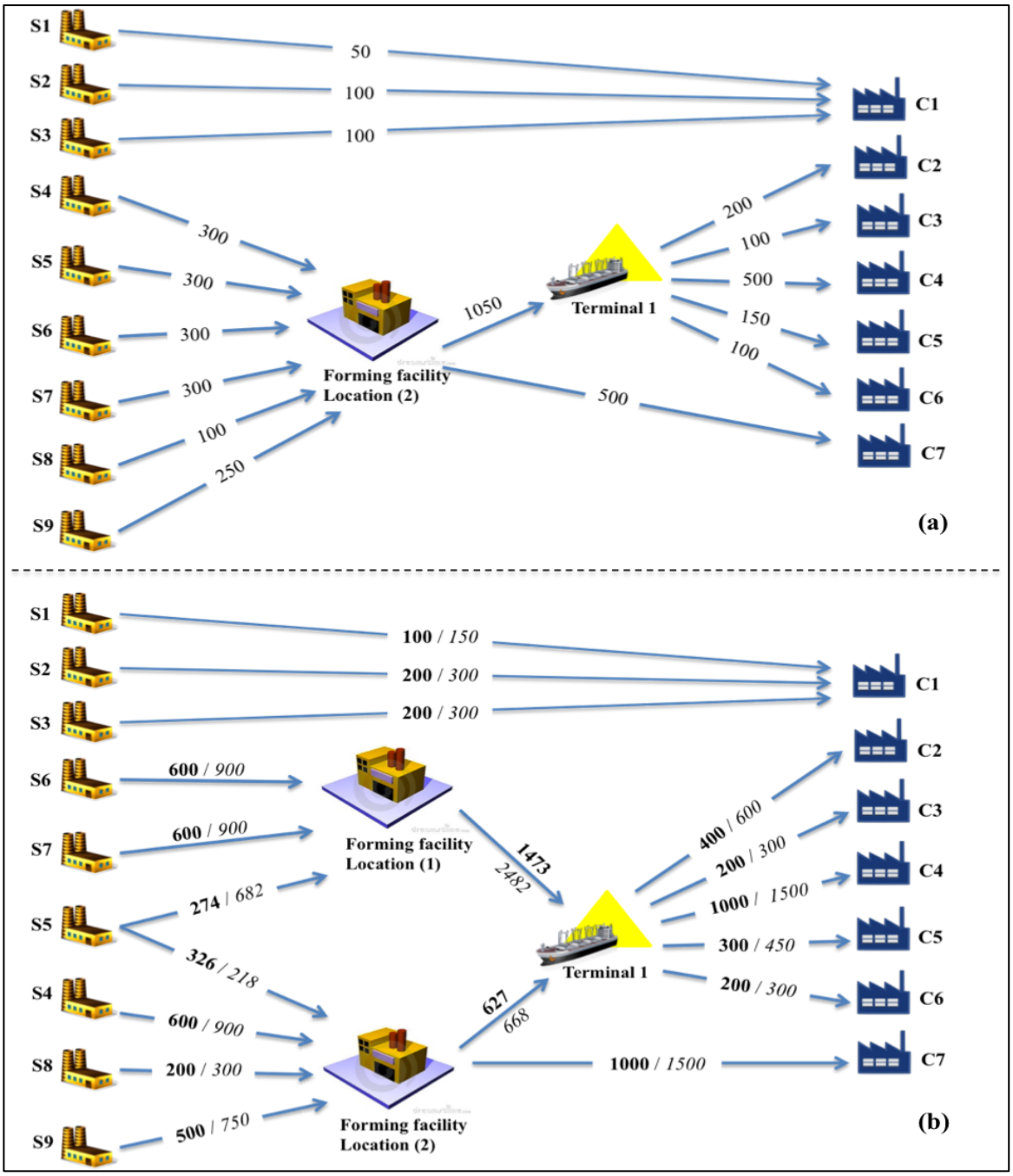

Figure 6.3 (a) Optimal supply chain configuration for the base case scenario and stream flowrates in kT yr^{-1}, **(b)** Optimal supply chain configurations for the 100% and 200% supply and demand increase scenarios and their corresponding stream flowrates (Bold – 100%, Italic – 200%) in kT yr^{-1}.

It shows all the interconnections among the nodes of the supply chain, as well as the corresponding stream flow rates. Table 6.7 lists the selected technologies and capacities

for the forming facilities, distribution centers and transportation modes for the three investigated scenarios. The stream results for the three investigated scenarios along with the corresponding transportation modes among the nodes of the supply chain are summarized in Table 6.8. Figure 6.3(a) shows the optimal configuration for the base case scenario. The output of suppliers 1 – 3 is sufficient to fulfill the demand of consumer 1 that is in their vicinity. The output of the remaining sulfur suppliers is sent to forming facilities to be later shipped to markets overseas (Consumers 2 – 7). Transportation of sulfur to markets in the United States (Consumer 7) can be achieved via rail. Figure 6.3(b) shows the optimal configuration for possible future scenarios. The stream results for the 100% increase in supply scenario are shown in bold font, and those for the 200% increase in supply scenario are shown in italic.

The establishment of sulfur forming facilities in the vicinity of each sulfur producer was not economically attractive as can be observed from the results (Figure 6.3). Having one or two forming facilities to serve several sulfur producers facilitates achieving economies of scale. These economies of scale manifest in the forming process, the storage of liquid and formed sulfur, and the distribution of sulfur to consumers (Table 6.8). Among all the potential locations for the sulfur forming facility, location two was always selected in all the investigated scenarios. Even though it is the farthest from all sulfur producers, the availability of access to both rail links at this location facilitates easier distribution of sulfur through both available export terminals, which are PCT and VW. Having access to both rail lines eliminates the cost of establishing rail line extensions, which is considerably high.

Increasing the sulfur forming capacity will be required if the production of sulfur increases from the sulfur recovery units and market demand for formed sulfur is available. As previously mentioned location two remains the preferred choice to allocate the sulfur forming units. However, the limited area required the establishment of forming facilities elsewhere as the production capacity increased. Location one is in very close proximity to most of the major sulfur producers in the industrial heartland and to the major rail lines compared to the remaining two locations, which justified its selection as it reduces the transportation cost of both liquid and formed sulfur. Even though location one was not justified to be the optimal choice for the base case scenario, the distribution of the forming capacity between the two selected forming facilities shows that it is more preferred due to its proximity to sulfur producers.

As the required capacity became large enough the Rotoform technology was no longer feasible. Even though they have higher capital and operating costs, the model optimal result was to select Enersul GX granulators due to limited space availability, which process considerably higher amounts of sulfur per footprint area. This is more economical than establishing many Rotoform units at several locations in AIH. The storage of formed sulfur in silos is preferable as their lower operating cost and footprint area justify their higher capital cost compared to other storage options. PCT is a closer distribution point to most of the concerned demand destinations and supply nodes, which makes it the preferred export terminal as can be observed from the results. The capacities of the available distribution centers are greater than the total demand for all the investigated scenarios, which eliminated the requirement of establishing new ones.

Table 6.8 Summary of forming facilities optimal results obtained for the base case, and 100% and 200% increase in supply and demand scenarios

	Base case	100% increase		200% increase	
Location	2	2	1	2	1
Technology (MT yr^{-1})	15RHS: 1.55	15RHS: 1.63	14RHS: 1.47	5GXM1: 2.15	5GXM1: 2.5
Storage (KT)	6L tanks: 8.5 1M shed: 20	6L tanks: 8.9 1M shed: 15	6L tanks: 8.1 10L silos: 44.2	8L tanks: 11.8 1M shed: 20	10L tanks: 13.8 1L shed: 40
Transportation (MT yr^{-1})	LT: 1.80 SR: 1.55	LT: 3.6 SR: 3.1		LT: 5.40 SR: 4.65	
Distribution center (KT)	PCT: 52.5	PCT: 105		PCT: 157.5	

L = Large, M = Medium, S = Small, LT = Liquid tanker truck, SR = Solid rail, SS = Solid ship

It can be observed from the results (Table 6.9) that tanker trucks are the only distribution mode selected for the transportation of liquid sulfur. This implies that tanker trucks are the preferred choice of distribution for short travel distances and small-to-moderate quantities of liquid sulfur transported from the several locations of recovery units. Liquid sulfur was delivered only to customers in the vicinity of the industrial heartland. It was economically more attractive to establish forming facilities and transport the sulfur in solid form than distributing it in liquid form. The establishment of liquid sulfur handling equipment and transportation infrastructure is considerably more expensive. The preferred mode of transportation for formed sulfur is by rail cars, the large quantities from the one or two locations of forming facilities transported over the long distance to export terminals justifies its selection. Transportation of formed sulfur by ship was required for overseas customers.

Table 6.9 Summary of stream results for steady state operation of the supply chain

			Flowrate, $Q_{ee'pt}$ (KT yr^{-1})		
From	**To**	**Mode**	**Base case**	**100%**	**200%**
S1	**C1**	TL	50	100	150
S2	**C1**	TL	100	200	300

S3	**C1**	TL	100	200	300
S4	**F1**	TL	0	0	0
S4	**F2**	TL	300	600	900
S5	**F1**	TL	0	274	682
S5	**F2**	TL	300	326	218
S6	**F1**	TL	0	600	900
S6	**F2**	TL	300	0	0
S7	**F1**	TL	0	600	900
S7	**F2**	TL	300	0	0
S8	**F2**	TL	100	200	300
S9	**F2**	TL	250	500	750
F1	**PCT**	SR	0	1473	2482
F2	**PCT**	SR	1050	627	668
F2	**C7**	SR	500	1000	1500
PCT	**C2**	SS	200	400	600
PCT	**C3**	SS	100	200	300
PCT	**C4**	SS	500	1000	1500
PCT	**C5**	SS	150	300	450
PCT	**C6**	SS	100	200	300

S = Supplier, C = Consumer, F = Forming facility at location *j*, TL = Tanker truck, SR = Solid rail, SS = Solid ship

The total cost breakdown summarized in Table 6.10 shows that a significant portion of the total annual cost is contributed to by transportation. This is expected due to the significant distances over which the large quantities of sulfur must be transported. The total annual cost increased with increasing capacity. Moreover, a considerable increase in operating cost occurred due to the switch to the granulation process when the capacity was increased from 100% to 200%. Its selection was more economical than establishing several rotoform pastillation facilities over the industrial heartland and also due to the limited space availability in the selected locations.

Table 6.10 Total cost breakdown for the base case, and 100% and 200% increase in supply and demand scenarios

	Base case	**100% increase**	**200% increase**
Capital cost ($)			
Forming and storage	1.04×10^7	1.53×10^8	7.42×10^7
Transportation	1.80×10^8	3.60×10^8	5.39×10^8
Total capital cost	1.90×10^8	5.08×10^8	6.13×10^8
Operating cost ($ yr^{-1})			
Forming and storage	2.38×10^9	5.17×10^8	1.00×10^9
Transportation	9.36×10^7	1.90×10^8	2.77×10^8
Total operating cost	3.32×10^8	7.20×10^8	1.28×10^9
Total annual cost ($ yr^{-1})	**5.22×10^8**	**1.23×10^9**	**1.89×10^9**

A sulfur forming and shipping facility project in AIH has been approved for construction. It has a capital cost of $30 M, which will be funded and completed by the HAZCO division of CCS Income Trust[39]. The proposed project includes forming and storage facilities, but it does not include emergency sulfur blocks. The forming technology to be implemented is Sandvik Rotoform, and the formed sulfur will be stored on engineered pads. The forming and liquid and solid storage capacities are 1.1 MT yr^{-1}, 3 KT, and 45 KT, respectively. Molten sulfur will be received by tanker trucks or pipelines and shipped by rail to export terminals. This facility will be established in one of the locations proposed in the presented case study, which is the optimal location suggested by the results obtained for the base case scenario (location 2). The results obtained about the forming facility for the base case scenario are comparable to those of this proposed project, which shows the adequacy of the proposed model. Another project is the Kinder Morgan sulfur forming and handling facility[40], which is deferred, and its establishment depends on the timing of construction of new upgraders in the industrial heartland. The facility is proposed to have forming units, liquid storage tanks and solid storage silos. It is

proposed to be established at location 1 shown in the presented case study. Assuming that it will be established when forming capacity expansions will be required, this information is in agreement with the results obtained for the case in which the supply and demand were increased by 100 and 200%.

6.6.2 Sulfur surplus accumulation

An important element of the sulfur supply chain is the emergency storage facilities, which are commonly available in the form of sulfur blocks. The surplus of sulfur supply could be due to increased operations or the establishment of gas plants, refineries and upgraders. It could also be due to a decrease in the sulfur market's demand. In order to investigate the effect of this, the supply was increased while keeping the demand constant. On the other hand, decreasing the demand for formed sulfur relative to a constant production level will eliminate the establishment of required sulfur forming facilities, which will contradict with the results obtained for the steady-state operation of the supply chain. The optimal configuration of the supply chain is shown in Figure 6.4. Summary of the stream results for the three investigated scenarios along with the corresponding transportation modes are listed in Table 6.10. The results regarding the additional capacity required for blocking the surplus sulfur for three investigated scenarios are summarized in Table 6.11.

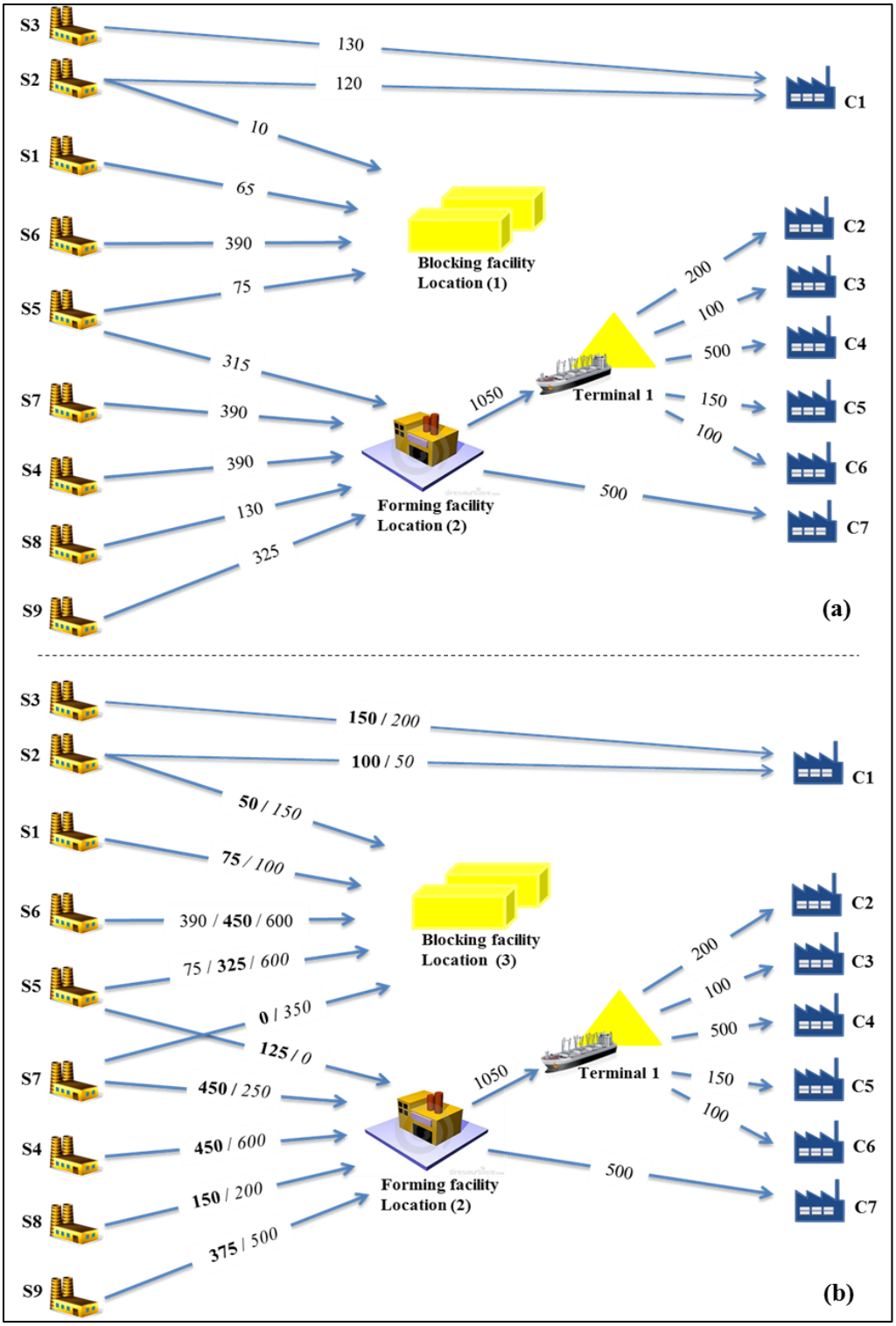

Figure 6.4 (a) Optimal supply chain configuration for the low supply accumulation scenario and stream flow rates in kT yr^{-1}, **(b)** Optimal supply chain configuration for the medium and high supply accumulation scenarios and stream flow rates (Bold – medium, Italic – high) in kT yr^{-1}.

The results obtained for the establishment of forming facilities were the same as those obtained for the base case scenario. The surplus of sulfur was stored into blocks. Three scenarios were investigated, which are associated with low, medium and high surplus of sulfur. These cases of supply increase over demand are quantified as ranges between 0 – 30%, 30% – 60%, 60% – 100%, respectively. Location 1 is selected when there is up to a 30% surplus of sulfur supply. However, higher amounts will require larger block storage capacities, and location 3 would then represent the optimal selection due to the space limitation (Table 6.11). The increase in liquid storage and transportation capacities are required for the operation of the new blocking facilities.

Table 6.11 Summary of blocking facilities optimal results obtained for low, medium and high sulfur surplus scenarios

Sulfur surplus	**Low**	**Medium**	**High**
Location	1	3	3
Blocks (MT)	1S**:** 1.1	1M**:** 1.8	2M**:** 3.6
Liquid Storage (KT)	2L**:** 3	4L**:** 5	7L**:** 9.9
Transportation (MT yr^{-1})	LT**:** 0.54	LT**:** 0.9	LT**:** 1.8

L = Large, M = Medium, S = Small, LT = Liquid tanker truck

Similar to the results obtained for steady state operation, tanker trucks remain the preferred mode of transportation for liquid sulfur (Table 6.12). It can also be observed from the stream results that all the sulfur produced by suppliers 1 and 6 are sent to blocking facilities, which represents an oversimplified assumption of the preference of sulfur suppliers regarding whether or not to send the sulfur to markets. It is a cheaper option to block sulfur than to send them to forming facilities; however it will not entail any revenues. As the surplus of sulfur produced increases, more of the output of suppliers

5 and 7 is also sent to blocking facilities. Therefore, for each supplier it might be required to constrain the share of sulfur that is sent to blocking facilities.

Table 6.12 Summary of stream results for sulfur surplus accumulation scenarios

			Flowrate, $Q_{ee'pt}$ (KT yr^{-1})		
From	**To**	**Mode**	**30%**	**50%**	**100%**
S1	**B1**	TL	65	0	0
S1	**B3**	TL	0	75	100
S2	**C1**	TL	120	100	50
S2	**B1**	TL	10	0	0
S2	**B3**	TL	0	50	150
S3	**C1**	TL	130	150	200
S4	**F2**	TL	390	450	600
S5	**B1**	TL	75	0	0
S5	**F2**	TL	315	125	0
S5	**B3**	TL	0	325	600
S6	**B1**	TL	390	0	0
S6	**B3**	TL	0	450	600
S7	**F2**	TL	390	450	250
S7	**B3**	TL	0	0	350
S8	**F2**	TL	130	150	200
S9	**F2**	TL	325	375	500
F2	**PCT**	RS	1050	1050	1050
F2	**C7**	RS	500	500	500
PCT	**C2**	SS	200	200	200
PCT	**C3**	SS	100	100	100
PCT	**C4**	SS	500	500	500
PCT	**C5**	SS	150	150	150
PCT	**C6**	SS	100	100	100

S = Supplier, C = Consumer, F = Forming facility at location *j*, B = Blocking facility at location *j*, TL = Tanker truck, SR = Solid rail, SS = Solid ship

Taking into account future increases in sulfur supply it is plausible to choose location 3 for the establishment of blocking facilities and location 1 for future forming capacity expansion. It is important to emphasize that blocking facilities represent a solution to an emergency situation occurring due to the volatility of the sulfur market that still has to be managed to reach the final market.

As can be observed from the cost breakdown in Table 6.13, the annual cost of managing the increased sulfur supply through blocking is considerably lower than forming it and distributing it to the final market. However, additional costs will eventually be incurred, as it will be required for blocked sulfur to be remelted, formed and sold to final consumers. Therefore, this temporary solution cannot be relied upon on the long-term as they also require a significant amount of space to establish them.

Table 6.13 Total cost breakdown for low, medium and high sulfur surplus scenarios

Sulfur surplus	**Low**	**Medium**	**High**
Capital cost ($)			
Forming and storage	9.79×10^7	1.04×10^8	1.17×10^8
Transportation	1.90×10^8	1.98×10^8	2.16×10^8
Total capital cost	2.88×10^8	3.02×10^8	3.33×10^8
Operating cost ($ yr^{-1})			
Forming and storage	3.37×10^8	4.31×10^8	4.20×10^8
Transportation	9.47×10^7	9.57×10^7	9.78×10^7
Total operating cost	4.32×10^8	5.26×10^8	5.17×10^8
Total annual cost ($ yr^{-1})	**7.20×10^8**	**8.28×10^8**	**8.50×10^8**

The proposed MILP model was solved by using the CPLEX solver version 11.0 accessed in the General Algebraic Modelling System[64]. The model statistics for the six investigated scenarios associated with steady state operation (1- base case, 2- 100%

increase and 3- 200% increase) and sulfur surplus accumulation (4- low, 5- medium and 6- high) are summarized in Table 6.14. As can be observed from the results in the table the required computational time are short and the relative optimality gaps are acceptable for all the investigated scenarios.

Table 6.14 Model computational results for all the investigated scenarios

	1	**2**	**3**	**4**	**5**	**6**
Constraints	5,126	5,126	5,126	5,143	5,143	5,143
Continuous variables	3,646	3,646	3,646	3,648	3,648	3,648
Integer variables	1,711	1,711	1,711	1,714	1,714	1,714
Optimality gap	0	0	0	0	0	0
CPU time (s)	0.049	0.047	0.048	0.053	0.053	0.053

6.7 Conclusions

The increasing development of the heavy oil industries as well as the reliance on increasingly sour crudes and gases accompanied with increasingly stringent environmental regulations impose the requirement of developing an effective management framework for future sulfur supply chains, which are expected to develop and change along with the projected increase in sulfur production in the future. Much of the previous research was directed towards developing and improving the efficiency and environmental sustainability of individual components of the supply chain, such as recovery, forming, storage and distribution. However, it is important to shed light on integrating these components within a single framework as it could provide significant potential economic benefits.

Therefore, the aim of this work is to develop a strategic decision support tool based on an optimization framework to facilitate the design and operation of sulfur supply chains. The formulated single-period MILP model is aimed at minimizing the total annual network

cost, and it is subject to material balance, capacity, space, and demand constraints. The decisions incorporated in the model include the allocation of forming and storage facilities, the selection of forming, storage and transportation technologies and their capacities, and the determination of flow rates among the nodes of the supply chain network. The applicability of the model was illustrated through the AIH case study. Due to the volatility of the sulfur market and the projected increase in sulfur production, it was important to investigate the effect of the supply and demand variability on the design of the supply chain. In one scenario steady state operation was assumed, and in another scenario temporary sulfur surplus accumulation was accounted for by incorporating long-term storage facilities (i.e. sulfur blocks).

The results obtained indicate that the optimal configuration of the sulfur supply chain in AIH might include medium-to-large forming facilities serving multiple sulfur producers. This achieves economies of scale compared to having individual forming facilities in the vicinity of each recovery unit. For small-to-medium scale of operation, it is preferred to select the sulfur pastillation technology, whereas for medium-to-large scale sulfur granulation is more economical. Silos are the preferred option for the storage of formed sulfur due to their lower operating cost and low footprint area requirements. Sulfur blocking is an extremely attractive option for managing increased sulfur supply for its low capital and operational costs; however, they require significant space, which renders their unreliable as a long-term solution. The locations selected for the establishment of the facilities are in very close proximity to both main rail lines in AIH and to most of the sulfur producer, which reduces logistical costs. Tanker trucks is the preferred mode of

transportation for delivering liquid sulfur to forming facilities, and rail transportation is preferred for formed sulfur transported to export terminals.

This work represents a starting point in understanding the important trade-offs involved in sulfur supply chains. It provides an indication of the important data required to support strategic decisions in their design and operation. It also provides an assessment of the applicability of implementing quantitative supply chain design models to solve these problems. At this stage, promising results were obtained from the proposed model. However, there are several aspects that require further improvement to develop a more sophisticated one. Several areas that could be investigated include the following:

- Develop a multiperiod optimization model to represent the supply chain network. Since a surplus of sulfur is expected to exist in the future, an idea that is being contemplated is to store the sulfur to avoid flooding the market and decreasing its value. Using a mutltiperiod model will assist in estimating optimal inventory levels, holding time and storage capacities. Moreover, a multiperiod will help account for the addition of remelted emergency sulfur blocks to the total supply of sulfur in future time periods and its distribution among forming facilities or demand nodes, which will affect the optimal configuration of the supply chain. It is also beneficial to better account for the unsteady-state operation of the sulfur supply chain, in which supply and demand are time variant.
- Pollutant emissions, such as, hydrogen sulfide, sulfur oxides and particulate matter are a major concern associated with the different forms of sulfur and their handling facilities and equipment. The inclusion of environmental constraints in the optimization model will assist in designing sulfur supply chains that comply

with environmental regulations at a minimum cost. Moreover, several mitigation technologies could be incorporated in the model, such as, hydrogen sulfide degassing systems, sulfur dust suppression systems and active air emission control technologies.

- It would be interesting to develop a comprehensive list of all existing technologies and applications which utilize sulfur as a feedstock. Then identify where these industries exist geographically to determine market locations. Then determine the optimal configuration to distribute the sulfur among these markets. Moreover, it could also be considered to extend the supply chain to include these downstream technologies. For example, the establishment of a sulfuric acid plant to serve the alkylation process typically used in refineries. This could create potential synergies and reduce the transportation and storage requirements of sulfur, which as observed from the results they constitute a significant portion of the total annual network cost.
- Finally, it is interesting to incorporate stochastic optimization techniques in the sulfur supply chain optimization model. This can allow handling the uncertainties associated with sulfur selling prices and demands.

Chapter 7

Conclusions

This thesis explored the effectiveness of various low carbon intensive energy production technologies (i.e. renewables, nuclear, and fossil fuel based integrated with carbon capture and sequestration) for carbon management of the energy infrastructure of energy intensive industries using the oil sands industry in Alberta as a case study. The results of this work support the design and implementation of effective carbon mitigation measures that result in the achievement of the highest possible emission reductions at the lowest possible costs. Similarly, the results obtained emphasize the significance of the effective management of the supply chain of excess by-products generated from oil sands industries (e.g. sulfur) that would otherwise hinder their operations if stockpiled in limited inventory.

Chapter 3 assessed the various renewable energy production options in Alberta that can be integrated in the energy infrastructure of oil sands operators. These included geothermal energy for the provision of heat, bioenergy (i.e. power, heat, hydrogen and biodiesel), electrolytic hydrogen from wind power. These technologies have been incorporated along with fossil fuel based technologies in an MINLP integrated energy optimization model. The model is utilized for the integrated planning of the energy infrastructure and the oil sands producers (i.e. oil sands production and bitumen upgrading routes). Capacity expansion decisions were incorporated along with the rolling horizon approach to determine the effect of the existing energy infrastructure of the current planning period on the new investment decisions of the following planning

period. The results obtained indicated that renewable energy technologies have significant potential in reducing emissions associated with oil sands production operations. Moreover, for some of the investigated scenarios the emission reduction target constraints were not achievable (i.e. infeasible solution) without the incorporation of renewable energy technologies, particularly geothermal energy and bioenergy (steam and hydrogen production). Heat production in the form of steam has been shown to account for the highest share in the generated emissions. As a result, bitumen upgrading routes that utilize hydrogen for cracking has been favored by the optimization model. Even though the results obtained have shown that renewable energy can play a significant role in achieving adequate emission reductions, these achievable reductions are expected to be offset by the forecasted significant increase in the oil sands production levels and their associated energy requirements. Therefore, it is required to expand the energy production mix incorporating various low carbon intensive technologies, as well as energy production technologies that utilize various fuel alternatives (e.g. petcoke) to natural gas. Moreover, the planning of the energy infrastructure of oil sands should simultaneously take place over a long planning horizon and take into account time dependent parameters. This was addressed in chapter 3, in which a multi-period generalized energy optimization model for the planning of energy intensive industries was proposed.

In chapter 4 an extensive superstructure of energy production technologies for energy intensive industries was proposed. The energy supply technologies considered included nuclear (PBMR, ACR-700, ACR-1000, CANDU, and HTGR) for power and heat production, natural gas combined cycle and oxyfuel for power production, pulverized

coal and coal oxyfuel for power production, SMR for hydrogen production, gasification (coal, petroleum coke, biomass, and asphaltenes) for power, hydrogen and thermal energy production, industrial natural gas combined heat and power production, natural gas boilers, integrated wind power, nuclear power and water electrolysis for power and hydrogen production, biodiesel, and geothermal energy. Carbon mitigation options also included carbon capture and sequestration, and purchase of carbon credits to satisfy emission targets. In addition, the model incorporated the possibility of selling excess power production to the Alberta grid, and excess hydrogen to the market. A deterministic multi-period MILP model that describes the superstructure was developed for the planning of energy production for energy intensive industrial operations. The optimization model is developed with the objective of identifying the optimal mix of energy supply and CO_2 emission mitigation options to satisfy a set of energy demands (e.g., power, heat, hydrogen, etc.) and emission targets at minimum cost. To accomplish this, an objective function is formulated that is geared toward the minimization of the net present value of the total cost of energy production over the entire planning period. Moreover, the model formulation incorporated time dependent parameters to account for the variability in major factors affecting the operations of the industry. These include energy demands, fuel prices, CO_2 emission reduction targets, CO_2 credit/tax cost, construction lead time, and techno-economic parameters of energy production technologies. The model was applied to a case study based on the energy-intensive oil sands operations in Alberta over the planning period 2015–2050.

A scenario based approach was used to investigate various carbon mitigation policies and to investigate variability in time dependent parameters. The total and unit energy

production costs ranged from CAD 446–2586 billion and 8.45–48.9 CAD/bbl SCO, respectively. The average annual emissions generated ranged from 1,100–12,000 tonne h^{-1}. The currently applied \$15/tonne CO_2 carbon tax in Alberta was not sufficient to achieve the required emission reduction targets. The model facilitated the investigation of the effect of various parameters on the planning of the energy infrastructure. This included variability in energy intensities, carbon mitigation policies, fuel prices, and price of energy commodities (e.g. power and H_2 selling price). Even though the buying and selling of surplus energy commodities such as power have been accounted for as variables in the optimization model, the effect of the penetration of large production capacities of energy production technologies such as wind, nuclear, natural gas combined heat and power on the operations (i.e. unit commitment) of the power generation units of the local Alberta grid is not accounted for. This has been addressed in chapter 4.

Chapter 5 investigated the integrated planning and scheduling of the decentralized energy infrastructure of oil sands. The superstructure of the energy production mix incorporates conventional, nuclear, and renewable energy production technologies. Power-to-gas is also considered for the management of the intermittent behavior of the wind-electrolysis system. Electrolytic hydrogen generated can be recovered via two pathways, which are power-to-gas (i.e. hydrogen sent to bitumen upgraders) and power-to-gas-to-power (i.e. hydrogen retrieved for HENG used in NGCC). A multi-period and multi-objective MILP model is generated and it takes into account the total system cost, grid cost, and total emissions. Unit commitment constraints are incorporated to manage the operations of the existing and new grid power generation units. This takes into account grid interactions with the penetration of additional power generation capacity to the energy infrastructure

of the oil sands industry, from which excess power is sent to the grid. The ranges of total system cost, grid cost, and total emissions were determined to be 6.02 – 127 billion CAD, 0.005 – 2.21 billion CAD, and 7.16 – 276.3 $MtCO_2$, respectively. The cost of wind power production had the highest share of the cost of the wind-electrolysis system, which in return had the highest share of the cost of electrolytic hydrogen production for bitumen upgrading. In order for wind-electrolysis to be competitive with conventional SMR a high weight has to be set on the emissions objective function. The cost of electrolytic hydrogen production was determined to be in the range of 5.97 – 17.5 CAD/kg H_2. Utilizing natural gas cogeneration facilities to its full potential in the oil sands industry can reduce the emissions of the power sector in Alberta by >40%. However, high penetration levels of cogeneration units impacts the planning of the wind-electrolysis system, as this impedes the penetration of renewable wind power generation capacity. It also affects the scheduling operations of the existing power generation units of the grid. The incorporation of nuclear energy facilitated the achievement of significant emission reductions at considerably lower system and grid operating costs. The integrated planning and scheduling of the energy infrastructure of oil sands and the Alberta grid's power generation units leads to the generation of large scale models, which are computationally expensive. A potentially promising approach that can be utilized in future work is the use of a data clustering approach. It will allow the reduction of the computational time of the model, the simultaneous planning and scheduling of multiple operational years, and the investigation of uncertain input data using stochastic optimization techniques.

In chapter 6 an extensive review was conducted of the individual components of sulfur supply chains, including recovery, forming, storage, and distribution. These components

were integrated within a single optimization-based framework in order to realize potential economic benefits. An MILP optimization model was developed for the planning of downstream sulfur supply chains. The model is geared towards the minimization of the annual network cost and was applied to a case study in the Alberta Industrial Heartland, for which material balance, capacity, space and demand constraints were incorporated. The results of the model, which included the allocation of forming and storage facilities, the selection of forming, storage and transportation technologies and their capacities, and the flow rates among the nodes of the supply chain network, provided an indication of the optimal configuration of the supply chain. The work provided a starting point for understanding the trade-offs involved in sulfur supply chains, and can be extended in future work to incorporate existing technologies and applications that utilize sulfur as a feedstock, then identify where these industries exist geographically to determine market locations and determine the optimal configuration to distribute the sulfur among these markets.

References

[1] Alberta's Oil Sands: The Facts. 2014. Alberta Government. Available online: http://www.energy.alberta.ca/OilSands/pdfs/AlbertasOilSandsFactsJan14.pdf

[2] Gordon, D. 2012. Understanding Unconventional Oil – The Carnegie Papers. Available online: http://carnegieendowment.org/files/unconventional_oil.pdf

[3] International Energy Agency – IEA. 2010. Unconventional Oil & Gas Production – Energy Technology Systems Analysis Programme. Available online: http://www.iea-etsap.org/web/E-TechDS/PDF/P02-Uncon%20oil&gas-GS-gct.pdf (Accessed April 2014).

[4] Ordorica-Garcia, G., Croiset, E., Douglas, P., Elkamel, A. and Gupta, M. Modeling the Energy Demands and Greenhouse Gas Emissions of the Canadian Oil Sands Industry. Energy & Fuels, 2007, vol. 21, pp. 2098 – 2111.

[5] Ordorica-Garcia, G., Elkamel, A., Douglas, P.L., Croiset, E. and Gupta, M. Energy Optimization Model with CO2-Emission Constraints for the Canadian Oil Sands Industry. Energy & Fuels, 2008, vol. 22, pp. 2660 – 2670.

[6] Betancourt-Torcat, A., Guiterrez, G., Elkamel, A. and Ricardez-Sandoval, L. Integrated Energy Optimization Model for Oil Sands Operations. Industrial & Engineering Chemistry Research, 2011, vol. 50, pp. 12641 – 12663.

[7] Betancourt-Torcat, A., Elkamel, A. and Ricardez-Sandoval, L. Optimal Integration of Nuclear Energy and Water Management into the Oil Sands Operations. AIChE journal, 2012, vol. 58 (11), pp. 3433 – 3453.

[8] Brooke, A., Kendrick, D., Meeraus, A. and Raman, R. 1998. GAMS: A User's Guide, Available online: http://www2.imm.dtu.dk/courses/02724/general_information/GAMS_userguide/GAMSUsersGuide.pdf

[9] Woynillowicz, D. 2005. Oil Sands Fever – The Environmental Implications of Canada's Oil Sands Rush. Available online: https://www.pembina.org/reports/OilSands72.pdf (Accessed December 2014).

[10] National Energy Board – Canada's Oil Sands Opportunities and Challenges to 2015: An Update. 2006. Available online: https://www.neb-

one.gc.ca/nrg/sttstc/crdlndptrlmprdct/rprt/archive/pprtntsndchllngs20152006/pprtntsndchllngs20152006-eng.pdf (Accessed November 2014).
[11] Oil Sands Discovery Centre – Facts about Alberta's oil sands and its industry. 2014. Available online: http://history.alberta.ca/oilsands/resources/docs/facts_sheets09.pdf (Accessed October 2014).
[12] Kubik, R. Canadian Oil Sands – 2013 Annual Report. 2013. Available online: http://www.cdnoilsands.com/files/FinancialReports/AnnualReport2013/2013%20Annual%20Report_Final_english_v001_r6d515.pdf (Accessed October 2014).
[13] World Oil Outlook – Organization of the Petroleum Exporting Countries. 2014. Available online: http://www.opec.org/opec_web/static_files_project/media/downloads/publications/WOO_2014.pdf (Accessed January 2015).
[14] Noronha, C. 2015. Canadian think-tank: Low oil prices may lead Alberta's oil-heavy economy to dip into recession – The Province. Available online: http://www.theprovince.com/business/Canadian+thinktank+prices+lead+Albertas+oilheavy+economy+into/10726034/story.html (Accessed February 2015).
[15] Isfeld, G. 2015. Low oil to have "both positive and negative effects" on Canadian economy, Ottawa told. Available online: http://business.financialpost.com/news/economy/low-oil-to-have-both-positive-and-negative-effects-on-canadian-economy-ottawa-told (Accessed April 2015).
[16] Mckenna, B. 2015. Oil prices could go lower, Bank of Canada. Available online: http://www.theglobeandmail.com/report-on-business/industry-news/energy-and-resources/oil-prices-could-go-lower-still-boc-says/article22427436/ (Accessed February 2015).
[17] Ferley, P., Hogue, R. and Janzen, N. 2014. Impact of Lower Oil Prices on the Canadian Economic Outlook: An Update. Available online: http://www.rbc.com/economics/economic-reports/pdf/other-reports/opi2.pdf (Accessed January 2015).
[18] Huot, M. and Grant, J. 2012. Clearing the air on oil sands emissions – The facts about greenhouse gas pollution from oil sands development. Available online:

http://www.pembina.org/reports/clearing-the-air-climate-oilsands.pdf (Accessed November 2014).
[19] Doritsch, D., Huot, M. and Partington, P. J. 2010. Canadian Oil Sands and Greenhouse Gas Emissions. Available online: https://www.pembina.org/reports/briefingnoteosghg.pdf (Accessed October 2014).
[21] Clarke, T. 2010. Tar Sands Watch: Tar Sands Showdown – Energy Security. Available online: http://www.tarsandswatch.org/files/Energy%20Security.pdf
[22] Doucet, J. 2007. Is Nuclear Technology an Appropriate Alternative to Natural Gas for Alberta's Oilsands? Available online: https://business.ualberta.ca/-/media/business/centres/cabree/documents/energy/renewables/wooley.pdf
[23] Betancourt-Torcat, A., Almansoori, A., Elkamel, A. and Ricardez-Sandoval, L. Stochastic Modeling of the Oil Sands Operations under Greenhouse Gas Emission Restrictions and Water Management. Energy & Fuels, 2013, vol. 27, pp. 5559 – 5578.
[24] Betancourt-Torcat, A., Elkamel, A. and Ricardez-Sandoval, L. A modeling study of the effect of carbon dioxide mitigation strategies, natural gas prices and steam consumption on the Canadian Oil Sands operations. Energy, 2012, vol. 45, pp. 1018 – 1033.
[25] Price Water House Coopers. 2009. Alberta Environment – Assessment of Selected Renewable Energy Technology and Potential In Alberta. Available online: eipa.alberta.ca/media/42554/assessment%20of%20selected%20renewable%20energy%20technology%20and%20potential%20in%20alberta.pdf (Accessed September 2014).
[26] Holm, A., Jennejohn, D. and Blodgett, L. 2012. Geothermal Energy Association – Geothermal Energy and Greenhouse Gas Emissions. Available online: http://geo-energy.org/reports/GeothermalGreenhouseEmissionsNov2012GEA_web.pdf
[27] Gray, D., Majorowicz, J. and Unsworth, M. Investigation of the geothermal state of sedimentary basins using oil industry thermal data: case study from Northern Alberta exhibiting the need to systematically remove biased data. J. Geophys. Eng., 2012, 9 (1), 534 – 548.
[28] Majorowicz, J., Unsworth, M., Chacko, T., Gray, A., Heaman, L., Potter, D., Schmitt, D. and Babadagli, T. Geothermal Energy as a Source of Heat for Oil Sands Processing in Northern Alberta, Canada, in Hein, F. J., Leckie, D., Larter, S. and Suter,

J., eds., Heavy oil and oil sand petroleum systems in Alberta and beyond: AAPG Studies in Geology, 2012, 64(1), 1 – 22.

[29] Pathak, V., Babadagli, T., Majorowicz, A. and Unsworth, M. Evaluation of Engineered Geothermal Systems as a Heat Source for Oil Sands Production in Northern Alberta. Natural Resources Research, 2013, 23(2), 247 – 265.

[30] Alberta Electric System Operator (AESO) – Wind Power in Alberta. 2012. Available online: http://poweringalberta.com/wp-content/uploads/2015/01/Wind_power_in_Alberta_WEB.pdf

[31] Bartholomy, O. 2005. Renewable hydrogen from wind in California. Proceedings, National Hydrogen Association Annual Conference, Washington, D.C., March 29 – April 1, 2005.

[32] Government of Canada – Climate: Hourly Wind Speed. Available online: http://climate.weather.gc.ca/climateData/generate_chart_e.html?timeframe=1&Prov=&StationID=8791&MeasTypeID=windspd&cmdB1=Go&Year=2001&Month=3&Day=18&cmdB1=Go# (Accessed October 2014).

[33] Sttaffel, I. 2012. Wind Turbine Power Curves. Available online: https://www.academia.edu/1489838/Wind_Turbine_Power_Curves (Accessed October 2014).

[34] Olateju, B. and Kumar, A. Hydrogen production from wind energy in Western Canada for upgrading bitumen from oil sands. Energy, 2011, 36, 6326 – 6339.

[35] Olateji, B., Monds, J. and Kumar, A. Large scale hydrogen production from wind energy for the upgrading of bitumen from oil sands. Applied Energy, 2014, 118, 48 – 56.

[36] Canada's Rivers at Risk – Environmental Flows and Canada's Freshwater Future. 2012. Available online: http://assets.wwf.ca/downloads/canadas_rivers_at_risk.pdf (Accessed November 2014).

[37] HATCH – Final Report for Alberta Utilities Commission: Update on Alberta's Hydroelectric Energy Resources. 2010. Available online: http://www.energy.alberta.ca/electricity/pdfs/auchydroelectricstudy.pdf (Accessed November 2014).

[38] Implications of a 2^{o}C global temperature rise on Canada's water resources – Athabasca River and oil sands development Great Lakes and hydropower production.

Available online: http://awsassets.wwf.ca/downloads/wwf_globalwarming_implicationsof2degressoncanadawaterresources.pdf (Accessed November 2014).

[39] Sarkar, S. and Kumar, A. Biohydrogen production from forest and agricultural residues for upgrading of bitumen for oil sands. *Energy*, 2010, 35, 582-591.

[40] Bradley, D. 2010. Canada Report on Bioenergy 2010. Available online: http://www.canbio.ca/upload/documents/canada-report-on-bioenergy-2010-sept-15-2010.pdf (Accessed November 2014).

[41] Kumarappan, S., Joshi, S. and MacLean, H. L. Biomass supply for biofuel production: Estimates for the United States and Canada. *BioResources,* 2009, 4(3), 1070-1087.

[42] Biomass CHP Catalog – Biomass Conversion Technologies, EPA Combined Heat and Power Partnership. 2010. Available online: www.epa.gov/chp/documents/biomass_chp_catalog_part5.pdf

[43] Black and Veatch. 2012. Cost report – Cost and performance data for power generation technologies prepared for the National Renewable Energy Laboratory. Available online: bv.com/docs/reports-studies/nrel-cost-report.pdf

[44] Common Boiler Formulas. 2006. Available online: http://steamcombustion.com/files/JBC_Common_Boiler_Formulas.pdf (Accessed September 2014).

[45] Garcia-Cortes, C., Tzimas, E., Peteves, S.D. 2009. Technologies for Coal based Hydrogen and Electricity Co-production Power Plants with CO2 Capture. European Commission Joint Research Centre Institute for Energy. Calgary, Canada, March 2008.

[46] Rubin, E.S., Rao, A.B., Chen, C. 2004. Comparative assessments of fossil fuel power plants with CO_2 capture and storage. Proceedings of the GHGT-7 Conference. Vancouver, Canada, September 2004.

[47] Demirel, Y. 2012. Energy, Green Energy and Technology. Springer-Verlag London Limited. Available online: http://www.springer.com/cda/content/document/cda_downloaddocument/9781447123712-c2.pdf?SGWID=0-0-45-1293540-p174262962

[48] International Energy Agency. 2010. Power Generation from Coal – Measuring and Reporting Efficiency Performance and CO2 emissions. Available online: https://www.iea.org/ciab/papers/power_generation_from_coal.pdf

[49] National Energy Strategy. 1992. Chapter 4 – Efficiency of Energy Conversion. Available online: http://www.ems.psu.edu/~radovic/Chapter4.pdf

[50] Simbeck, D., Chang, E. 2002. Hydrogen Supply: Cost estimate for Hydrogen Pathways – Scoping Analysis. Report NREL/SR-540-32525. National Renewable Energy Laboratory. Colorado, United States.

[51] Simbeck, D. R. 2004. Hydrogen Costs with CO2 Capture. Proceedings of the GHGT-7 Conference. Vancouver, Canada, September 2004.

[52] Chiesa, P., Consonni, S., Kreutz, T., Williams, R. 2005. Co-production of hydrogen, electricity, and CO2 from coal with commercially ready technology. Part A: Performance and emissions. International Journal of Hydrogen Energy. 30:747, 2005.

[53] Jechura, J. 2015. Hydrogen from Natural Gas via Steam Methane Reforming (SMR). Available online: http://inside.mines.edu/~jjechura/EnergyTech/07_Hydrogen_from_SMR.pdf

[54] Maxwell, G. (2004). Synthetic Nitrogen Products – A Practical Guide to the Products and Processes. Kluwer Academic Publishers, New York, New York, USA.

[55] Meyers, R. A. 1984. Handbook of Synfuels Technology. McGraw-Hill: New York.

[56] OTPI Canada. 2002. OPTI Canada Long Lake Project Application for Commercial Approval; OPTI Canada: Calgary, Alberta, Canada, Vol. 1, Sections A – C.

[57] Yui, S. and Chung, K. 2001. Processing Oil Sands Bitumen is Syncrude's R&D Focus. Oil and Gas Journal, 99(17), 46 – 53.

[58] Refining Process Handbook. 2004. Hydrocarbon Processing Magazine, Gulf Publishing Company: Houston, TX.

[59] Sunderland, B. 2001. Hydrogen Production, Recovery and Use at Syncrude. EFI Conference on Technologies to Enable the Hydrogen Economy, Tucson, AZ.

[60] Schumacher, M. 1982. Heavy Oil and Tar Sands Recovery and Upgrading International Technology; Noyes Data Corporation: Park Ridge, NJ.

[61] Van Driesen, R., Caspers, J., Campbell, A. R. and Lunin, G. 1979. LC-Fining Upgrades Heavy Crudes. Hydrocarbon Process, 58 (5).

[62] Fichter, T., Trieb, F. and Moser, M. Optimized Integration of Renewable Energy Technologies Into Jordan's Power Plant Portfolio. Heat Transfer Engineering, 2014, vol. 35(3), pp. 281 – 301.

[63] Fichter, T., Trieb, F., Moser, M. and Kern, J. Optimized integration of renewable energies into existing power plant portfolios. Energy Procedia, 2014, vol. (49), pp. 1858 – 1868.

[64] Investing in our Future: Responding to the Rapid Growth of Oil Sands Development. 2006. Available online: http://www.energy.alberta.ca/pdf/OSSRadkeReportInvesting2006.pdf (Accessed December 2014).

[65] Harrel, G. 2002. Steam System Survey Guide. Report ORNL/TM-2001/263. Oak Ridge National Laboratory. Tennessee, United Sates.

[66] Canadian Association of Petroleum Producers (CAPP). 2014. Crude Oil Forecast, Markets & Transportaion. Available online: www.capp.ca/getdoc.aspx?DocId=247759&DT=NTV

[67] McColl, D., Mei, M, Millington, D. and Kumar, C. 2008. Canadian Energy Research Institute – Green Bitumen: The Role of Nuclear, Gasification, and CCS in Alberta's Oil Sands. Available online: www.ceri.ca/docs/CERIOilSandsGHG-PartII.pdf

[68] Bunse, K, Vodicka, M, Schönsleben, M, Brülhart, M, Ernst, F. Integrating energy efficiency performance in production management e gap analysis between industrial needs and scientific literature. Journal of Cleaner Production. 2011;19(1):667-679.

[69] Energy and Mine's Ministers' Conference. Maximizing Canada's Energy Advantage – Canadian Industrial Energy Efficiency. 2015; Available online: https://www.nrcan.gc.ca/sites/www.nrcan.gc.ca/files/www/pdf/publications/emmc/15-0138_Industrial%20report_e_acc.pdf

[70] Responsible Action: A Plan for Alberta's Oil Sands. 2009; Available online: http://www.energy.alberta.ca/pdf/OSSgoaResponsibleActions_web.pdf

[71] Mech, M. A comprehensive guide to the Alberta oil sands. 2011; Available online: http://www.greenparty.ca/sites/default/files/a_comprehensive_guide_to_the_alberta_oil_sands_-_may_2011_-_last_revised_march_2012.pdf

[72] Woynillowicz, D. Oil Sands Fever – The Environmental Implications of Canada's Oil Sands Rush. 2005; Available online: https://www.pembina.org/reports/OilSands72.pdf

[73] National Energy Board – Canada's Oil Sands Opportunities and Challenges to 2015: An Update. 2006; Available online: https://www.neb-one.gc.ca/nrg/sttstc/crdlndptrlmprdct/rprt/archive/pprtntsndchllngs20152006/pprtntsndchllngs20152006-eng.pdf

[75] Findlay, J. The Future of the Canadian Oil Sands – Growth potential of unique resource amidst regulation, egress, cost, and price uncertainty. 2016; Available online: https://www.oxfordenergy.org/wpcms/wp-content/uploads/2016/02/The-Future-of-the-Canadian-Oil-Sands-WPM-64.pdf

[76] Nuwer, R. Oil Sands Mining Uses Up Almost as Much Energy as It Produces. 2013; Available online: http://insideclimatenews.org/news/20130219/oil-sands-mining-tar-sands-alberta-canada-energy-return-on-investment-eroi-natural-gas-in-situ-dilbit-bitumen

[77] Ouellette, A, Rowe, A, Sopinka, A, Wild, P. Achieving emissions reduction through oil sands cogeneration in Alberta's deregulated electricity market. Energy Policy. 71(1):13-21.

[78] Environment Canada. Canada's Emissions Trends. 2014; Available online: https://ec.gc.ca/ges-ghg/E0533893-A985-4640-B3A2-008D8083D17D/ETR_E%202014.pdf

[79] Moorhouse, J, Doritsch, D, Woynillowicz, D. Life cycle assessments of oilsands greenhouse gas emissions. 2011; Available online: https://www.pembina.org/reports/pembina-lca-checklist.pdf

[80] Chan, G, Reilly, J, Paltsev, S, Chen, Y. Then Canadian oil sands industry under carbon constraints. Energy Policy. 2012;50(1):540-550.

[81] Finan, A, Miu, K, Kadak, A. Nuclear Technology & Canadian Oil Sands: Integration of Nuclear Power with In-Situ Oil Extraction. 2011; Available online: http://web.mit.edu/pebble-bed/papers1_files/OilSands.pdf

[82] McColl, D. Green Bitumen: The Role of Nuclear, Gasification and CCS in Alberta's Oil Sands. 2009; Available online: http://climateactionnetwork.ca/2009/02/18/09-02-ceri-

green-bitumen-the-role-of-nuclear-gasification-and-ccs-in-alberta%E2%80%99s-oil-sands/
[83] Becera, G, Esparza, E, Finan, A. Nuclear Technology & Canadian Oil Sands – Integration of Nuclear Power with In-Situ Oil Extraction. 2005; Available online: https://canes.mit.edu/publications/nuclear-technology-and-canadian-oil-sands-integration-nuclear-power-situ-oil-extraction
[84] Gandrik, A, Patterson, M, Mills, P. HTGR-Integrated Oil Sands Recovery via Steam-Assisted Gravity Drainage. 2011; Available online: https://art.inl.gov/NGNP/INL%20Documents/Year%202011/HTGR-Integrated%20Oil%20Sands%20Recovery%20Via%20Steam-Assisted%20Gravity%20Drainage.pdf
[85] Gibbs, G, Asgarpour, S. Integration of High Temperature Gas-cooled Reactor Technology with Oil Sands Processes. 2011; Available online: http://www.ptac.org/attachments/1393/download
[86] Doucet, J. Is Nuclear Technology an Appropriate Alternative to Natural Gas for Alberta's Oilsands? 2007; Available online: https://business.ualberta.ca/-/media/business/centres/cabree/documents/energy/renewables/wooley.pdf
[87] Olateju, B, Kumar, A. Hydrogen production from wind energy in Western Canada for upgrading bitumen from oil sands. Energy. 2011;36:6326-6339.
[88] Olateji, B, Monds, J, Kumar, A. Large scale hydrogen production from wind energy for the upgrading of bitumen from oil sands. Applied Energy. 2014; 118:48-56.
[89] Sarkar, S, Kumar, A. Biohydrogen production from forest and agricultural residues for upgrading of bitumen for oil sands. Energy. 2010; 35:582-591.
[90] Majorowicz, J, Moore, M. The feasibility and potential of geothermal heat in the deep Alberta foreland basin-Canada for CO2 savings. Renewable Energy. 2014; 66(1):541-549.
[91] Holm, A, Jennejohn, D, Blodgett, L. Geothermal Energy Association – Geothermal Energy and Greenhouse Gas Emissions. 2012; Available online: http://geo-energy.org/reports/GeothermalGreenhouseEmissionsNov2012GEA_web.pdf
[92] Gray, D, Majorowicz, J, Unsworth, M. Investigation of the geothermal state of sedimentary basins using oil industry thermal data: case study from Northern Alberta

exhibiting the need to systematically remove biased data. J. Geophys. Eng. 2012; 9 (1):534-548.
[93] Majorowicz, J, Unsworth, M, Chacko, T, Gray, A, Heaman, L, Potter, D, Schmitt, D, Babadagli, T. Geothermal Energy as a Source of Heat for Oil Sands Processing in Northern Alberta, Canada, in Hein, FJ, Leckie, D, Larter, S, Suter, J, eds., Heavy oil and oil sands petroleum systems in Alberta and beyond: AAPG Studies in Geology. 2012; 64(1):1-22.
[94] Pathak, V, Babadagli, T, Majorowicz, A, Unsworth, M. Evaluation of Engineered Geothermal Systems as a Heat Source for Oil Sands Production in Northern Alberta. Natural Resources Research. 2012; 23(2):247-265.
[95] McKellar, J, Bergerson, J, MacLean, H. Replacing Natural Gas in Alberta's Oil Sands: Trade-Offs Associated with Alternative Fuels. Energy Fuels. 2010; 24(1):1687-1695.
[96] Furimsky, E. Gasification of oil sands coke: Review. Fuel Processing Technology. 2010; 56(1):263-290.
[97] El Gemayel, J, Macchi, A, Hughes, R, Anthony, E. Simulation of the integration of a bitumen upgrading facility and an IGCC process with carbon capture. Fuel. 2014; 117(1):1288-1297.
[98] Doulweera, G, Jordaa, S, Moore, M, Keith, D, Bergerson, J. Evaluating the role of cogeneration for carbon management in Alberta. Energy Policy. 2011; 39(12):7963-7974.
[99] Ordorica-Garcia, G, Nikoo, M, Carbo, M, Bolea, I. Technology Options and Integration Concepts for Implementing CO_2 Capture in Oil-Sands Operations. Journal of Canadian Petroleum Technology. 2012; 1(1):362-375.
[100] Ordorica-Garcia, G, Croiset, E, Douglas, P, Elkamel, A, Gupta, M. Modeling the Energy Demands and Greenhouse Gas Emissions of the Canadian Oil Sands Industry. Energy & Fuels. 2007; 21(1):2098-2111.
[101] Ordorica-Garcia, G, Elkamel, A, Douglas, PL, Croiset, E, Gupta, M. Energy Optimization Model with CO_2-Emission Constraints for the Canadian Oil Sands Industry. Energy & Fuels. 2008; 22(1):2660-2670.

[102] Betancourt-Torcat, A, Guiterrez, G, Elkamel, A, Ricardez-Sandoval, L. Integrated Energy Optimization Model for Oil Sands Operations. Industrial & Engineering Chemistry Research. 2011;50:12641-12663.

[103] Betancourt-Torcat, A, Elkamel, A, Ricardez-Sandoval, L. Optimal Integration of Nuclear Energy and Water Management into the Oil Sands Operations. AIChE journal. 2012; 58 (11):3433-3453.

[104] Betancourt-Torcat, A, Almansoori, A, Elkamel, A, Ricardez-Sandoval, L. Stochastic Modeling of the Oil Sands Operations under Greenhouse Gas Emission Restrictions and Water Management. Energy & Fuels. 2013; 27(1):5559-5578.

[105] Betancourt-Torcat, A, Elkamel, A, Ricardez-Sandoval, L. A modeling study of the effect of carbon dioxide mitigation strategies, natural gas prices and steam consumption on the Canadian Oil Sands operations. Energy. 2012; 45(1):1018-1033.

[106] Government of Alberta. Technical Guidance for Offset Project Developers. 2013; Available online: http://environment.gov.ab.ca/info/library/8525.pdf

[107] Wheler, J. Alberta's Climate Change Strategy and Regulations – A review of the first six years of the Specified Gas Emitters Regulation. 2014; Available online: http://cmcghg.com/wp-content/uploads/2014/01/J_Wheler-CMC-Workshop-SGER-Renewal-2014_01_27_v2.pdf

[108] Lattanzio, R. Canadian Oil Sands: Life-Cycle Assessments of Greenhouse Gas Emissions. 2014; Available online: https://www.fas.org/sgp/crs/misc/R42537.pdf

[109] Bramley, M, Huot, M, Dyer, S, Horne, M. Responsible action? An assessment of Alberta's greenhouse gas policies. 2011; Available online: http://www.pembina.org/reports/responsible-action.pdf

[110] Bakken, B, Skjelbred, H, Wolfgang, O. eTransport: Investment planning in energy supply systems with multiple energy carriers. Energy. 2007; 32(11):1676-1689.

[111] Zhang, D, Ma, L, Liu, P, Zhang, L, Li, Z. A multi-period superstructure optimization model for the optimal planning of China's power sector considering carbon dioxide mitigation Discussion on China's carbon mitigation policy based on the model. Energy Policy. 2012; 41(1):173-183.

[112] Mirzaesmaeeli, H, Elkamel, A, Douglas, P, Croiset, E, Gputa, M. A multi-period optimization model for energy planning with CO_2 emission consideration. Journal of Environmental Management. 2010; 91(1):1063-1070.

[113] Cormio, C, Dicorato, M, Minoia, A, Trovato, M. A regional energy planning methodology including renewable energy sources and environmental constraints. Renewable and Sustainable Energy Reviews. 2003; 71(1):99-130.

[114] Sirikitputtisak, T, Mirzaesmaeeli, H, Douglas, P, Croiset, E, Elkamel, A, Gupta, M. A multi-period optimization model for energy planning with CO_2 emission considerations. Energy Procedia. 2009; 1(1):4339-4346.

[115] Ding, J, Somani, A. A Long-Term Investment Planning Model for Mixed Energy Infrastructure Integrated with Renewable Energy. Proceedings of the Green Technologies Conference, IEEE 2010, Grapevine, TX, April 15 – 16, 2010.

[116] Bagchi, D, Biswas, S, Narahari, Y, Suresh, P, Lakshmi, L, Viswanadham, N, Subrahmanya, S. Carbon Footprint Optimization: Game Theoretic Problems and Solutions. ACM SIGecom Exchanges. 2012; 11(1):34-38.

[117] Garcia-Cortes, C, Tzimas, E, Peteves, SD. Technologies for Coal based Hydrogen and Electricity Co-production Power Plants with CO2 Capture. European Commission Joint Research Centre Institute for Energy. Calgary, Canada, March 2008.

[118] Rubin, ES, Rao, AB, Chen, C. Comparative assessments of fossil fuel power plants with CO_2 capture and storage. Proceedings of the GHGT-7 Conference. Vancouver, Canada, September 2004.

[119] Demirel, Y. Energy, Green Energy and Technology. Springer-Verlag London Limited. 2012; Available online: http://www.springer.com/cda/content/document/cda_downloaddocument/9781447123712-c2.pdf?SGWID=0-0-45-1293540-p174262962

[120] International Energy Agency. Power Generation from Coal – Measuring and Reporting Efficiency Performance and CO_2 emissions. 2010; Available online: https://www.iea.org/ciab/papers/power_generation_from_coal.pdf

[121] National Energy Strategy. Chapter 4 – Efficiency of Energy Conversion. 1992; Available online: http://www.ems.psu.edu/~radovic/Chapter4.pdf

[122] Simbeck, D, Chang, E. Hydrogen Supply: Cost estimate for Hydrogen Pathways – Scoping Analysis. 2002; Report NREL/SR-540-32525. National Renewable Energy Laboratory. Colorado, United States.
[123] Simbeck, DR. Hydrogen Costs with CO2 Capture. Proceedings of the GHGT-7 Conference. Vancouver, Canada, September 2004.
[124] Chiesa, P, Consonni, S, Kreutz, T, Williams, R. Co-production of hydrogen, electricity, and CO2 from coal with commercially ready technology. Part A: Performance and emissions. International Journal of Hydrogen Energy. 2005; 30(1):747.
[125] Jechura, J. Hydrogen from Natural Gas via Steam Methane Reforming (SMR). 2015;Available online: http://inside.mines.edu/~jjechura/EnergyTech/07_Hydrogen_from_SMR.pdf
[126] Maxwell, G. Synthetic Nitrogen Products – A Practical Guide to the Products and Processes. New York: Kluwer Academic Publishers, 2004.
[127] Turchi, C, Zhu, G, Wagner, M, Williams, T, Wendt, D. Geothermal/Solar Hybrid Designs: Use of Geothermal Energy for CSP Feedwater Heating. 2014; Available online: https://inldigitallibrary.inl.gov/sti/6330917.pdf
[128] Jamel, M, Rahman, A, Shamsuddin, A. Advance in the integration of solar thermal energy with conventional and non-conventional power plants. Renewable and Sustainable Energy Reviews. 2013; 20(1):71-81.
[129] Bruhn, M. Hybrid geothermal–fossil electricity generation from low enthalpy geothermal resources: geothermal feedwater preheating in conventional power plants. Energy. 2002; 27(4):329-346.
[130] Twa, B, Butler, D. Use of Low Grade Heat from Existing Coal Plant in Alberta. 2013; Available online: http://www.ai-ees.ca/media/12503/use_of_low_grade_heat_from_coal_plants_11jun13.pdf
[131] Beihong, Z, Weiding, L. An optimal sizing method for cogeneration plants. Energy and Buildings. 2006; 38(1):189-195.
[132] Liu, P, Pistikopoulos, E, Li, Z. A Multi-Objective Optimization Approach to Polygeneration Energy Systems Design. AIChE Journal. 2010; 56(5):1218-1234.

[133] Azargohar, R, Gerspacher, R, Dalai, A, Peng, D. Co-gasification of petroleum coke with lignite coal using fluidized bed gasifier. Fuel Processing Technology. 2015; 134(1):310-316.
[134] Georgeson, A. Modeling, optimization and economic evaluation of residual biomass gasification. Master of Science thesis, Texas A&M University, 2010.
[135] Orhan, O, Alper, E, McAlpine, K, Daly, S, Sycz, M, Elkamel, A. Gasification of Oil Refinery for Power and Hydrogen Production. Proceedings of the 2014 International Conference on Industrial Engineering and Operations Management Bali, Indonesia, January 7 – 9, 2014.
[136] Canadian Energy Research Institute. Oil Sands Industry Energy Requirements and Greenhouse Gas (GHG) Emissions Outlook (2015 – 2050). 2015; Available online: https://www.ceri.ca/s/CERI-Study-151-Final-Report.pdf
[137] Price Water House Coopers. Alberta Environment – Assessment of Selected Renewable Energy Technology and Potential In Alberta. 2009; Available online: eipa.alberta.ca/media/42554/assessment%20of%20selected%20renewable%20energy%20technology%20and%20potential%20in%20alberta.pdf
[138] The Centre for Spatial Economics. Economic Impacts of a Nuclear Accident at the Pickering or Darlington Nuclear Stations. 2011; Available online: http://www.greenpeace.org/canada/Global/canada/report/2011/09/Accident%20impact.pdf
[139] SBC Energy Institute. Hydrogen-Based Energy Conversion – More than storage: system flexibility. 2014; Available online: https://www.sbc.slb.com/~/media/Files/SBC%20Energy%20Institute/SBC%20Energy%20Institute_Hydrogen-based%20energy%20conversion_FactBook-vf.pdf
[140] Nyboer, J, Groves, S, Baylin-Stern, A. A Review of Existing Cogeneration Facilities in Canada. 2013; Available online: http://www2.cieedac.sfu.ca/media/publications/Cogeneration_Report_2013__2012_data__Final_-_May_3.pdf
[141] James, D. Biomass Energy Possibilities for Alberta to 2100. 2009; Available online: http://www.ai-ees.ca/media/6950/biomass_energy_possibilities_for_alberta_to_2100.pdf

[142] Tesfa, B, Mishra, R, Gu, F, Powles, N. Prediction models for density and viscosity of biodiesel and their effects on fuel supply system in CI engines. Renewable Energy. 2010; 35(1):2752-2760.

[143] U. S. Environmental Protection Agency Combined Heat and Power Partnership. 2007. Biomass Combined Heat and Power Catalog of Technologies.

[144] JACOBS Consultancy. Control Technologies Review, Cogeneration Units. 2010; Available online: http://ceaa.gc.ca/050/documents_staticpost/cearref_37519/44867/m.pdf

[145] HATCH – Alberta Innovates - Energy and Environment Solutions & BIO. Alberta Biomass and Gas to Liquids (BGTL) Scoping Study. 2014; Available online: http://bio.albertainnovates.ca/media/75733/hybrid_bgtl_final_report_rev._c.pdf

[146] Lower and Higher Heating Values of Gas, Liquid and Solid Fuels. 2013; Available online: http://cta.ornl.gov/bedb/appendix_a/Lower_and_Higher_Heating_Values_of_Gas_Liquid_and_Solid_Fuels.xls

[147] AB 1007 Fuel Price Forecast. 2015; Available online: http://www.energy.ca.gov/ab1007/documents/2007-10-09_workshop/presentations/AB_1007_Fuel_Price_Forecast.pdf

[148] Canadian Energy Research Institute. Western Canada Natural Gas Forecasts and Impacts (2015 – 2035). 2015; Available online: http://static1.squarespace.com/static/557705f1e4b0c73f726133e1/t/56a7f347c21b86130c778c3f/1453847367830/CERI+Study+149+-+Executive+Summary.pdf

[149] Subramanyam, V, Paramashivan, D, Radpour, S, Shah, T, Kumar, A. Identification of Best Energy-Efficiency Opportunities in Alberta's Energy Sector Phase II. 2013; Available online: http://www.ai-ees.ca/media/13033/kumar2_2013-11-18_final_report_on_assessment_of_energy_efficiency_scenarios_wit.pdf

[150] Duffey, R, Kuranb, S, Millera, A. Applications of Nuclear Energy to Oil Sands and Hydrogen Production. Available online: http://www-pub.iaea.org/MTCD/publications/PDF/P1500_CD_Web/htm/pdf/topic5/5S11_R.B.%20Duffey.pdf

[151] Bersak, A, Kadak, A. Integration of Nuclear Energy with Oil Sands Projects For Reduced Greenhouse Gas Emissions and Natural Gas Consumption. 2007; Available online: http://web.mit.edu/finana/Public/oilsands/MITWhitePaper.pdf
[152] Taljan, G, Canizares, C, Fowler, M, Verbic, G. The feasibility of hydrogen storage for mixed wind-nuclear power plants. 2007; Available online: https://ece.uwaterloo.ca/~ccanizar/papers/GregorTaljan.pdf
[153] Brooke, A, Kendrick, D, Meeraus, A, Raman, R. GAMS: A User's Guide. 1998; Available online: http://www2.imm.dtu.dk/courses/02724/general_information/GAMS_userguide/GAMSUsersGuide.pdf
[154] Kalkbrenner, A. Environmental Assessment of Nuclear Power Plants in Alberta – Canadian Institute of Resource Law. 2013; Available online: http://dspace.ucalgary.ca/bitstream/1880/49993/1/NuclearOP43w.pdf
[155] Aplin, S. Embrace nuclear energy, Alberta: it's the only way to lower oil sands GHGs – Canadian Energy Issues. 2013; Available online: http://canadianenergyissues.com/2013/04/05/embrace-nuclear-energy-alberta-its-the-only-way-to-lower-oilsands-ghgs/
[156] Backus, W. Carbon Capture Technology – A Technoeconomic Evaluation of Absorption, Gasification and Oxy-Coal Combustion for Coal Power Plants. 2010; Available online: https://engineering.wustl.edu/current-students/student-services/ecc/Documents/Backus.pdf
[157] Brandt, A, Heath, G, Kort, E, Sullivan, F, Petron, G, Jordaan, S . . . Harriss, R. Methane Leaks from North American Natural Gas Systems. Science. 2014; 343(1):733-735.
[158] Norgate, T, Haque, N, Koltun, P. The impact of uranium ore grade on the greenhouse gas footprint of nuclear power. Journal of Cleaner Production. 2014; 84(1):360-367.
[159] Warner, E, Heath, G. Life Cycle Greenhouse Gas Emissions of Nuclear Electricity Generation. Journal of Industrial Ecology. 2012; 16(1):73-92.
[160] Stephen, J, Wood-Bohm, S. Biomass Innovation – Canada's Leading Cleantech Opportunity for Greenhouse Gas Reduction and Economic Prosperity – Alberta Innovates

Bio Solutions. 2016; Available online: http://wsca.ca/wp-content/uploads/2016/03/Biomass_GHGEconomy_Canada_2016.pdf

[161] Sikka, M, Thornton, TF, Worl, R. Sustainable biomass energy and indigenous cultural models of well-being in an Alaska forest ecosystem. Ecology and Society. 2013; 18(3): 38

[162] Nuclear Energy Agency. The Role of Nuclear Energy in a Low-Carbon Energy Future. 2012; Available online: https://www.oecd-nea.org/nsd/reports/2012/nea6887-role-nuclear-low-carbon.pdf

[163] Bunse, K.; Vodicka, M.; Scheonsleben, M.; Breulhart, M.; Ernst, F. Integrating energy efficiency performance in production management e gap analysis between industrial needs and scientific literature. *J Clean Prod*. 2011, 19(1):667–679.

[164] Energy and Mine's Ministers' Conference. Maximizing Canada's Energy Advantage—Canadian Industrial Energy Efficiency. 2015. Available at: https://www.nrcan.gc.ca/sites/www.nrcan.gc.ca/files/ www/pdf/publications/emmc/15-0138_Industrial%20report_e_acc.pdf

[165] Kubik, R. 2013. Canadian Oil Sands—2013 Annual Report, Available online: https://www.cdnoilsands.com/files/FinancialReports/AnnualReport2013/2013%20Annual%20ReportFinalenglishv001r6d515.pdf

[166] Mech, M. A Comprehensive Guide to the Alberta Oil Sands. 2011. Available at: https://www.greenparty.ca/sites/default/files/a_comprehensive_guide_to_the_alberta_oil_sands_-_may_2011_-_last_revised_ march_2012.pdf

[167] Woynillowicz, D. Oil Sands Fever—The Environmental Implications of Canada's Oil Sands Rush. 2005. Available at: https://www.pembina.org/reports/OilSands72.pdf

[168] Demirel, Y., 2012. Energy, Green Energy and Technology. Springer-Verlag London Limited, Available online: https://www.springer.com/cda/content/document/cdadownloaddocument/9781447123712c2.pdf?SGWID=0-0-45-1293540-p174262962

[169] Findlay, J. The Future of the Canadian Oil Sands—Growth Potential of Unique Resource Amidst Regulation, Egress, Cost, and Price Uncertainty. 2016. Available at: https://www.oxfordenergy.org/wpcms/wp-content/uploads/2016/02/The-Future-of-the-Canadian-OilSands-WPM-64.pdf

[170] Doritsch, D.; Huot, M.; Partington, P.J. 2010. Canadian Oil Sands and Greenhouse Gas Emissions, Available online: https://www.pembina.org/reports/briefingnoteosghg.pdf
[171] Nuwer, R. Oil Sands Mining Uses Up Almost as Much Energy as It Produces. 2013. Available at: https://insideclimatenews.org/news/20130219/oil-sands-mining-tar-sands-alberta-canada-energy-return-oninvestment-eroi-natural-gas-in-situ-dilbit-bitumen
[172] Environment Canada. Canada's Emissions Trends. 2014. Available at: https://ec.gc.ca/ges-ghg/E0533893-A985-4640-B3A2-008D8083D 17D/ETR_E%202014.pdf
[173] Moorhouse, J.; Doritsch, D.; Woynillowicz, D. Life cycle assessments of oil sands greenhouse gas emissions. 2011. Available at: https:// www.pembina.org/reports/pembina-lca-checklist.pdf
[174] Finan, A; Miu, K; Kadak, A. Nuclear Technology & Canadian Oil Sands: Integration of Nuclear Power with In-Situ Oil Extraction. 2011. Available at: https://web.mit.edu/pebble-bed/papers1_files/OilSands.pdf
[175] McColl, D. Green Bitumen: The Role of Nuclear, Gasification and CCS in Alberta's Oil Sands. 2009. Available at: https://climateactionnetwork.ca/2009/02/18/09-02-ceri-green-bitumen-the-role-of-nuclear-gasification-and-ccs-in-alberta%E2%80%99s-oil-sands/
[176] Olateji, B.; Monds, J.; Kumar, A. Large scale hydrogen production from wind energy for the upgrading of bitumen from oil sands. *Appl. Energ*. 2014, 118:48–56.
[177] Sarkar, S.; Kumar, A. Biohydrogen production from forest and agricultural residues for upgrading of bitumen for oil sands. *Energy*, 2010; 35:582–591.
[178] Majorowicz , J.; Moore, M. The feasibility and potential of geothermal heat in the deep Alberta foreland basin-Canada for CO_2 savings. *Renew. Energ*. 2014, 66(1):541–549.
[179] Pathak, V.; Babadagli, T.; Majorowicz, A.; Unsworth, M. Evaluation of engineered geothermal systems as a heat source for oil sands production in Northern Alberta. *Nat Resour Res*. 2012, 23(2):247–265.
[180] McKellar, J.; Bergerson, J.; MacLean, H. Replacing natural gas in alberta's oil sands: trade-offs associated with alternative fuels. *Energ Fuel*. 2010, 24(1):1687–1695.

[181] Furimsky, E. Gasification of oil sands coke: review. *Fuel Process Technol*. 2010, 56(1):263–290.
[181] El Gemayel, J.; Macchi, A.; Hughes, R.; Anthony, E. Simulation of the integration of a bitumen upgrading facility and an IGCC process with carbon capture. *Fuel*. 2014, 117(1):1288–1297.
[182] Ouellette, A.; Rowe, A.; Sopinka, A.; Wild, P. Achieving emissions reduction through oil sands cogeneration in Alberta's deregulated electricity market. *Energ. Policy*. 2016, 71(1):13–21.
[183] Doulweera, G.; Jordaa, S.; Moore, M.; Keith, D.; Bergerson, J. Evaluating the role of cogeneration for carbon management in Alberta. *Energ. Policy*. 2011, 39(12):7963–7974.
[184] Betancourt-Torcat, A.; Guiterrez, G.; Elkamel, A.; Ricardez-Sandoval, L. Integrated energy optimization model for oil sands operations. *Ind. Eng. Chem. Res*. 2011, 50:12641–12663.
[185] Betancourt-Torcat, A.; Elkamel, A.; Ricardez-Sandoval, L. Optimal integration of nuclear energy and water management into the oil sands operations. *AIChE J*. 2012, 58(11):3433–3453.
[186] Betancourt-Torcat, A.; Almansoori, A.; Elkamel, A.; Ricardez-Sandoval, L. Stochastic modeling of the oil sands operations under greenhouse gas emission restrictions and water management. *Energ. Fuel*. 2013, 27(1):5559–5578.
[187] Elsholkami, M.; Elkamel, A.; Vargas, F. Optimized integration of renewable energy technologies into Alberta's oil sands industry. *Comp. Chem. Eng*. 2016, 90(1):1–22.
[188] Elsholkami, M.; Elkamel, A. General Optimization Model for the Energy Planning of Industries Including Renewable Energy: A Case Study on Oil Sands. *AIChE J*. 2017, 63(2):610–638.
[189] Gamage, G. Assessing the Effectiveness of Wind Power and Cogeneration for Carbon Management of Electric Power Systems. 2011. Available at: http://keith.seas.harvard.edu/files/tkg/files/th12_gamage_2011.pdf
[190] Wilson, N. Alberta Oil Magazing: Ramped up to its full potential in the oil sands, cogeneration could be an environmental game changer. 2016. Available at:

https://www.albertaoilmagazine.com/2016/09/cogeneration-one-efficient-energy-sources-whats-holding-back/

[191] Somma, M.;Yan, B.; Bianco, N.; Graditi, G.; Luh, P.B.; Mongibello, L; Naso, V. Multi-objective design optimization of distributed energy systems through cost and exergy assessments. *App. Energ*. 2017, 204(1):1299-1316.

[192] Majewski, D.; Wirtz, M.; Lampe, M.; Bardow, A. Robust multi-objective optimization for sustainable design of distributed energy supply systems. *Comp. Chem. Eng*. 2017, 102(1):26-39.

[193] Falke, T.; Krengel, S.; Meinerzhagen, A.K.; Schnettler, A. Multi-objective optimization and simulation for the design of distributed energy systems. *App. Energ*. 2016, 184(1):1508-1516.

[194] Haikarainen, C.; Pettersson, F.; Saxen, H. An MILP Model for Distributed Energy System Optimization. *Chem. Eng. Trans*. 2013, 35(1):295-300.

[195] Barbato, A.; Bolchini, C.; Geronazzo, A.; Quintarelli, E.; Palamarciuc, A.; Piti, A.; Rottondi, C.; Verticale, G. Energy Optimization and Management of Demand Response Interactions in a Smart Campus. *Energies*. 2016, 398(9):1-20.

[196] Abujarad, S.; Mustafa, M.W.; Jamian, J.J. Recent approaches of unit commitment in the presence of intermittent renewable energy resources: A review. *Renew. Sus. Energ. Rev*. 2017, 70(1):215-223.

[197] Govardhan, M.; Roy, R. Economic analysis of unit commitment with distributed energy resources. *Int. J. Elec. Pow. Energ. Sys*. 2015, 71(1):1-14.

[198] Yang, Z.; Li, K.; Niu, Q.; Xue, Y. A comprehensive study of economic unit commitment of power systems integrating various renewable generations and plug-in electric vehicles. *Energ. Conv. Manag*. 2017, 132(1):460-481.

[199] Bashiri, M.; Badri, H.; Talebi, J. A New Approach to Tactical and Strategic Planning in Production–distribution Networks. *A*
pp. Math. Model. 2012, 36(4):1703-1717.

[200] Hemmati, R.; Saboori, H.; Jirdehi, M.A. Stochastic planning and scheduling of energy storage systems for congestion management in electric power systems including renewable energy resources. *Energy*. 2017, 133(1):380-387.

[201] Hemmati, R.; Saboori, H.; Siano, P. Coordinated short-term scheduling and long-term expansion planning in microgrids incorporating renewable energy resources and energy storage systems. *Energy*. 2017, 134(1):699-708.
[202] Vahid-Pakdel, M.J.; Nojavan, S.; Mohammadi-ivatloo, B.; Zare, K. Stochastic optimization of energy hub operation with consideration of thermal energy market and demand response. *Energ. Conv. Manag*. 2017, 145(1):117-128.
[203] AESO 2015 Long-term Transmission Plan. Available at: https://www.aeso.ca/assets/Uploads/2015-Long-termTransmissionPlan-WEB.pdf
[204] AESO – Current Supply and Demand Report. 2017. Available at: http://ets.aeso.ca/ets_web/ip/Market/Reports/CSDReportServlet
[205] AESO 2017 Long-term Outlook. 2017. Available at: https://www.aeso.ca/download/listedfiles/AESO-2017-Long-term-Outlook.pdf
[206] Fakhfakh, M.; Loulou, M.; Masmoudi, N. A novel heuristic for multi-objective optimization of analog circuit performances. *Analog. Integ. Circ. Signal. Proc*. 2009, 61(1):47-64.
[207] Liu, S.; Papageorgiou, L.G. Multi objective optimization of production, distribution and capacity planning of global supply chains in the process industry. *Omega*. 2013, 41(2), 369-382.
[208] Beihong, Z.; Weiding, L. An optimal sizing method for cogeneration plants. *Energ. Build*. 2006, 38(1):189–195.
[209] Nyboer, J.; Groves, S.; Baylin-Stern, A. A Review of Existing Cogeneration Facilities in Canada. 2013. Available at: http://www2.cieedac.sfu.ca/media/publications/Cogeneration_Report_2013__2012_data__Final_-_May_3.pdf
[210] Santoli L, Lo Basso G, Bruschi D. Energy characterization of CHP (combined heat and power) fueled with hydrogen enriched natural gas blends. Energy. 2013; 60(1):13-22.
[211] Coster, E.J.; Myrzik, J.M.A.; Kling, W.L. Grid interaction of MV-connected CHP-plants during disturbances. Power & Energy Society General Meeting, 2009. PES '09. IEEE 2009, Calgary, AB, Canada, July 26-30, 2009.
[212] CANWEA - Wind Energy in Alberta. 2017. Available at: https://canwea.ca/wind-energy/alberta/

[213] Price Water House Coopers. Alberta Environment—Assessment of Selected Renewable Energy Technology and Potential In Alberta. 2009. Available at: eipa.alberta.ca/media/42554/assessment%20of%20selected%20renewable%20energy%20technology %20and%20potential%20in%20alberta.pdf

[214] Giudici, F.A. Feasibility study of hydrogen production using electrolysis and wind power in Patagonia, Argentina. 2008. Available at: http://ufdcimages.uflib.ufl.edu/UF/E0/02/23/29/00001/giudici_f.pdf

[215] Eichman, J.; Harrison, K.; Peters, M. Novel Electrolyzer Applications: Providing More Than Just Hydrogen. 2014. Available at: https://www.nrel.gov/docs/fy14osti/61758.pdf

[216] Murillo, C. Canadian Energy Research Institute. Oil Sands Industry Energy Requirements and Greenhouse Gas (GHG) Emissions Outlook (2015-2050). 2015. Available at: https://www.generationenergy.ca/images/documents/CERI/Study_151_Full_Report.pdf

[217] Wheler, J. Alberta's Climate Change Strategy and Regulations—A review of the first six years of the Specified Gas Emitters Regulation. 2014. Available at: http://cmcghg.com/wp-content/uploads/2014/01/J_Wheler-CMC-Workshop-SGER-Renewal-2014_01_27_v2.pdf

[218] Lattanzio, R. Canadian Oil Sands: Life-Cycle Assessments of Greenhouse Gas Emissions. 2014. Available at: https://www.fas.org/sgp/crs/misc/R42537.pdf

[219] Bramley, M.; Huot, M.; Dyer, S.; Horne, M. Responsible action? An assessment of Alberta's greenhouse gas policies. 2011. Available at: http://www.pembina.org/reports/responsible-action.pdf

[220] Taljan, G.; Canizares, C.; Fowler, M.; Verbic, G. The Feasibility of Hydrogen Storage for Mixed Wind-Nuclear Power Plants. 2007. Available at http://psrc.iiit.ac.in/resources/Conf.Proc/NAPS%202008/Paperlist/Papers/4.pdf

[221] Saur, G.; Ramsden, T. Wind Electrolysis: Hydrogen Cost Optimization. 2016. Available at: https://www.nrel.gov/docs/fy11osti/50408.pdf

[222] Beccali, M.; Brunone, S.; Finocchiaro, P.; Galleto, J.M. Method for size optimisation of large wind–hydrogen systems with high penetration on power grids. *App. Energ*. 2013, 102(1):534-544.

[223] Finan, A.; Miu, K.; Kadak, A. Nuclear Technology & Canadian Oil Sands: Integration of Nuclear Power with In-Situ Oil Extraction. 2011. Available at: http://web.mit.edu/pebble-bed/papers1_files/OilSands.pdf

[224] Gibbs, G.; Asgarpour, S. Integration of High Temperature Gas-cooled Reactor Technology with Oil Sands Processes. 2011. Available at: http://www.ptac.org/attachments/1393/download

[225] McColl, D. Green Bitumen: The Role of Nuclear, Gasification and CCS in Alberta's Oil Sands. 2009. Available at: http://climateactionnetwork.ca/2009/02/18/09-02-ceri-green-bitumen-the-role-of-nuclear-gasification-and-ccs-in-alberta%E2%80%99s-oil-sands/

[226] Jechura, J. Hydrogen from Natural Gas via Steam Methane Reforming (SMR). 2015. Available at: http://inside.mines.edu/~jjechura/EnergyTech/07_Hydrogen_from_SMR.pdf

[227] Canadian Energy Research Institute. Oil Sands Industry Energy Requirements and Greenhouse Gas (GHG) Emissions Outlook (2015–2050). 2015. Available at: https://www.ceri.ca/s/CERI-Study-151-Final-Report.pdf

[228] Canadian Energy Research Institute. Western Canada Natural Gas Forecasts and Impacts (2015–2035). 2015. Available at: http://static1.squarespace.com/static/557705f1e4b0c73f726133e1/t/56a7f347c21b86130c778c3f/1453847367830/CERI+Study+149+-+Executive+Summary.pdf

[229] Duffey, R.; Kuranb, S.; Millera, A. Applications of Nuclear Energy to Oil Sands and Hydrogen Production. Available at: http://www-pub.iaea.org/MTCD/publications/PDF/P1500_CD_Web/htm/pdf/topic5/5S11_R.B.%20Duffey.pdf

[230] Nuclear Energy Institute. Nuclear Costs in Context. 2017. Available at: https://www.nei.org/CorporateSite/media/filefolder/Policy/Papers/Nuclear-Costs-in-Context.pdf?ext=.pdf

[231] Independent Power Producers Society of Alberta. Trends in GHG Emissions in the Alberta Electricity Market – Impact of fuel switching to natural gas. 2013. Available at: http://www.ippsa.com/IP_pdfs/Analysis%20of%20GHG%20Emissions%20in%20the%20Alberta%20Electricity%20Market%20-%20May%202,%202013.pdf

[232] Parker, N. Using Natural Gas Transmission Pipeline Costs to Estimate Hydrogen Pipeline Costs. 2005. Available at: https://escholarship.org/content/qt9m40m75r/qt9m40m75r.pdf

[233] Yang, C.; Ogden, J. Determining the lowest-cost hydrogen delivery mode. *Int. J. Hyd. Energ*. 2007, 32(1):268-286.

[234] Market Intelligence and Data Analysis Corporation. Grid Integrated Electrolysis – Facilitating Carbon Emission Reductions in the Transportation, Industrial and Residential Sectors. 2016. Available at: http://www.ieso.ca/-/media/files/ieso/document-library/engage/esf/esf-20170217-midac.pdf?la=en.

[235] Alberta's Oil Sands Projects and Upgraders. 2017. Available at: http://www.energy.alberta.ca/LandAccess/pdfs/OilSands_Projects.pdf

[236] Layzell, D.; Klein, M. The Globe and Mail: It's time to put an end to Alberta's energy waste. 2015. Available at: https://www.theglobeandmail.com/opinion/its-time-to-put-an-end-to-albertas-energy-waste/article26061509/?arc404=true

[237] Yu, R. What are we going to do with all that Sulphur, 2005. http://www.business.ualberta.ca/Centres/CABREE/NaturalResources/~/media/business/Centres/CABREE/Documents/NaturalResources/CumulativeEffectsManagement/RonnieYuOilSandsFinal.ashx (Accessed March 20th 2013).

[238] Louie, D. *Handbook of Sulphuric Acid*. DKL Engineering, Inc.: Thornhill, ON, 2005.

[239] Johnson, G.; Lang, L. Sulphur Handling Forming, Storage and Shipping, 2010. http://www.scribd.com/doc/45851897/Sulfur-Handling-Forming-Storage-and-Shipping (Accessed October 25th 2013).

[240] Ye, E. Alternative Sulfur Management Solutions to Help Refiners Meet Clean Fuel and Environmental Challenges.10th Biennial Sulfur Market Symposium; 2006 April 4 – 6; Beijing, China.

[241] Jula, P. and Zschocke, M. Dynamic simulation of a push-pull distribution system. Proceedings of the 2005 Winter Simulation Conference; 2005 Dec 4 – 7; Florida, USA.

[242] Mackenzie, N. Government of Alberta – The elemental sulphur management framework for the industrial heartland, 2007. http://environment.gov.ab.ca/info/library/8412.pdf (Accessed October 15th 2013).

[243] Clark, P.; Dowling, N.; Hyne, J. Understanding and Mitigating Corrosion During Handling and Transportation of Elemental Sulphur. Alberta Sulphur Research Ltd Quarterly Bulletin. 1996, 33 (1), 15 – 28.
[244] Clark, P. A Review of Solid and Liquid Sulfur Specifications with Emphasis on Handling and Transportation. Alberta Sulphur Research Ltd Quarterly Bulletin. 1996, 33 (1), 1 – 14.
[245] Clark, P.; Bernard, F.; Davis, P. Storage of Solid and Liquid Sulfur: Safeguarding the Environment and Product Integrity. Alberta Sulphur Research Ltd Quarterly Bulletin. 2004, 40 (4), 23 – 35.
[246] Clark, P. Technology for Utilization of Excess Sulfur and New Approaches for Sour Gas Production that Eliminate CO2 Emission. Alberta Sulphur Research Ltd Quarterly Bulletin. 2006, 43 (3), 1 – 8.
[247] Clark, P. Injection of SO2 into Disposal Reservoirs – Energy Production from Excess Sulfur and Sulfur Management for Hydrocarbon Development. Alberta Sulphur Research Ltd Quarterly Bulletin. 2006, 43 (3), 9 – 48.
[248] Clark, P.; Dowling, N.; Huang, M. The chemistry and Kinetics of Claus Tail Gas Incineration-Improving Efficiency. Alberta Sulphur Research Ltd Quarterly Bulletin. 2008, 45 (2), 21 – 55.
[249] Clark, P.; Hornba, D. Preventing Corrosion in Sulfur Storage Tanks. Alberta Sulphur Research Ltd Quarterly Bulletin. 2008, 45 (2), 1 – 20.
[250] Clark, P.; Dowling, N. Corrosion Pathways in Liquid Sulfur Run-Down Pits and Other Liquid Sulfur Handling Facilities. Proceedings Brimstone Sulfur Symposium; 2009 Sep 14 -18; Colorado, USA.
[251] Clark, P.; Davis, P.; Marriott, R.; Wan, H.; Bernard, F. Development of Technologies for Utilization and Storage of Excess Sulphur. Alberta Sulphur Research Ltd Quarterly Bulletin. 2008, 45 (1), 56 – 65.
[252] Clark, P.; Huang, M.; Dowling, N.; Shields, M. New Technologies for Sulfur Recovery at the 1-10 ton/day Scale. Alberta Sulphur Research Ltd Quarterly Bulletin. 2008, 44 (4), 5 – 13.
[253] Clark, P. The Chemist's Guide to Building a Sulfur Block in the Refinery Parking Lot. Proceeding Brimstone Sulfur Symposium; 2009 Sep 14 – 18; Colorado, USA.

[254] Shamskar, K. The effect of quenching temperature on structural and mechanical properties of sulfur prills. *Powder Tech.*. 2008, 217, 128 – 133.

[255] Mokhatab, S.; Poe, W. Sulfur Recovery and Handling (1st Ed.), Handbook of Natural Gas Transmission and Processing; Gulf Professional Publishing: Houston, TX, 2012; pp. 291 – 316.

[256] Wang, H.; Fang, D.; Chuang, K., A sulphur removal and disposal process through H_2S adsorption and regeneration: Ammonia leaching regeneration, *Process Safety and Environmental Protection*. 2008, 86 (4), 296 – 302.

[257] Ordorica-Garcia, G.; Elkamel, A.; Douglas, P.; Croiset, E.; Gupta, M. Energy Optimization Model with CO2-Emission Constraints for the Canadian Oil Sands Industry, *Energy & Fuels*. 2008, 22 (1), 2660 – 2670.

[258] Betancourt-Torcat, A.; Guiterrez, G.; Elkamel, A.; Ricardez-Sandoval, L. Integrated Energy Optimization Model for Oil Sands Operations, Ind. Eng. Chem. Res. 2011, 50 (1), 12641 – 12663.

[259] Lambiase, A.; Mastrocinque, E.; Miranda, S.; Lambiase, A. Strategic planning and Design of Supply Chain: a Literature Review. *Int. J. Eng. Bus. Manag.*, 2013, 5, 49 – 60.

[260] AlMansoori, A.; Shah, N. Design and operation of a future hydrogen supply chain. Chemical Engineering Research and Design. 2006, 84 (A6), 423 – 438.

[261] Paquet, M.; Martel, A.; Desaulniers, G. Including technology selection decisions in manufacturing network design models. *Int. J. Comp. Int. Mfg*. 2004, 17 (2), 117 – 125.

[262] Tsiakis, P.; Papageorgiou, L. Optimal production allocation and distribution supply chain networks. *Int. J. Prod. Econ*. 2008, 111, 468 – 483.

[263] You, F. and Grossmann, I. Integrated Multi-Echelon Supply Chain Design with Inventories under Uncertainty: MINLP Models, Computational Strategies, *AIChE J*. 2010, 56 (2), 419 – 440.

[264] Rodriguez, M.; Vecchietti, A.; Harjunkoski, I.; Grossmann, I. Optimal supply chain design and management over a multi-period horizon under demand uncertainty. Part I: MINLP and MILP models, *Comp. & Chem. Eng*. 2014, 62 (1), 194 – 210.

[265] Melo, M.; Nickel, S; Gama, F. Dynamic multi-commodity capacitated facility location: a mathematical modeling framework for strategic supply chain planning, *Comp. & Ops. Res*. 2006, 33 (1), 181 – 208.

[266] Yan, H.; Yu, Z.; Cheng, T. A strategic model for supply chain design with logical constraints: formulation and solution, *Comp. & Ops. Res*. 2003, 30 (14), 2135 – 2155.

[267] Sabri, E. and Beamon, B. A multi-objective approach to simultaneous strategic and operational planning in supply chain design, *Omega*. 2000, 28 (5), 581 – 598.

[268] Tsou, S. Strategic design for imported liquefied petroleum gas distribution systems in East China. 2002, Unpublished Master's thesis, Massachusetts Institute of Technology, Massachusetts, USA.

[269] D'Aquin, G. Sulfur Overview North America. IFA Production and International Trade Conference; 2002 October 16 – 18; Quebec City, Canada.

[270] Crawford, P. Are we there yet?, 2009. http://www.enersul.com/docs/elp_articles_are_we_there_yet.pdf (Accessed November 18th 2013).

[271] Harbaugh, E.; Baker, J. Enersul Loading Up Liquid, 2013. http://www.enersul.com/Docs/Enersul_loading_up_liquid.pdf (Accessed February 3rd 2014).

[272] Harbaugh, E. Enersul Building Blocks, 2011. http://www.enersul.com/Docs/enersul_building_blocks.pdf (Accessed February 3rd 2014).

[273] Marsh, R., Parks, K. and Crowfoot, C. Alberta's Energy Reserves 2012 and Supply/Demand Outlook 2013 – 2022, 2013. http://www.aer.ca/documents/sts/ST98/ST98-2013.pdf (Accessed November 15th 2013).

[274] Project Status – Alberta's Industrial Heartland: Active Projects Announced or Under Construction, 2014. http://www.industrialheartland.com/index.php?option=com_content&view=article&id=130:project-status&catid=53&Itemid=160 (Accessed February 15th 2014).

[275] Application For Approval Alberta Sulphur Terminals Ltd. – HAZCO Sulphur Management Facility Bruderheim, Alberta, 2005. http://www.scribd.com/doc/91796143/Sulphur-Handling-Terminal-Alberta-Environment-28102005 (Accessed November 3rd 2013).

[276] Kinder Morgan Canada Terminals Heartland Regional Sulphur Forming and Handling Terminal, 2007.

http://s3.amazonaws.com/zanran_storage/www.kindermorgan.com/ContentPages/12491989.pdf (Accessed December 9th 2013).

[277] Canadian Association of Petroleum Producers (CAPP) – Statistical handbook for Canada's upstream petroleum industry, 2013. http://www.capp.ca/library/statistics/handbook/Pages/default.aspx (Accessed December 4th 2014).

[278] Alberta's International Exports by Industry - A 10-Year Review, 2013. http://www.albertacanada.com/files/albertacanada/SP-EH_AIME-10-year-review.pdf (Accessed November 15th 2013).

[279] Clark, P., Davis, P., Marriott, R., Bernard, F., Wan, H., Fitzpatrick, E., Giri, G. and Alere, P. Technical and commercial considerations for sulphur management. Sour gas 2010 – 3rd annual meeting; 2010 January 31; Abu Dhabi, UAE.

[280] Fertecon Sulphur Report – A Review of the International Sulphur Market, 2012. http://fertecon.agra-net.com/wp-content/uploads/2012/05/Sulphur-report.pdf (Accessed January 4th 2014).

[281] Teare, M.; Burrowes, A.; Baturin-Pollock, C.; Tamblyn, C.; Ito, S.; Willwerth, A. Energy Resources Conservation Board (ERCB) – Alberta's Energy Reserves 2012 and Supply/Demand Outlook 2013 – 2022, 2013. http://www.aer.ca/documents/sts/ST98/ST98-2013.pdf (Accessed February 14th 2014).

[282] Board Decision Report: Alberta Sulphur Terminals Ltd. Sulphur Forming and Shipping Facility, 2009. https://nrp.nrcb.ca/Projects/CompletedProjects/AlbertaSulphurTerminalsLtd.aspx (Accessed January 2nd 2014).

[283] Montgomery, K. Sulphur forming and handling – Middle East and Caspian. IFA conference; 2004 October 3 – 5; Dubai, UAE.

[284] GASCO award AED 4bn contracts for sulphur plant projects. Emirates News Agency, 2011. https://www.zawya.com/story/GASCO_awards_AED_4bn_contracts_for_Sulphur_plant_projects-WAM20110101075023125/ (Accessed November 22nd 2013).

[285] Enersul Brochure – Sulphur Granulation: A Premium Product, 2013. http://www.enersul.com/Docs/ES-Brochure-SPgMnt-Eng.pdf (Accessed November 25th 2013).

[286] Sandvik Brochure – Sulphur solidification and handling system, 2013. http://www2.sandvik.com/sandvik/0140/internet/s002582.nsf/0/BC7D901D03D8DE7CC12574E4004A6B70/$file/Sulphur%20saleskit%208.7.2008.pdf?OpenElement (Accessed November 25th 2013).

[287] North American Oil Sands Upgrader Project – StatoilHydro Canada Ltd. Upgrader Project Supplemental Information, 2008. http://www.statoil.com/no/EnvironmentSociety/Environment/impactassessments/pipelines/Downloads/Volume%201.pdf (Accessed December 4th 2013).

[288] Turton, R.; Bailie, R.; Whiting, W.; Shaeiwitz, J. Analysis, Synthesis and Design of Chemical Processes (3rd Ed.); Pearson Education: Upper Saddle River, NJ, 2008.

[289] Leslie, W. Strategic analysis of a bulk terminal, 2005. Unpublished Master's Thesis, Simon Fraser University, Burnbay, British Colombia, Canada.

[290] Baumgartner, K. Optimization Approaches for the Design of Realistic Supply Chains: Examples from the Chemical Industry; Kölner Wissenschaftsverlag: Cologne Metropolitan Area, Germany, 2010.

[291] Baumgartner, K.; Fuetterer, A.; Thonemann, U. Supply chain design considering economies of scale and transport frequencies. *EU. J. of Op. Res.*; 2012, 218, 789 – 800.

[292] d'Aquin, G.; Fell, R. Sulfur and Sulfuric Acid (11th Ed.), Kent and Riegel's Handbook of Industrial Chemistry and Biotechnology; Springer Science: New York, NY, 2007; 1157 – 1183.

[293] National Energy Board – Reasons for Decision In the Matter of Westcoast Energy Inc. Application for Pine River Plant and Grizzly Pipeline System Expansion, 1993. http://publications.gc.ca/collections/Collection/NE22-1-1993-7E.pdf (Accessed January 5th 2014).

[294] Stone, K. Sulphur. Canadian minerals yearbook, 2008. http://www.nrcan.gc.ca/sites/www.nrcan.gc.ca/files/mineralsmetals/pdf/mms-smm/busi-indu/cmy-amc/2008revu/pdf/sul-sou-eng.pdf (Accessed March 11th 2014).

[295] Western Canadian Shippers' Coalition (WCSC) – Rail Freight Service Review Panel, 2010. http://www.tc.gc.ca/media/documents/policy/092-western-canadian-chippers-coalition-eng.pdf (Accessed March 11th 2014).

[296] ISL Engineering and Land Services – Alberta Infrastructure and Transportation Capital Region Integrated Growth Management Plan Final Report on Core Infrastructure, 2007. http://www.municipalaffairs.gov.ab.ca/documents/CRIGMP_Core_Infrastructure_November_2007_Section_3.pdf (Accessed January 5th 2014).

[297] Meyer, R. Canadian National Railway (CN) – Transportation Solutions for Oil Sands Production Phase. Transportation Innovation in Alberta Oil Sands: A Summit; 2009 May 13; The Van Horne Institute, Calgary, Alberta, Canada.

[298] Avison Young – The Industrial Report, 2011. http://www.avisonyoung.com/sites/default/files/market-intelligence/2011Q2_Industrial_Report.pdf (Accessed March 11th 2014).

[299] Messick, D. World Sulphur Outlook – The Sulphur Institute, 2010. http://www.firt.org/sites/default/files/DonMessick_Sulphur_Outlook.pdf (Accessed December 15th 2013).

Appendix

Appendix A

In this appendix, the data that is required to apply the proposed mathematical model to the investigated case study is summarized. The economic and operational parameters for the considered energy production technologies are presented in Table A1. These data were obtained from multiple sources in the literature [176, 189-197, 216-251]. It is important to note that bioenergy and nuclear facilities are assumed to be low-carbon emitting. Based on several studies in the literature, life cycle analyses show total GHG reductions of up to 95% from baseline when agricultural residues or forest biomass are used as a feedstock for energy and fuel production. According to a study conducted by the Nuclear Energy Agency, on the long run nuclear facilities will remain to be a very low-carbon technology even when considering all the energy intensive steps in their life cycle. It is important to note that this input data is just used to illustrate the applicability of the model proposed. The results and conclusions drawn might vary if another set of input data is used. Figure A1 represents the six demand levels investigated, which represent different energy intensities for oil sands operations. The variation in energy intensity arises based on three factors, which are business as usual scenario, improved energy efficiency, and deteriorated reservoir quality. The data presented in Figure A2 is used to derive the different carbon mitigation policies investigated. For each emission level, the different carbon credit price levels are considered, as well as the unavailability of carbon credits, which results in a total of six investigated carbon mitigation policy scenarios. Figure A3 shows the different levels of fuel prices considered in the investigated case study.

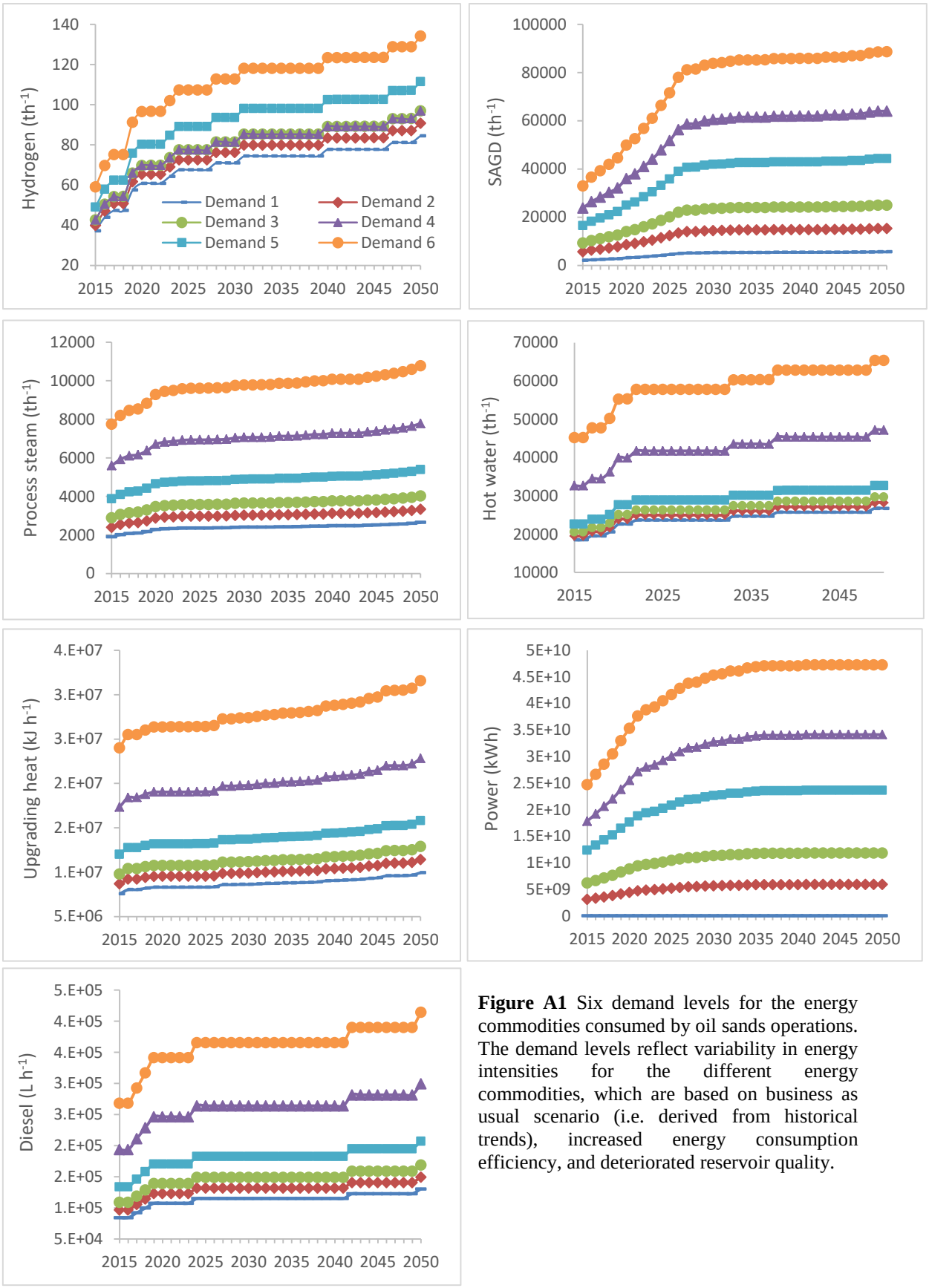

Figure A1 Six demand levels for the energy commodities consumed by oil sands operations. The demand levels reflect variability in energy intensities for the different energy commodities, which are based on business as usual scenario (i.e. derived from historical trends), increased energy consumption efficiency, and deteriorated reservoir quality.

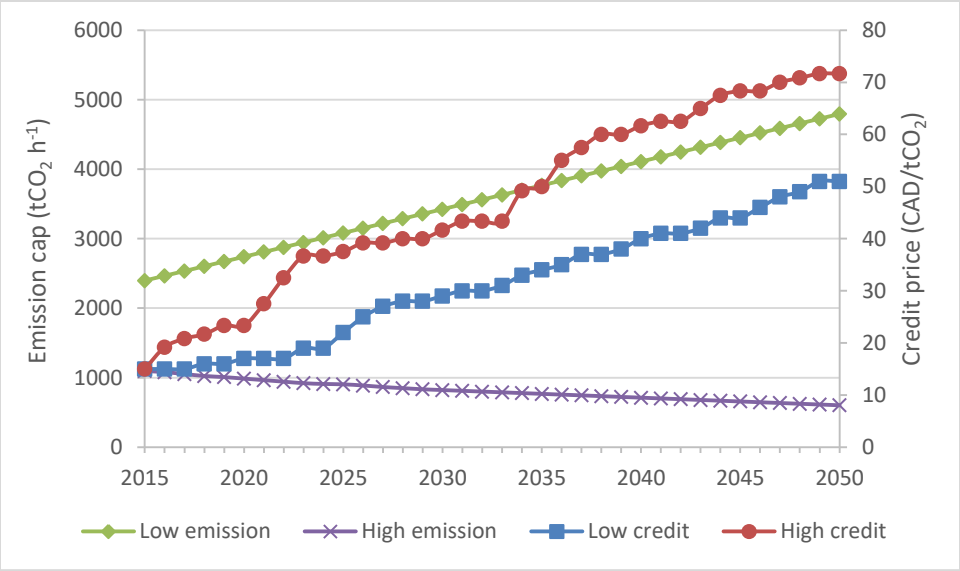

Figure A2 CO_2 emission targets proposed for oil sands operations, and prices of carbon credit purchased to offset emissions for energy production

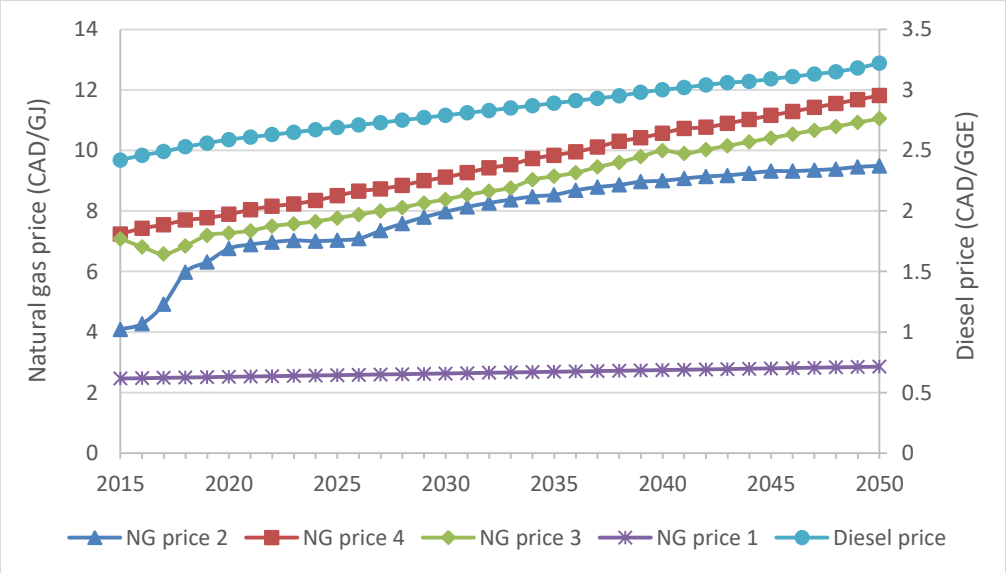

Figure A3 Different levels of fuel prices considered in the investigated case study

Table A9-a Economic and operational parameters for new energy production technologies. The table represents the total capacity, and capital and operating costs of single units and units retrofitted with carbon capture and sequestration. All the presented costs are estimated in terms of 2014 Canadian dollars

Technology	Capacity	Capital	F-O&M (%)	V-O&M	CO_2	Yield	CCS (%)	Lead time
NGCC	507 MW	567 CAD/kW	1	0.00102 CAD/kWh	0.367 tCO2/MWh	7.17 MJ/kWh	-	4
NGCC wCC	432 MW	931 CAD/kW	1	0.0034 CAD/kWh	0.043 tCO2/MWh	8.4 MJ/kWh	88%	4
PC	524 MW	1234 CAD/kW	1.5	0.0046 CAD/kWh	0.811 tCO2/MWh	9.16 MJ/kWh	-	4
PC wCC	492 MW	1983 CAD/kW	1.5	0.0097 CAD/kWh	0.107 tCO2/MWh	12 MJ/kWh	88%	4
NGOX wCC	539 MW	1246 CAD/kW	1	0.0107 CAD/kWh	0.012 tCO2/MWh	7.69 MJ/kWh	90%	4
Coal OX wCC	448 MW	1952 CAD/kW	1.5	0.0148 CAD/kWh	0.084 tCO2/MWh	9.72 MJ/kWh	90%	4
WT - Vestas 1.8	1.8 MW	785 CAD/kW	10	0.023 CAD/kWh	0	-	-	3
SMR	6.25 th^{-1}	11.2M CAD/th^{-1}	1	76 CAD/t	8.992 tCO_2/tH_2	174886 MJ/tH_2	-	4
SMR wCC	6.25 th^{-1}	17.8M CAD/th^{-1}	1	121 CAD/t	1.05 tCO_2/tH_2	204174 MJ/tH_2	88%	4
Electrolyzers	5 th^{-1}	35M CAD/th^{-1}	1	103 CAD/t	0	0.0000187 tH_2/kWh	-	3
NGB - SAGD	120 th^{-1}	377K CAD/th^{-1}	0.5	9.8 CAD/t	0.218 tCO_2/t	-	-	1
NGB - PS and HW	300 th^{-1}	290K CAD/th^{-1}	0.5	7.6 CAD/t	0.129 tCO_2/t	-	-	1
Geothermal - HW	300 th^{-1}	136K CAD/th^{-1}	1	10.4 CAD/t	0	-	-	4
Geothermal - PS	300 th^{-1}	472K CAD/th^{-1}	1	11.3 CAD/t	0	-	-	4
Geothermal - SAGD	300 th^{-1}	528K CAD/th^{-1}	1	13.1 CAD/t	0	-	-	4
GT CHP - P & SS	200 MWt/Mwe	525 CAD/kWe	1	0.0031 CAD/kWh	0.45 tCO_2/MWh	-	-	4
GT CHP wCC - P & SS	200 MWt/Mwe	630 CAD/kWe	1.5	0.0047 CAD/kWh	0.052 tCO_2/MWh	-	95%	4
GT CHP - P & PS	200 MWt/Mwe	500 CAD/kWe	1	0.00247 CAD/kWh	0.37 tCO_2/MWh	-	-	4
GT CHP wCC - P & PS	200 MWt/Mwe	595 CAD/kWe	1.5	0.0027 CAD/kWh	0.041 tCO_2/MWh	-	95%	4
ST CHP - P, PS & HW	50 MWt/Mwe	980 CAD/kWe	1	0.008 CAD/kWh	0.37 tCO_2/MWh	-	-	4
ST CHP wCC - P, PS & HW	50 MWt/Mwe	1300 CAD/kWe	1.5	0.011 CAD/kWh	0.041 tCO_2/MWh	-	95%	4

IGCC - P	440 MW	1764 CAD/kW	1.5	0.0046 CAD/kWh	0.8 tCO2/MWh	8.757 MJ/kWh	-	4
IGCC wCC - P	532 MW	1886 CAD/kW	1.5	0.006 CAD/kWh	0.131 tCO2/MWh	11.06 MJ/kWh	85%	4
IGCC - H2	32.09 tH_2/h	23.8M CAD/th^{-1}	1.5	97 CAD/t	18.7 tCO_2/tH_2	174888 MJ/tH_2	-	4
IGCC wCC - H2	32.09 tH_2/h	25.1M CAD/th^{-1}	1.5	101.86 CAD/t	1.5 tCO_2/tH_2	204174 MJ/tH_2	90%	4
Biogas - SS	120 t/h	520K CAD/th^{-1}	1	13.8 CAD/t	0	-	-	3
Biogas - PS & HW	300 th^{-1}	415K CAD/th^{-1}	1	11.3 CAD/t	0	-	-	3
Biogas - P & SS	100 Mwe/MWt	4805 CAD/kWe	4.3	0.0160/kWh	0	-	-	4
Biogas - P & PS	60 Mwe/MWt	5100 CAD/kWe	4	0.012/kWh	0	-	-	4
Biogas - H2 (1)	10.5 tH_2/h	30.8 CAD/th^{-1}	1	135 CAD/t	0	0.0834 $tH_2/tbio$	-	4
Biogas - H2 (2)	20.85 tH_2/h	45.8 CAD/th^{-1}	1	128 CAD/t	0	0.0834 $tH_2/tbio$	-	4
Biodiesel (1)	0.46 th^{-1}	2330K CAD/th^{-1}	1.5	123 CAD/t	0	500L/tbio	-	3

Table A1-b Economic and operational parameters for new energy production technologies. The table represents the total capacity, and capital and operating costs of single units and units retrofitted with carbon capture and sequestration. All the presented costs are estimated in terms of 2014 Canadian dollars

Biodiesel (2)	0.91 th^{-1}	3600K CAD/th^{-1}	1.5	103 CAD/t	0	500L/tbio	-	3
Biodiesel (3)	1.68 th^{-1}	4500K CAD/th^{-1}	1.5	91 CAD/t	0	500L/tbio	-	3
PCK/A gas - P	120 th^{-1}	2.96M CAD/th^{-1}	1.5	42 CAD/t	0.837 $tCO_2/tPCK$	0.83MWh/t Syn	90%	4
PCK/A gas - H2	88 th^{-1}	3.1M CAD/th^{-1}	2.5	44.8 CAD/t	0.837 $tCO_2/tPCK$	0.18 $tH_2/tsyn$	90%	4
PCK/A gas- P & H2	212 th^{-1}	3.4M CAD/th^{-1}	1.5	41.26 CAD/t	0.837 $tCO_2/tPCK$	-	90%	4
PCK/A gas - P, H2 & Steam	303 th^{-1}	4.1M CAD/th^{-1}	3.4	49 CAD/t	0.837 $tCO_2/tPCK$	0.296tSS/tsyn	90%	4
PCK/A gas - P & Steam	260 th^{-1}	3.2M CAD/th^{-1}	1.5	46 CAD/t	0.837 $tCO_2/tPCK$	0.37tPS/tsyn	90%	4
Nuclear PBMR - P	172 MW	4.3 CAD/MW	1.5	0.00897 CAD/kWh	0	-	-	6
Nuclear ACR - 700 - P	703 MW	3.74 CAD/MW	1.5	0.00997 CAD/kWh	0	-	-	6
Nuclear ACR - 1000 -P	1150 MW	4.4 CAD/MW	1.5	0.0462 CAD/kWh	0	-	-	6
Nuclear CANDU - P	728 MW	4.38 CAD/MW	1.5	0.0523 CAD/kWh	0	-	-	6
Nuclear PBMR - SS	550 t/h	900K CAD/th^{-1}	1.5	10.3 CAD/t	0	-	-	6

Nuclear PBMR - P & SS	500 MWth	871K CAD/MWt	1.5	54 CAD/MWh	0	0.096 MWe/MWt	-	6
Nuclear HTGR - P & SS	2400 MWth	1887K CAD/MWt	1.5	62 CAD/MWh	0	0.046 MWe/MWt	-	6
Nuclear HTGR - P, SS, PS, UH & H2	2965 MWth	2750K CAD/MWt	1.5	67 CAD/MWh	0	0.11 MWe/MWt	-	6
Nuclear PBMR - Power, PS & HW	500 MWth	770K CAD/MWt	1.5	43 CAD/MWh	0	0.096 MWe/MWt	-	6
Nuclear PBMR - PS, HW & UH	600 MWth	700K CAD/MWt	1.5	42 CAD/MWh	0	-	-	6
Nuclear ACR - 700 - P, PS, HW, UH, H2	2100 MWth	4056K CAD/MWt	1.5	68.8 CAD/MWh	0	0.096 MWe/MWt	-	6

Technologies – NGCC: Natural gas combined cycle, PC: Pulverized coal, NGOX: Natural gas oxyfuel, Coal OX: Coal oxyuel, WT: Wind turbines, SMR: Steam methane reforming, NGB: Natural gas boilers, CHP: Combined heat and power, GT: Gas turbines, ST: Steam turbines, IGCC: Integrated gasification combined cycle, Biogas: Biomass gasification, PCK/A gas: Petcoke/asphaltene gasificaition, CC: Carbon capture and sequestration**. Energy commodities** – P: Power, SS: SAGD steam, PS: Process steam, HW: Hot water, H2: Hydrogen, UH: Upgrading heat.

Table A10 Key techno-economic parameters required for the optimization model

CO_2 pipeline length	6 km/100
Compression power for CO_2 trans (kWh/tonne CO_2/100 km)	1.34
Cost of carbon transport (CAD/tCO_2/100 km)	1.3
Cost of carbon storage (CAD/tCO_2)	7
Emission factor for diesel (tCO_2/L Diesel)	0.00267
Emission factor for process fuel natural gas (tCO_2/Nm^3 NG)	0.00179
Emission factor for process fuel coal (tCO_2/t coal)	1.702
Diesel cost (CAD/L)	1.25
Heating value of process fuel natural gas (MJ/kg)	43
Heating value of process fuel coal (MJ/kg)	24
Heating value of biomass (MJ/kg)	18
Heating value of syngas (MJ/kg)	48
Total cost of a nuclear accident (CAD)	1.28E+11
Probability of occurence of a nuclear accident (reactor yr-1)	0.000001
Factor associated with individual risk perception	385
Biomass availability (t/hr)	2512
Boiler supplementary boiler efficiency	85%
Gas turbine electricity generation efficiency	30%

HRSG heat recovery efficiency	50%
HRSG supplemental firing efficiency	95%

Appendix B

This appendix includes operating data for the Alberta grid existing power generation units, which is utilized in chapter 5.

Table B1 Detailed operating data of the units belonging to the Alberta grid.

Unit	BUS	Pmin (MW)	Pmax (MW)	Type	Heat rate (GJ/MWh)	Ramp rate (MW/min)	Start-up fuel (GJ)	Min. up time (hr)	Min. down time (hr)
i1	3	60	149	PC	12	2	2500	48	24
i2	3	60	155	PC	12	2	2500	48	24
i3	3	147	385	PC	11	3	3000	48	24
i4	4	154	400	PC	10	3	3000	48	24
i5	4	154	400	PC	10	3	3000	48	24
i6	4	158	466	SCPC	9	5	3000	48	24
i7	6	60	144	PC	16	2	3000	48	24
i8	4	152	395	PC	10	3	3000	48	24
i9	4	152	395	PC	10	3	3000	48	24
i10	1	151	463	PC	11	3	3000	48	24
i11	1	151	400	PC	11	3	3000	48	24
i12	4	112	390	PC	11	3	3000	48	24
i13	4	112	280	PC	11	3	3000	48	24
i14	4	141	280	PC	11	3	3000	48	24
i15	4	162	368	PC	11	3	3000	48	24
i16	4	141	406	PC	10	3	3000	48	24
i17	4	160	406	PC	10	3	3000	48	24
i18	4	112	401	PC	12	2	3000	48	24
i19	2	5	120	CCGT	8	12	180	4	2
i20	2	15	320	CCGT	8	12	480	4	2
i21	2	3	73	CCGT	10	16	110	4	2
i22	2	10	210	CCGT	8	12	315	4	2
i23	2	5	120	CCGT	8	12	180	4	2
i24	2	35	860	CCGT	7	9	1290	4	2
i25	6	13	63	SCGT	13	5	164	1	1
i26	6	1	7	SCGT	13	5	18	1	1
i27	6	2	10	SCGT	13	6	26	1	1
i28	6	3	15	SCGT	13	4	39	1	1

i29	6	10	48	SCGT	13	3	125	1	1
i30	6	20	101	SCGT	12	5	263	1	1
i31	6	20	101	SCGT	17	6	263	1	1
i32	6	10	48	SCGT	16	6	125	1	1
i33	6	10	48	SCGT	12	5	125	1	1
i34	4	10	48	SCGT	17	3	125	1	1
i35	4	1	6	SCGT	16	4	16	1	1
i36	4	3	16	SCGT	13	4	42	1	1
i37	4	1	6	SCGT	13	5	16	1	1
i38	1	3	15	SCGT	12	6	39	1	1
i39	1	1	7	SCGT	17	6	18	1	1
i40	1	1	6	SCGT	16	5	16	1	1
i41	6	2	8	SCGT	13	5	21	1	1
i42	6	2	11	SCGT	12	4	29	1	1
i43	6	2	9	SCGT	14	3	23	1	1
i44	6	21	105	SCGT	16	4	273	1	1
i45	6	10	48	SCGT	17	5	125	1	1
i46	6	10	50	SCGT	17	3	130	1	1
i47	6	4	20	SCGT	16	6	52	1	1
i48	6	10	50	SCGT	12	6	130	1	1
i49	6	10	50	SCGT	13	5	130	1	1
i50	6	4	20	SCGT	13	5	52	1	1
i51	5	39	195	COGEN	7.5	7	52	4	3
i52	5	19	96	COGEN	7.5	4	26	4	3
i53	6	9	45	COGEN	7.5	2	12	4	3
i54	6	10	50	COGEN	7.5	2	13	4	3
i55	3	13	64	COGEN	7.5	2	17	4	3
i56	3	7	36	COGEN	7.5	1	10	4	3
i57	5	1	5	COGEN	7.5	1	1	4	3
i58	5	41	203	COGEN	7.5	8	54	4	3
i59	2	2	10	COGEN	7.5	1	3	4	3
i60	6	19	95	COGEN	7.5	4	25	4	3
i61	5	20	101	COGEN	7.5	4	27	4	3
i62	3	65	326	COGEN	7.5	12	87	4	3
i63	5	3	13	COGEN	7.5	1	3	4	3
i64	5	95	473	COGEN	7.5	18	126	4	3
i65	1	40	199	COGEN	7.5	8	53	4	3
i66	5	20	98	COGEN	7.5	4	26	4	3
i67	2	95	474	COGEN	7.5	18	126	4	3
i68	5	17	84	COGEN	7.5	3	22	4	3
i69	5	3	16	COGEN	7.5	1	4	4	3
i70	5	40	202	COGEN	7.5	8	54	4	3
i71	5	41	205	COGEN	7.5	8	55	4	3

i72	5	36	180	COGEN	7.5	7	48	4	3
i73	5	40	202	COGEN	7.5	8	54	4	3
i74	5	39	195	COGEN	7.5	7	52	4	3
i75	5	44	220	COGEN	7.5	8	59	4	3
i76	5	75	376	COGEN	7.5	14	100	4	3
i77	4	20	100	COGEN	7.5	4	27	4	3
i78	4	9	47	COGEN	7.5	2	13	4	3
i79	4	9	46	COGEN	7.5	2	12	4	3
i80	6	4	19	COGEN	7.5	1	5	4	3
i81	5	102	510	COGEN	7.5	19	136	4	3
i82	6	2	12	COGEN	7.5	1	3	4	3
i83	6	8	39	COGEN	7.5	1	10	4	3
i84	3	0	120	HYDRO	-	24	0	0	0
i85	2	0	320	HYDRO	-	64	0	0	0
i86	3	0	350	HYDRO	-	70	0	0	0
i87	1	0	32	HYDRO	-	6	0	0	0
i88	3	0	15	HYDRO	-	3	0	0	0
i89	2	0	15	HYDRO	-	3	0	0	0
i90	3	0	7	HYDRO	-	1	0	0	0
i91	3	0	21	HYDRO	-	4	0	0	0
i92	1	0	14	HYDRO	-	3	0	0	0
i93	6	20	131	BIO	12	2.2	10	4	3
i94	6	6	42	BIO	12	0.7	10	4	3
i95	1	8	52	BIO	12	0.9	10	4	3
i96	1	2	11	BIO	12	0.2	10	4	3
i97	3	1	5	BIO	12	0.1	10	4	3
i98	3	4	27	BIO	12	0.5	10	4	3
i99	6	2	16	BIO	12	0.3	10	4	3
i100	6	1	9	BIO	12	0.2	10	4	3
i101	6	8	50	BIO	12	0.9	10	4	3
i102	6	3	18	BIO	12	0.3	10	4	3
i103	6	7	48	BIO	12	0.8	10	4	3
i104	6	4	25	BIO	12	0.4	10	4	3
i105	1	457	3,045	WIND	-	-	0	0	0

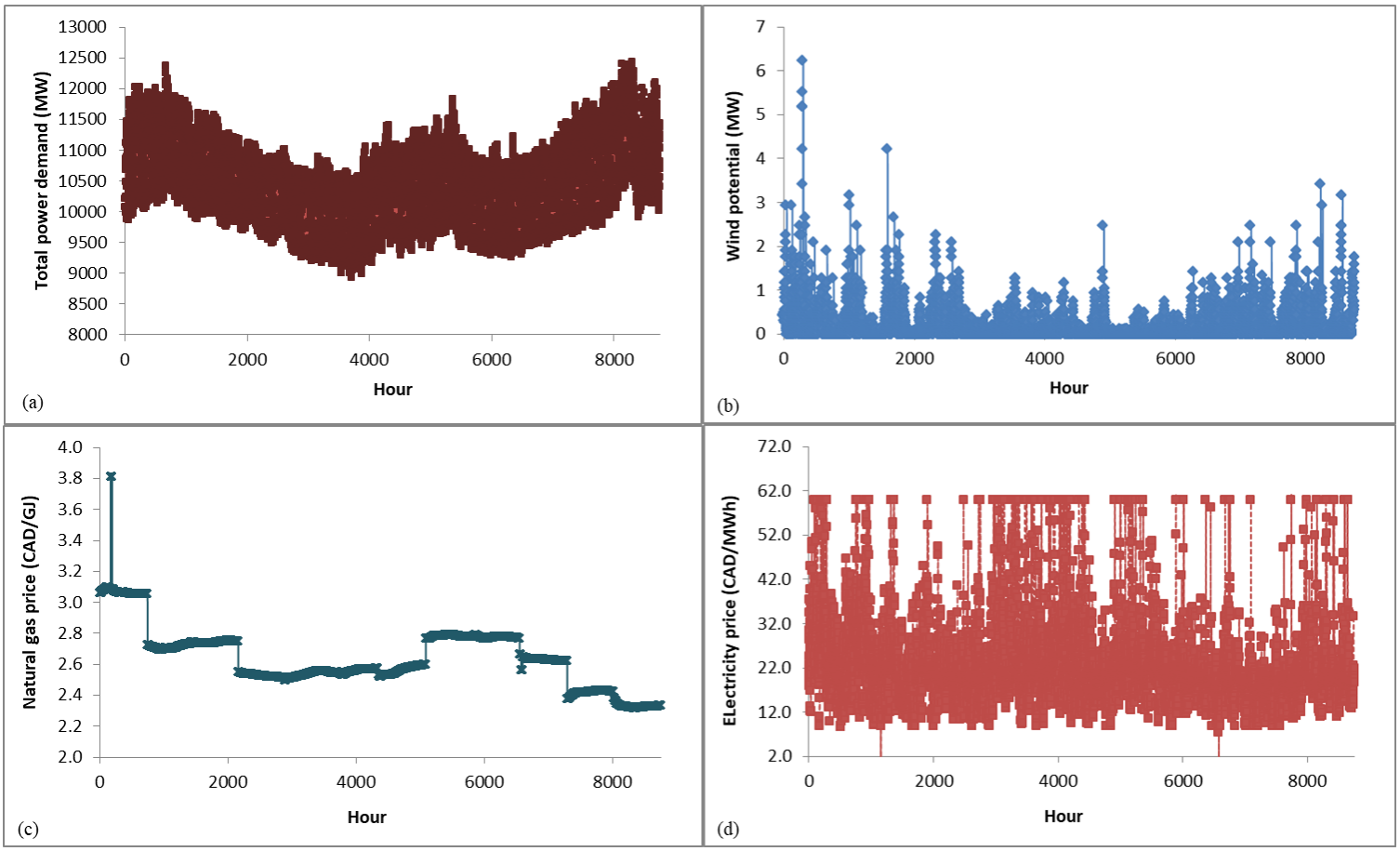

Figure B1 (a) Total power demand (MW), (b) Total wind potential (MW), (c) Natural gas price (CAD/GJ), (d) Electricity price (CAD/MWh)